Laura Mercantili

Sonochemically induced reactions of oils

CRANFIELD HEALTH

Ph.D. Thesis

Academic years 2009-2012

Supervisors: Professor Séamus P. J. Higson

Dr. Frank Davis

October 2012

CRANFIELD HEALTH

Ph.D. Thesis

Academic years 2009-2012

Laura Mercantili

Sonochemically induced reactions of oils

Supervisors: Professor Séamus P. J. Higson

Dr. Frank Davis

October 2012

This thesis is submitted in partial fulfilment of the requirements for the degree of Doctor of Philosophy

Abstract

This work will describe the use of the ultrasonic power for the modification of a wide range of oils from vegetable, through to mineral and synthetic oils. It will be shown that ultrasound is effective in cleaving the chains of carbon-based oils with the generation of products with a lower viscosity. The proposed mechanism through which these less viscous products are generated involves the formation of radical species which can be either oxygen or non-oxygen related. The process can be improved by the addition of nucleating agents, with the achieved lower viscosity being stabilised by the addition of radical scavengers.

It will be also shown that ultrasound is effective as a power source to drive organic chemistry reactions such as the alkaline hydrolysis of triglycerides (saponification reaction).

Benefits of this work will be related to the possible production of more easily degradable oils and to the possibility of using such oils as alternative energy sources, with a particular interest in investigating the environmental and energetic benefits of this approach.

Ackowledgements

First of all I would like to thank my supervisor, Professor Séamus Higson, for his help, encouragement, guidance and great patience throughout these three years. It was deeply appreciated!

My deepest gratitude is also extended to Dr. Frank Davis for co-supervising this work, Dr. Stuart Collyer and Dr. Jo Holmes for their friendship and for all the advices, valuable criticisms and suggestions they gave me during these years…not only about research!

I also wish to thank all the past and present university friends and colleagues whit whom I shared this experience; I can now count some of them as my great friends, they made these years more enjoyable and their friendship and support is still appreciated more than they know.

I am also grateful to my Italian best friends Silvia, Elisa, Bianca and Tiziana, for their constant presence in my life even from so far away.

A special thank you must also go to Domenico, who has been there for me with great patience throughout this thesis and for countless more reasons.

Last but not least, a special thank you goes to my family for their continuous support and encouragement, particularly to my parents for everything they have done to get me to this point. All my love, thank you!

"What we know is a drop, what we don't know is an ocean"

Sir Isaac Newton (1643 - 1727)

Declaration

This is a declaration to certify that the contents of this thesis have not been submitted for any other academic or professional award or published in any other form and the contents of this thesis represents entirely my own work.

Laura Mercantili

October 2012

Table of Contents

List of Figures

List of Tables

Nomenclature/Abbreviation

λ	wavelength (cm^{-1})
μ	dynamic viscosity (cP)
ρ	medium density ($kg\ m^{-3}$)
ρF	fluid density ($kg\ m^{-3}$)
ρS	sphere density ($kg\ m^{-3}$)
c	speed of the sound ($m\ s^{-1}$)
f	frequency (Hz)
g	gravitational acceleration ($9.8\ m\ s^{-2}$)
BR	burning rate (mg/min)
CV	calorific value ($MJ\ kg^{-1}$)
D	diameter of the sphere (m)
E	Young's elastic modulus ($N\ m^{-2}$)
M	mass (kg)
S	specific heat ($J\ g^{-1}°C$)
T	period
$\mathcal{V}$	terminal velocity of the sphere ($m\ s^{-1}$)

A	Ampere
atm	atmosphere (1.01325 bar)
C	Celsius
cP	centiPoise ($0.001\ Pa\ s$)
g	gram
h	hour
Hz	Hertz
J	Joule ($N\ m$)
K	Kelvin
m	metre
min	minute
ml	millilitre
mT	millitesla ($\mathrm{T} = \mathrm{V}\ s\ m^2$)

N	Newton ($kg\ m\ s^{-2}$)
P	Poise ($g\ cm^{-1}\ s^{-1}$)
Pa	Pascal ($N\ m^{-2}$)
s	second
V	Volt ($W\ A^{-1}$)
W	Watt ($kg\ m^2\ s^{-3}$)

ATD-GCMS	Automated Thermal Desorption Gas Chromatography – Mass Spectrometry
CNTs	carbon nanotubes
CP	carbon black
CPLS	carbon plasma black
DLS	Dynamic Light Scattering
ESR	Electron Spin Resonance
FTIR	Fourier Transform Infrared Spectroscopy
HC	total unburned hydrocarbons
HHV	Higher Heating Value
KOH	potassium hydroxide
LAB	linear alkyl-benzenes
LC/MS	Liquid Chromatography – Mass Spectrometry
LHV	Lower Heating Value
LPG	Liquefied Petroleum Gas
PBN	N-tert-butyl-α-phenil nitrone
PCB	polychlorinated biphenyls
PDMS	polydimethylsiloxane
Ph	4-tert-butylphenol
PM	particulate matter
PTC	phase transfer catalysts
SEM	Scanning Electron Microscopy
SIFT	Selected Ion Flow Tube - Mass Spectrometry
TIC	total ion chromatogram
WCO	waste cooking oil

Part 1

Introduction and Methodology

Chapter 1

Introduction

1.1 Rationale

The increasing consumption of petroleum products and of the other conventional energy sources has caused a decrease in reserves along with an increase in price, so that the development of newer and greener energy sources is of the utmost interest. These factors, coupled with the issues related to the treatment of oil waste and to the remediation of oil-contaminated lands, underpin the development of a new process for the recovery/generation of energy from the degradation of oil and oil waste.

The most commonly used processes for the generation of alternative energy sources are biological and thermochemical processes which convert biomatter into fuels such as bio-ethanol, bio-methanol, bio-hydrogen, or biodiesel. Even though these processes match the criteria for the production of greener and renewable energy sources compared with the conventional cracking processes, they still have some disadvantages such as the generation of high temperatures or pressures generally required to drive these processes, or the addition of chemicals and the formation of by-products as in the case of the classic transesterification reaction for the production of biodiesel.

A common point of these thermal processes, such as pyrolysis or other forms of cracking, and of the transesterification reaction is that they have, or can have, vegetable oil as substrate and their action results in the cleaving of the carbon chains of the oil with a subsequent lowering of the viscosity of the product. This last characteristic is of particular interest for the present work since a similar effect has been demonstrated for the cavitation process applied to samples containing polymeric chains.

Cavitation, a physical phenomenon which implies the formation, growth, and implosive collapse of micro-bubbles, can be induced in liquids either from the application of a mechanical force - hydrodynamic cavitation - or from the application of an acoustic field - sonication. The latter is of particular interest since the use of ultrasound is well established in many chemistry processes from its use to facilitate chemical reactions, through to its use in polymer synthesis and degradation.

Ultrasound is defined as a sound of frequencies above the threshold for human hearing; the term sonication defines the use of the acoustic energy to produce physical and/or chemical changes in fluids. During cavitation a localised release of high temperatures and pressures takes place; this is responsible for the physical and chemical changes which affect the substrate under analysis. In the case of polymeric chains, the cavitating micro-bubble generates shear forces which stretches the coiled polymeric chains till they are cleaved from the forces generated by the micro-bubble's collapse. It has been demonstrated that this process leads to the generation of highly reactive radical species and results in the decrease of the viscosity of the substrate.

The starting point of this work is therefore the possibility to generate low viscous products with the application of an ultrasonic field to oil samples with a polymeric-like structure. The possible applications of this process range from its use in the treatment of oil waste - as the obtained products will be more easily degradable, through to its use in the food processing for food with a high oil/fat content, its use in the remediation of contaminated lands, and also to the production of an alternative biofuel or to improve the existing processes for the production of biofuel.

1.2 Aim and Objectives

The primary aim of this research project will be to study and characterise the sonochemical breakdown of oils from different sources, vegetable, mineral, and synthetic, in order to obtain products more easily degradable and possibly coupling a way to recover energy from the process.

The main objectives to achieve this aim will include: *1)* to test the efficiency of the sonication process on the different kinds of oils; *2)* to stabilise the products obtained with the sonication in order to allow future applications of the sonicated products; *3)* to investigate the oils' properties and chemical composition before and after sonication; *4)* to hypothesise a mechanism responsible for the generation of the products; *5)* to evaluate the energy required to drive the sonication; *6)* to investigate the combustion properties of the sonicated products.

Chapter 2

Literature Review

2.1 Ultrasound

2.1.1 Sound and ultrasound

Sound is a phenomenon caused by the vibration of an oscillating body in an elastic medium (air, liquid, solid). This vibration causes a local movement of the particles in the medium, leading to the formation of waves which are described in terms of frequency and intensity.

Sound waves are longitudinal in nature, in which particles movement in the medium is parallel to wave's direction of travel. The acoustic impulse, generated by the oscillating body, compresses the particles in the medium (high pressure), although this compression is limited by the elasticity of the medium itself which creates a rarefaction (low pressure). Compression and rarefaction alternate till the oscillation reaches its end and the medium goes back to equilibrium [1]. This phenomenon can be seen in figure 2.1; at equilibrium all the particles in the medium have a characteristic distance between them. When an acoustic field is applied, the distance between the particles changes according to the intensity and the frequency of the sound waves. The bar within figure 2.1 indicates the local particles' concentration within the medium – where the particles are more concentrated due to compression the bar is darker; where the particles are less concentrated due to rarefaction the bar is brighter [2; 3].

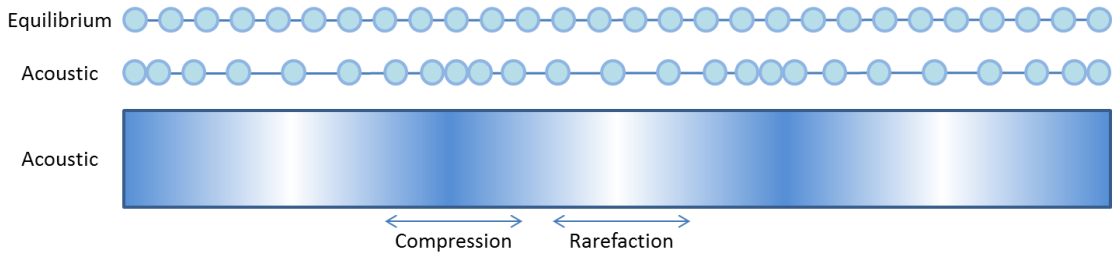

Figure 2.1 Compression and rarefaction waves graphic representation [adapted from 2].

The frequency represents the number of oscillations (one cycle of compression and rarefaction) per second and is measured in Hertz (Hz) which is the number of cycles per second; the relationship between frequency and oscillation is defined by equation 2.1:

Equation 2.1 $$f = {}^{1}/_{T}$$

where f is frequency and T is period (time required to complete a full cycle).

The acoustic intensity is the ratio between wave's power and the surface covered by the sound wave, its unit of measurement is the decibel.

The wavelength is the space covered by a sound wave during a complete oscillation and is related to frequency by equation 2.2:

Equation 2.2 $$\lambda = c \cdot T = c/f$$

where λ is wavelength and c is the speed of the sound.

The velocity at which the sound is propagated depends on the density and the elasticity of the medium; the velocity is directly proportional to the elasticity of the medium and inversely proportional to the density of the medium; this relationship is described by equation 2.3:

Equation 2.3 $$c = k \sqrt{E/\rho}$$

where c is the speed of the sound in the specific medium, k is a constant, E is Young's elastic modulus ($N\ m^{-2}$) and ρ is medium density ($kg\ m^{-3}$).

Since the human ear is able to hear sounds of frequency from about 20 Hz to 20 kHz, ultrasound may be defined as sounds of particular frequencies above the acoustic range. As demonstrated in figure 2.2, ultrasound is suitable for a number of different uses at distinct frequencies: high frequency – low power for non destructive testing (NDE) and

medical imaging for diagnostic (2-25 MHz); low frequency – high power for sonochemistry in terms of synthesis and catalysis within chemical reactions and for cavitational studies (20-100 kHz); medium frequency for medical and destructive purposes in water and sewage treatment (300-1000 kHz) [3; 4-8].

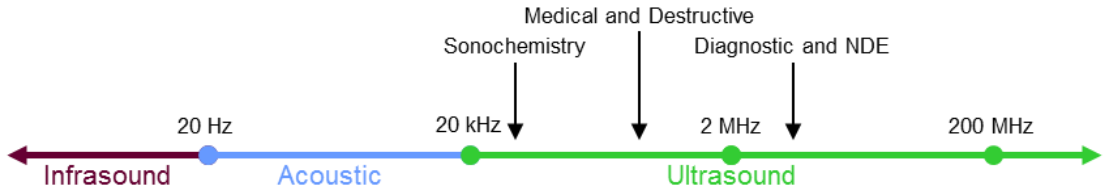

Figure 2.2 Sound and ultrasound range diagram.

Ultrasound is also widely used in industry and in engineering processes. One of the most common applications is the use of ultrasound for cleaning and decontaminating purposes, this can be from small objects, such as surgical and dental instruments or analytical equipments, through to very large items, such as engine blocks in factories [8; 9]. Other industrial applications include the welding of metals or thermoplastic articles, the cutting of materials, and atomization of samples [8]. Important uses are also found in the pharmaceutical and food industries where ultrasound is utilised for sterilisation, mixing, emulsification, extraction, microencapsulation, and crystallisation purposes [7; 10].

2.1.2 Generation of ultrasound

Ultrasound can be produced by an electronic generator which transforms normal alternating current (AC – a/c) line power to a 1000 V and 20 kHz signal that drives a piezoelectric convertor/transducer [11]. A material is defined as piezoelectric if it shows electrical charge when subjected to mechanical stress (direct effect) or if it deforms its shape under an electric field (indirect effect). The transducer converts the electrical signal into a mechanical vibration of the particles in the medium creating the ultrasound [3; 8; 12].

Another way to produce ultrasound is via the use of magnetic transducers; a variable magnetic field is applied to particular materials, such as nickel or iron-cobalt alloys, which deform their shapes accordingly with the frequency of the applied field and this produces the longitudinal vibration of a bar thus generating the ultrasonic waves [3; 8].

The literature reports also the presence of mechanical generators such as Galton and Hartmann whistles (figure 2.3a); this rationale is based upon air jets that induce cavity resonance, by the movement of the internal piston, and thus ultrasound [3; 13; 14], or more recently liquid whistles (figure 2.3b). This last category is used for homogenisation or mixing processes. A fluid jet is generated by a pump which forces the heterogeneous mixture through an orifice. This jet collides with steel blades producing a vibration that leads to the mixing of the medium [3; 8].

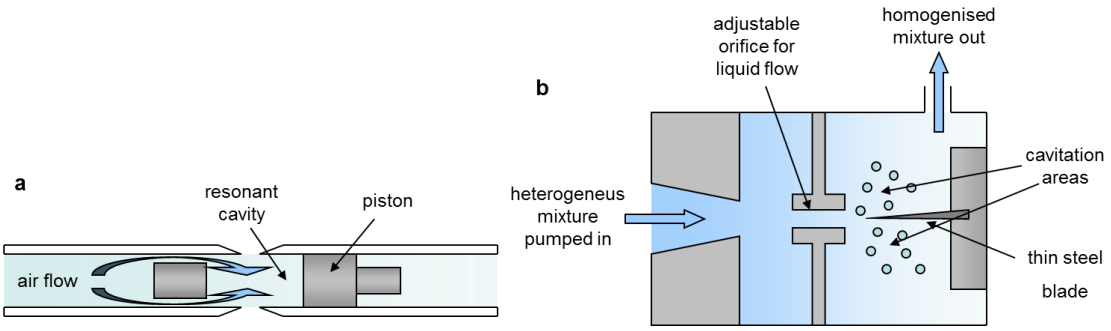

Figure 2.3 Examples of Galton (a) and liquid (b) whistles [adapted from 3].

When the generation of ultrasound, through one of these processes, is applied to a horn or a probe inserted in a fluid, the resulting phenomenon is known as sonication, which is defined as the use of acoustic energy to produce physical and/or chemical changes in fluids. In sonication the transducer amplifies and transmits the mechanical vibration to the tip of the horn or probe which expands and contracts itself in a longitudinal way and causes the cavitation phenomenon [12].

Cavitation phenomena can be generated in different ways and are classified as: acoustic cavitation when the driving force is the acoustic field obtained with ultrasound as described above; hydrodynamic cavitation is induced when the liquid medium is forced through orifices at different speed to generate kinetic energy and pressure variation

(Venturi's effect) - the obtained conditions are similar to acoustic cavitation but the energy requirements are lower; optic cavitation induced by a laser; particle cavitation in which elementary particles, such as neutron beams, can induce the formation of micro-bubbles (bubble chambers phenomenon). Nevertheless only acoustic and hydrodynamic cavitations are able to induce the necessary conditions, in terms of high temperature and pressure, to drive physical changes and chemical reactions [10; 15; 16].

2.1.3 Acoustic cavitation

Liquid ultrasonic irradiation is useful for many chemical reactions at high energy through cavitation, a physical phenomenon which involves the formation, growth and collapse of micro-bubbles. This phenomenon generates very extreme temperatures (1000-5000 K) and pressures (200-5000 atm) for a very short time (<10 ms) at millions of localised places simultaneously, defined as "Hot Spots" [3; 4; 10; 15; 17]. These high temperatures catalyse chemical reactions and radical formation, whereas the strong shear gradient is responsible for the mechanical effects induced by cavitation [18].

Acoustic cavitation is a three step process and occurs when the cycles of rarefaction of the ultrasound generate a negative pressure which exceeds the tensile strength of the liquid (the point at which the medium is no more able to counteract the applied force, in this case the rarefaction waves) causing molecular breakaway to form cavities made of vapour and micro-bubbles filled with gas [4; 19]. This phenomenon, which represents the first step of the process, is known as nucleation. Nucleation can be defined as homogeneous when it is caused by momentary micro-voids within the liquid due to the liquid particles motion following temperature variations; or heterogeneous when it takes place at pre-existing weak points of the liquid, such as the interface between the liquid and the wall of the reactor, small contaminant particles (impurities) suspended within the liquid, or micro-bubbles of contaminant gas [20]. Once formed, the micro-bubbles continue to absorb energy and interchanges of gas takes place between the micro-bubbles and the surrounding liquid so that they grow, under the action of the

rarefaction waves, till they reach the maximum volume allowed (figure 2.4). The phenomenon which regulates these gas interchanges is called rectified diffusion; during rarefaction the pressure outside the micro-bubble is higher than at equilibrium causing the gas to diffuse into the micro-bubble expanding its surface area, during compression the phenomenon is reversed causing the gas to diffuse out of the micro-bubble, at the next rarefaction the amount of gas which can diffuse into the micro-bubble is higher due to the larger surface area generated during the previous cycle thus leading to a greater expansion of the micro-bubble [3]. The speed of this step depends on the intensity of the sound waves applied to the liquid - with high power (low frequency) ultrasound the growth rate of the cavity is faster (*transient cavitation*), whereas with lower power (high frequency) ultrasound many more acoustic cycles are needed (*stable cavitation*).

During *transient cavitation*, when the micro-bubbles reach the maximum volume in which they cannot absorb more energy and gas to sustain themselves, an implosive collapse takes place with the release of high temperatures and pressures (figure 2.4). The intensity of this release and then of the entire process depends on the size of the cavity, with bigger cavities giving rise to greater temperature and pressure releases [4; 10; 15; 19].

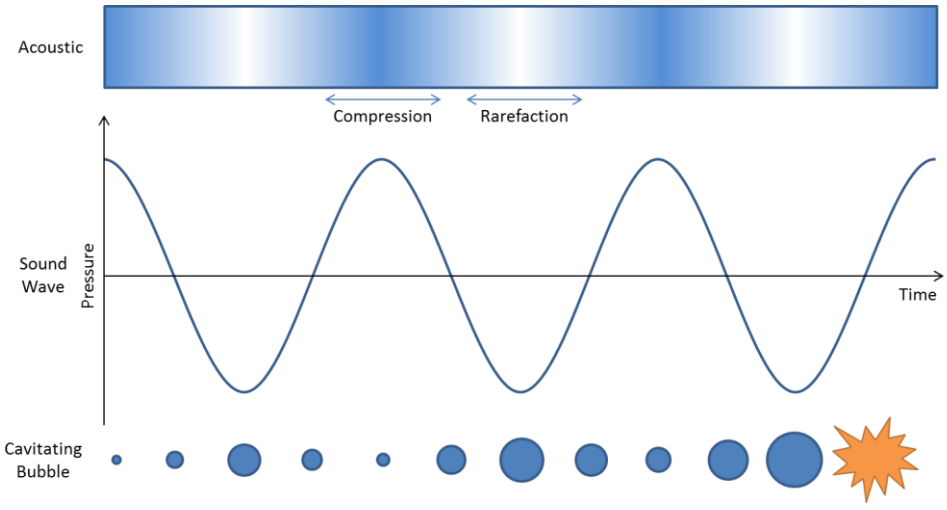

Figure 2.4 Cavitating bubbles growth and implosive collapse [adapted from 18].

Stable cavitation takes place when the energy of the acoustic field is not sufficient to induce micro-bubbles' collapse. The micro-bubbles undergo thousands of cycles of oscillation without reaching the maximum size thus not leading to high energy release. At the same time the micro-bubbles' vibration causes formation of local turbulences with the formation of micro-currents into the surrounding liquid, a phenomenon generally known as micro-streaming. Energy release of this kind of cavitation gives rise to effects which are typically smaller than the effects of transient cavitation [10; 15; 19].

In addition to frequency, other factors can influence cavitation intensity. One factor is the ambient operational temperature; higher temperatures are characterised by high vapour pressure which decreases the tensile strength leading to a faster production of the micro-bubbles, although the released energy during the collapse is of lower intensity. Viscosity is another factor which affects cavitation intensity; when the viscosity of the liquid medium is high, ultrasonic waves cannot penetrate it thus decreasing the efficiency of the phenomenon [3]. Surface tension and density of the liquid have, also, been found to attenuate the effects of cavitation in a similar way to viscosity [21]. The solution to all these problems, and to obtain a useful intensity of cavitation, can be to use low frequencies (high power) of about 20 kHz [19].

Cavitation can affect different systems in dissimilar ways influencing chemical reactions. When ultrasound is used on homogeneous liquid phase systems – including both aqueous and non-aqueous organic solvents – the cavitational collapse leads to the formation of highly reactive free radical species (hydroxyl, hydrogen or organic radicals). These radicals – which can be formed both from molecular fragmentation, caused by the dissociation of vapours which fill the micro-bubbles, and from chemical bonds breaking, due to shear forces of the liquid filling the cavity – are responsible for the catalysing effect on chemical reactions and their propagation under ambient conditions [4; 12].

For homogeneous liquid systems, there is a strong correlation between the frequency of the ultrasound and the site of the reactions, and this influences the kind of chemical reaction that is driven by cavitation. With low frequency ultrasound, the growth of the

micro-bubble requires many cycles during which volatile solutes and solvent vapours flow into the internal gas phase, and this inhibits the mass transfer from inside to outside the micro-bubble, allowing chemical reactions to take place within the micro-bubbles or at the interface between the micro-bubble and the surrounding liquid (figure 2.5). This process primarily affects hydrophobic solutes. When using medium frequency ultrasound, the growing and the collapse of the micro-bubbles is very rapid leading to a high energy release in the surrounding liquid which catalyses oxidation processes in the solution bulk (figure 2.5) [4].

Ultrasound on liquid-liquid heterogeneous systems, such as oil/water systems, increases the interface between them causing higher reaction rates and thus promoting the emulsification of non-miscible liquids; this emulsion is more stable and requires less or no surfactant in comparison to conventional techniques (figure 2.5) [15; 17; 22].

In heterogeneous solid/liquid systems, ultrasound can be used for increasing the reaction surface area through the activation of solid catalysts by the high speed liquid inrush in the cavity (micro-jets) subsequent to the non-spherical collapse of the micro-bubble near the solid surface [17], and through solid's disruption due to the energy released by the collapse [4]. The micro-jets are responsible for localised erosion which is at the basis of the above mentioned changes in morphology and reactivity of the solid surface, and also of the use of ultrasound for cleaning purposes [17]. In these reactions, cavitation intensity must be controlled so as to not detrimentally affect the thermodynamic of the reaction itself [15].

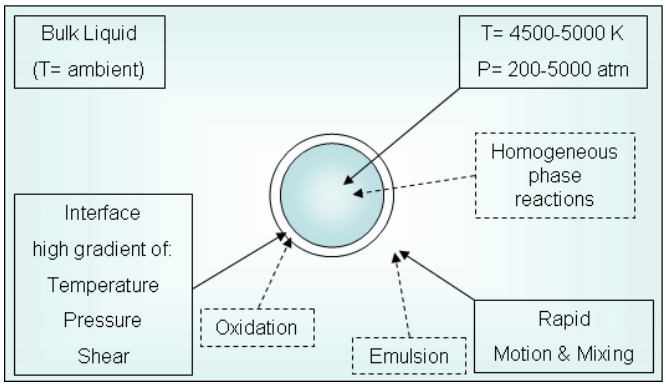

Figure 2.5 Cavitation phenomenon and possible sites for chemical reactions in the surrounding of a cavitating bubble [adapted from 4 and 22].

2.1.4 Reactor optimisation

Two strategies are generally accepted for maximising reaction efficiency. The first strategy is the optimisation of power and reactor configuration. The first step is selecting the most appropriate transducer, between piezoelectric and magnetic materials, for a particular application. Piezoelectric transducers are the most widely used because they allow the production of the whole range of ultrasound frequencies, although magnetic materials are still used - and research in this context for improving the efficiency for both is on-going [8]. The second choice is between probe or plate type generators matching the volume and the viscosity of the medium by enhancing the efficiency of the power delivered. This can be achieved by choosing probe type generators when in presence of low reaction volume, since a smaller tip delivers high intensity but low frequency ultrasound within small area; or choosing plate type generators which are characterised by lower intensity but high frequency ultrasound, when in presence of larger reaction volume [4]. As cavitation intensity diminishes while increasing the distance from the horn [21], another solution is the use of multiple transducers, and in this case the optimal conditions, in term of intensity and frequency of irradiation, can be reached by changing and improving the geometrical arrangements of the transducers [10].

The second strategy is to enhance the cavitation for increasing reaction yields or rates, and this could be done, for example, by adding a soluble gas to the solution during all the sonication period thus providing an excess of cavitation nuclei that speed up the start of the process [4]. Other parameters to be considered to enhance the cavitation, which are interrelated with the reactor configuration, are the maximal size of the cavity achieved before the collapse which influences the intensity of the process, and the life of the cavity which determines the areas of the reactor in which the cavitation phenomenon takes place. Maximising these parameters is possible through an adequate reactor design [15].

2.1.5 Ultrasound application

One important application of ultrasound is within the field of polymer materials chemistry. Studies are on-going in both polymer synthesis and polymer degradation, and the latter is of particular interest [18]. This degradation is a result of a physical-mechanical cleavage at pre-existing weak points of the chain; as it is shown in figure 2.6 the coiled polymeric chain is stretched under the shear gradient induced by the micro-bubbles growth, when the micro-bubble collapses the shear is sufficient to cleave the intra-molecular bonds mainly near the middle of the chain; this is in contrast to thermal degradation processes which cause cleavage at random points of the chain [17; 18; 22; 23]. The effect is irreversible and the new formed smaller chains are characterised by a Gaussian distribution of molecular weights. The speed of the process is influenced by the chain length, with ultrasonic degradation being faster for polymers with high molecular weights and tending to a limit under which the degradation does not occur; this is most efficient with high intensity ultrasound [17; 22; 23]. These chains are moreover highly reactive and can undergo intra- and inter- molecular rearrangements, with this last feature being utilised for ultrasound driven polymer and copolymer synthesis. This allows a great level of control on the properties of the resulting polymers in terms of molecular weight and polydispersity, which is a measure of the distribution of the molecular weight in the polymer sample [18; 22; 23].

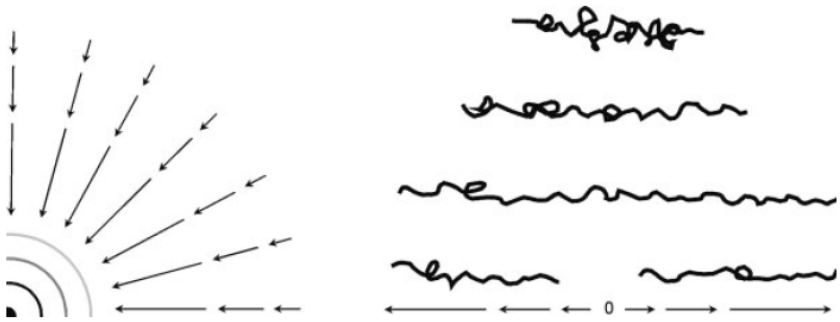

Figure 2.6 Collapsing bubble's shear gradient (left) and its action on polymeric chains (right) [18].

The reactivity of the chains is due to the formation of radical species, the nature of which was first described by Rice [24] in his work on hydrocarbons pyrolysis, and then further investigated, using ultrasound, by Suslick [25] and Gopinath [12]. According to these works the treatment of alkane species of different nature with ultrasound leads to the formation of free radicals by C-C bond cleavage which, during the propagation phase, may react with other hydrocarbons to give other primary radicals, or react with hydrogen atoms leading to the formation of hydrogen radical and alkenes, or decompose to give smaller compound with or without internal radical (secondary radicals); when two radicals collide (alkyl-alkyl, alkyl-hydrogen, hydrogen-hydrogen) the termination phase occurs (figure 2.7). This mechanism of radical formation, propagation and termination is generally defined as the *Rice Radical Chain Mechanism* [12; 25].

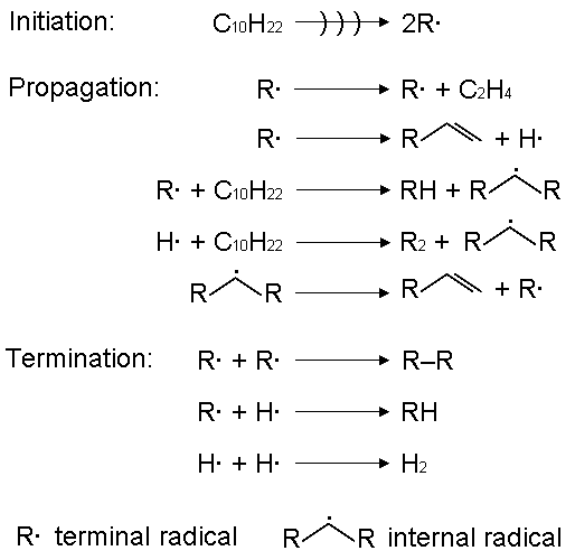

Figure 2.7 Example of the mechanism of radical formation and reactions after ultrasound treatment of *n*-decane based upon the *Rice Radical Chain Mechanism* [25].

This mechanism applies also to the polymeric cleavage driven by the shear gradient produced by the micro-bubbles collapse; in this case the scission of each polymeric chain produces two smaller highly reactive radical polymeric chains which can then react and terminate, by recombination or disproportionation, leading to the formation of new polymeric chains (figure 2.8) [26].

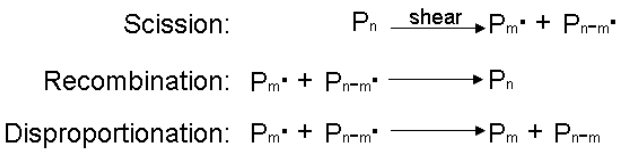

Figure 2.8 Examples of polymeric scission and termination by means of shear gradient [26].

A very interesting example of the use of ultrasound for the degradation of polymeric-like chains is the hydrolysis of vegetable oils to obtain free fatty acids and glycerol [27]. Pandit and Joshi, in their work, were among the first in testing the ability of cavitation to drive such degradation without the addition of any chemicals and at room temperature and pressure, in contrast to the stringent conditions generally required by organic reactions like hydrolysis [27].

2.1.6 Saponification reaction

As stated before, ultrasound is widely used to facilitate organic chemistry reactions; an example is the saponification reaction. Saponification (literally soap-making) is the alkaline hydrolysis of triacylglycerols (from fats or oils) which produce glycerol and the salts of the carboxylic acids, called soaps (figure 2.9). The hydrolysis of the fats/oils is typically conducted in a water bath with the addition of an alkaline solution (sodium or potassium hydroxide in water). The reaction requires heating up to 100°C and stirring; when the reaction is complete the soap can be separated and purified through several precipitation steps by adding sodium chloride. Glycerol is the by-product of the reaction and is recovered from the aqueous phase by distillation [28; 29].

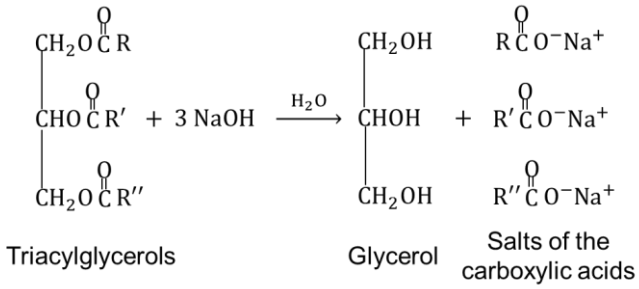

Figure 2.9 Alkaline hydrolysis of triacylglycerols [28].

The soaps thus obtained have a non-polar (hydrophobic) alkyl chain and a polar (hydrophilic) carboxylate group; when in water they form micelles with the sodium/potassium ions dispersed in the aqueous phase. The micelles are thus negatively charged and repel each other. The structure of the soaps and their chemical behaviour is the basis of their effectiveness as "cleaning agents"; the alkyl chains can penetrate the fat/oil layer which surrounds the dirt, thus generating micelle-like aggregates which can be dispersed in the polar aqueous phase (figure 2.10).

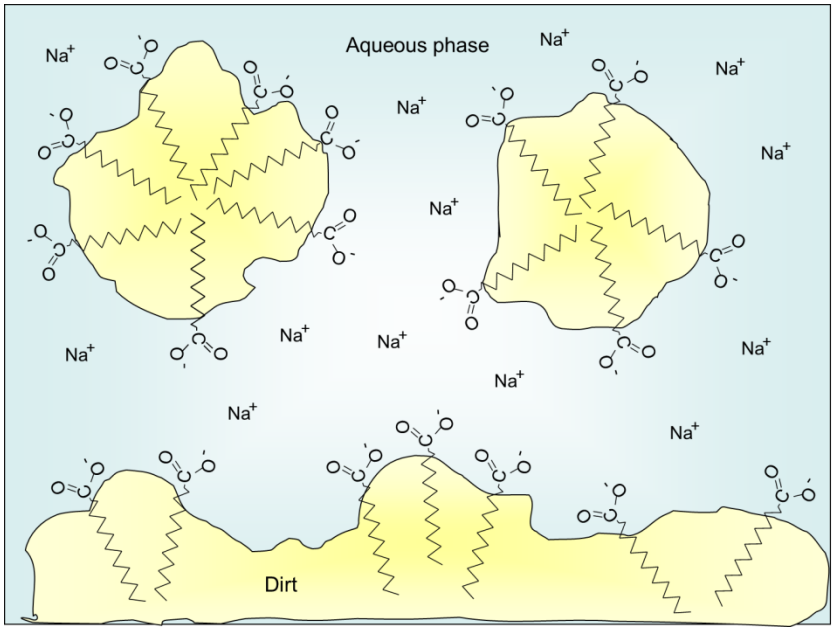

Figure 2.10 Soap micelles and their action on dirt particles [28].

The efficiency of the ultrasound in assisting the saponification of various substrates has been studied in the last few years by several groups (table 2.1). The work of Moon *et al*. [30] was one of the earliest in investigating the ultrasound assisted saponification reaction of some chemical compounds, such as methyl benzoate. This, along with another similar work performed on wool grease [31; 32], highlighted the feasibility of the process. Other later works used vegetable oils as substrates for the saponification reaction in conjunction with ultrasound; the reaction in these studies was catalysed by phase transfer catalysts (PTC), ionic compounds bearing alkyl chains which favour the transport of the salts into the organic phase thus facilitating the mixing of the reactant. When PTCs are used in conjunction with ultrasound, the levels of saponification achieved are comparable to those achieved with the traditional thermal reaction while lowering the temperature and thus the energy required for the reaction. The main works in this area are those of Samant *et al*. [33] who achieved a final yield of 97%, and of Entezari *et al*. [34] who achieved a final yield of 94%. In the first work the reaction was performed on sunflower oil samples in the presence of cetyl trimethyl ammonium bromide (CTAB) as a phase transfer catalyst under sonication (35±3 kHz) and stirring with a temperature of 35±2°C and a reaction time of 180 minutes [33]. The second work was performed on several oils obtaining the maximum reaction yield on a sample of castor oil sonicated with a horn sonicator (20 kHz) for 12 minutes at 60°C using CTAB

as the phase transfer catalyst [34]. Other studies concentrate on the application of ultrasound to the enzyme-catalysed saponification reaction of soy oil. These studies coupled the sonic power to heating (up to 55°C) for reaction times comprised between 1 and 5 hours obtaining good yields, while still requiring further purification steps [35; 36].

The similar transesterification reaction, where alkali catalyses the reaction of the triglycerides with methanol, has been also investigated with ultrasound. A typical work in this area combined NaOH catalysis with a methanol/hexane extraction in the presence of ultrasound obtaining reaction yield which doubled those obtained without ultrasound [37]. A similar reaction was performed on rice bran while coupling ultrasound with heating up to 60°C obtaining 80% yield in 4 hours of reaction [38]. A two-step acid and then based catalysed transesterification of *Jatropha curcas L* oil was also studied in the presence of ultrasound yielding 96% of free fatty acids [39]. Finally a recent work [40] has investigated the ultrasonic assisted transesterification of waste palm oil with ethanol/sulphuric acid at 60°C, yielding 97.3% of free fatty acids in 45 minutes of reaction time.

However, in all the mentioned saponification or transesterification reactions, excess of either alkali or methanol was required and also extra chemicals and/or further heating for product purification would be needed. As such the energy required to drive these reactions, which use ultrasound, heating and, in some cases, stirring, is still quite high; therefore it might be worthwhile investigate new processes to further improving the energy efficiency of these reactions.

Table 2.1 Comparative summary of previous works on saponification reaction. Yield values are reported as found in the literature; white cells are left for data not discussed/available. RT= room temperature.

Method	Heat	Ultrasound	Stirring	Alkali	Other chemicals	Reaction time	Purification steps	Substrate	Yield
Traditional [28; 29]	100°C	No	Yes	KOH	For purification	1-4 h	Sodium chloride	Fats/oils	100%
Moon (1979) [30]		Bath 20 kHz		NaOH (20%)		10 min		Methyl benzoate	98%
Davidson (1987) [31; 32]	60°C	Bath or Homogeniser (whistle)			PTC	Fast	Liquid extraction (70°C)	Wool grease	
Samant (1998) [33]	35°C	Bath 35 kHz - 120 W	Yes	KOH	PTC	180 min	Yes	Sunflower oil	97%
Entezari (2001) [34]	60°C	Probe 20 kHz - 39 W	No	KOH	PTC	12 min	Yes	Castor oil	94%
Siatis (2006) [37]	RT	Bath 35 kHz		NaOH/ methanol		30 min	Methanol/hexane extraction	Oil-bearing seeds	85-93%
Liu (2008) [35]	55°C	Bath 28 kHz - 1.20 W cm^{-2}		No	Lipase 1% Buffer pH 7.7	5 h	Ether-ethanol	Soy oil	60 Acid Value
Yustianingsih (2009) [38]	60°C	Bath 35 kHz - 500 W	Yes	No	Methanol Sulphuric acid	4 h	n-hexane extraction, acidification	Rice bran	80%
Deng (2010) [39]	60°C	Bath 210 W	Yes	Two steps: Acid - Base	Methanol	1.5 h	Yes	*Jatropha curcas* oil	96.4%
Huang (2010) [36]	45°C	1.64 W cm^{-2}		No	Lipase 3 mg/ml Buffer pH 7.7	60 min	Ether-ethanol	Soy oil	1.3 mol/m^3
Lima (2012) [40]	60°C	42 kHz - 160 W (80%)		No	Ethanol Sulphuric acid	45 min	Water 50°C Drying 110°C	Waste palm oil	97.3%

2.2 Fuels and combustion

The word fuel commonly defines a wide range of substances used to provide heat or power usually by being burned. The first major distinction for fuels is between conventional and alternative fuels. Conventional fuels include natural gas, petroleum products, and coal, while alternative fuels are those derived from biomasses and hydrogen. Differences between these two categories arise not only from the properties of the source materials, but also from the manufacturing processes. All the fuels can be then classified according to their physical state as: gaseous, liquid, and solid fuels.

2.2.1 Conventional fuels processing

The major constituents of conventional fuels are hydrocarbons with a relative concentration of 83-87% C and 11-13% H, plus traces of sulphur, oxygen, and nitric compounds. These hydrocarbons can be in the form of long saturated aliphatic chains (paraffinic), cyclic saturated chains (naphthenic) or aromatics like benzene and its homologues [41]. The nomenclature and general molecular formula of the main hydrocarbons involved in the processing of conventional fuels are listed in table 2.2; the common names which are in use in the fuel technology sector are also reported here.

Table 2.2 Nomenclature and general molecular formula of the main hydrocarbon series in fuel technology [adapted from 41].

Series Name			Description	General Molecular Formula
Overall	**Organic Chemistry**	**Fuel Technology**		
Aliphatic	Alkanes	Paraffins	Open-chain saturated (C-C)	C_nH_{2n+2}
	Alkenes	Olefins	Open-chain unsaturated (C=C)	C_nH_{2n}
	Alkynes	Acetylenes	Open-chain unsaturated (C≡C)	C_nH_{2n-2}
Carbocyclic – Alycyclic	Cycloalkanes	Naphthenes or Cycloparaffins	Closed-chain saturated	$(CH_2)_n$
Carbocyclic – Aromatics	Aromatics	Aromatics	Closed-chain resonance	
			Monocyclic	C_nH_{2n-6}
			Polycyclic	C_nH_{2n-12}

2.2.1a Solid fuels

Natural solid fuels are mainly derived from vegetable substrates through a process of carbonization, also known as coking or coalification. This process consists of an anaerobic decomposition of the vegetable mass which, progressively, loses its humidity while becoming enriched in carbon. The solid fossil fuel is naturally produced over geological era, but the same effects can be reproduced with a combination of high temperature and pressure with the aid of anaerobic bacteria which start the process.

According to the degree of carbonization, from the vegetable source to the last level of coal, the solid fuels can be classified into the following: *1)* wood is the fresh vegetable source, is characterised by a high content of water (50%) which decrease to 15% when dried, and is mainly constituted of cellulose and lignin; *2)* peat is the first level of coalification, it retains most of the characteristics of the vegetable source and, when burned, produces a high level of ashes; *3)* lignite is the result of a more in-depth

coalification process than peat, it tends to exfoliate when dry so it is generally shaped in the form of small bricks; *4)* sub-bituminous coal is a very hard and compact material, the fibrous structure is no longer visible, it has a low humidity and, when burned, generates very few ashes; *5)* anthracite is the last step of the conversion process, it has a graphite-like appearance, its ignition is very difficult and is mainly used in industrial furnaces [41]. The term charcoal mainly identifies a kind of coal which was historically produced from the slow pyrolysis of vegetable material in purposefully built log chimneys; the properties and purity of this coal vary according to the characteristics of starting material. When burned, charcoal generates a high level of ashes.

The main component of artificial solid fuels is coke. This material is obtained from the dry distillation (temperature between 1000-1200°C and absence of air) of coal or from the crude oil processing; other products of this process are bitumen and some gases which need to be further purified to be used as energy sources.

All solid fuels benefit from low cost due to the relatively high availability and ease of production, but their combustion efficiency is low with the formation of high levels of ash, so that their impact on the environment is very high. These fuels are mainly used in the metallurgical industries [41].

2.2.1b Liquid fuels

The vast majority of conventional liquid fuels are petroleum products derived by the processing of crude oil. The crude oil refining process involves an initial first step of physical settling to separate the oil from the sludge. The oil is then heated in a furnace and enters the fractionating tower where the constituents of the oil separate according to their boiling point.

The fractionating tower is a heated column constituted of around forty fractionating trays; the temperature decreases from the bottom to the top of the column allowing the formation of an upward mobility vapour stream. The volatile components move to the

top of the column, while the non-volatile remain on the bottom. The fractionating trays are designed so as to allow the passage of the vapour stream towards the top, but they also redirect the condensed fraction to the lower tray forming a downwards liquid stream, hence the name continuous distillation (figure 2.11). A full-load sensor monitors the conditions of the tray, so that the liquid fraction can be extracted from the column to avoid overloads. The main fractions separated from the top to the bottom of the column are: petroleum gases, kerosene, gas oil, heavy gas oil, and non-boiling residues such as bitumen [41].

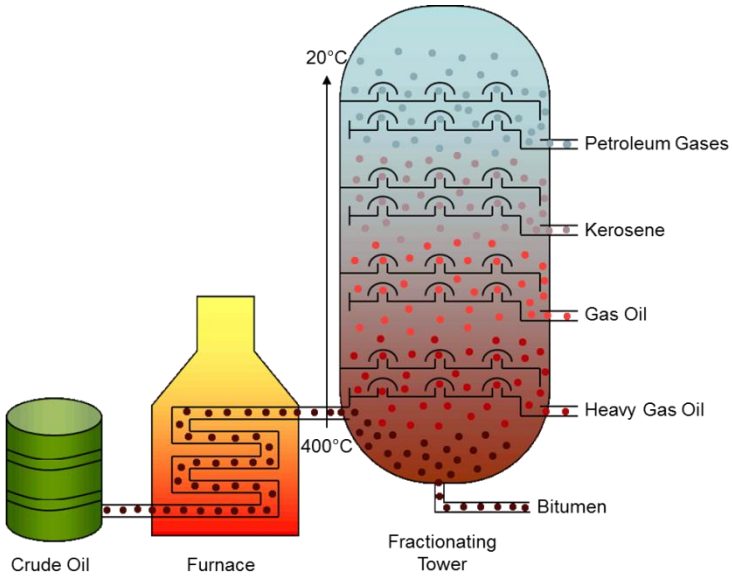

Figure 2.11 Fractionating tower and main fractions separated.

The gaseous products undergo a stabilisation step and then the propane fraction is purified to a very high standard and liquefied to obtain Liquefied Petroleum Gas (LPG); the gas is cleaned from heavier hydrocarbons, H_2S, and CO_2, compressed and cooled to below its dew point to attain the liquefaction of the gas. All the other gaseous fractions are then converted to gasoline through different processes; the aim is to increase the production of gasoline as it is the most required fuel for the transport sector. The target of these processes is the production of gasoline with a high octane number which positively influences its combustion efficiency. The butane fraction is subject to alkylation with olefins to give highly branched iso-paraffins which will constitute gasoline with a high octane number. The naphthenic fraction (C_6-C_{10}) undergo the catalytic reforming in order to obtain branched or aromatic products; this step is

performed at 500°C and at a pressure between 15-40 atm, while the catalyst is Pt on Al_2O_3 (platinum on alumina). Other processes are polymerisation of olefins and the lighter fractions to give gasoline, and isomerisation of paraffins into branched products which are used in gasoline blending [41].

The kerosene and the gas oil fractions are hydrotreated to lower the sulphur content. Hydrotreatment is performed with the aid of catalysts such as cobalt/molybdenum or nickel/molybdenum on heated alumina base. The process effectively removes about 90% of the sulphur; the main drawback is that sulphur acts as a natural antioxidant and lubricant, so additives must be added after the treatment. The main use of kerosene is fuel for the air transport sector, while treated gas oil constitutes diesel fuel for the road transport sector.

From the heavy gas oil fraction are derived a number of products such as lubricant oils, gasoline, and coke. One of the main treatments performed on the heavy gas oil fraction is thermal cracking which occurs at temperatures between 400-500°C; the aim is to break the long chains of heavy gas oils in order to obtain lighter products. The catalytic cracking works at lower temperatures, but in the presence of a catalyst such as silica or alumina, the resulting product has a high level of aromatics and is utilised in gasoline blending. Hydrocracking is performed in the presence of hydrogen and of catalysts (sulphur and oxides on silica); this process gives a higher yield of paraffins and monocyclic aromatics which will be the major constituent of gasoline. The residual fuels of the heavy gas oil fraction are converted into distillates through visbreaking, which is a less severe form of thermal cracking to lower the viscosity and pour point. Coking is the process performed on the non-boiling residues; it is a severe form of thermal cracking with temperatures of about 650°C, with products including olefinic distillates and coke as mentioned in the artificial solid fuels section (section 2.2.1a) [41].

Other processes are then required before it is possible to commercialise the petroleum products; some are: deodorising, cleansing, stabilisation, blending, addition of detergents for the fuels designed for the transport sector.

Some of the characteristics of the liquid fossil fuels obtained after refining of crude oil are listed in table 2.3. The products are listed as they exit the fractionating tower, as can be seen the volatility increases for products with a low number of carbons, while the presence of aromatic compounds is major for products with a high number of carbons. The more volatile compounds have higher calorific values, while the density increases with the number of carbons.

Table 2.3 Characteristics of liquid fossil fuels obtained after refining of crude oil.

	N° of C	**N° of H**	**Aromatics**	**Volatiles**	**Calorific Value**	**Density (kg/L)**
LPG	C_1-C_4	↑	↓	↑	↑	
Gasoline	C_5-C_9					0.72-0.75
Kerosene	C_{10}-C_{13}					0.80
Gas oil	C_{12}-C_{20}					0.84
Fuel oil	C_{14}-C_{30}					0.95-0.97

Liquid fossil fuels have high combustion efficiency; they are in general easy to store and transport, and their impact on the environment is variable from the low impact of LPG to the higher impact of fuel oil [41].

2.2.1c Gaseous fuels

The main distinction for gaseous fuels is between those whose origin is from fossil natural materials, and those which are processed by-products of solid or liquid raw materials. To the first class belong: *1)* natural gas, mainly methane and traces of ethane, propane, nitric and sulphur compounds; *2)* petroleum gases, mainly propane and butane with traces of ethane. To the second class belong gases from coal or biomasses, and water gas.

Natural gas is extracted from geological deposits and its purity depends on the geographical location of the reservoir. After the extraction methane is purified

remaining occasional water, which might be present in the reservoir, and condensable hydrocarbons. It is widely used as heating source, in the chemical industry, and in the transport sector. Recent developments in the anaerobic fermentation field made it possible to increase the production of natural gas. Therefore it became a renewable energy source; as fuel the natural gas gives lower emission than petroleum products, however its efficiency in automotive applications is lower than that of gasoline [41].

As previously described, the refining process of crude oil allows the separation of volatile products of which LPG is the most purified; other less purified gaseous fractions are obtained from fuel cracking and reforming; these fractions contain methane, carbon dioxide, hydrogen, and traces of olefins and nitric compounds. LPG can also be obtained from biogas produced during the processing of solid waste. The efficiency of LPG as fuel is comparable to that of gasoline with the advantage of being less polluting and giving lower emission of carbon dioxide.

The gaseous products obtained from the gasification of solid fuels, such as coal or biomasses, contains 20-30% CO, 10-20% H_2, 3-10% CO_2, and 45-55% N_2. A fraction of the energy originally contained in the starting material is lost during the gasification process, so that these fuels can not be used in the automotive sector, but are mainly employed for industrial processes [41].

Water gas derives from the combustion of natural fuels with water vapour; possible products of this process are methanol, liquid hydrocarbons, carbon dioxide, and hydrogen. Variability on the products depends on the chosen substrate fuel, while the general reaction is reported in equation 2.4.

Equation 2.4 $$H_2O + C \rightarrow CO + H_2$$

Some of the advantages of gaseous fuels include: high combustion efficiency, high stability which influences their storage and transport, and low level of contaminants which lowers their impact on the environment. Some disadvantages include them being high flammable and the high costs associate to constructing and maintaining pipelines.

2.2.2 Alternative fuels

During the last two centuries the development of the industrial and transport sectors have led to an increase on the demand of energy, particularly in the form of coke at the beginning, and petroleum products at a later stage, in order to fulfil the demands of the fast-growing modern world. The constant increasing consumption of the conventional energy sources has equally caused a decrease in the reserves of these materials, so that it has become necessary to develop alternative energy sources. For the transport sector, which is one of the most affected, the main alternative or substitute fuels developed and under development are: oxygenate compounds; hydrogen, and biofuels [41].

The term oxygenate compounds refers to alcohols and ethers. Methanol can be produced from the destructive distillation of wood, or through a synthetic process which can use natural gas, biomatter, residual fuel oil, coal. The gasification of black-liquor to obtain methanol is also possible, but the black-liquor is of most use in the process for the production of pulp and paper [42]. The main drawback of methanol is its corrosiveness to metal and some plastics. Ethanol can be derived from petroleum products, but its main attractiveness as an alternative fuel arise from the possibility to obtain it from yeast-mediated fermentation of carbohydrates contained in any organic matter with a high content of simple or complex sugars, such as starch and cellulose contained in vegetables and plants [41; 42]. Ethers can be derived from gasoline or from methanol or ethanol to give tertiary amylmethylether, butylmethylether and butylethylether respectively, which are the main ethers of interest as engine fuels.

Hydrogen has been mentioned in section 2.2.1c as a possible product of the production of water gas. Advantages of hydrogen as a fuel are its abundance in the environment, its high energy, and its clean combustion. Main products of combustion are water vapour and NO_x [41]. Hydrogen can be produced through water electrolysis, but the process is inefficient as more energy is required to drive the process than the final energy obtained from the produced hydrogen. Other cheaper ways to produce hydrogen involve a series of reaction which start from methane or carbon to give hydrogen and carbon di- and/or mono- oxide as by-product; these reactions are similar to the general reaction reported

in equation 2.4. Microorganisms may be also used to produce hydrogen; cyanobacteria use their photosynthetic process to decompose water, while anaerobic bacteria can convert organic substrates into hydrogen as a result of their metabolic processes [42]. Disadvantages of hydrogen as a fuel are the generally high costs associated with its production, the fact it has to be stored and maintained at -253°C under pressure, and the safety issues related to its handling [41].

The term biofuels comprises all the products generated from the physical and chemical processing of biomatter, such as woods, vegetables substrates from crops, vegetable oils, solid municipal waste and sewage sludge. As mentioned in section 2.2.1a woods can undergo incomplete combustion or carbonization to give charcoal with a high specific energy. As an alternative, the cellulose of woods and other vegetable substrates can be hydrolysed to obtain sugars which can then be converted to bio-ethanol through fermentation, or bio-methanol through anaerobic digestion. Application of pyrolysis or gasification to these vegetable substrates allows the conversion of the solid matter to gaseous fuels. The pyrolysis and gasification processes mainly differ in the source of heat, external and internal with limited air respectively. A very interesting source of biomatter to be converted into biofuels using these processes is salt-water algae. Advantages of algae are that irrigation is obviously not required, and more important that no land, currently used for the production of food, has to be devoted to the production of biofuels, which is a major issue when considering the economic aspects in the development of biofuels. For the production of biofuels from solid waste and sewage sludge a first step is the shredding and sorting of the waste, which can be then further processed with one of the following techniques: pyrolysis, treatment with carbon monoxide and water, anaerobic digestion, or yeast fermentation. Through these processes the waste can be converted in methane-rich gases, ethanol, or gaseous and liquid fuels of different nature [41].

One of the most famous biofuels is biodiesel which derives from the transesterification of the triglycerides of the vegetable oil in the presence of ethanol or methanol to obtain the esterified fatty acids. The transesterification reaction may also be obtained using an enzymatic catalyst such as lipase and, while the biodiesel product is easily separated,

the catalyst is very expensive and the conventional way is preferred. The reaction converts the oil to obtain a less viscous product with a viscosity comparable to that of the common diesel fuel. For ease of understanding, a nomenclature has been adopted which refer to biodiesel and diesel/biodiesel blends as BXX, where XX represents the percentage of the volume of biodiesel in the blend; pure biodiesel is B100, B2 means that 2% of biodiesel is contained within the blend, while petroleum diesel is commonly referred as D2 diesel fuel [42].

2.2.3 Combustion reaction

Combustion is defined as an exothermic reaction which involves a combustible material and a combustive agent, typically the atmospheric oxygen, with the release of energy in the form of heat [41]. The reaction involves four main steps: the even mixing of the molecules of the combustible material with the air; a pre-combustion step, at 400-600°C, with the formation of extremely reactive species (radicals and free unstable atoms) which are responsible for the speed-up of the following steps; the real combustion where the free radicals react with the oxygen and the combustible to give complete and incomplete oxidation products and other radicals; post-flame reactions which involve the chemical recombination of the combustion-step products to give the final products of the combustion reaction, during this step part of the heat is also transferred to the exterior of the combustion chamber by the low-temperature products (smoke). The combustion reaction is defined as complete when all the oxidisable elements of the combustible material are oxidised; in table 2.4 are listed the main products found in the smoke emissions for complete and incomplete combustions.

Table 2.4 Smoke compositions after complete and incomplete combustion.

Oxidisable compounds found in the combustible material	**Smoke compositions**	
	Incomplete combustion	**Complete combustion**
C	CO_2 + CO + volatiles organic compounds	CO_2
H	$H_2O + H_2$	H_2O
S	$SO_2 + SO_3$	SO_2
N	$N_2 + NO + NO_2$	N_2

An example of a very simple complete combustion is the combustion of methane which is reported in equation 2.5. Products of this reaction are carbon dioxide, water which is usually released as water vapour, and, as the reaction is exothermic, energy in the form of heat. Another advantage of this reaction is that few if any other by-products are released, making natural gas the cleanest of the fossil fuels.

Equation 2.5 $$CH_4 + 2O_2 \rightarrow CO_2 + 2H_2O + Energy$$

A combustible material, to be of practical interest, should be easy to extract and manipulate, be free from poisonous substances, have good combustion properties, and be of relative low cost. Some of the most important parameters which define a generic combustible are: the calorific value, the theoretical and real quantity of air necessary to develop the reaction, the volume and composition of the smokes, the theoretical temperature of combustion, the ignition temperature, and the flammability limits.

The calorific value (or heating value) is the quantity of heat generated during the complete combustion of 1 kg of liquid or solid combustible or 1 m^3 of gas combustible, and it is expressed in $MJ\,kg^{-1}$ for liquids and solids and $MJ\,m^{-3}$ for gaseous combustibles. The calorific value can be expressed as higher heating value (HHV) when the water at the end of the combustion is present as vapour, so it includes the heat necessary to vaporize the water, or lower heating value (LHV) when this heat is not

included as the water is present in the liquid form. For extension it can be said that the heating value relates to the energy content of the combustible [41].

The theoretical air of combustion is the necessary volume of air which allows the complete combustion of the combustible. Air is a mixture of different gases, 78% nitrogen, 21% oxygen and 1% rare gases such as argon and carbon dioxide; their composition percentage is important for the determination of the composition of the smoke.

The term smoke indicates all the gaseous products of the combustion reaction excluding the potential suspended solid particles; the smoke obtained after water condensation is called anhydrous. The volume of the smokes is calculated from the balanced chemical reaction, considering that all the air nitrogen is found within the smoke.

The theoretical temperature of combustion, sometimes known as flame temperature, is the maximum temperature achievable if the combustion with the theoretical air is complete and all the heat generated from the process is used to heat the exhaust smokes. This temperature is practically never achieved because of the unavoidable losses of heat during the combustion, but it is important to calculate it to determine whether the combustible under analysis is useful for a particular application. The ratio between the effective temperature of combustion and the theoretical temperature of combustion is defined as the thermal efficiency of combustion.

The ignition temperature is the lowest temperature to which the combustible-combustive agent mixture must be heated in order to start the combustion reaction; the minimum and maximum percentage of the combustible in the mixture indicate the flammability limits for the reaction; outside of these values the combustion can not start and develop.

2.2.4 Combustion and emission characteristics of fuels

There are several properties which influence the combustion characteristics of fuels; some of these are specific either for diesel or gasoline fuel, while others are of general importance. The ignition delay is an important parameter for diesel engine fuels, it represents the time that elapses between the injection of the fuel in the combustion chamber and the start of the combustion; this parameter is influenced by the cetane number, the greater the cetane number of the fuel the lower the ignition delay [43; 44]. The cetane number depends on the length and saturation characteristics of the hydrocarbon chains constituting the fuel; the longer and more saturated the chains, the higher the cetane number [42]. The octane number is characteristic for gasoline fuel and represents the anti-knock properties of the fuel in the mixture with air; if the octane number is high the mixture can withstand great compression in the combustion chamber without knocking thus avoiding self-ignition prior to the controlled spark. The viscosity and density of the fuel influence the atomization characteristics of the fuel in the combustion chamber; an inefficient atomization, due to high viscosity fuel, leads to an inefficient combustion. The viscosity is also critical for the cold flow behaviour of the fuel; in particular the pour point is the lowest temperature at which flow is still visible, while the cloud point is the temperature at which there is the formation of solid particulates within the fuel (wax). These parameters should be below the freezing point of the fuel [44]. The heating value was defined in section 2.2.3; it is an important parameter in engine fuel combustion as it influences the specific fuel consumption and the attainable power and speed, being the specific fuel consumption the unit of fuel consumed per unit of power in a defined time, characteristic heating values for some fuel are reported in table 2.5. The flash point is the minimal temperature at which the vapours of a fuel ignite in the presence of a flame. This parameter greatly influences the transportation, storage, and handling of the fuel, and thus should be as high as possible. Other important parameters are the sulphur content, the carbon residues, and the ashes which influence not only the exhaust emissions after combustion, but also the formation of residues and the corrosions on engine parts [44].

Table 2.5 Lower and higher eating values for some fuels.

Fuel	Heating Value (MJ/kg)	
	Lower (LHV)	**Higher (HHV)**
Crude oil	42.7	45.5
Petroleum diesel	42.8	45.8
Low sulphur diesel	42.6	45.5
Gasoline	43.4	46.5
Methanol	20.1	22.8
Ethanol	26.9	29.8
Biodiesel	37.5	40.2
Coal	22.7	23.9

With regards to the exhaust emissions associated with the combustion of engine fuels, the main emissions are: *1)* carbon monoxide (CO) – due to incomplete combustion is a toxic gas with no odour, colour, or taste, and when the level CO is above 150-200 ppm it can cause poisoning and death; *2)* carbon dioxide (CO_2) – a naturally occurring gas linked to global warming issues, therefore every method to decrease the CO_2 emissions has environmental benefits; *3)* nitrogen oxides (NO_x) – which are indicated as all the gases containing nitrogen and oxygen, from nitric oxide to nitrates - these gases have effects both on health giving rise to respiratory problems, and on the environment as causes of ground-level ozone (also known as smog) and acid rain; *4)* sulphur oxides (SO_x) – formed from the combustion of fuel and from the heating of the lubricant oil, in conjunction with NO_x are responsible for the formation of acid rain; *5)* total unburned hydrocarbons (HC) – these can be released in the form of linear C_1-C_{22} hydrocarbons or in the form of polycyclic aromatic hydrocarbons (PAH) which are suspected to be carcinogenic; *6)* particulate matter (PM) – is a by-product of internal combustion and comprises particles of different size and complexity; the expression PM2.5 indicates particulates with a diameter equal or less than 2.5 µm, while PM10 indicates particulates with a diameter equal or less than 10 µm; these particles can lead to development of respiratory problems by accumulating in the respiratory system and can also react with NO_x or SO_x contributing to the creation of smog.

2.2.5 Combustion efficiency of biodiesel

The use of vegetable oil as a fuel dates back to the Paris Exposition of the 1900 when Rudolph Diesel used peanut oil to fuel his engine [45]. As petroleum was at the time cheaper, the use of vegetable oil as engine fuel was disregarded favouring the development of petroleum products to suit the engine requirements; since then the diesel engine and petroleum diesel fuel have developed and evolved together. During World War II vegetable oil was used again as engine fuel due to the scarcity of petroleum supplies. Recently more interest was placed on the possibility to use vegetable oil as engine fuel due to limited crude oil resources, its increase in price, and the concerns for the environment [44].

Biodiesel is a renewable and biodegradable resource, moreover it is non-toxic, free of sulphur, and oxygenated which means that the combustion of biodiesel is more efficient, complete, cleaner, and produces less white smoke when compared to the combustion of conventional diesel [42; 46-48]. The white smoke is generally produced during the cold start of the engine, before it reaches the operational temperature and it is mainly composed of water vapour and unburned hydrocarbons [41]. The combustion of B100 results in 90% decrease in the level of total unburned hydrocarbons when compared to the combustion of petroleum diesel, with particulates and carbon monoxide emissions also being greatly lowered. These effects are mainly due to the presence of oxygen in the molecular structure of the biodiesel and to the absence of aromatic compounds, which are the main reason for the formation of PM [49]. The oxygen promotes the combustion and leads to an increase in the combustion temperature which influences the NO_x emissions [43]. Different authors reported somewhat inconclusive, and sometimes contradictory, results about the emissions associated to the combustion of biodiesel, in particular with nitrogen oxides emissions. In general it can be said that NO_x emissions are increased, but this is mainly dependent on the engine and the operational conditions; these emissions are lower when the engine is operated at lower loads and speed [46; 48]. The production of NO_x can also depend on the maximum combustion temperature, and if the combustion efficiency and temperature are low the emissions are lower [43; 45]. Another parameter which can influence HC and NO_x

emissions is the degree of unsaturation; the more unsaturated fatty acids present in the biodiesel, the greater the emissions of HC and NO_x [48].

The lubricant properties of biodiesel are much better than that of petroleum diesel, so addition of lubricant additives is not necessary. Moreover biodiesel has better ignition properties than petroleum diesel, due to its fatty acid chains being longer and the cetane number higher. Other advantages of biodiesel over conventional diesel are that it is non-flammable and non-explosive with a flash point of 423 K, while petroleum diesel has a flash point of 337 K [42]. These features mean that biodiesel is easy to handle, transport and store while maintaining the same infrastructure of conventional diesel [46].

The composition in saturated fatty acids and the properties of a biodiesel vary according to type of oil used to produce the biodiesel [48]. Biodiesel with a high content of saturated fatty acids has, as mentioned, higher cetane number, and low iodine value. This last parameter is an index of the formation of deposits on the engine and the quality of lubrication; a higher iodine value means that more deposits are formed and the lubricating properties of the biodiesel are lower [47]. The high content of saturated fatty acids lowers the cold flow properties of the fuels leading to problems at the start of combustion when in use in cold climates. Moreover, as shown in table 2.4, the heating value of the methyl esters is lower than that of conventional diesel - this characteristic reflects on the specific fuel consumption during combustion, with the value being higher for biodiesel due to its lower energy content [45; 46]. This also reflects on lower engine speed and power when biodiesel is compared to conventional diesel [42].

Wear and corrosion are other issues which may be related to the use of biodiesel as an engine fuel. Some studies have shown that biodiesel has better lubricant properties in the short term, but these properties may be lost on the long term due to some auto-oxidation phenomena. The auto-oxidation is related to the content of free fatty acids. A high acid value indicates the presence of free fatty acids which are subjected to oxidation and can cause engine wear [47]. Biodiesel is also more hygroscopic than conventional diesel and thus is more prone to absorb the air humidity; the presence of

water in the fuel enhances microbial growth which, in conjunction with the auto-oxidation phenomenon, may lead to the corrosion of engine parts [50].

Some economic issues arise with the production of biodiesel: biodiesel is more expensive than conventional diesel due to the starting vegetable oil being more expensive than crude oil, with this accounting for the 80% of the total cost of production. Since 95% of the starting material is edible vegetable oil, the production of biodiesel competes with the food industry for the usage of crop land [42]. This last issue may be partially overcome by producing biodiesel from waste cooking oil (WCO), namely the oil obtained after one or more frying of foods in vegetable oil [44]. Another advantage is that WCO is cheaper than fossil fuel and has the added benefit of recycling an otherwise very polluting waste product [51; 52]. The main disadvantages related to the use of biodiesel from waste cooking oil are similar to those reported for the biodiesel produced from fresh vegetable oil, and relate in particular to the emissions and some loss of power due to the lower heating value of WCO compared to petroleum diesel [52]. Also in this case the results concerning emissions are not conclusive among the different studies. In some studies WCO was used without any further purification and was found to have similar combustion characteristics as conventional diesel, but CO, NO_x, and SO_x emissions were higher and some tar-like deposits were found after the combustion at high temperatures due to an incomplete combustion of the heavier constituents of the oil [51; 52]. Other studies produced biodiesel through the transesterification of WCO, in this case emission of NO_x and particulates were increased, while emission of CO and SO_x were lower when compared to those of petroleum diesel [53].

Although the variability in the emissions profile of biodiesel, which is mainly due to the different feedstocks, and the concerns related to its production from fresh vegetable oil, biodiesel still remains a viable alternative to petroleum diesel. Studies are on-going to improve the characteristics of biodiesel, through the use of additives to prevent and lower the emissions, and to obtain more conclusive results on its combustion properties. One of the remaining main goals for biodiesel use is the possibility to utilise it as fuel with minor or no modification within existing diesel engines [46; 49].

2.3 Oils: characteristics and problems

2.3.1 Oils of interest

Sunflower (*Helianthus annus*) seed oil is one of the major vegetable oils in world production, being used in food and in cosmetic industries.

Sunflower oil is a mixture of different triglycerides, which are fatty acids esterified with glycerol, with typical fatty acid profiles: 48-74% linoleic acid, 14-40% oleic acid, 4-9% palmitic acid, and 1-7% stearic acid (figure 2.12). Fatty acids composition per 100 g of sunflower oil is typically: 11.9 g saturated, 20.2 g monounsaturated, 63.0 g polyunsaturated [54]. Variations in the unsaturated fatty acids profile are due to genetic and climatic conditions among the different world's production sites.

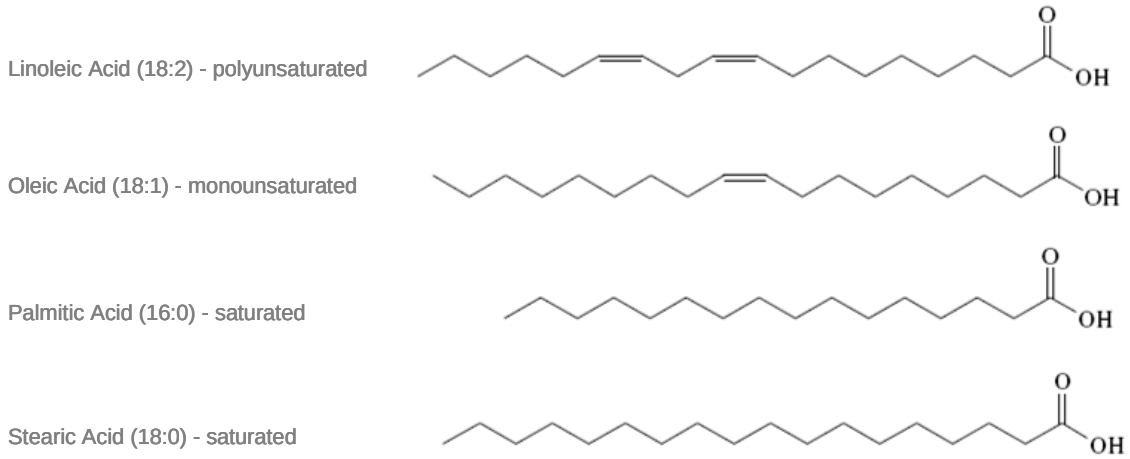

Figure 2.12 Structure of the fatty acids constituting sunflower oil triglycerides.

Sunflower linoleic acid oil is the original sunflower oil and is rich in polyunsaturated fatty acids and in vitamin E. Variations with higher oleic content were developed; examples include NuSun mid oleic sunflower oil and HighSun or HOSO high oleic sunflower oil with at least 80% of monounsaturated, oleic, fatty acids [55; 56].

Cable and transformer oil are generally known as lubricant oils. Lubricant oils can be classified as paraffinic, naphthenic and synthetic oil. Paraffinic and naphthenic oil are

refined from crude oil and are distinguished by their molecular structure; the first one is composed by long linear hydrocarbon chains and contains wax, whereas the second is characterised by cyclic hydrocarbons. Synthetic lubricants are formed by chemical synthesis and they show better characteristics than mineral oils in term of oxidation stability, viscosity, pour point and friction coefficient which allow their use with either very high or very low temperatures [57].

Cable oil is a synthetic mixture of linear alkyl-benzenes (LAB, figure 2.13), designed for electrical cables lubrication, with aliphatic chains which may contain from 12 to more than 22 carbon atoms [58; 59].

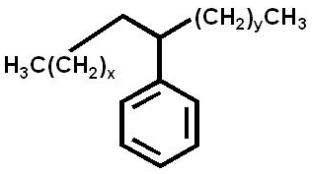

Figure 2.13 Linear alkyl-benzenes (LAB) general structure.

Transformer oil is a highly-refined mineral oil, with excellent properties in terms of high temperature stability and electrical insulation, which was historically characterized by high content of polychlorinated biphenyls (PCB, figure 2.14) [60].

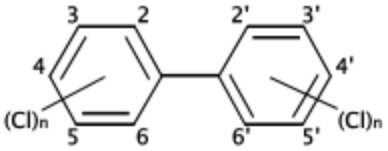

Figure 2.14 Polychlorinated biphenyls (PCB) general structure.

Such oils have good resistance to acids, bases and oxidising agents, a very low solubility in water, and they also have good thermal stability and are generally inert. All these aspects concur to negatively affect their biodegradability.

This aspect is of primary importance since many studies were conducted and are still on-going on waste oil degradation and on soil and groundwater remediation after contamination due to oil leaks.

Liquid silicone oils belong to a class of synthetic polymers whose core molecular structure is based on Si-O bonds, the most common of these polymers being polydimethylsiloxane (PDMS) (figure 2.15). According to the number and kind of substituent and to the presence of long lateral chains on the core structure, silicones can exist in the form of liquids/oils, greases/pastes, foam, rubber or solids; this leads to a wide variety of uses from healthcare-food-cosmetics industries to electronic and mechanical engineering applications [61].

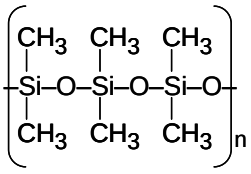

Figure 2.15 Polydimethylsiloxane (PDMS) general structure.

Silicone fluids have good dielectric properties, high compressibility, good hydrodynamic lubricant properties, high thermal resistance and low flammability; with all of these properties leading to their use in transformers and other electrical appliances [61].

Motor oils are a wide range of lubricating oils used mainly in internal combustion engines to avoid the friction of the moving parts and to carry away the heat generated by the engine. These oils can be either synthetic or derived from petroleum products (section 2.2.1b); their general structure consist in medium/long chains hydrocarbons molecules containing 18-34 carbon atoms (figure 2.16). Various additives, such as detergents, corrosion inhibitors and acid oxidation neutralizers are generally added to the oil to avoid the deposition of sludge on the engine's parts and the subsequent corrosion [41].

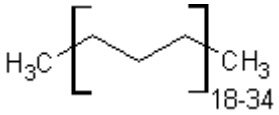

Figure 2.16 General structure of motor oil.

As discussed in section 2.2.1b, diesel fuel is a product of the refinery of crude oil and its main application is within the road transport sector. The general structure of diesel consists of short/medium chains hydrocarbons molecules with 9-21 atoms of carbon (figure 2.17). Diesel is treated to lower the sulphur content and has detergents added to maintain the operational conditions of the engine [41].

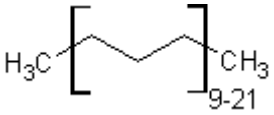

Figure 2.17 General structure of diesel fuel.

2.3.2 Soil and groundwater remediation

After an oil spillage, the processes, under study and in use, for soil and groundwater remediation present slight differences from one to another on the basis of the chemical composition of the oil.

Enzymatic biodegradation is one of the main processes in use for soil and groundwater remediation. With the term enzymatic biodegradation are defined both processes using free enzymes and processes using microorganisms which contain the specific enzyme required for the remediation. The first advantage of this technique is the possibility to obtain an *in situ* remediation that is of primary importance since many leaks occur in urban areas where it is not possible to excavate the soil and transfer it to a treatment area [58; 59].

Enzymatic biodegradation can be either aerobic or anaerobic depending on the chemical composition of the oil as source of carbons, the presence of oxygen, nitrates, sulphates

and iron in the soil, the microorganisms existing in the medium and those added to increase the rates of bioremediation [58; 60]. Although aerobic degradation is well studied and its pathways are commonly known, anaerobic degradation is a relatively new technique and its main benefit is the *in situ* remediation of anaerobic regions of the soil where aerobic degradation can not take place due to the absence of oxygen [58].

Aerobic and anaerobic biodegradation have great benefits on soil and groundwater remediation, with their effect being increased when used together through a mix of different indigenous microorganisms [60].

An example of enzymatic biodegradation is the use of nitrate reductase to attain reductive dechlorination of PCB in contaminated soils; this process can take place in both aerobic and anaerobic condition [62].

In a significant study, Montagnolli *et al.* [63] compare the effectiveness of biodegradation on various oils through the respirometry technique which evaluates CO_2 production from the degradation of organic compounds by microorganisms. The oils taken into account included samples of synthetic lubricant oil, semi-synthetic lubricant oil, mineral lubricant oil, used lubricant oil and vegetable oil. This study showed that used lubricant oil undergoes a better biodegradation than all the other samples, that microorganisms action on mineral and semi-synthetic lubricant oil is better than on synthetic oil, and that vegetable oil is the compound on which biodegradation is least effective. A reported explanation for the massive effect of biodegradation on used lubricant oil is that the heat, to which the oil is exposed while in use, causes breaks in the hydrocarbon chains, leading to a partial deterioration of the compounds that makes it easier for the biodegradation by microorganisms. The same could be said also for cooked vegetable oil, but the presence of antioxidants (added during the refining process) such as citric acid and 2-(1,1-Dimethylethyl)-1,4-benzenediol (TBHQ), preserves the oil from the action of the microorganisms [63].

Techniques other than enzymatic for soil and groundwater remediation include photo-degradation and the Fenton advanced oxidation process; these processes use the

light-induced generation of radicals, such as hydroxyl radicals ($^{\bullet}OH$) and superoxide ion ($^{\bullet}O_2^-$), which interact with organic compounds to induce degradation reactions [64; 65].

Another proposed technique is phytoextraction. The rationale of this procedure is to plant seeds in the contaminated soil, so that the plants, while growing, absorb and accumulate the contaminant through the root. When the plants are mature, they are harvested and burned as solid waste. *Cucurbita* genus plants are the most suitable for this purpose, but the process still has some limitations since low concentrations of the accumulated contaminant are obtained (and in particular with hydrophobic molecules) with a negative benefit/cost balance compared to other techniques [66].

2.3.3 Waste oil degradation

In the case of waste oil degradation, the general trend is to recycle waste edible and non-edible oils in order to develop alternative energy sources.

Transesterification is one of the most widely studied techniques to convert vegetable oils into biodiesel by reacting them with methanol or ethanol to give the resulting fatty acid methyl or ethyl esters; the preferred catalyst is sodium hydroxide because of its low cost and high reaction yield. The by-product of the reaction is glycerol which is recovered and used in many different industrial products, from food to cosmetic, pharmaceutical, and also explosives production [67; 68]. The main purpose of transesterification is to diminish the viscosity of the oil in order to use it as fuel in existing diesel engines without further modifications [69; 70]. One disadvantage related to this process is the temperature needed to drive the reaction which leads to high energy consumption [71].

Pyrolysis is a severe form of thermal cracking, which when used on waste oil leads to the formation of different bio-fuels depending on the temperature, on the presence of a catalyst (catalytic thermal cracking), and on the chemical composition of the starting

material [68]. At relatively low temperatures (400-600°C) it is possible to obtain fuels similar in nature to gasoline or diesel, while at higher temperatures (800°C) synthesis gas, methane and ethylene can be obtained [70]. Although there are many benefits by having a wide range of possible products, problems relate to the quality of these final products which are influenced by the quality of the starting material, and also to the costs associated with the generation of those high temperatures [71].

Hydroprocessing is a general word to indicate a class of processes which use transition metals as catalysts and are able to produce diesel-like "super cetane" products, generally used as diesel fuel additives, from vegetable oils [70]. Specifically, hydro-cracking breaks long chain molecules. Hydro-treating refers to oxygen removal from the starting material, and hydrogenation leads to the saturation of the double bonds of the chains [72]. The main problem related to these processes is the high pressure needed to drive the conversion [68].

An alternative method for recycling waste oils is the catalytic steam reforming process which leads to eventual hydrogen production [70; 73]. Vegetable oils are, with the aid of a nickel-based catalyst, converted into hydrogen with high yield because of their low oxygen content [73]. A disadvantage of this technique is the high furnace temperature which drives steam formation (500-600°C).

A novel technique for waste oil degradation is microwave-activated cracking; this process generates high temperatures and pressures through microwave absorption due to the addition of sensitizers or catalysts which leads to the production of fuel of superior quality than that obtained from other techniques, with low sulphur and other metals content. Metals and soil sediments can be separated from the reacting oil by a mechanism which induces oil swirling in the reaction chamber [74].

2.3.4 Rationale for the use of ultrasound

The techniques mentioned above, although useful in generating new energy sources from waste edible and non-edible oils, still suffer some disadvantages such as the requirement for high temperatures or pressures generally required to drive these processes; as a consequence new methods for the treatment of waste oils should be considered and ultrasound might be one of the answers to make progresses in this field.

Evidence in this direction come from the above mentioned effects of cavitation on polymeric degradation [27] and from the use of ultrasound as a way to improve the efficiency of the transesterification reaction to produce biodiesel. To this last category belong many studies which compare the benefit of ultrasound driven transesterification to conventional reaction, which implies, for example, the possibility to drive the reaction at room temperature, the lower amounts of catalyst required to drive the reaction, and the shorter reaction times with the same high reaction yield [75-78].

Further support comes from microwave-activated cracking, which, in the same way as ultrasound, involves the formation of localised high pressures and temperatures to drive oil cracking, as well as from the use of ultrasound to improve oil extraction from tar sand and from contaminated soils. Some pilot tests indicate that ultrasound is able to enhance pollutant extraction in the soil-flushing method, and that it can be used to affect deep regions of multiphase system soils, which are not accessible with other extraction methods [11; 79].

Chapter 3

Materials and Methods

3.1 Reagents and materials

Sunflower oil (Flora, Princes Ltd., UK), 'Total' motor oil (Quartz Ineo ECS 5W-30), 'Comma' motor oil (Multigrade Premium 20W-50), 'Halfords' motor oil (Classic Oil 20W-50), and diesel fuel were purchased from local shops; cable and transformer oils were obtained from National Tray Transco (UK), while silicone oil was purchased from Dow Corning (Barry, UK). The oil lamps containing vegetable oil were obtained from Agowa (Denmark).

Potassium hydroxide, ammonium acetate, sodium acetate, N-tert-Butyl-α-phenylnitrone, carbon black, glyceryl trilinoleate, and glyceryl trioleate were obtained from Sigma-Aldrich (Gillingham, UK). Carbon nanotubes were provided from the School of Engineering (Cranfield University, UK), while carbon plasma black was supplied by Gasplas (University of East Anglia, UK). Acetone and 4-tert-butylphenol were supplied by Acros Organics (Geel, Belgium). Isopropanol and methanol were supplied by Fisher Scientific (Loughborough, UK). Acetic acid and glass spheres were purchased from BDH (Poole, UK).

All chemicals were used without further purification.

3.1.1 Reagents characterisation

Carbon black, carbon plasma black and carbon nanotubes were characterised prior to use in order to obtain data on their size and three-dimensional structure.

The specifications provided for carbon black (CP) were: chemical formula C; molecular weight 12.01 AMU; size 2-12 μm. These particles were analysed with Scanning Electron Microscopy (SEM) before and after sonication.

A liquid suspension of CP in deionised water was formed and a drop of this suspension was placed on a silicon surface, allowed to dry and analysed with SEM. The formation of a liquid suspension of very small particles, as those analysed here, makes the deposition of the particles on the silicon surface easier. At the same time, the analysis can not be performed on a liquid sample since this would damage the SEM instrument, so the drying step – which occurs at room temperature (23°C) – is necessary.

As can be seen in figure 3.1, CP is in the form of beads which size is congruent with that reported in the "house" supplied specification.

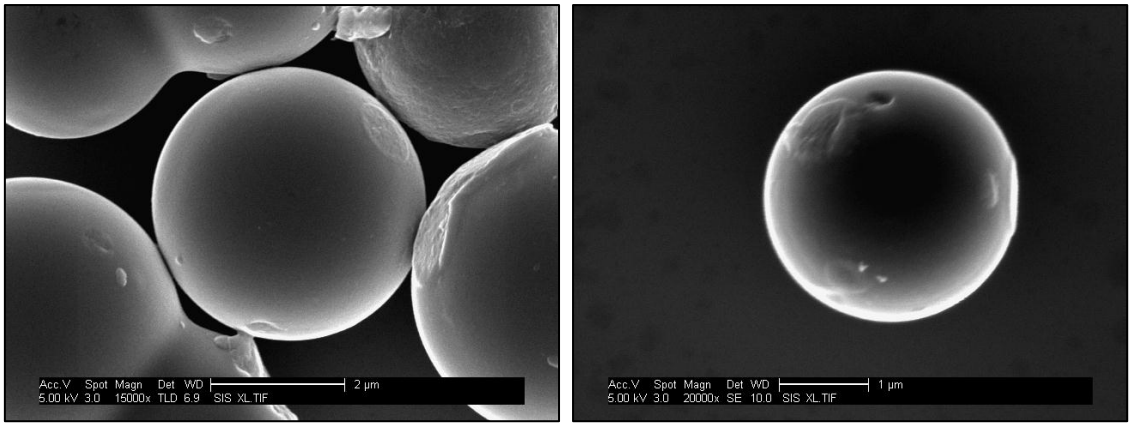

Figure 3.1 SEM images of carbon black.

Carbon black was then suspended either in deionised water or in sunflower oil; the two suspensions were sonicated for 60 minutes in a bath sonicator at 35 kHz frequency. A drop of the CP suspension in deionised water was dried on the silicon surface and analysed with SEM. The nature of sunflower oil does not allow it to dry at ambient conditions, so many trials to wash the particles from the oil were performed using a number of different solvents. The best results were obtained with chloroform, and so after this treatment, a drop of the particles' suspension was left to dry on the silicon surface and then analysed.

As can be seen in figures 3.2 a and b, the ultrasound seems to partially affect the three-dimensional structure of the particles; some of the beads are, in fact, broken or fragmented, though the vast majority retain the bead-like shape. Figures 3.2 c and d

show the particles after sonication in sunflower oil; as can be seen not all the oil was removed by the treatment with chloroform; for this reason in-depth imaging was not performed to avoid possible damage to the instrument. Despite this unexpected difficulty, the images seem to confirm the results obtained for the particles sonicated in deionised water.

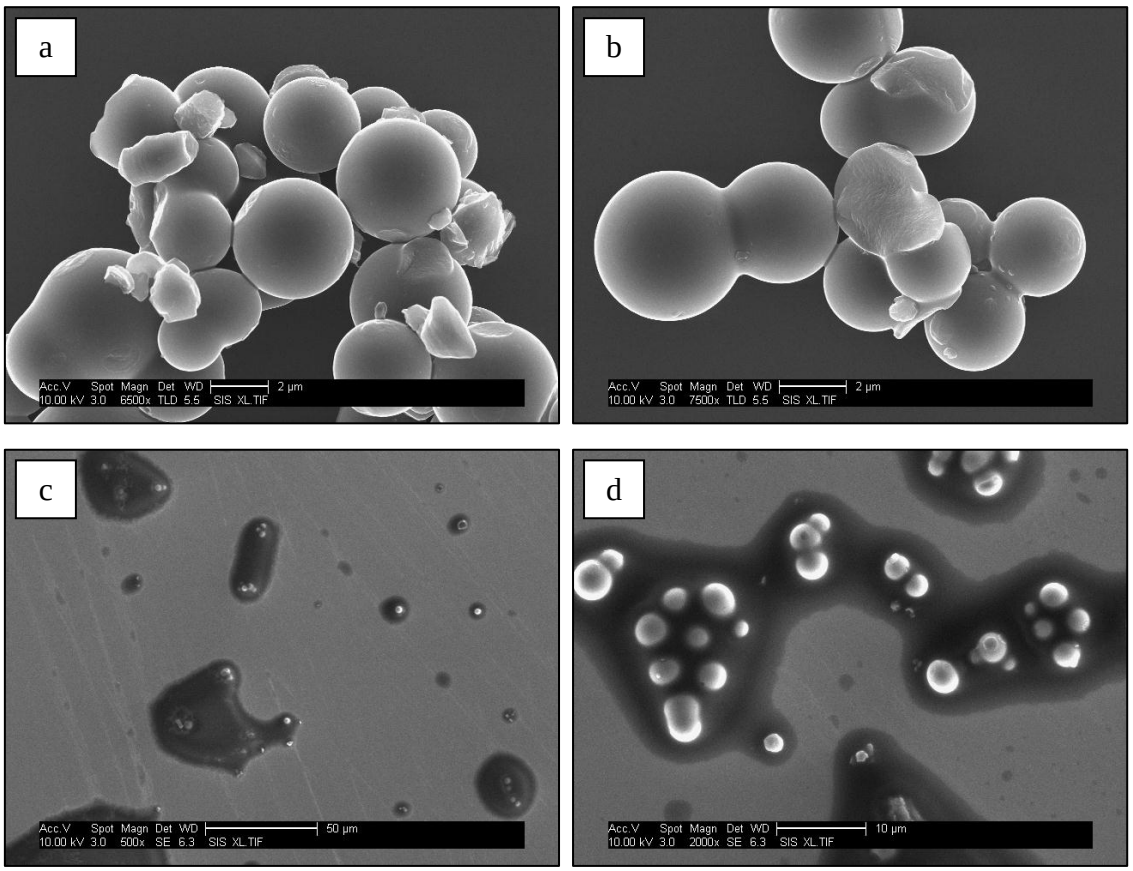

Figure 3.2 SEM images of carbon black after sonication in deionised water (a and b), and in sunflower oil (c and d).

No specification was supplied with the carbon plasma black (CPLS) particles, and so the SEM analysis was necessary to understand the nature of the particles. CPLS was suspended in water and then a drop was dried and analysed with SEM. As can be seen in figure 3.3, CPLS present as carbon agglomerates in the range of 1-10 μm, formed by many layers. The bead-like protrusions (figure 3.3 right) are in the range 20-200 nm.

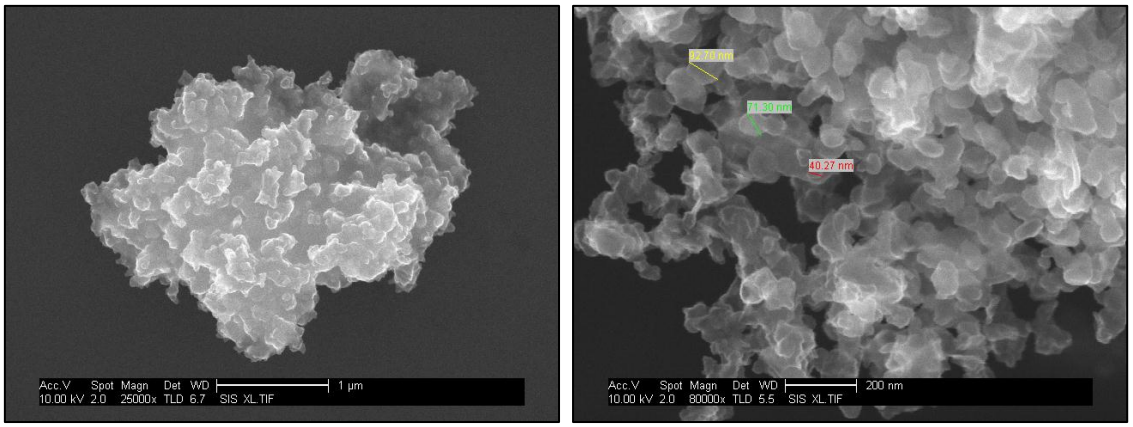

Figure 3.3 SEM images of carbon plasma black.

Carbon plasma black was then suspended either in deionised water or in sunflower oil; the two suspensions were sonicated for 60 minutes in a bath sonicator at 35 kHz frequency. A drop of the CPLS suspension in deionised water was dried on the silicon surface and analysed with SEM. As previously described for carbon black, a wash step is necessary prior to performing the analysis on the particles which were suspended and sonicated in sunflower oil. The same trials were performed with chloroform being found to give the best results, and so a drop of the treated suspension was left to dry on the silicon surface and then analysed.

As can be seen in figure 3.4, CPLS particles seem to retain the agglomerate conformation whether they were sonicated in deionised water or sunflower oil, however, it may be possible that this conformation is favoured by the washing and drying steps which are part of the method of analysis.

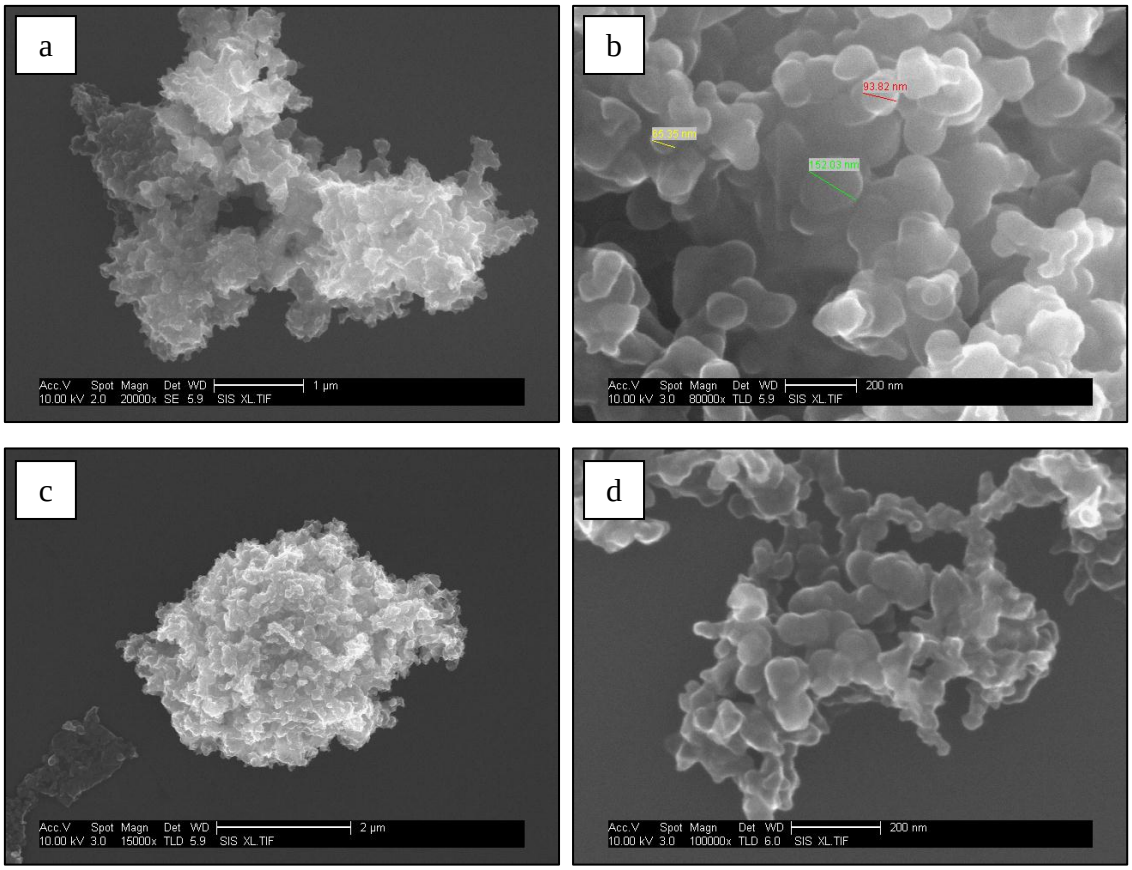

Figure 3.4 SEM images of carbon plasma black after sonication in deionised water (a and b), and in sunflower oil (c and d).

Carbon nanotubes (CNTs) were provided without specification, and for this reason they were suspended in water and then analysed with Dynamic Light Scattering (DLS), Nanosight, and SEM, to evaluate their size, length, and three-dimensional structure. The analysis revealed the presence of agglomerates of CNTs with a size distribution of 450-750 nm, while the individual length of the CNTs is in the range of 60-150 nm as can be seen in the plot of figures 3.5 and 3.6. The SEM images reported in figure 3.7 show the diameter of the CNTs to be in the range of 15-20 nm.

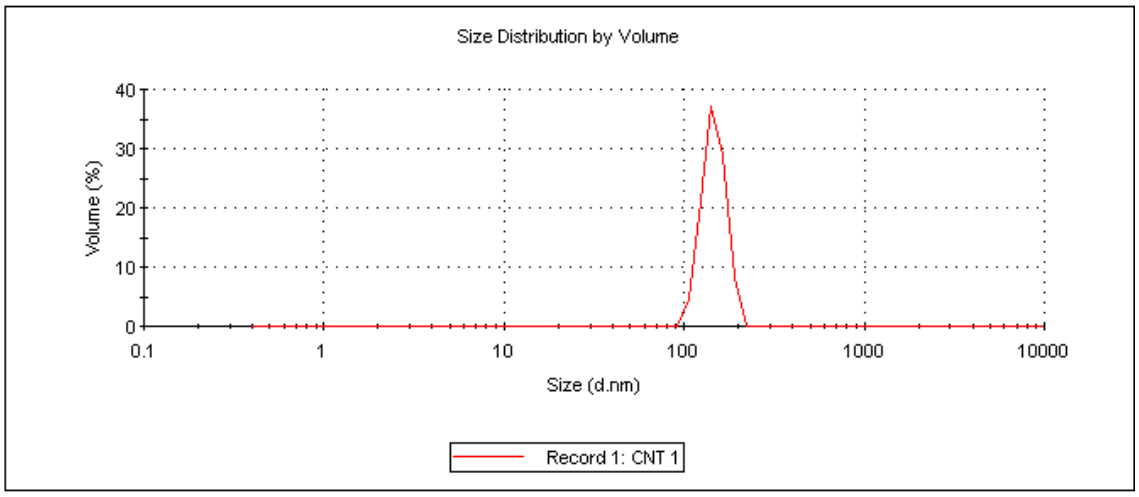

Figure 3.5 Dynamic Light Scattering of carbon nanotubes. The plot was obtained from a Zetasizer Nano instrument.

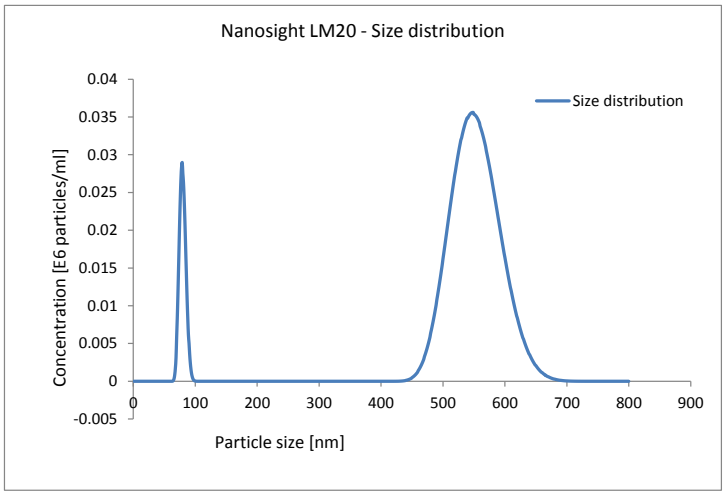

Figure 3.6 Size distribution of carbon nanotubes. The graph was obtained from a Nanosight LM20 instrument.

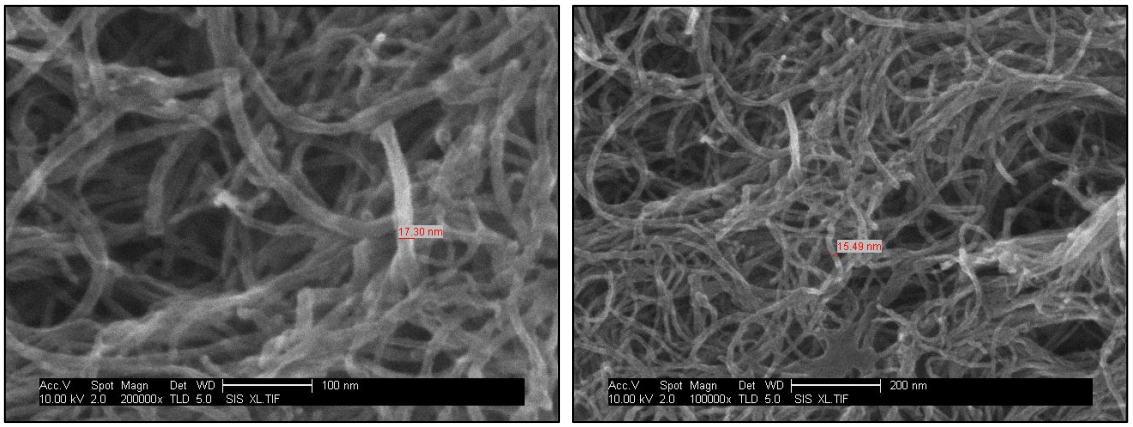

Figure 3.7 SEM images of carbon nanotubes.

3.2 Apparatus

3.2.1 Sonication

For the viscosity investigation experiments two ultrasonic water baths were used: Camlab Transsonic T460 (Camlab, Cambridge, UK) at 35 kHz frequency and 85 W power output (figure 3.8a); Ultrawave U100 (Ultrawave Ltd., Cardiff, UK) at 44 kHz frequency and 35 W power output (figure 3.8b) - hereafter referred to respectively as Camlab and Ultrawave water baths. For the saponification reaction experiments a probe sonicator at 40 kHz frequency and 50 W power output, Miniprobe 40 (Kerry Ultrasonics Ltd, Hitchin, UK; now Guyson International Ltd) was used (figure 3.9). A custom-built ultrasonic water tank linked to a 1 kW ultrasonic generator, Ultrawave SFE590 (Ultrawave Ltd., Cardiff, UK), was used for the scale-up of the process (figure 3.10) - hereafter referred to as custom-built water tank; this tank is provided with five transducers positioned under its base: one in each corner and one in the centre.

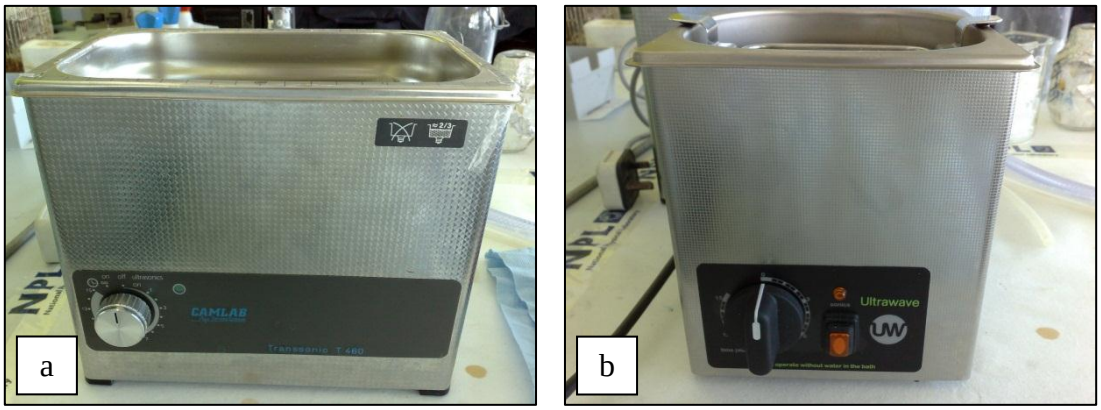

Figure 3.8 Ultrasonic water baths. a) Camlab Transsonic T460. b) Ultrawave U100.

Figure 3.9 Probe sonicator Miniprobe 40.

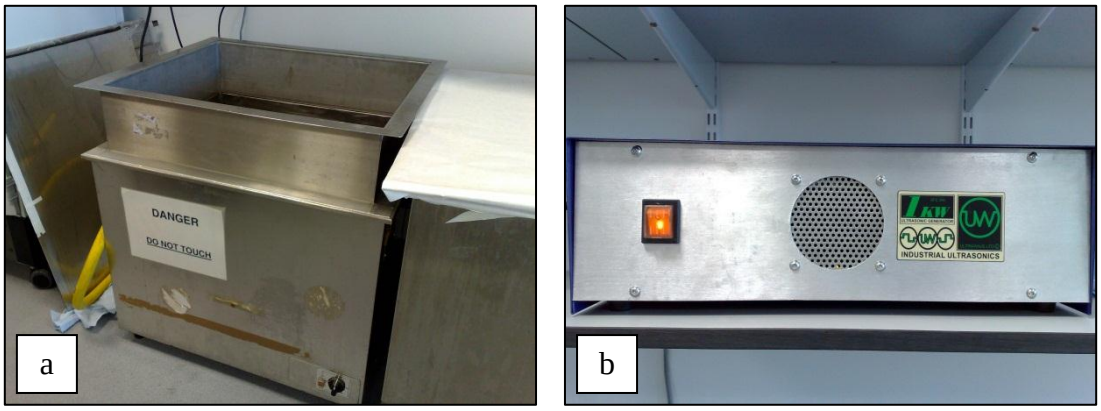

Figure 3.10 Custom-built water tank (a) linked to the ultrasonic generator Ultrawave SFE590 (b).

3.2.2 FTIR

For the Fourier Transform Infrared Spectroscopy analysis an Equinox 55 (Bruker Optik GmbH, Ettlingen, Germany) running the OPUS-NT 3.1 spectroscopic software was

used. The spectra were measured in the attenuated total reflection (ATR) mode using a ZnSe (Zinc Selenide) prism mounted on a Specac Gateway Multi-Reflection ATR (Specac Ltd., Slough, UK). The use of FTIR in the total reflection mode has been widely accepted as quantitative analytical method and as an alternative to other techniques, such as gas chromatography and titration, in various applications when on-line real time data are needed or when the use of solvents for sample preparation has to be avoided to not detrimentally affect the sample [80-87]. To perform the analysis a drop of the sample was spread on the prism surface (figure 3.11) and then the FTIR/FTNIR spectra was taken in the spectral range 400-4000 cm^{-1}, with a maximum spectral resolution of 0.20 cm^{-1}.

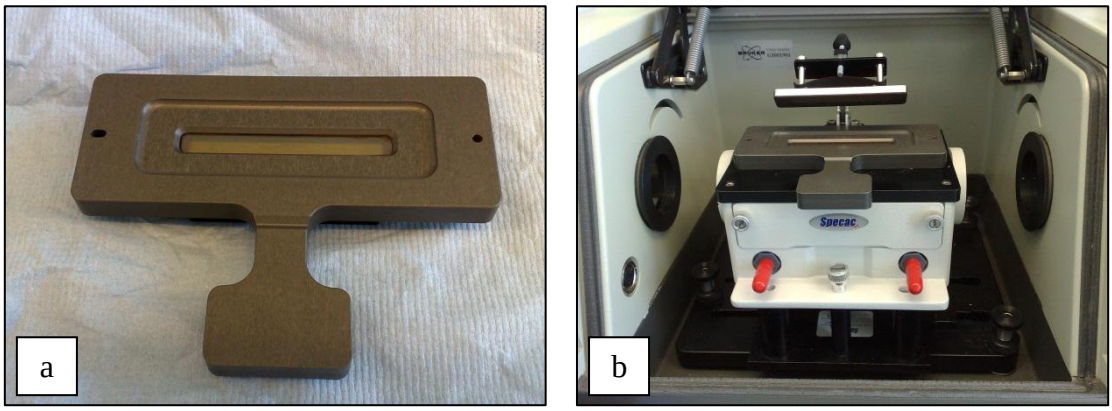

Figure 3.11 ZnSe prism (a) mounted on the Specac Gateway Multi-Reflection ATR (b) inside the spectrometer.

3.2.3 SIFT-MS

The Selected Ion Flow Tube - Mass Spectrometry analysis of the volatiles were performed using a Profile 3 SIFT-MS (Trans Spectra - Instrument Science, Crewe, UK). The principle of this method is based on the generation of precursor ions species (H_3O^+, NO^+, O_2^+) which are injected into a flow tube where a carrier gas (helium) is rapidly flowing. The precursor ions are generated by a 2.45 GHz microwave discharge. These ions, after having adjusted to the temperature of the carrier gas (300 K), collide with the helium atoms and then react with the traces of the samples' volatile components

creating ionized product species. Both the precursor and the product species then pass into the mass spectrometer where the ionised products are analysed according to their mass/charge ratio [88].

For the experiments, the liquid samples were injected into bags made of polyethylene terephthalate (Nalophan), which were then filled with zero grade air. The bags were then linked to the apparatus and the headspace volatiles were collected at 0.62 $torr\ L\ s^{-1}$ flow rate for an average time of 30 seconds via a heated calibrated capillary. The bags were allowed to equilibrate at 30°C for 15 minutes before the analysis, and the same temperature was maintained during the collection. The analysis was performed using the full-scan mode by selecting the mass-charge ratio (m/z) range between 10 and 200 m/z. The products identified in the samples were then normalised to the products identified from the analysis of a control bag just filled with the zero grade air.

3.2.4 ATD-GCMS

The Automated Thermal Desorption Gas Chromatography – Mass Spectrometry anlaysis of the volatiles were performed on a Perkin Elmer combining a TurboMass MS 4.1, Autosystem XL GC and Automated Thermal Desorption system ATD 400 (Perkin Elmer, Wellesley, MA). The column used was a wall-coated Zebron XB624 (Phenomenex, Torrance, CA), with dimensions of 30 m x 0.4 mm x 0.25 mm (internal diameter), the liquid phase comprising a 0.25 µm layer of 6% cyanopropylphenyl and 94% methylpolysiloxane; the carrier gas was CP grade helium (BOC Gases, Guildford, UK).

The volatiles of the oils were adsorbed on TD (thermal desorption) tubes containing 50% Tenax TA and 50% Carbotrap (Markes International Ltd, Llantrisant, UK) at a temperature of 30°C. The tubes were then desorbed on the ATD for 2 minutes at room temperature followed by 5 minutes at 300°C (ATD valve temperature 180°C). The

volatiles were captured in primary and secondary cold traps maintained at 30°C; the primary trap was then heated to 320°C for 5 minutes while the volatiles were transferred to the GC via a transfer line heated to 210°C. The temperature in the GC oven was maintained at 50°C for 4 minutes and then raised at increments of 10°C per minute until reaching 220°C and then held for 9 minutes. The products were then conveyed to the MS via a heated line at 240°C, where they were ionised to generate a full scan of mass/charge ratios from 33 to 350 m/z with a scan time of 0.3 seconds and 0.1 seconds delay - producing mass spectra with a total ion chromatogram (TIC).

3.2.5 LC/MS

Liquid Chromatography – Mass Spectrometry (LC/MS) analysis were performed using an Agilent HPLC 1290 Infinity – 6540 UHD (Ultra High Definition) coupled with an Accurate-Mass QTOF MS detector. For the separation, a Zorbax Eclipse Plus C18 (50 mm) column was used and the elution solvent consisted of 18% isopropanol in methanol with the addition of 0.1% acetic acid, 0.05% ammonium acetate, and 0.001% sodium acetate, as described in the work of Zeb and Murkovic [89]. The solvent for the standards and the samples was 50% acetone and 50% of a solution of 18% isopropanol in methanol. Both the standards and the samples were diluted to a concentration of 1 mg/ml and then injected at a dilution of 100 μg/ml. The column was maintained at a temperature of 30°C, while the gas temperature and the drying gas temperature were at 325°C. The fragment voltage was 150 V and the capillary voltage was 4000 V. The flow rate was 0.25 ml/min and the separation time was 35 minutes. The ion polarity was on the positive mode and the ESI-MS spectra range was 100-1000 m/z. The reference ion masses taken into account were those for acetate (121 m/z and 922 m/z) since it is the main component comprising the elution solvent.

3.2.6 ESR

Electron Spin Resonance (ESR) analysis were performed at room temperature on a Jeol JES-FA200 spectrometer (Jeol Ltd., Welwyn Garden City, UK). The samples were either injected in glass capillaries, which were then sealed using gas flame and placed in a cylindrical quartz cell for the analysis, or injected in cap-sealable quartz capillaries which would fit the spectrometer chamber (figure 3.12). The machine operated at 9 GHz microwave frequency, while the microwave power level was kept around 6.7 mW. The scanned magnet field was between 0 and 1000 mT, the modulation width was 2 mT, and the amplitude was 400 mT with a time constant of 0.3 seconds.

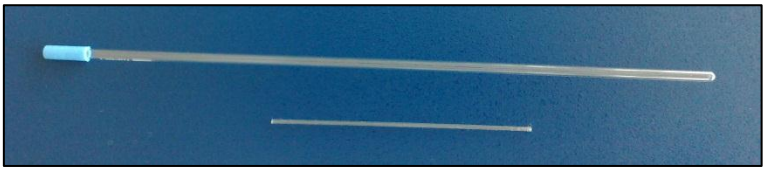

Figure 3.12 Sealable quartz capillary with blue cap (top) and open glass capillary (bottom).

3.3 Experimental methodology

3.3.1 Ultrasound intensity mapping

The intensity and region of action of the ultrasound within the ultrasonic water baths and tank was carried out using a "foil test" [3; 90]. Clean pieces of aluminium foil, with consistent sizes relevant to the bath or tank under analysis, were suspended vertically in the ultrasonic baths and tank following the scheme in figure 3.13. The foils were sonicated in a stationary position, either simultaneously in groups of three (group 1 foils *A*, *B*, *C*; group 2 foils *D*, *E*, *F*) or singularly (figure 3.14), for 2 to 10 minutes. The foils were then carefully removed and images obtained in order to allow investigations on the intensity and regions of perforation, thus determining the site of maximum cavitation effect within the tested sonicators.

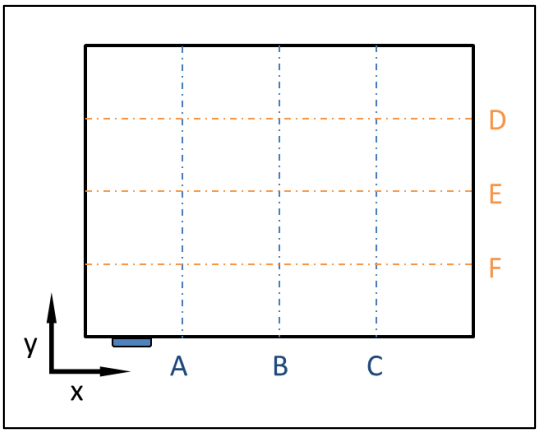

Figure 3.13 General foil positioning within the ultrasonic baths and tank (top view).

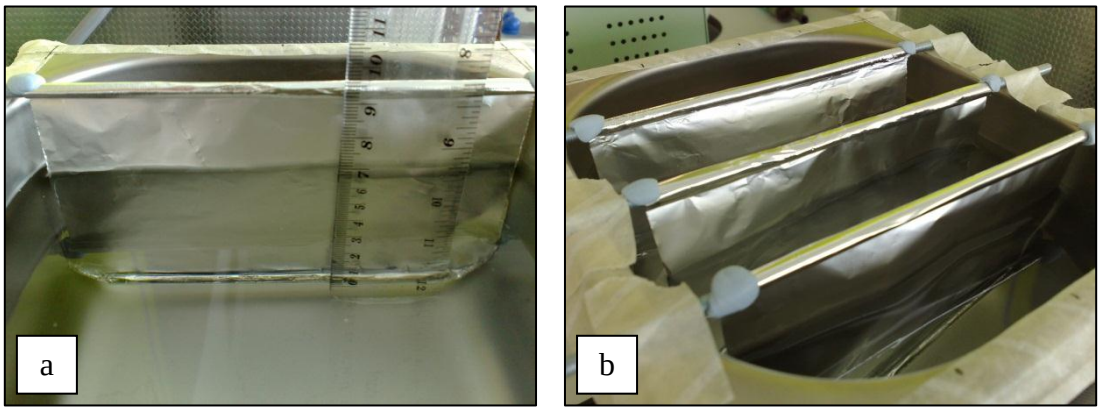

Figure 3.14 Method to suspend the aluminium foils within the sonicators. Single foil sonication (a) and simultaneous sonication (b).

The "foil test" was also performed on clean pieces of aluminium suspended within a glass beaker filled with 25 ml of water or sunflower oil (figure 3.15) to test the interference of a glass wall on the propagation of the ultrasonic waves in the two different media. The foils were sonicated for 2 to 60 minutes.

Figure 3.15 "Foil test" on aluminium foils suspended within a glass beaker.

3.3.2 Viscosity measurements

For all the viscosity measurements a dropping ball viscometer was used (figure 3.16). This type of viscometer is based upon Stokes' Law for flows around submerged objects [91]. According to this law, the forces which act on a sphere settling through a fluid are the force of gravity, the drag forces and the buoyant force; when the drag forces acting on the sphere become equal to the gravity force, the sphere falls at a constant velocity termed terminal velocity (equation 3.1):

Equation 3.1 $$\mathcal{V} = [D^2 \mathfrak{g} (\rho S - \rho F)]/(18\mu)$$

where $\mathcal{V}$ is the terminal velocity of the sphere ($m\ s^{-1}$), D is the diameter of the sphere (m), $\mathfrak{g}$ is the gravitational acceleration ($\mathfrak{g} = 9.8\ m\ s^{-2}$), ρS is the density of the sphere ($kg\ m^{-3}$), ρF is the density of the fluid through which the sphere is settling ($kg\ m^{-3}$), μ is the viscosity of the fluid ($Pa\ s$).

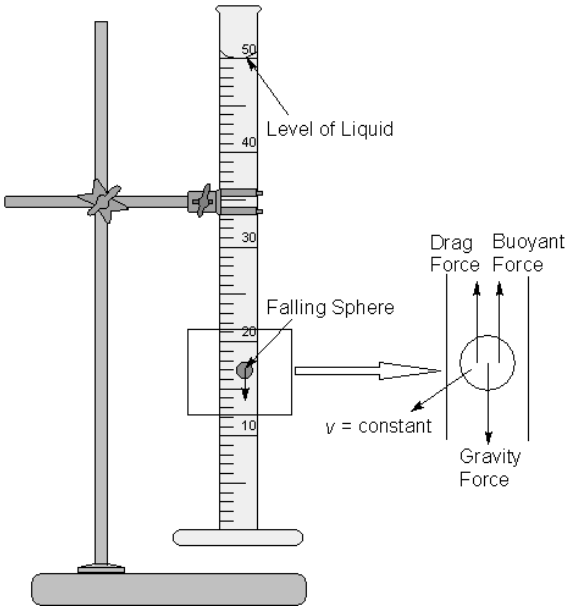

Figure 3.16 Schematic representations of a falling ball viscometer and of the forces acting on the falling sphere.

By rearranging this equation it is possible to determine the viscosity of a fluid by measuring the terminal velocity of the sphere (equation 3.2). The unit of measure of the viscosity obtained in this way is $Pa\ s$; for simplicity all the viscosity values are here reported in cP being 1 cP = 0.001 $Pa\ s$ (dynamic viscosity).

Equation 3.2 $$\mu = [D^2 \mathrm{g}\,(\rho S - \rho F)(\tfrac{1}{v})]/18$$

The terminal velocity of the sphere has been recorded with the aid of a video camera and the videos were analysed with a free video analysis and modelling software (Tracker 4.50 - Open Source Physics).

3.3.3 Determination of the calorific value

The calorific value has been described in section 2.2.3 as the quantity of heat generated during the complete combustion of 1 kg of a combustible material. The calorific value

has been measured by means of a "home-made" calorimeter which comprises an oil lamp below a suspended beaker of deionised water (figure 3.17).

Figure 3.17 "Home-made" calorimeter. The beaker of deionised water is placed over the oil lamp by means of a retort stand.

This calorimeter evaluates the heat produced, expressed as the rise in water temperature, during the burning of a defined amount of oil. In order to achieve this, a known mass of water is placed over a lighted oil lamp for a defined amount of time at a consistent height; the mass of the oil is measured before and after burning as well as the temperature of the water. The calorific value (CV) has been determined using equation 3.2:

Equation 3.2 $$CV = [M \cdot S\,(T_2 - T_1)]/(W_1 - W_2)$$

where M is the mass of the deionised water (g), S is the specific heat of water ($4.81\,J\,g^{-1}\,°C$), T_1 and T_2 represent the temperature of the water before and after the burning, W_1 and W_2 represent the mass of the oil before and after the burning (g).

3.3.4 Saponification reaction

As described in section 2.1.6 the saponification reaction requires heating to 100°C and is time consuming; in this work ultrasound was used as the heating source in an attempt to use less energy and to diminish the time required to drive the reaction.

All the reactions were performed on sunflower oil samples with the addition of potassium hydroxide in the form of fine powder or aqueous solutions at different concentrations (0.8, 1.6, and 3 mol/L). A probe sonicator at 40 kHz frequency was used, with the application of the power being pulsed (five minutes application and five minutes rest) to avoid overheating the oil. The reactions were driven until most of the oil was converted into a solid and the application of the ultrasound on the sample was no longer possible due to the separation of the semi-solid sample from the probe (reaction end-poin); the yield of the reaction was then measured with FTIR in the ATR mode (see section 3.2.2).

Part 2

Results and Discussion

Chapter 4

Preliminary investigations

4.1 Introduction

As discussed in section 2.1, the application of an acoustic field to a liquid medium generates cavitation phenomenon with the formation, growth and implosive collapse of micro-bubbles [20]. Polymeric chains surrounding the micro-bubbles can be affected by both the high temperature release and the shear forces generated by the growth and collapse of the micro-bubbles. Temperature effects lead to a randomised breaking of the chain within weakest intra-molecular bonds, while shear forces are known to cause the breakage of the chains from the middle, with the formation of radicals and products with lower molecular weight [18]. From these collective effects a decrease in the viscosity of oils, characterised by medium-long chains, could be suggested and is therefore investigated in this work.

4.2 Viscosity investigation for a range of oils

The first investigation was carried out on samples of sunflower oil as a model of vegetable oil, and on transformer and cable oil as models of mineral and synthetic oils, respectively. The Camlab bath sonicator at 35 kHz frequency was used as the ultrasound source, and the samples were sonicated for a total amount of 60 minutes. The viscosity was measured before the sonication, after 30 minutes of sonication and finally after the 60 minutes sonication period. Before each measurement, the samples were allowed to cool down to room temperature in order to avoid any possible temperature effects on the viscosity (resting time 30 minutes). This measure was taken since it is generally known that the viscosity of any liquid sample is affected by temperature variations [18] and a generalised increase of the temperature of the whole sample is expected after sonication, as explained in section 2.1.3. In this particular case the temperature of the samples after sonication was found to be increased by about 20°C; being the aim of the present investigation to determine solely the physical-mechanical effects induced by the cavitation phenomenon, it was decided to allow the temperature of the samples to cool down back to room temperature before proceeding with the analysis.

Figure 4.1 shows the plot of the viscosity of the samples against the experimental time; in this chart 0h represents the viscosity measurements taken before the sonication, 1h the measurements taken after 30 minutes of sonication plus 30 minutes of the cooling down period, and 2h represents the measurements taken after the further 30 minutes of sonication (which equates to 60 total minutes of sonication plus two cooling down periods of 30 minutes each).

As can be observed from figure 4.1, the ultrasound is effective in lowering the viscosity for all the samples; this decrease is clearly related to the sonication time. In particular, after 60 minutes of sonication, sunflower oil decreases by 10.4% (figure 4.1a), transformer oil 20.6% (figure 4.1b), and cable oil 29.2% (figure 4.1c), from their non-sonicated viscosity values. The higher viscosity of sunflower oil might be responsible for the lower viscosity decrease obtained in this sample when compared with the decrease achieved in the other two samples since, as described in section 2.1.3, the highest the viscosity of the medium the lowest the cavitation intensity. According to these data the hypothesis of the viscosity decrease, related to the effect of the high temperatures and shear forces generated by the ultrasound, can be accepted.

Further investigations will analyse and describe the nature of this physical behaviour, and will try to relate this information to the possible chemical changes which the oils undergo during sonication.

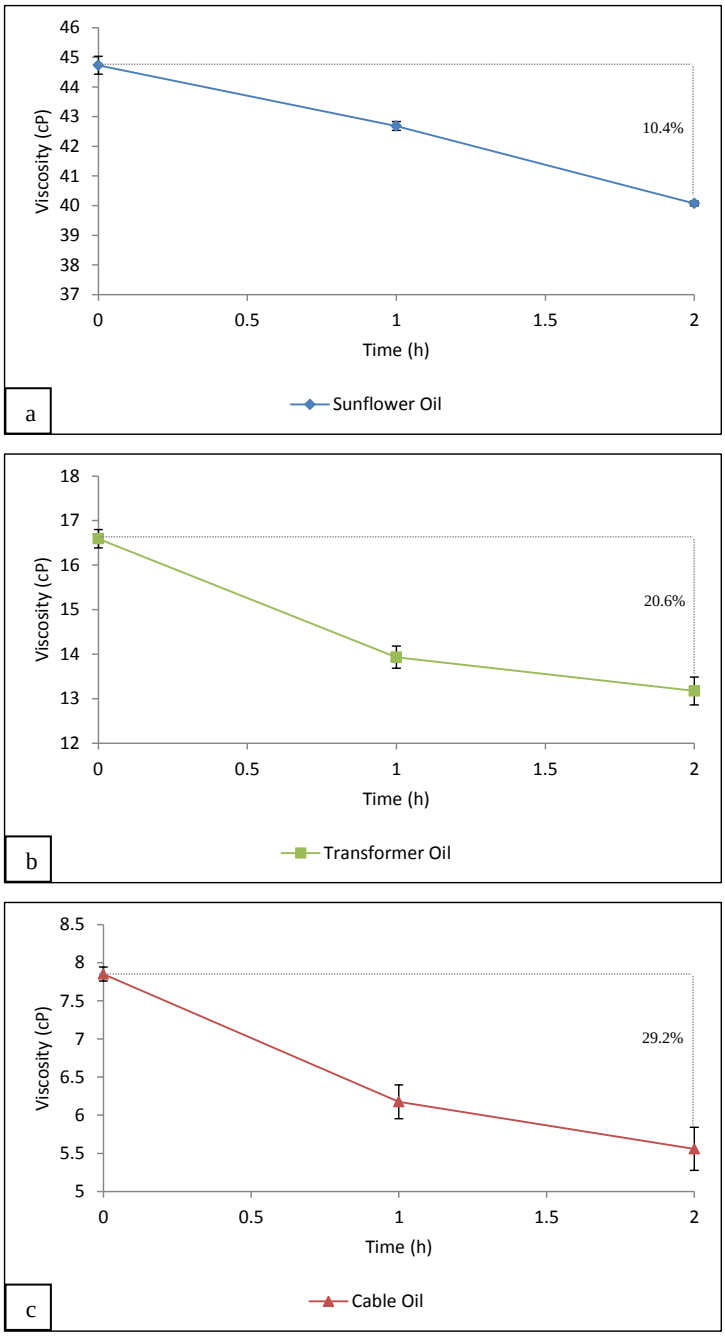

Figure 4.1 Effects of ultrasound on the viscosity of sunflower oil (a), transformer oil (b), cable oil (c). The measurements were performed in triplicate with the standard error being shown.

4.3 Efficiency investigations for the sonochemical reactors

Having established the effectiveness of the ultrasound in lowering the viscosity of sunflower, transformer, and cable oil (section 4.2), it is of importance to investigate the efficiency of the different ultrasound equipment in delivering the sonic power to the sample. This step is necessary in order to determine if any of the equipment has a greater efficiency and which is the optimum area of effect for each of the sonicators. In the following sections sunflower oil will be used as the model oil to carry out the mapping of the available sonochemical reactors described in section 3.2.1 (Camlab and Ultrawave water bath and Ultrawave custom-built water tank).

4.3.1 Camlab Transsonic T460

The general procedure adopted for the mapping of the intensity of the ultrasound is described in section 3.3.1. The sizes of the aluminium foils for the Camlab water bath were 12x10 cm for positions *A*, *B*, and *C*, and 23x10 cm for positions *D*, *E*, and *F*. The foils' positions within the bath are shown in figure 4.2. The foils were sonicated in the stationary position for 2 minutes since a large number of perforations were already visible after this time period.

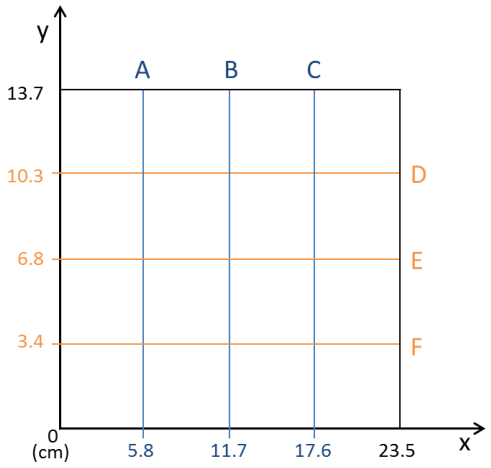

Figure 4.2 Foils positions relatively to the Camlab bath sonicator (top view).

As can be seen in figures 4.3, 4.4, and 4.5, the major perforations were observed for the foils placed in positions *A*, *B*, and *E* (see figure 4.2) indicating the central position as preferential in obtaining the maximum perforation effects (and therefore the maximum ultrasonic intensity) during sonication for this particular tank. From most of the images it appears that the cavitation phenomenon occurs along horizontal planes parallel to the surface of the liquid medium and that the region of major effect is located within the first 4-5 cm from the bottom of the tank. These horizontal planes occur at half the wavelength ($\lambda/2$) of the sonic waves where the antinodes regions are located. In particular in this system they occur about every 2 cm since the wavelength, calculated using equation 2.2 (section 2.1.1), was found to be 4.3 cm. From these results it appears that the region of maximum cavitation is directly above the transducer which is placed centrally in the base of the water bath. The perforations appeared to be more intense when the foils were sonicated simultaneously. This might be due to the generation of more aluminium debris when three foils are sonicated simultaneously. It is possible that these debris might act as nucleating agents increasing the rate of cavitation thus augmenting the perforations of the foil.

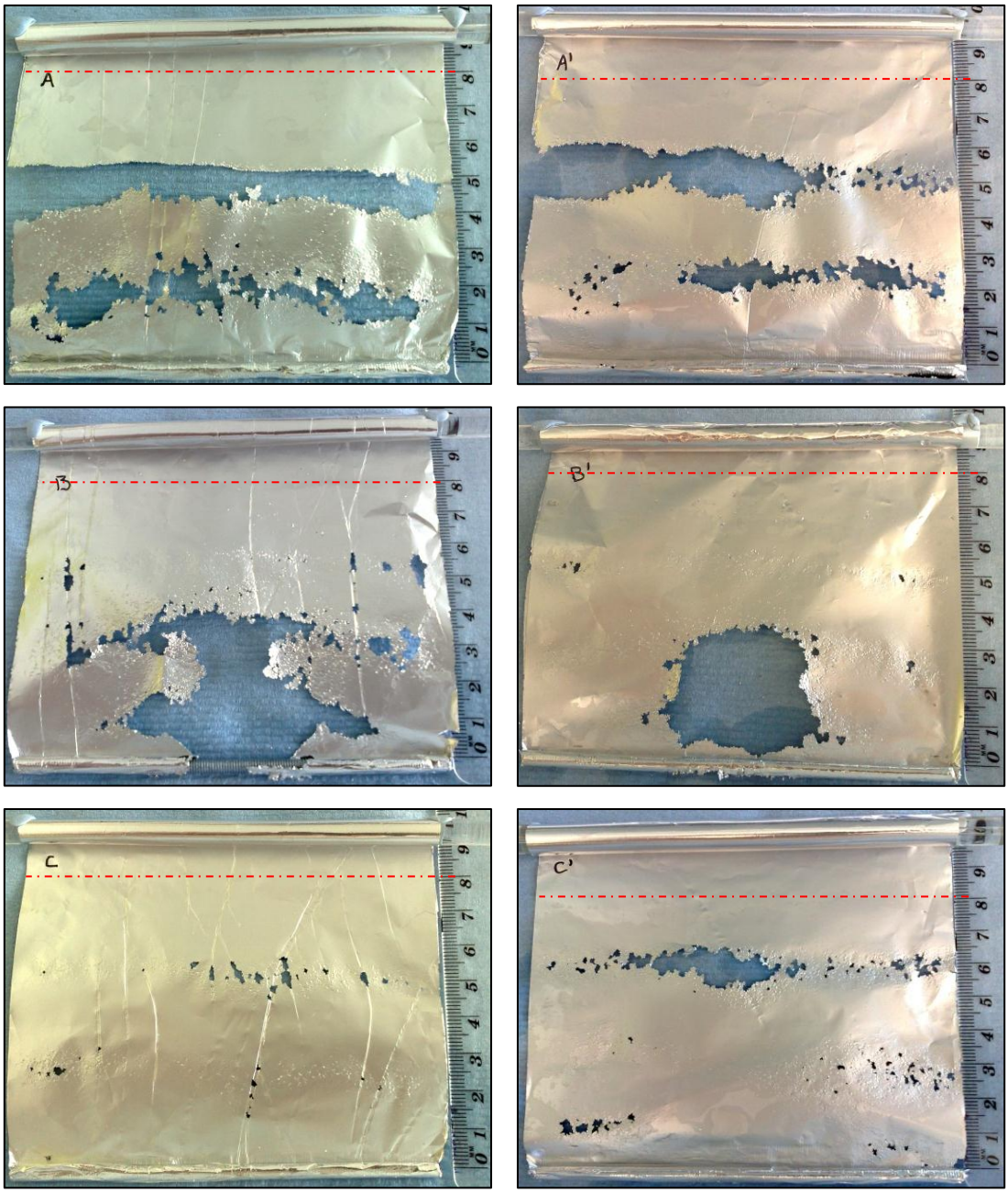

Figure 4.3 "Foil test" for Camlab bath sonicator in positions *A*, *B*, and *C*. The captions *A*, *B*, *C* indicate that the foils were sonicated simultaneously (left hand side), while *A'*, *B'*, *C'* indicate foils placed in the same positions within the sonicator but sonicated singularly (right hand side). The foils were sonicated for 2 minutes. The red dotted line indicates the water level; the scale bar shows cm.

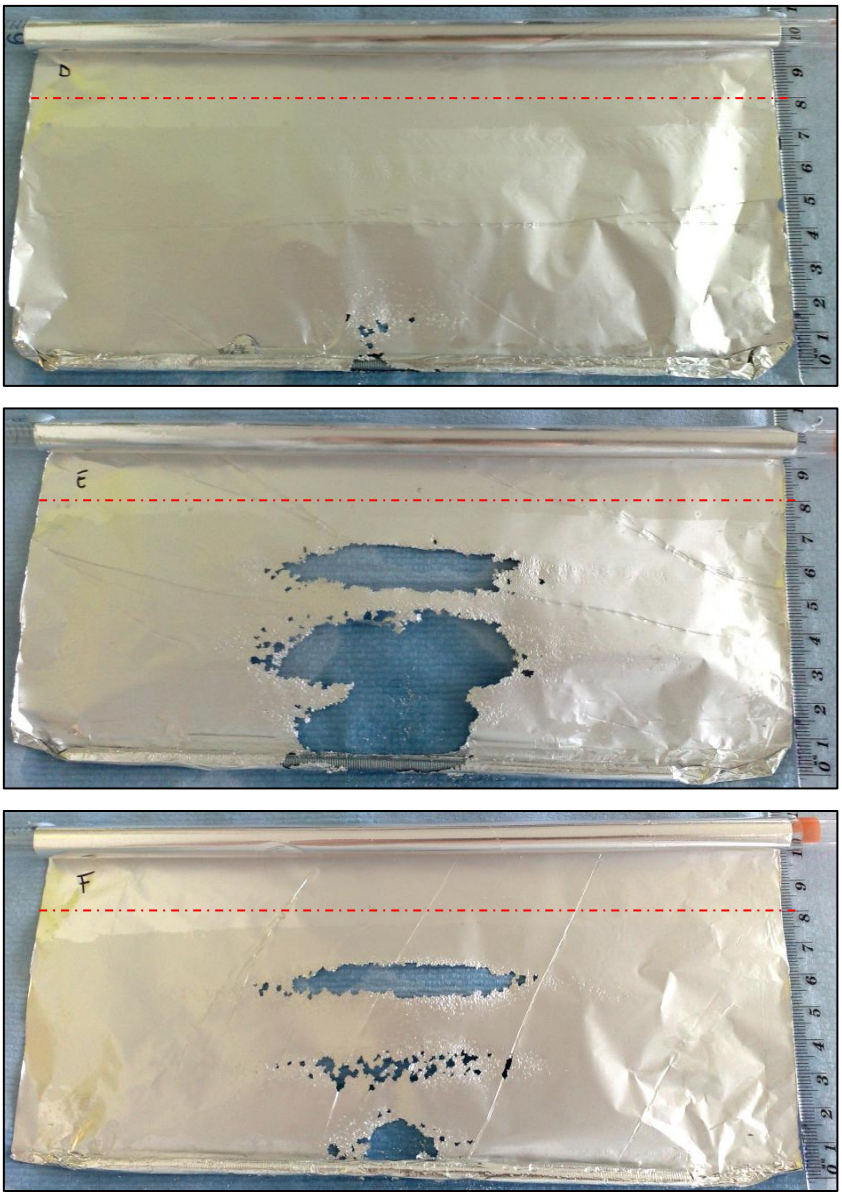

Figure 4.4 "Foil test" for Camlab bath sonicator in positions *D*, *E*, and *F*. The foils were sonicated simultaneously for 2 minutes. The foils were sonicated for 2 minutes. The red dotted line indicates the water level; the scale bar shows cm.

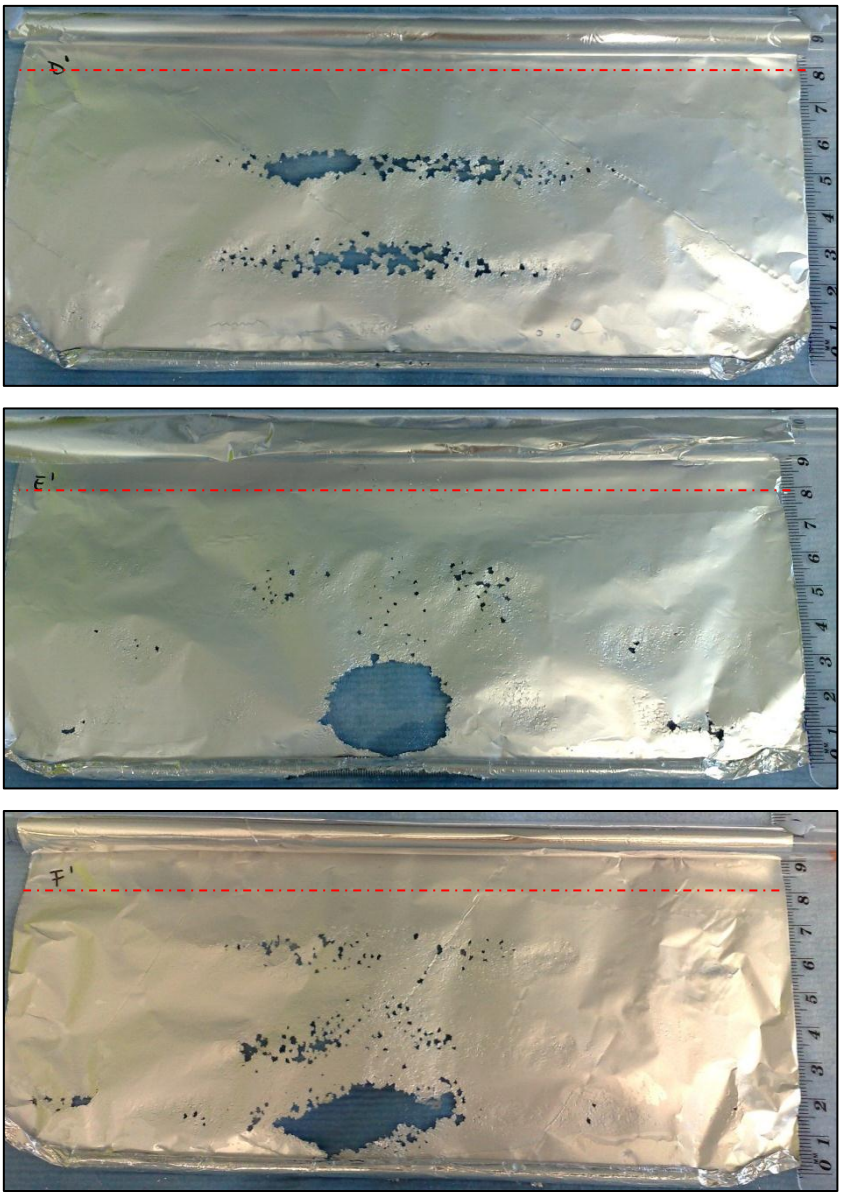

Figure 4.5 "Foil test" for Camlab bath sonicator in positions *D*, *E*, and *F*. The captions *D'*, *E'*, *F'* indicate that the foils were sonicated singularly. The foils were sonicated for 2 minutes. The red dotted line indicates the water level; the scale bar shows cm.

A foil sample was also sonicated whilst placed inside a beaker filled with either water or sunflower oil to test the hindrance of the glass wall of the beaker on the propagation of the ultrasonic waves in the two different media; the foil sample size was 4x6 cm. The foil placed in sunflower oil was sonicated for a total amount of 60 minutes in a pulsed mode (15 min on/10 min off) as no foil damage was seen for the shorter times of sonication previously employed. The foil placed in water was sonicated for a total amount of 15 minutes, while being checked after 2 minutes of sonication. The beaker

was placed in a central position within the bath and over a tray which was raised 4 cm from the bottom of the tank.

As shown in figure 4.6a, the foil sonicated in sunflower oil did not show any visible damage, whilst some damage was visible for the foil sonicated in water after 15 minutes of sonication (figure 4.6c). It has to be noted that the beaker was placed on a tray 4 cm from the bottom of the tank to avoid any possible damage induced by the direct contact of the beaker with the base of the water bath. This position is at the limit of the region of stronger effect identified during the mapping of the sonicator; this might explain why few perforations were visible in the foil sonicated in water. The viscosity of sunflower oil might also further diminish the intensity of cavitation since, as discussed in section 2.1.3, the ultrasonic waves cannot penetrate efficiently liquids with high viscosity [3], and thus no perforations are visible. In both cases the interference to the propagation of the ultrasonic power, generated by the presence of the glass wall, adds to the previously described effects, further lessening the number of perforations when compared with those obtained when the foils were sonicated directly in the water bath.

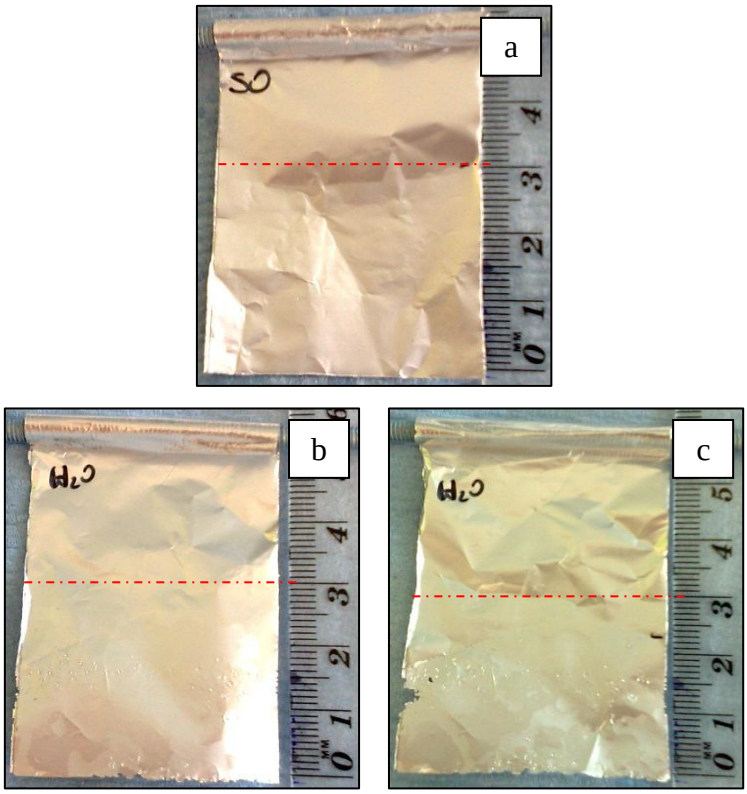

Figure 4.6 "Foil test" performed on foils placed inside a beaker. a) foil sonicated in sunflower oil for a total amount of 60 minutes; b) foil sonicated in water for 2 minutes; c) foil sonicated in water for 15 minutes. The red dotted line indicates the water level; the scale bar shows cm.

4.3.2 Ultrawave U100

The mapping was performed on the Ultrawave U100 water bath. The sizes of the aluminium foils for this water bath were 12x10 cm for positions *A*, *B*, and *C*, and 14x10 cm for positions *D*, *E*, and *F*. The foils' positions within the bath are shown in figure 4.7. The foils were sonicated in a stationary position for 10 minutes. This time was chosen since few perforations were visible after 2 minutes of sonication. The sonication was continued with the level of perforations being checked every 2 minutes of sonication, and stopped when the level of perforations obtained was similar to those obtained with the Camlab water bath (figures 4.3 – 4.5), reaching a total of 10 minutes of sonication.

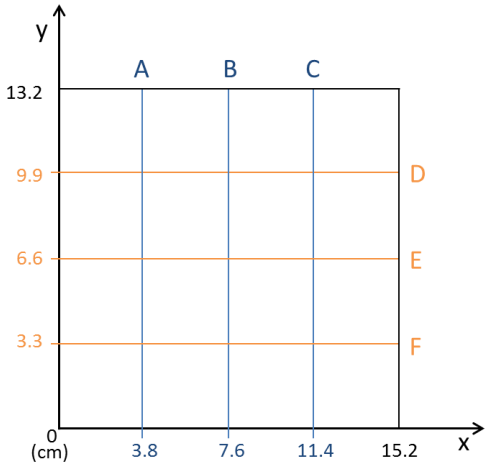

Figure 4.7 Foils positions relatively to the Ultrawave bath sonicator (top view).

As can be seen in figures 4.8 and 4.9, the major perforations were seen for the foils placed in positions *B*, *C*, *E*, and *F*, again indicating the central position as preferential in obtaining the maximum effect during sonication. As shown for the Camlab water bath in section 4.3.1, it appears that the cavitation phenomenon occurs along horizontal planes parallel to the surface of the liquid medium, but the region of major effect for the Ultrawave water bath is more uniform than observed for the Camlab water bath and is located within the first 7 cm from the bottom of the tank. In this case the perforation appeared to be more intense when the foils were sonicated singularly. It is possible to hypothesise that the aluminium foils show more perforation when sonicated singularly since the delivery of the ultrasonic power in the Ultrawave water bath is more uniform than it is in the Camlab water bath, and the presence of more foils in the bath would act more like a physical barrier inhibiting the propagation of the sound waves through the liquid.

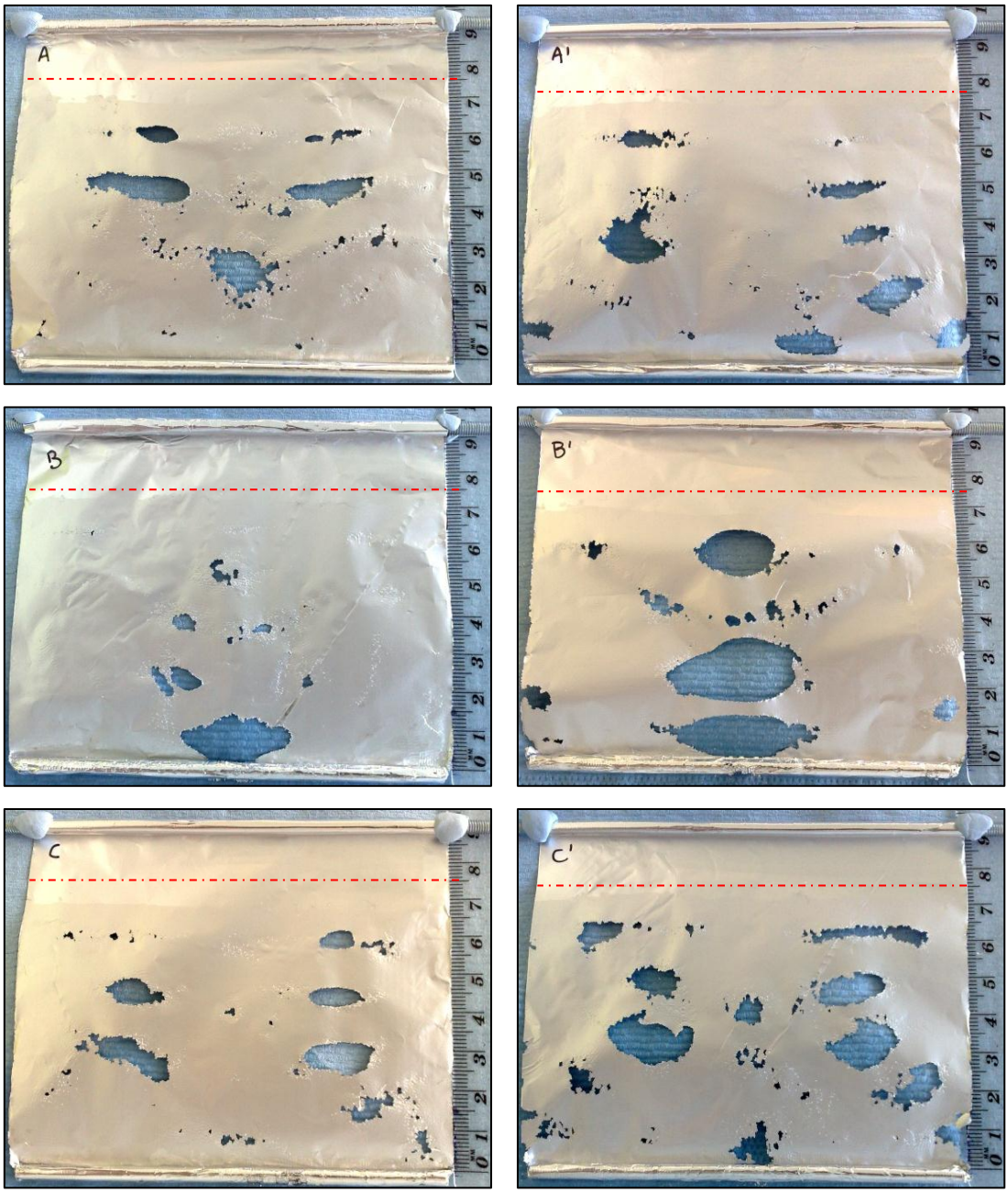

Figure 4.8 "Foil test" for Ultrawave bath sonicator in positions *A*, *B*, and *C*. The captions *A*, *B*, *C* indicate that the foils were sonicated simultaneously (left hand side), while *A'*, *B'*, *C'* indicate foils placed in the same positions within the sonicator but sonicated singularly (right hand side). The foils were sonicated for 10 minutes. The red dotted line indicates the water level; the scale bar shows cm.

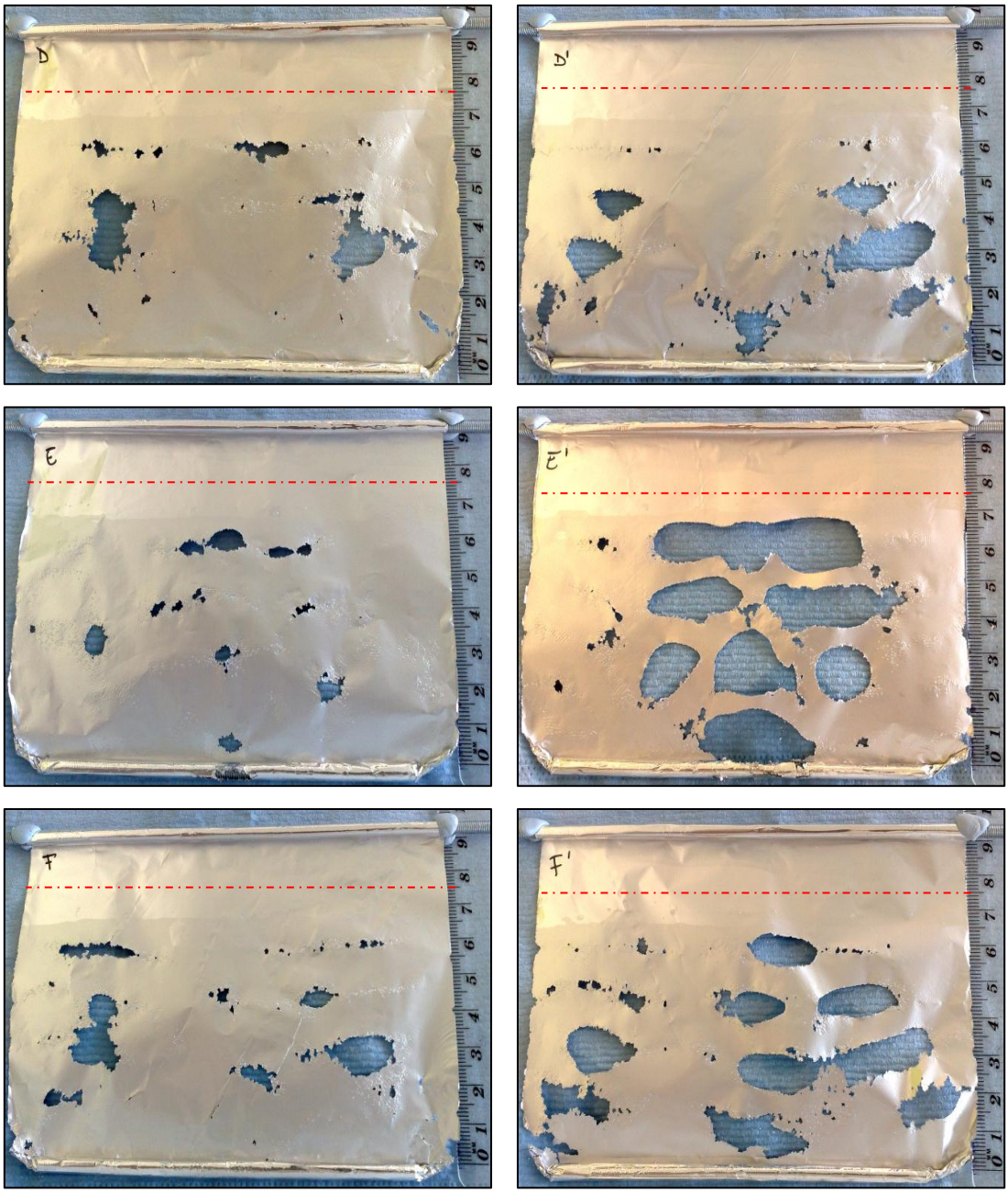

Figure 4.9 "Foil test" for Ultrawave bath sonicator in positions *D*, *E*, and *F*. The captions *D*, *E*, *F* indicate that the foils were sonicated simultaneously (left hand side), while *D'*, *E'*, *F'* indicate foils placed in the same positions within the sonicator but sonicated singularly (right hand side). The foils were sonicated for 10 minutes. The red dotted line indicates the water level; the scale bar shows cm.

A foil sample was again sonicated while placed inside a beaker filled with either water or sunflower oil to test the interference of the glass wall of the beaker on the propagation of the ultrasonic waves in the two different media; the foil size was 4x6 cm.

The foils were sonicated for a total amount of 20 minutes (10 min on/10 min off) and pictures of the foils were taken after 2, 10, and 20 minutes of sonication (see figure 4.10). The beaker was placed in a central position within the bath and over a tray which was raised 1.5 cm from the bottom of the tank.

It can be observed in figure 4.10, that the foil sonicated in sunflower oil shows some perforation events after 10 minutes of sonication; these are increased after 20 minutes of sonication. The foil sonicated in water shows perforations after 2 minutes of sonication, and these are greatly increased after 10 and 20 minutes of sonication. As was discussed in section 4.3.1 for the Camlab water bath, the glass wall of the beaker interferes with the propagation of the ultrasonic power causing a lower amount of perforations when compared with those obtained when the foils were sonicated directly in the water bath. The difference in the rate of perforations between the foil sonicated in water and the foil sonicated in sunflower oil may be again related to the difference in the viscosity of the two media, being higher for the latter so that less perforations are visible for the foil sonicated in sunflower oil.

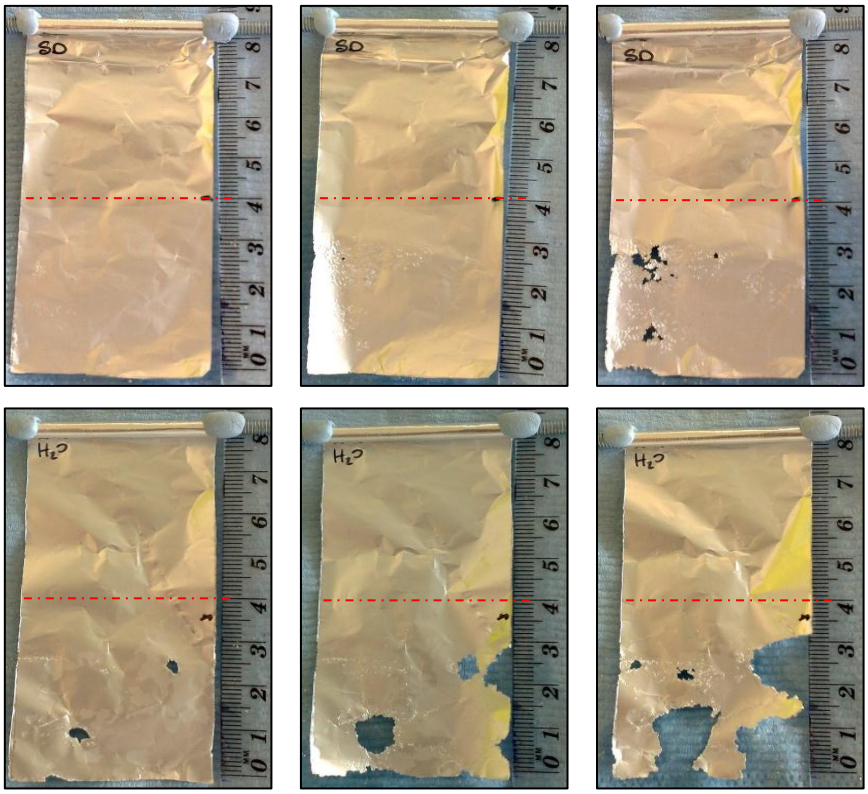

Figure 4.10 "Foil test" performed on foils placed inside a beaker. Above from left to right images of the foil sonicated in sunflower oil taken respectively after 2, 10, and 20 minutes of sonication. Below from left to right images of the foil sonicated in water taken respectively after 2, 10, and 20 minutes of sonication. The red dotted line indicates the water level; the scale bar shows cm.

4.3.3 Ultrawave SFE590 custom-built water tank

The mapping procedure was performed on a custom-built water tank linked to a 1 kW ultrasonic generator (Ultrawave SFE590); this test was performed in order to obtain preliminary data for an eventual possible scale-up of the sonication process. The size of the aluminium foils employed in this instance was 45x53 cm for all the positions. The foils' positions within the tank are shown in figure 4.11. The foils were sonicated in a stationary position for 10 minutes. This time was chosen since few perforations were visible after 2 minutes of sonication. The sonication was continued with the level of perforations being checked every 2 minutes of sonication, and stopped when the level of

perforations obtained was similar to those obtained previously with the smaller water baths, reaching a total of 10 minutes of sonication.

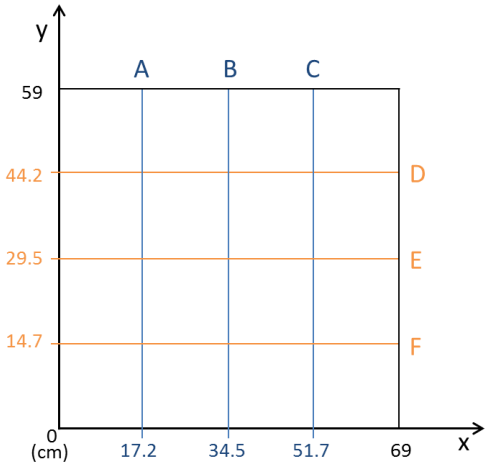

Figure 4.11 Foils positions relatively to the custom-built water tank (top view).

As can be seen in figures 4.12 and 4.13, the major perforations were seen for the foils placed in positions *B*, *E*, and *F* indicating the central position near the front of the tank as preferential to obtain the maximum effect during sonication. These positions are very similar to the positions of maximum perforations observed for the previous smaller water baths. As observed previously for the smaller water baths, it appears that the cavitation phenomenon occurs along horizontal planes parallel to the surface of the liquid medium and again are evenly spaced at half the wavelength of the sound waves; this is particularly evident in the images taken for positions *E* and *F*. There does not seem to be much difference in the level of the perforation obtained between the foils sonicated in groups and the foils sonicated singularly. This might be due to the larger size of the custom-built water tank in relationship with the dimension and position of the aluminium foils within. In particular, the relative space between the foils while sonicated simultaneously in the larger water tank would be greater when compared to the relative space between the foils sonicated in the smaller water baths; this might favour a more homogenous distribution of the ultrasonic power throughout the water tank while avoiding the barrier-like effect of the aluminium foils described for the Ultrawave water bath in section 4.3.2.

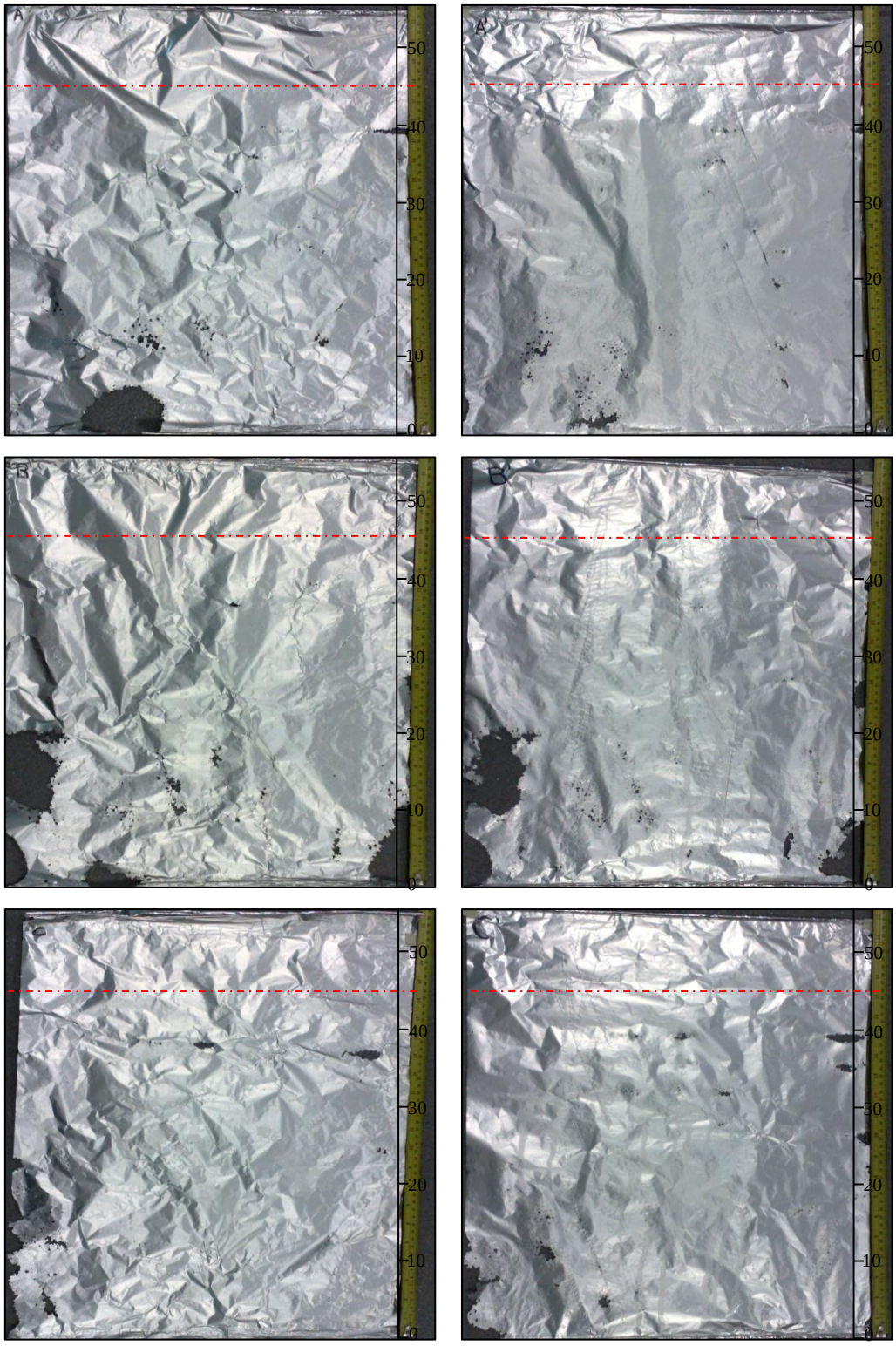

Figure 4.12 "Foil test" for the custom-built ultrasonic water tank in positions *A*, *B*, and *C*. The captions *A*, *B*, C indicate that the foils were sonicated simultaneously (left hand side), while *A'*, *B'*, *C'* indicate foils placed in the same positions within the sonicator but sonicated singularly (right hand side). The foils were sonicated for 10 minutes. The red dotted line indicates the water level; the black scale bar shows 10 cm intervals.

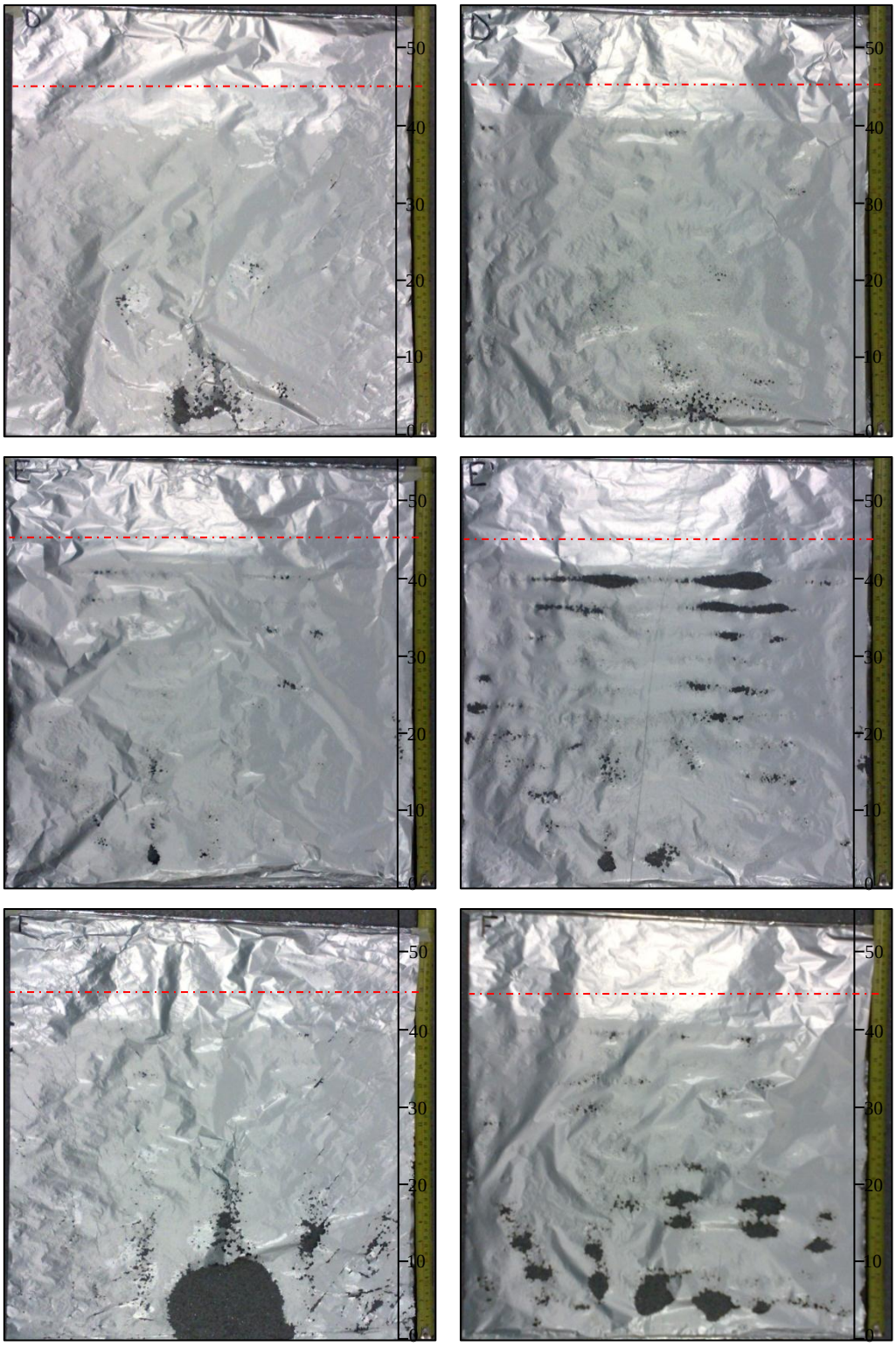

Figure 4.13 "Foil test" for the custom-built ultrasonic water tank in positions *D*, *E*, and *F*. The captions *D*, *E*, *F* indicate that the foils were sonicated simultaneously (left hand side), while *D'*, *E'*, *F'* indicate foils placed in the same positions within the sonicator but sonicated singularly (right hand side). The foils were sonicated for 10 minutes. The red dotted line indicates the water level; the black scale bar shows 10 cm intervals.

A foil sample was again sonicated while placed inside a 2 litre glass bottle filled with either water or sunflower oil to test the interference of the glass wall of the bottle on the propagation of the ultrasonic waves in the two different media; the foil size was 26x3 cm. The foil placed in water was sonicated for a total amount of 20 minutes (10 min on/10 min off) and pictures of the foil were taken after 10 and 20 minutes of sonication. The foil placed in sunflower oil was sonicated for a total amount of 60 minutes (10 min on/10 min off) and pictures of the foil were taken every 10 minutes of sonication. The bottle was placed in a central position within the tank and over a tray which was raised 25 cm from the bottom of the tank.

As can be observed in figure 4.14, the foil sonicated in sunflower oil shows some small perforations after 40 minutes of sonication, these are increased after 50 and 60 minutes of sonication. The foil sonicated in water shows perforations after 10 minutes of sonication, and these are greatly increased after 20 minutes of sonication (figure 4.15). As discussed previously for the two smaller water baths (sections 4.3.1 and 4.3.2), the glass wall interferes with the propagation of the ultrasonic power generating a lower amount of perforations when compared with those generated when the foils were sonicated directly in the water tank. Again the higher viscosity of sunflower oil is responsible for the lower efficiency of the ultrasound in generating perforations, when compared with those generated for the foil sonicated in water.

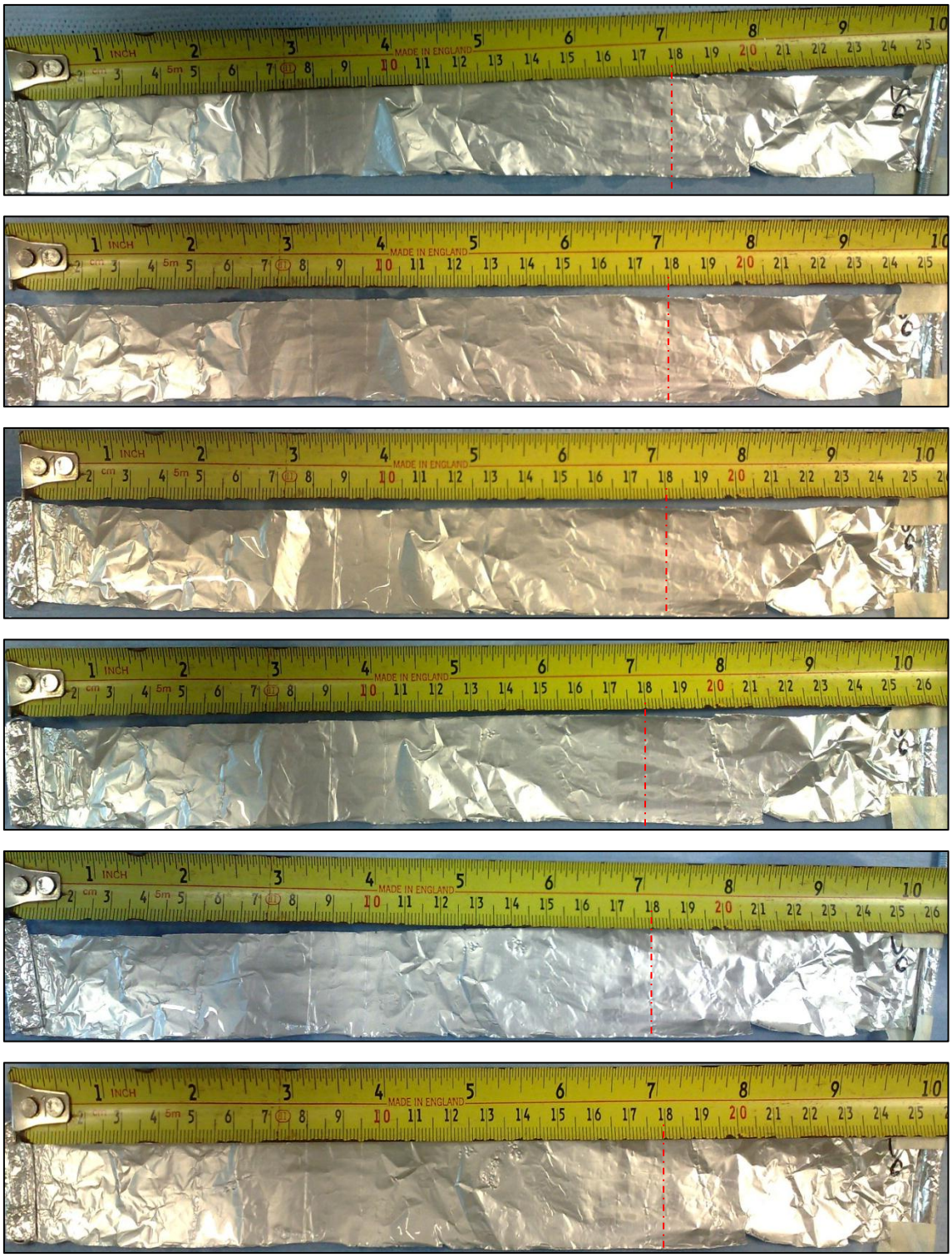

Figure 4.14 “Foil test” performed on foils sonicated inside a bottle filled with sunflower oil. The sonication time was respectively 10, 20, 30, 40, 50, and 60 minutes from top to bottom. The red dotted line indicates the water level; the scale bar shows inches and cm.

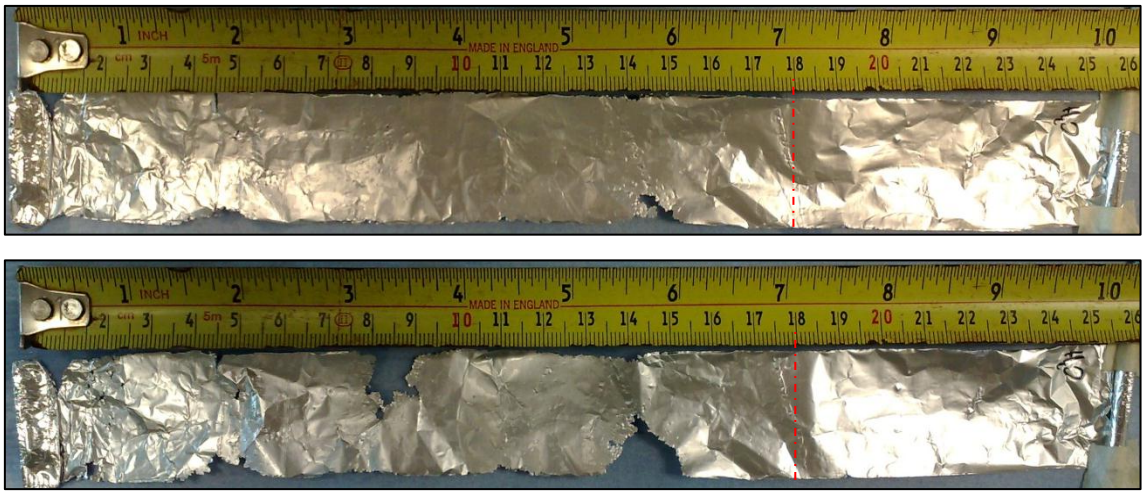

Figure 4.15 “Foil test” performed on foils sonicated inside a bottle filled with water. Above foil sonicated for 10 minutes, below foil sonicated for 20 minutes. The red dotted line indicates the water level; the scale bar shows inches and cm.

4.4 Mapping of the sonochemical reactors

The “foil tests” described in section 4.3 highlighted the presence of horizontal regions of weaker and stronger effect of the sound waves across the baths and tank sonicators; these regions correspond respectively to the nodes and the antinodes of standing waves generation during sonication [3; 90]. The standing waves are generated from the superposition of two waves with the same frequency travelling in different or opposite directions. As it is shown in figure 4.16 the points where the two travelling waves cross each other are termed nodes; in an ideal system if the two waves have the same amplitude they will cancel each other so that the amplitude at the nodes is equal to zero (zero displacement). The regions where the two travelling waves are at the maximum distance apart are the antinodes; in these regions the amplitudes of the two waves add to each other to give a greater amplitude (maximum displacement). The amplitude at the nodal and antinodal regions of the standing waves determines the extent of perforations obtained during the sonication; in particular the areas of the aluminium foil characterised by a greater amount of perforations correspond to the antinodal regions, while the areas of the foil with lower or no perforations correspond to the nodal regions [3; 90].

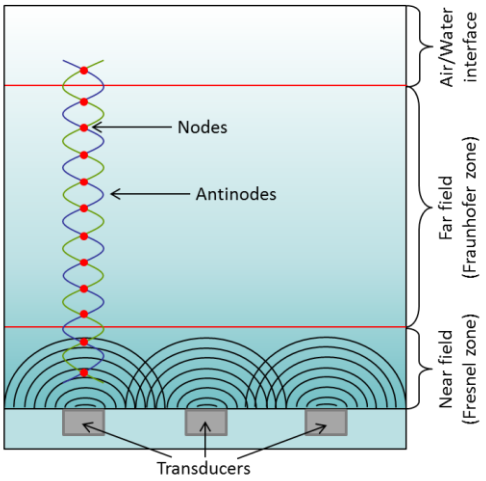

Figure 4.16 Diagram showing the interference of multiple sound waves (black). Blue and green lines represent two travelling waves overlapping and generating the standing waves; red dots indicate the nodes point.

In order to investigate the effects of nodal/antinodal positions within the sonicator systems, samples of sunflower oil were sonicated inside a measuring cylinder placed at different heights from the bottom of the bath/tank. This experiment was performed for the Camlab Transsonic T460 water bath and for the Ultrawave ultrasonic water tank since both showed regions of maximum and minimum effect; in particular the region of stronger effect identified for the water bath is below the level of the tray which raises the sample by 4 cm from the bottom of the bath. The Ultrawave U100 water bath has not been used for this investigation since it has shown a more uniform effect in the "foil test" (section 4.3.2), and its tray raises the sample only by 1.5 cm from the bottom maintaining it in the optimal region of maximum effect.

4.4.1 Camlab water bath

A sample of sunflower oil was sonicated in the Camlab water bath sonicator at 35 kHz frequency for a total amount of 60 minutes. The viscosity of the sample was measured before the sonication and after 30 minutes from the sonication to allow the sample to cool down to room temperature in order to avoid the mere temperature effect on the viscosity. The sample was sonicated inside a cylinder placed on the bottom of the bath; this raises the oil by 1.5 cm from the bottom while the meniscus is at 5 cm from the bottom of the bath, the volume of the oil being 25 ml (figure 4.17). The percentage of viscosity decrease achieved after the sonication, was compared to that achieved in the previous experiment (section 4.2) where the beaker was placed on the bath tray (which was raised 4 cm from the bottom of the bath).

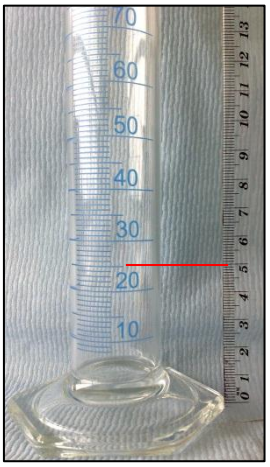

Figure 4.17 Cylinder used for the sonication, the cylinder was placed on the bottom of the bath. The red line indicates the level reached by the meniscus of the oil.

As can be seen in figure 4.18, the sonication in the lower region of the bath gave a viscosity decrease of 14.9%, whereas the decrease achieved in the upper region was 10.4% (figure 4.1a). Even though the sonication in the lower region of the bath gives a greater decrease, matching the predictions of the "foil test", the two results are still in good agreement.

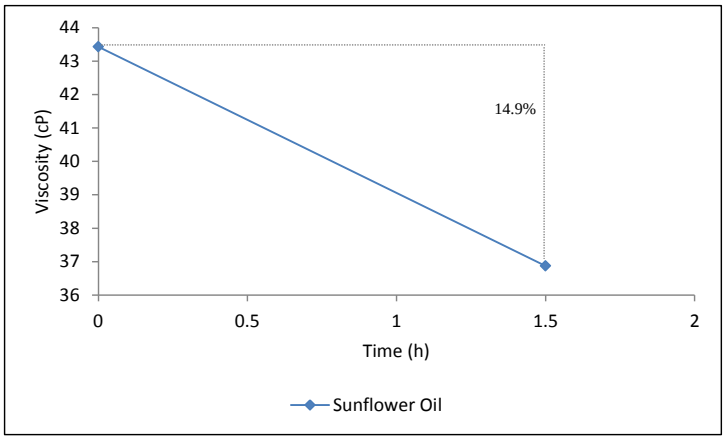

Figure 4.18 Effects of ultrasound on the viscosity of sunflower oil while sonicated in the Camlab water bath. The measurements were performed in triplicate with the standard error being shown.

4.4.2 Compared efficiency of Camlab and Ultrawave water baths

Having established the effectiveness of the ultrasound in lowering the viscosity of several differing oil samples (section 4.2), an experiment was performed in order to compare the efficiency of the two smaller ultrasonic water baths (Camlab Transsonic T460 and Ultrawave U100) in delivering the ultrasonic power to the sample.

Two individual samples of sunflower oil were sonicated in each of the water baths in a pulsed mode (15 min on/5 min off) for a total amount of 60 minutes. The viscosity of the samples was measured before sonication, after each 15 minute cycle of sonication, and 30 minutes after the sonication period to allow the samples to cool back down to room temperature.

As can be seen in figure 4.19, both the ultrasonic baths are similarly effective in lowering the viscosity of the oil; after 60 minutes of sonication, the decrease in the measured viscosity is similar for both sonicators: 23.4% for the Camlab and 25.3% for the Ultrawave sonicator, indeed the trend of viscosity decrease is consistent across the full time range investigated for both the baths. Even though the "foil test" described in

sections 4.3.1 and 4.3.2 highlighted the need to increase the time of sonication in the Ultrawave water bath to obtain the same level of perforations which were obtained in the Camlab water bath (from 2 to 10 minutes of sonication), this result shows that the two water baths have a comparable efficiency in lowering the viscosity of the oil in particular after 60 minutes of sonication.

One important detail to remember while performing the sonication in any type of water baths is that not all the nominal power of the sonicator is delivered to the sample, but some of it is dissipated through the water; this phenomenon is proportional to the volume of water contained in the water bath. According to this is it possible to explain why the two water baths here investigated have a comparable efficiency for longer times of sonication, in fact even though the Camlab water bath has a higher power output (85 W) than the Ultrawave water bath (35 W), it has to be noted that also its volume capacity is bigger (2.75 litre Camlab, 1.5 litre Ultrawave) so that, in this instance, more power is dissipated before reaching the sample. This might indicate that, for longer times of sonication, the efficiency of the two water baths are comparable due to a "generalised" homogeneity being reached in terms of the delivery of the ultrasonic power to the sample. For this reason the two water baths might be used interchangeably when longer sonication exposure periods are being considered.

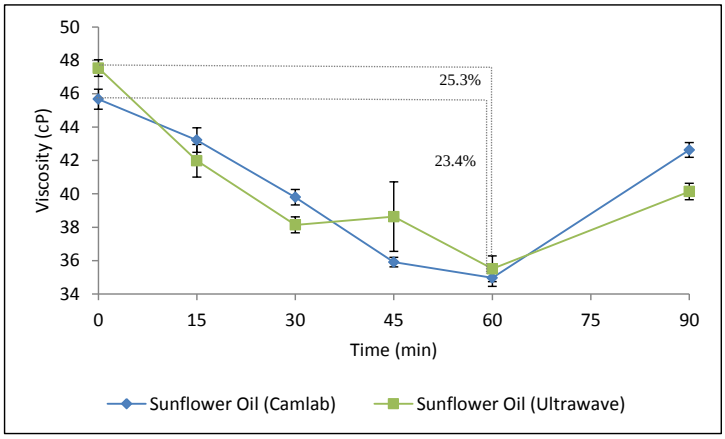

Figure 4.19 Comparison of the efficiency of the Camlab and Ultrawave bath sonicators in lowering the viscosity of sunflower oil. The measurements were performed in triplicate with the standard error being shown.

4.4.3 Custom-built water tank

A sample of sunflower oil was sonicated in the custom-built Ultrawave water tank in a pulsed mode (15 min on/10 min off) for a total amount of 60 minutes. The viscosity of the sample was measured before the sonication, immediately after the sonication, and 30 minutes after the sonication (to allow the sample to cool down to room temperature). The sample was sonicated inside a 2 litre bottle placed on a tray which raises the sample by 25 cm from the bottom of the tank (figure 4.20). Since the analysis of the viscosity is performed on a limited volume of sample, it is required to get a representative sample out of the 2 litres of oil. In order to do this, three samples of oil were taken at random levels from the 2 litre sample, the viscosity measurements were performed, and then the oil was remixed with the rest in the 2 litre bottle; this procedure was repeated for each of the points where the viscosity was measured. The percentage of viscosity decrease achieved after the sonication was compared to that achieved in the experiments performed with the smaller bath sonicators (sections 4.2 and 4.4.1).

Figure 4.20 Sunflower oil sample sonicated in the custom-built water tank. The sample was placed on a tray (red arrow) raised 25 cm from the bottom of the tank.

Figure 4.21 shows that the sonication performed in the custom-built water tank does not seem to overly affect the viscosity of the oil sample. Possible explanations for this phenomenon could be either differences in the delivery of the sonic power to the sample due to the increased volume of the sample, or differences of the amount of power

delivered to the sample between the small water bath and the larger water tank. These possibilities will therefore be investigated with further experiments.

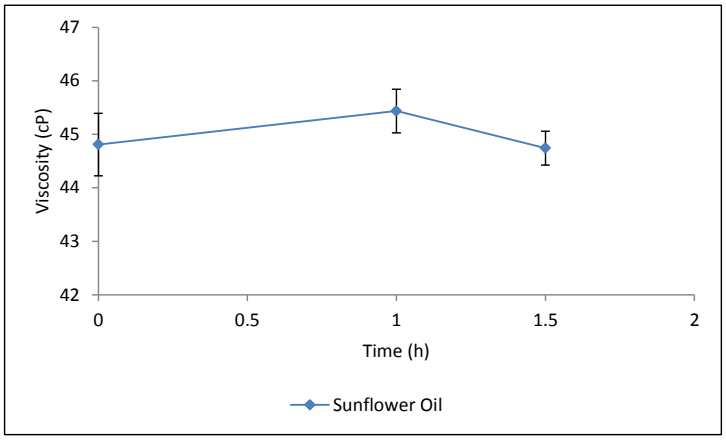

Figure 4.21 Effects of ultrasound on the viscosity of sunflower oil while sonicated in the custom-built ultrasonic water tank. The measurements were performed in triplicate with the standard error being shown.

4.4.4 Custom-built water tank efficiency

As shown in the previous section (4.4.3), the viscosity of large samples (2 litre) of sunflower oil is not affected by the sonication performed in the custom-built Ultrawave water tank, and no direct comparison with the smaller water baths is possible due to the larger volume sonicated in this instance. To gain a better understanding of the efficiency of this larger water tank sonicator and to obtain data comparable with those from the smaller water baths, samples of sunflower oil (25 ml) were placed in a central position within the tank and sonicated at different heights from its base, where the transducers are located. A long glass tube, provided with a 25 ml capacity bulb on one end, was used for this purpose (figure 4.22); since the sample here is contained within a space of 5 cm diameter, the height of each sample measurement was increased by 5 cm for every sonication event. The samples were sonicated for 60 minutes in a pulsed mode (15 min on/10 min off), and for each sonication a fresh sample of sunflower oil was used. The viscosity of the samples was measured before and immediately after the sonication. The

percentage of viscosity decrease obtained during the sonication was calculated from the viscosity level measured before exposure to sonication.

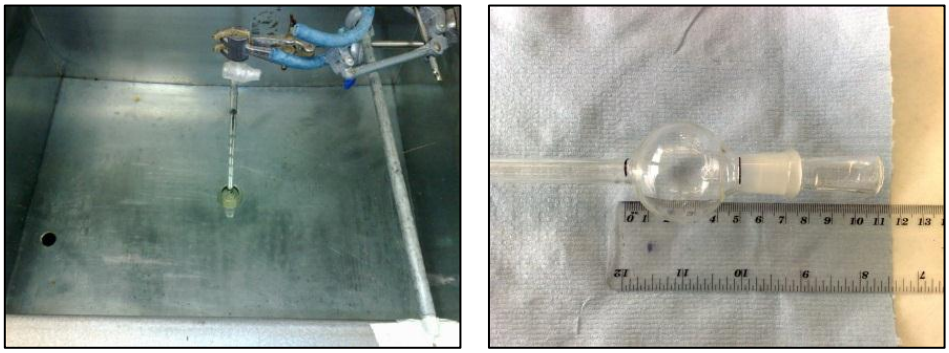

Figure 4.22 Sunflower oil sample sonicated in a central position within the custom-built water tank (left). The sample was placed inside a tube which is provided with a bulb of 25 ml capacity at its end (right).

Figure 4.23 shows the percentage of viscosity decrease obtained after the sonication of each sample when placed over the 45 cm (9 x 5 cm increments) of vertical alignment. As observed the maximum viscosity decrease obtained is 4.1% which is about 25% of the average viscosity decrease obtained with the smaller ultrasonic water baths (sections 4.2, 4.4.1, and 4.4.2). The greatest viscosity decrease is obtained for the samples sonicated in the central region at heights between 15 and 30 cm from the transducers. Positions between 0 and 10 cm from the transducers might be influenced by the irregular wave pattern which characterise the area near the five transducers (section 3.2.1) known as near field or Fresnel zone (figure 4.16 in section 4.4); in this area the travelling and standing waves interfere and cancel each other giving a lower ultrasonic efficiency. The region beyond the near field is known as far field of Fraunhofer zone, in this area the sonic field is more homogeneous and the sonic waves have the major efficiency. According to the literature the length of the near field is directly proportional to the square value of the radius of the transducer and inversely proportional to the wavelength [90] This is in good agreement with the results obtained. Positions at 35 and 40 cm from the transducers are closer to the air/water interface which is characterised by the presence of reflected standing waves which interfere and cancel each other, since the interface acts as a free boundary. For these reasons both the lower and higher

regions gave a lower efficiency in lowering the viscosity of sunflower oil, as observed and confirmed in figure 4.23.

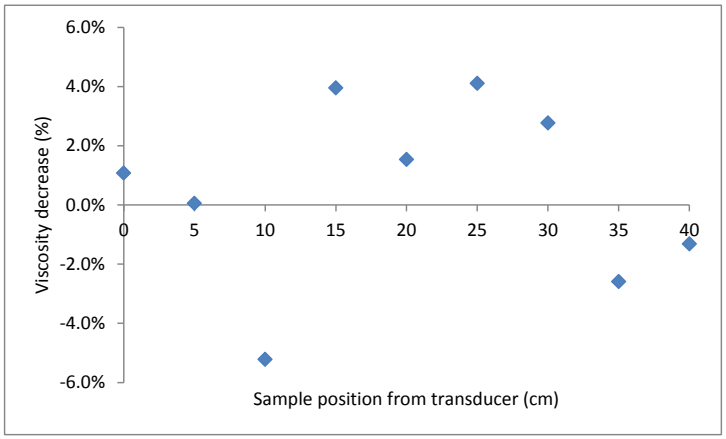

Figure 4.23 Percentage of viscosity decrease for sunflower oil while sonicated in the custom-built ultrasonic water tank at different heights from the transducers (n=1).

As shown in the "foil test" performed in section 4.3.3, areas of different efficiency can be identified within the water tank, in particular in the front and central areas. The water tank was then divided into nine areas (figure 4.24a) and each has been tested for its efficiency in lowering the viscosity of sunflower oil. The previous experiment was repeated in these nine areas concentrating on heights comprised between 15 and 30 cm from the bottom of the tank, since those gave better results previously (figure 4.23). The viscosity of the samples was measured before and after the sonication, and the percentage of viscosity decrease, obtained during the sonication period, was calculated from the value change of the viscosity level measured before sonication exposure.

The results reported in figure 4.24 seem to confirm the findings elucidated from the "foil test" experiments (section 4.3.3), where the areas with the greater efficiency are those placed in the front of the tank (areas *B*, *C*, *I*) and in the centre (areas *A* and *D*). In particular from figure 4.24b it is visible that areas *F* and *G* are those with the lowest viscosity decrease, leading to the suggestion of a lower efficiency of the transducer placed in the top right corner (under area *G*). Area *B* and *D* seem to have the greater viscosity decrease since they are influenced by ultrasonic waves coming from three different transducers each, being the transducers placed under areas *E*, *A*, and *C* for area

D, and under areas *C*, *A*, and *I* for area *B*. As can be seen in figure 4.24c, the percentage of viscosity decrease seem to be homogeneous throughout the vertical alignment for each of the areas investigated, with peaks of major effect in positions at 20-25 cm from the transducers.

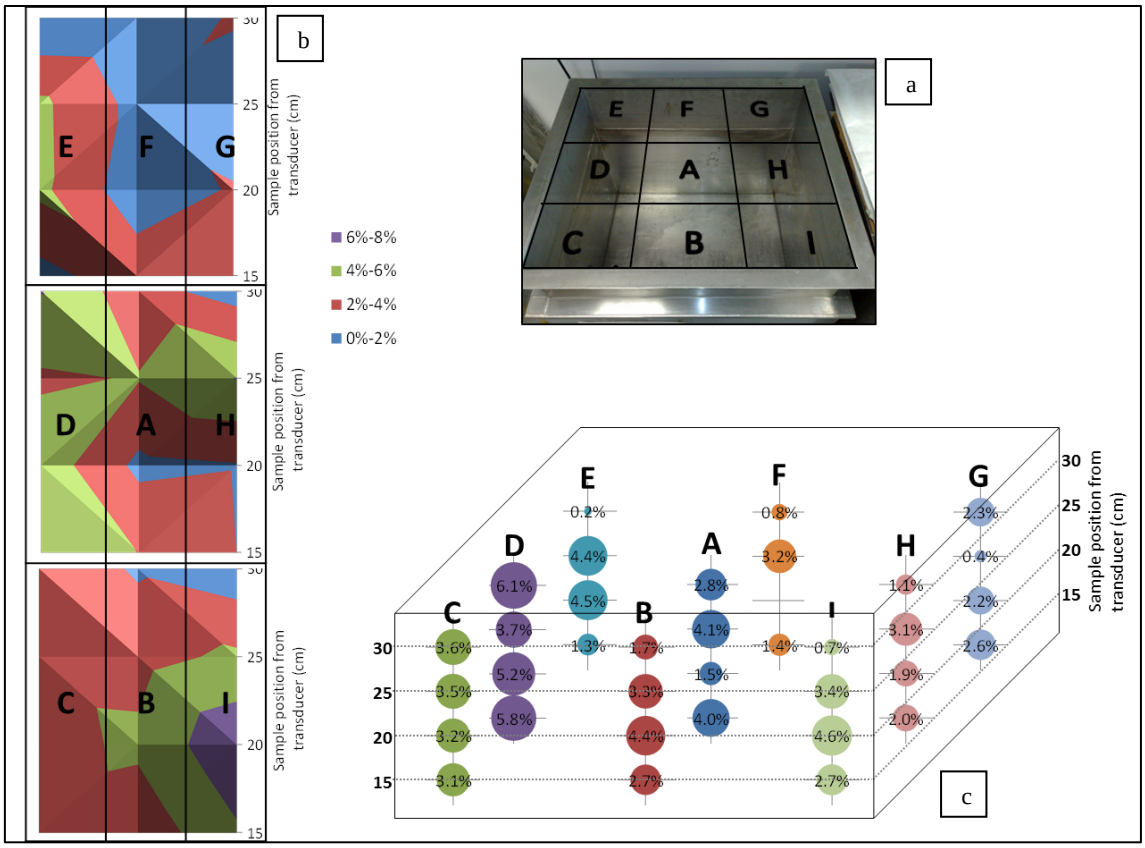

Figure 4.24 Mapping of the efficiency of the custom-built ultrasonic water tank. a) picture of the ultrasonic water tank showing the grid of the areas investigated; b) map showing the range of viscosity decrease obtained for each area; c) spheres showing the percentage of viscosity decrease for each of the positions analysed in their vertical alignment.

4.5 Chapter summary

This chapter has shown that ultrasound is effective in lowering the viscosity of a range of oil samples and that this decrease is related to the sonication time. The efficiency of different sonicators in delivering the sonic power has been tested. The two bench-sized water baths (Camlab Trannsonic T460 and Ultrawave U100) have a similar effect on the viscosity of the samples; the region of maximum effect is for both the central area of the bath which is located directly above the single transducer horn.

It has also been found that the efficiency of the custom-built water tank is about 25% of the average viscosity decrease obtained with the two smaller water baths, and that the regions of maximum effect are located in the central area near the front of the tank. In order to allow the scale-up of the process, it remains to be established the effects of the sonication of an increased volume of sample within the custom-built water tank, and also the effects of increasing the time of sonication.

The following chapters will investigate the physical and chemical effects induced by the ultrasonic power generated by the water baths on the different oils analysed. Since the investigations undertaken so far have demonstrated the two smaller water baths to be comparable, resulting in an essentially identical efficiency in lowering the viscosity of the oil, they will be used interchangeably throughout the remaining investigations.

Chapter 5

The effects of ultrasound on oil viscosity

5.1 Introduction

The previous chapter has established that ultrasound may be effective in lowering the viscosity of some model oils, and has also shown the efficiency of differing apparatus available in doing so. It is therefore now important to evaluate how stable the effect on the viscosity is and whether this decrease is permanent or transient. These characteristics will influence the possible future applications of this process, which can range from methods to improve the transportation of the oil, to alternative degradation systems, and also possibly biofuel production.

5.2 Storage effects on viscosity of oils

In order to obtain information on the storage effects on viscosity, sunflower, transformer and cable oil were sonicated in a bath sonicator at 35 kHz frequency for a total time of 60 minutes; the samples were then stored at room temperature in glass bottles for 7 days within a dark cabinet. The viscosity was measured before sonication, after 30 and 60 minutes of sonication, and every day during the storage time. To avoid the effects caused by the generalised heating of the samples generated by the sonication process, the samples were allowed to cool down to room temperature before measuring the viscosity (resting time 30 minutes).

As can be seen in figure 5.1, all the samples undergo a viscosity decrease following sonication, as described previously. Following 24 hours from the sonication, the viscosity increases again over a period of days, but does not reach the level it had before the sonication. As can be seen the viscosity settles at a value 2-5% lower with respect to the value measured prior to sonication exposure (results shown in table 5.1). A possible explanation for this behaviour could be related to the radicals formed during the cavitation phenomenon, and it seems likely that the smaller reactive chains react among themselves to give rearranged chains which are shorter and of new lower molecular weight than the original chains. This phenomenon might, thus, have parallels to the *Rice Radical Chain Mechanism* described in section 2.1.5.

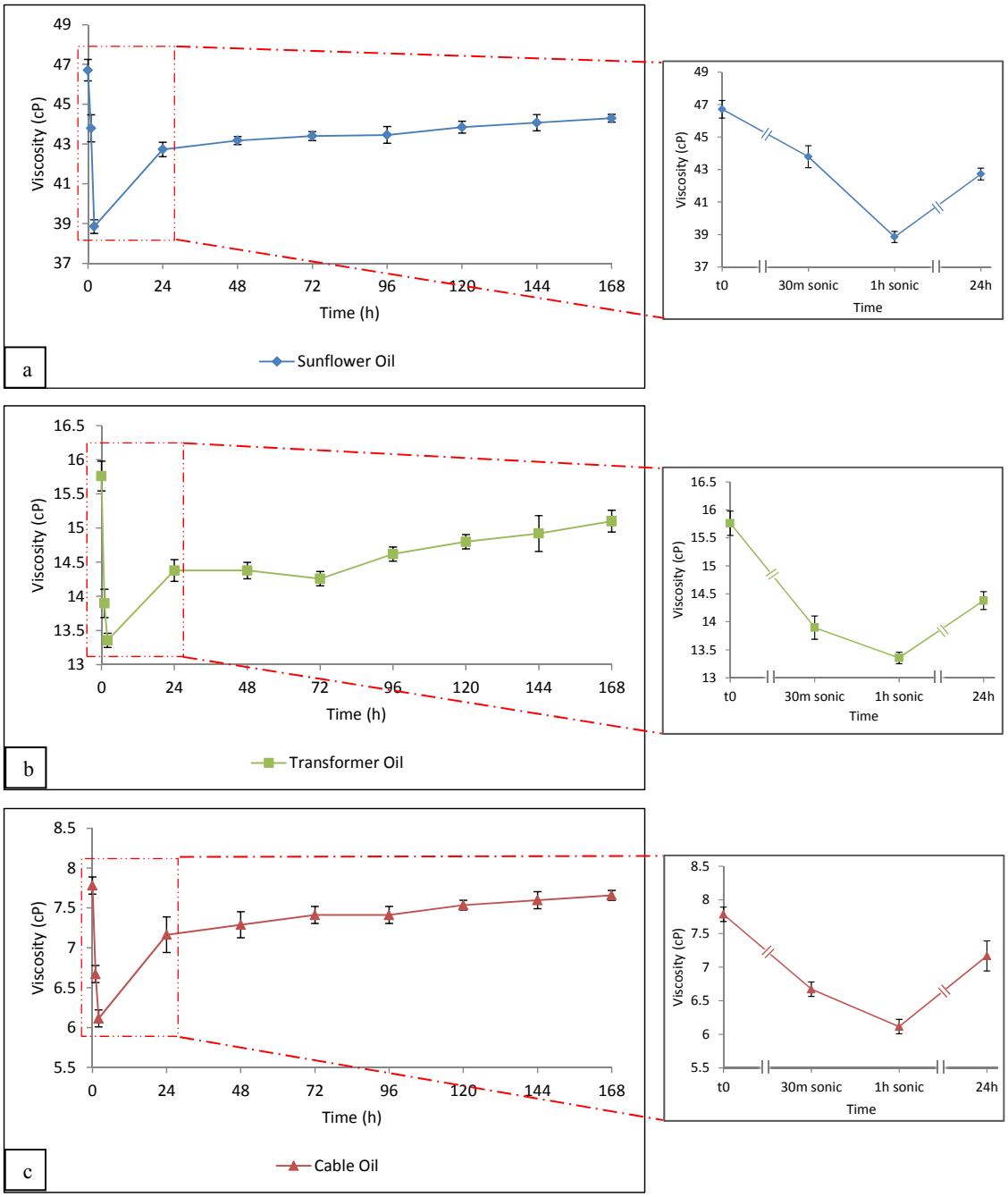

Figure 5.1 Effects of storage on the viscosity of sunflower oil (a), transformer oil (b), cable oil (c). The measurements were performed in triplicate with the standard error being shown.

Table 5.1 Viscosity values for the examined oils before the sonication (initial), after 1 hour of sonication (minimum), and after the storage time (final). The percentage of viscosity decrease at the minimum value after the sonication is also shown.

Oil	Initial viscosity (cP)	Minimum viscosity (cP)	Final viscosity (cP)	Viscosity drop at minimum value
Sunflower oil	46.7	38.8	44.3	16.8%
Transformer oil	15.8	13.4	15.1	15.3%
Cable oil	7.8	6.1	7.7	21.4%

5.3 Viscosity decreases for oils while increasing the sonication time

In parallel with the work on the effects of the storage on the viscosity, the effects of an increased sonication time on both the viscosity and the storage characteristics were investigated. For this purpose sunflower, transformer and cable oil were again sonicated at 35 kHz frequency in a bath sonicator for a total amount of 4 hours. The viscosity measurements were made before sonication, after each hour of sonication to more accurately follow the decrease, and every day of storage time (3 days at room temperature within a dark cabinet). On the day of sonication (day 0), the samples were allowed to cool down to room temperature before each measurement was made in order to avoid any temperature effects (resting time 30 minutes).

Figure 5.2 and table 5.2 show the effects of the increased sonication time; the viscosity value lowers for increasing times of sonication, reaching a maximum of decrease after 4 hours of sonication of 22.2%, 25.4% and 27.2% respectively for sunflower (figure 5.2a), transformer (figure 5.2b) and cable oil (figure 5.2c). The increased sonication time does not seem to affect the behaviour of the viscosity during the later storage time; in fact after 24 hours from the sonication the viscosity increases again following the same trend described in section 5.2. This tendency seems to support the chains rearrangement hypothesis previously described (section 2.1.5).

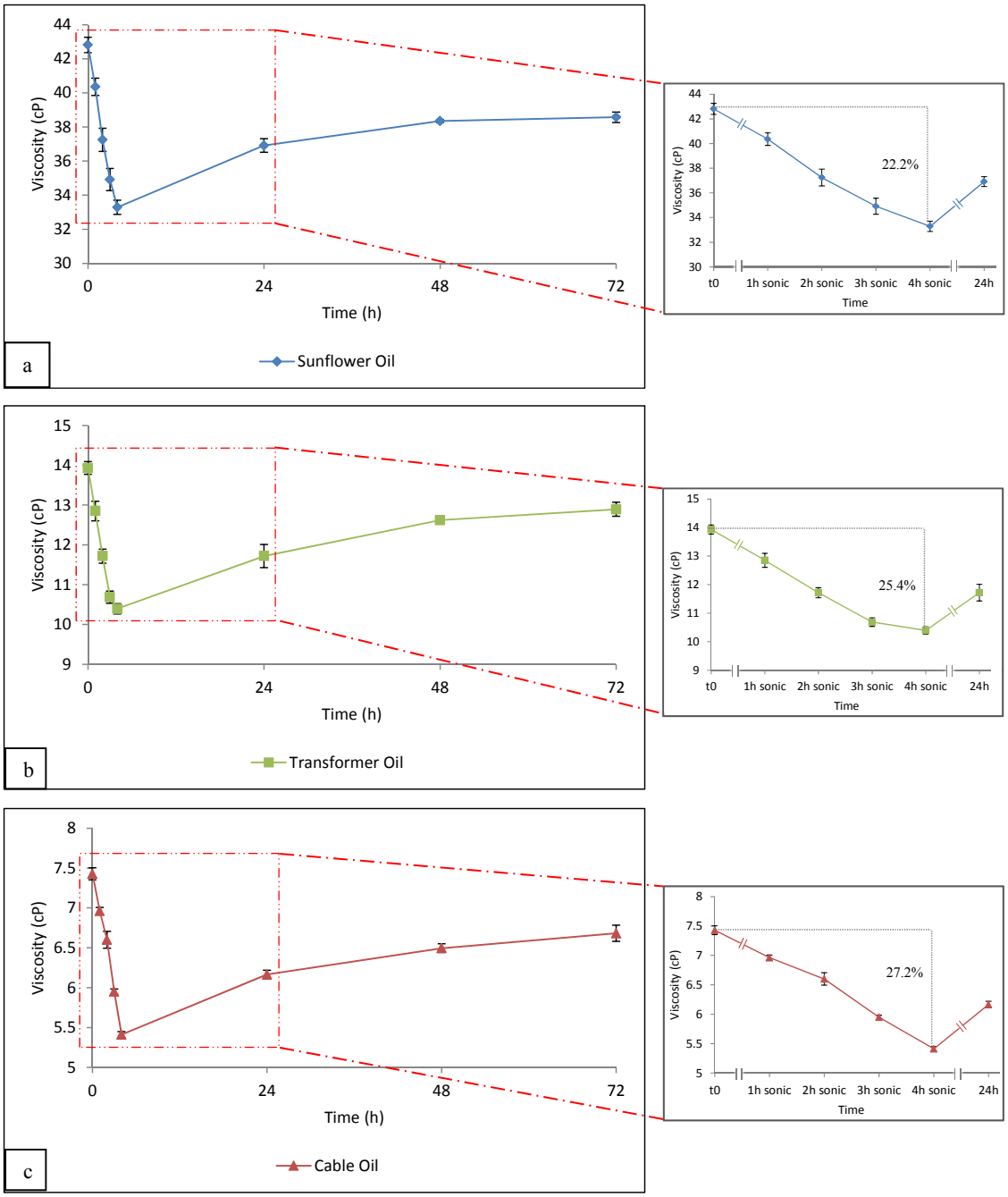

Figure 5.2 Effects of long time sonication on the viscosity of sunflower oil (a), transformer oil (b), cable oil (c). The measurements were performed in triplicate with the standard error being shown.

Table 5.2 Viscosity values for the examined oils before the sonication (initial), after 4 hours of sonication (minimum), and after the storage time (final). The percentage of viscosity decrease at the minimum value after the sonication is also shown.

Oil	Initial viscosity (cP)	Minimum viscosity (cP)	Final viscosity (cP)	Viscosity drop at minimum value
Sunflower oil	42.8	33.3	38.6	22.2%
Transformer oil	13.9	10.4	12.9	25.4%
Cable oil	7.4	5.4	6.7	27.2%

5.4 Viscosity and the effects of introducing a nucleating agent

As reported in the literature [20; 92], the cavitation effects can be improved by enhancing the cavitation rate by adding to the sonication medium gases or particles which increase the numbers of nuclei; with this purpose carbon black (CP) was added to sunflower oil as a nucleating agent. Samples of sunflower oil with carbon black (0.1% – 1% – 2% w/w) and sunflower oil without carbon black (control) were sonicated for 60 minutes in a bath sonicator at 35 kHz frequency and were then stored at room temperature for 5 days within a dark cabinet. Following the sonication, the samples to which carbon black was added were centrifuged at 4000 rpm for 15 minutes in order to remove the carbon to allow the viscosity measurements (the effects of the centrifugation procedure on these samples are reported in section 6.2). The viscosity was measured before the sonication, following sonication (having allowed the samples to cool down to room temperature - resting time 30 minutes), and each day of storage.

As shown in figure 5.3, the viscosity decrease for the control sample is 2.0% (blue line), while for the samples to which carbon was added is more pronounced reaching 5.1% when 0.1% carbon black is added (green line), 6.9% for 1% carbon sample (red line), 9.4% for 2% carbon sample (purple line). As reported in table 5.3, 24 hours after the sonication a further viscosity decrease could be seen for all the samples to which CP was added, reaching 9.4% for the 0.1% carbon sample, 10.9% for the 1% carbon sample and 13.2% for the 2% carbon sample, while the control sample shows an increase in the

viscosity as previously described. In this way carbon seems not only to increase the rate of cavitation during ultrasound irradiation, but also possibly to "protect" the broken chains from early rearrangements while favouring some scission processes during the first 24 hours after the sonication. After 48 hours from the sonication, and during the following days, the viscosity shows a tendency to increase again but without reaching the value measured before the sonication.

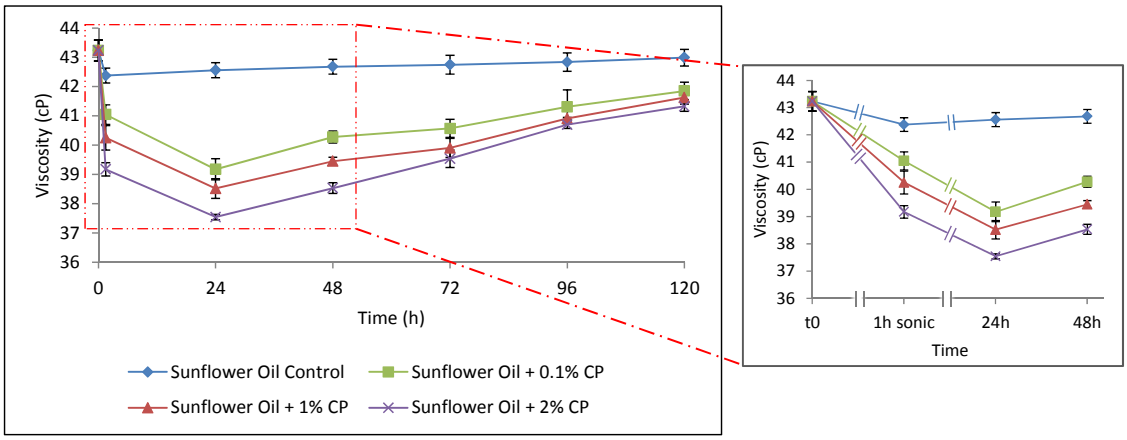

Figure 5.3 Effects of nucleating agent on viscosity. The measurements were performed in triplicate with the standard error being shown.

Table 5.3 Viscosity values for sunflower oil samples sonicated in the presence of different concentrations of carbon black (CP) before the sonication (initial), after 1 hour of sonication, after 24 hours from the sonication, and after the storage time (final). The percentage of viscosity decrease at the minimum value after the sonication is also shown.

Oil	**Initial viscosity (cP)**	**Viscosity after 1 hour sonication (cP)**	**Viscosity after 24 hours from sonication (cP)**	**Final viscosity (cP)**	**Viscosity drop at minimum value**
Sunflower oil control	43.2	42.3	42.5	42.9	2.0%
Sunflower oil + 0.1% CP	43.2	41.0	39.2	41.8	9.4%
Sunflower oil + 1% CP	43.2	40.2	38.5	41.6	10.9%
Sunflower oil + 2% CP	43.2	39.2	37.5	41.3	13.2%

5.5 Viscosity minimum investigation

In order to investigate the effects of the nucleating agent during the first 24 hours after sonication and to determine the minimum value reached by the viscosity of the oil when the nucleating agent is added, a time course experiment was undertaken. Samples of sunflower oil with carbon black (0.1% and 1% w/w) (CP) and sunflower oil without carbon black (control) were sonicated for 60 minutes in a bath sonicator at 35 kHz frequency. The samples to which carbon black was added were then centrifuged at 4000 rpm for 15 minutes to remove the carbon. The viscosity measurements were made before sonication, after the sonication (having allowed the samples to cool down to room temperature - resting time 30 minutes), and every 6 hours for a total of 48 hours. The samples were stored at room temperature in glass bottles within a dark cabinet.

As could be seen in figure 5.4, the further decrease in the viscosity, obtained in the samples to which the nucleating agent was added, mainly occurs during the first 30 hours after sonication, with a minimum being observed after 24 hours. Between a period of 30 and 42 hours after the sonication, an increase could be seen in the viscosity and this follows the trend described in section 5.4.

Since there appears to be relatively small differences between the viscosity decrease obtained with the higher concentrations of carbon (1% and 2% w/w) and the lowest concentration (0.1% w/w), possibly due to an effective saturation of the solution, the 0.1% w/w concentration was therefore been chosen for the following experiments.

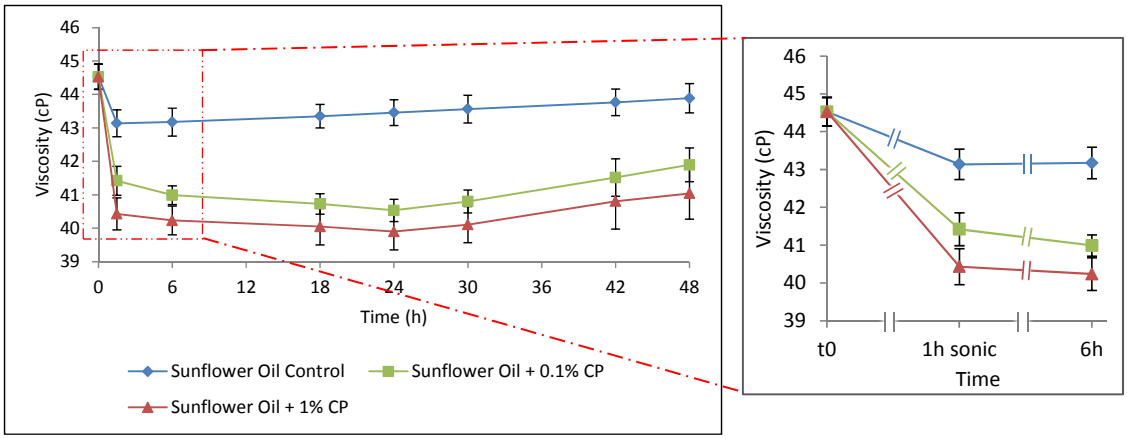

Figure 5.4 Effects of nucleating agent on viscosity during the first 48 hours. The measurements were performed in triplicate with the standard error being shown.

5.6 Use of carbon nanotubes as nucleating agents

The efficiency of carbon black (CP) as nucleating agent was compared to that of carbon nanotubes (CNTs) in order to establish which of these compounds yielded enhanced viscosity decreases. One sample of sunflower oil was added with 0.1% w/w carbon black, while another sample was added with 0.1% w/w carbon nanotubes; these two samples plus another sample of fresh sunflower oil (control) were sonicated in a bath sonicator at 35 kHz frequency for 60 minutes. After the sonication, the samples to which the nucleating agents were added were centrifuged at 6000 rpm for 15 minutes. The viscosity measurements were made before sonication, after the sonication (having allowed the samples to cool down to room temperature - resting time 30 minutes), and every 24 hours after the sonication for 72 hours. The samples were stored at room temperature in glass bottles within a dark cabinet.

As can be seen in figure 5.5, carbon nanotubes act as effective nucleating agents since they give rise to an enhanced drop in the viscosity compared to that achieved by the ultrasound itself. In this context carbon black is still, however, the most effective nucleating agent. It should be noted that, in a recent communication, the UK Health and Safety Executive has pointed out that CNTs may cause lung inflammation and fibrosis, and so are potentially harmful and require specific facilities to be used [93]. Having

shown that the effect of CNTs is lower than that achieved with carbon black and taking into account the HSE communication, CNTs were therefore not used any further in this work.

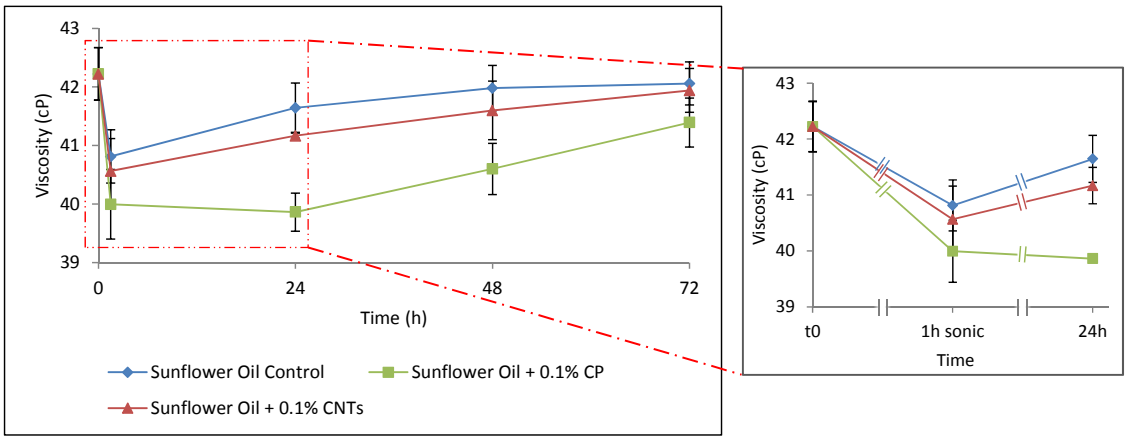

Figure 5.5 Efficiency of carbon nanotubes as nucleating agent. The measurements were performed in triplicate with the standard error being shown.

5.7 Use of carbon plasma black as nucleating agents

The efficiency of carbon black (CP) as a nucleating agent was compared to that of carbon plasma black (CPLS) in order to establish which of these compounds gave the better viscosity decrease. One sample of sunflower oil was added with 0.1% w/w carbon black, while another sample was added with 0.1% w/w carbon plasma black; these two samples plus another sample of fresh sunflower oil (control) were sonicated in bath sonicator at 35 kHz frequency for 60 minutes. After the sonication, the samples to which the nucleating agents were added were centrifuged at 6000 rpm for 15 minutes. The viscosity measurements were made before sonication, after the sonication (having allowed the samples to cool down to room temperature - resting time 30 minutes), and every 24 hours after the sonication for 72 hours. The samples were stored at room temperature in glass bottles within a dark cabinet.

As shown in figure 5.6, carbon plasma black and carbon black seem to have a similar effect as nucleating agents. While the effects on the viscosity are comparable, it is

important to notice that CP is easily removed from the sample through the centrifugation process. In contrast CPLS can not be easily removed by centrifugation (figure 5.7) and because of this, carbon black was used as the preferred nucleating agent for all the following work.

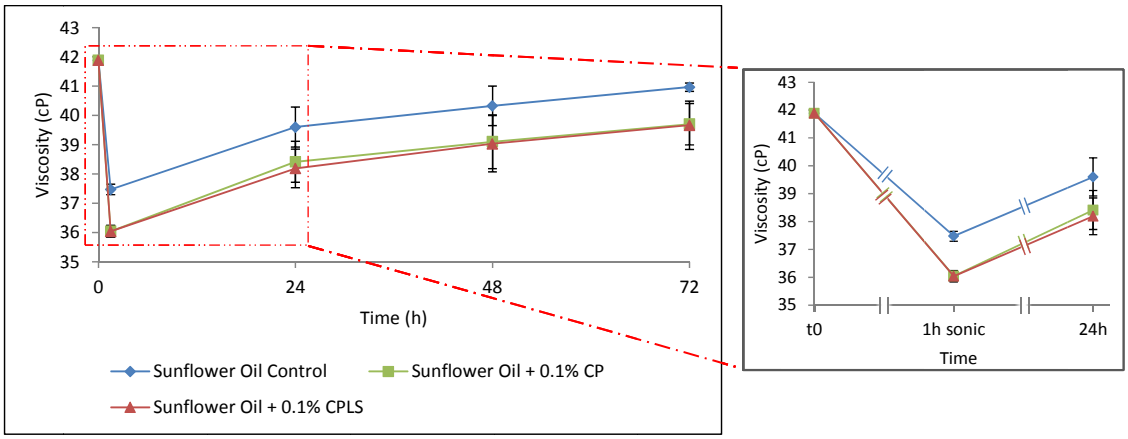

Figure 5.6 Efficiency of carbon plasma black as nucleating agent. The measurements were performed in triplicate with the standard error being shown.

Figure 5.7 Picture of the samples after centrifugation at 6000rpm for 15 minutes. From left to right: sunflower oil control, sunflower oil + 0.1% carbon black, sunflower oil + 0.1% carbon plasma black.

5.8 Chapter summary

This chapter has shown that ultrasound is effective in lowering the viscosity of the analysed oils in a time dependent way and that this decrease can be further increased by the addition of nucleating agents. Carbon black is the preferred nucleating agent for its ease of use, optimal results obtained, and safety. The achieved lower level of viscosity, with or without the nucleating agent, is however not stable and the viscosity increases during further storage. A possible explanation for this behaviour is the formation, during sonication, of low molecular weight radical species which, if left free, react with themselves forming new chains thus increasing the viscosity of the sample. The formation of radical species during sonication will be further investigated in the following chapter.

Chapter 6

The radical theory

6.1 Introduction

As discussed in section 2.1.5, many studies describe the generation of radical species during treatment with ultrasound and highlight that these are responsible for inter- and intra-molecular rearrangements within the sample, so that ultrasound is commonly applied in polymer and copolymer synthesis [18; 22; 23]. In this section the generation of radicals during sonication and their action will be investigated in order to confirm this radical theory in the range of oils under study in this work.

6.2 Viscosity is stabilised via the addition of a radical scavenger

As discussed before (section 5.2), the generation of radicals during sonication is likely to induce chain rearrangement during the storage time and therefore a radical scavenger (4-tert-butylphenol) was consequently used in order to confirm this hypothesis.

One sample of each sunflower, transformer and cable oil was added with 0.1% w/w carbon black (CP). These samples plus another fresh sample of each of the oils (control) were sonicated in the bath sonicator at 35 kHz frequency for 60 minutes. Immediately after the sonication, the samples to which carbon black was added were centrifuged at 4000 rpm for 15 minutes in order to remove the carbon. After 24 hours from the termination of sonication 4-tert-butylphenol at 0.1 mM was added to these samples. As previously reported (sections 5.4 and 5.5), 24 hours is the point at which the viscosity is at the lowest level for this procedure. After sonication all the samples were stored at room temperature for 9 days within a dark cabinet. The viscosity measurements were made before sonication, after the sonication having allowed the samples to cool down to room temperature (resting time 30 minutes), after 24 hours from the sonication terminating (before the addition of the scavenger), and every day of storage.

As could be seen in figure 6.1 the addition of 4-tert-butylphenol, to the sample to which carbon black was added, stabilises the recorded sample viscosity at the minimum value reached after 24 hours from the sonication. In this way 4-tert-butylphenol acts as a chain

terminator preventing the chain rearrangements responsible for the increase of the viscosity which characterises the control sample, as described in section 5.2.

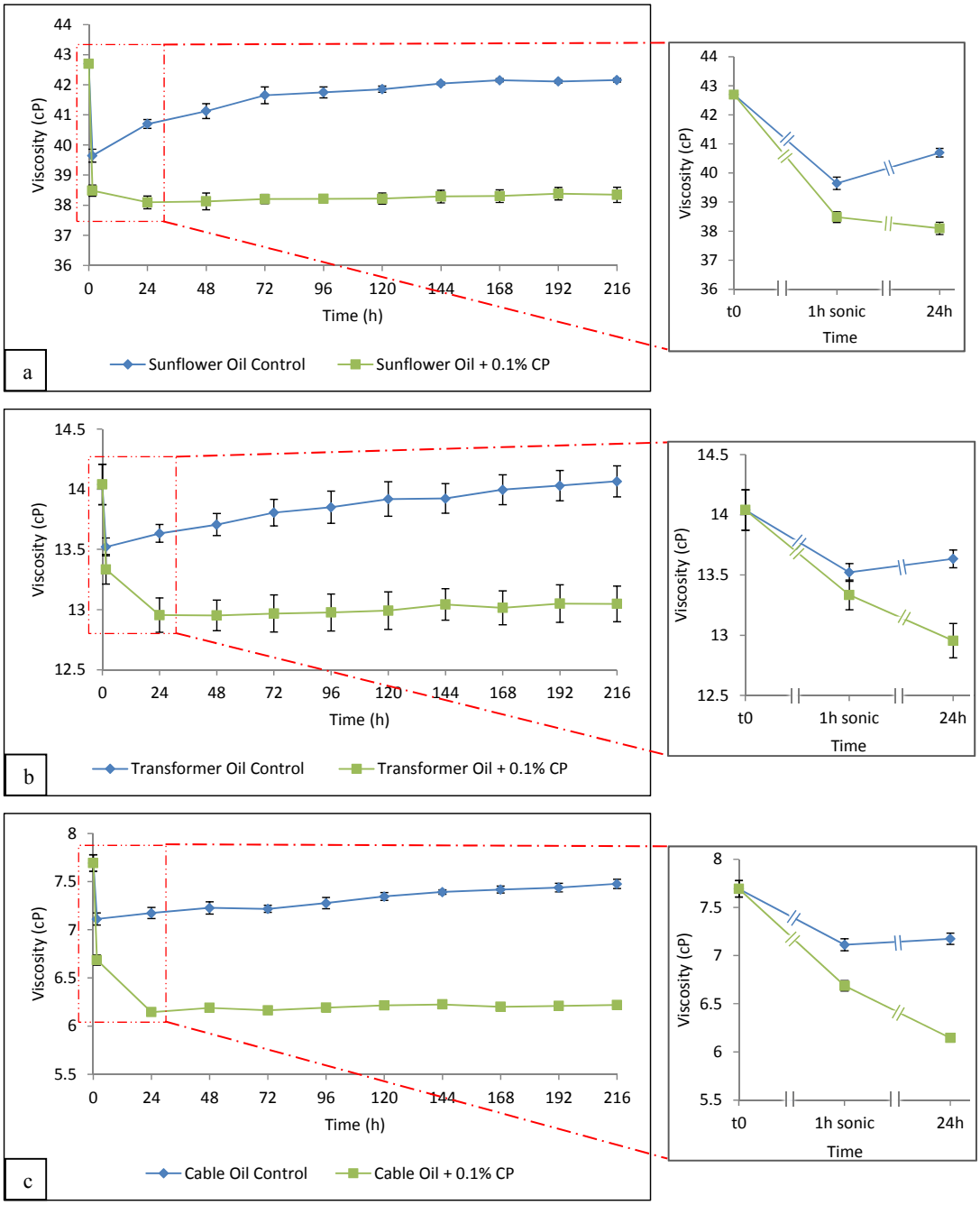

Figure 6.1 Effects of the radical scavenger on sunflower oil (a), transformer oil (b), cable oil (c). 4-tert-butylphenol was added after 24 hours from the sonication to the samples which were sonicated in the presence of carbon black (green line). The measurements were performed in triplicate with the standard error being shown.

In a control experiment three samples of sunflower, transformer and cable oil were sonicated in a bath sonicator at 35 kHz frequency for 60 minutes. Following sonication one of the samples was centrifuged at 4000 rpm for 15 minutes, the viscosity of this sample was then measured and then 4-tert-butylphenol at 0.1 mM was immediately added to act as radical scavenger. After 24 hours from this initial sonication period 4-tert-butylphenol 0.1mM was then added to another of the sonicated samples for the same purpose; the third sample (control) was just sonicated with no scavenger added. Viscosity measurements were taken before sonication, 30 minutes after the sonication, and then every 24 hours for 3 days. Measurements were taken before the addition of the scavenger when required. The samples were stored at room temperature in glass bottles within a dark cabinet.

As it is shown in figure 6.2, 4-tert-butylphenol stabilises the obtained lower level of viscosity for each of the samples to which is added - independently from any treatment (centrifugation) performed on the samples. It can therefore be said that the centrifugation procedure does not seem to have any effect on the viscosity since, for the sample which was centrifuged, the viscosity measured 30 minutes after the sonication is very similar to that of the samples which did not undergo this procedure.

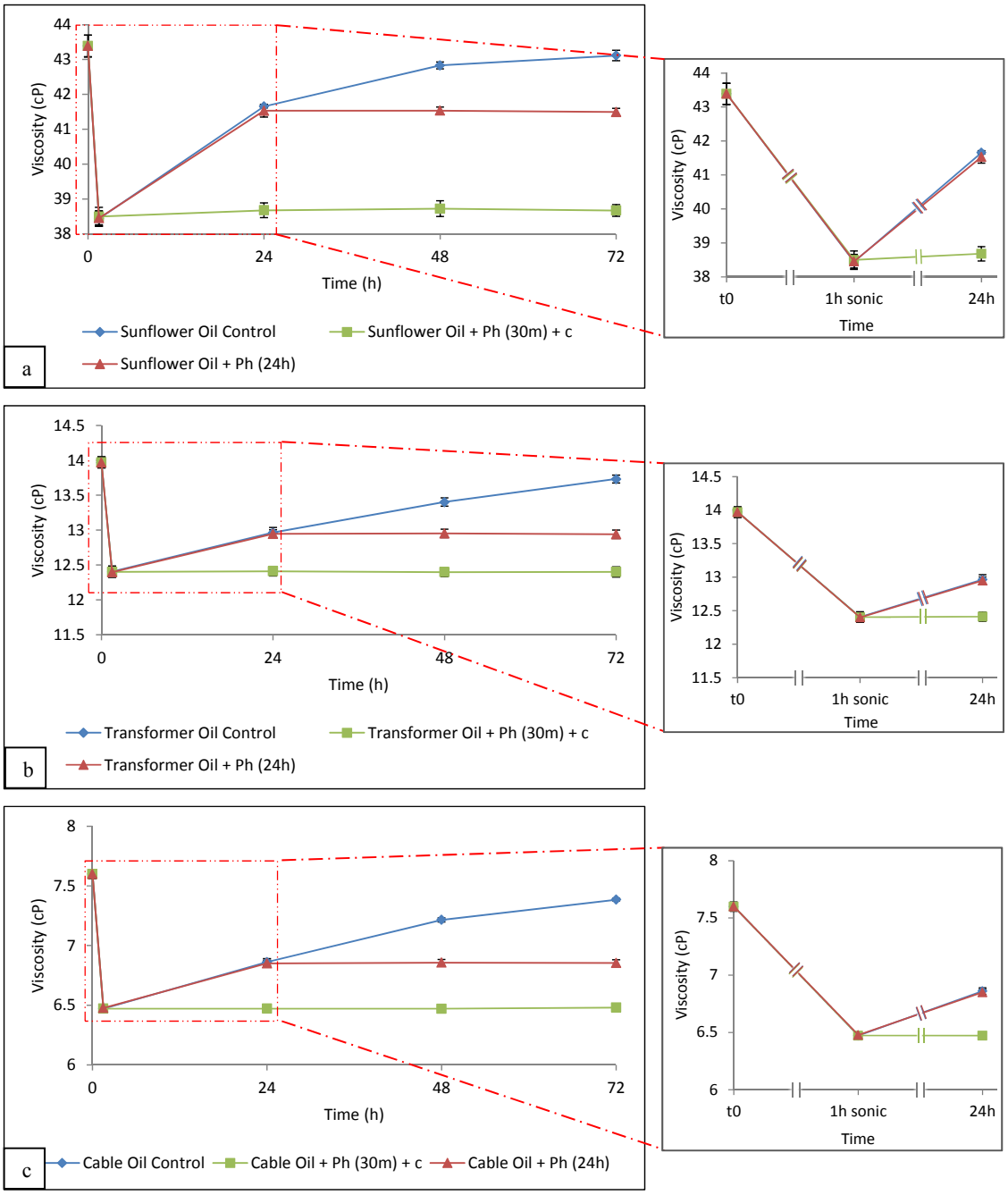

Figure 6.2 Effects of the radical scavenger on sunflower oil. 4-tert-butylphenol (Ph) was added to two of the samples after 30 minutes from the sonication (green line) and after 24 hours from the sonication (red line). The first of these two samples was also centrifuged at 4000 rpm for 15 minutes prior to the addition of the scavenger (green line). The measurements were performed in triplicate with the standard error being shown.

6.3 Viscosity of oils and the effects of sonication time when the nucleating agent is used

The effects described in section 5.4 and in section 6.2 were then investigated in addition to the effects of an increased sonication time on the viscosity of two samples of sunflower, transformer and cable oil. To one sample (of each of the oils), 0.1% w/w of carbon black (CP) was added to increase the cavitation events; the other sample was left untreated (control). All the samples were then sonicated at 35 kHz frequency in a bath sonicator for a total amount of 4 hours. Immediately after the sonication, the samples to which carbon black was added were centrifuged at 4000 rpm for 15 minutes in order to remove the carbon. After 24 hours from the termination of the sonication 4-tert-butylphenol at 0.1 mM was added to these samples. Viscosity measurements were made before sonication, after the total sonication time (having allowed the samples to cool down to room temperature - resting time 30 minutes), after 24 hours from the sonication (but before the addition of the scavenger), and every 24 hours for a total amount of 72 hours. The samples were stored at room temperature in glass bottles within a dark cabinet.

As can be seen in figure 6.3, the addition of the nucleating agent greatly enhances the viscosity lowering effect for all the measured samples. In particular, after 4 hours of sonication, sunflower oil viscosity decrease reaches 1.9% without carbon and 3.9% with carbon (a), transformer oil 12.6% and 16.9% without and with carbon (b), cable oil 11.8% and 20.1% without and with carbon (c). After 24 hours from the sonication period the samples to which carbon was added, show further viscosity decreases reaching 4.9%, 17.3%, 20.3% respectively, as reported in section 5.4. The addition of the radical scavenger to the samples to which carbon was added, stabilises the lower viscosity level as previously reported in section 6.2.

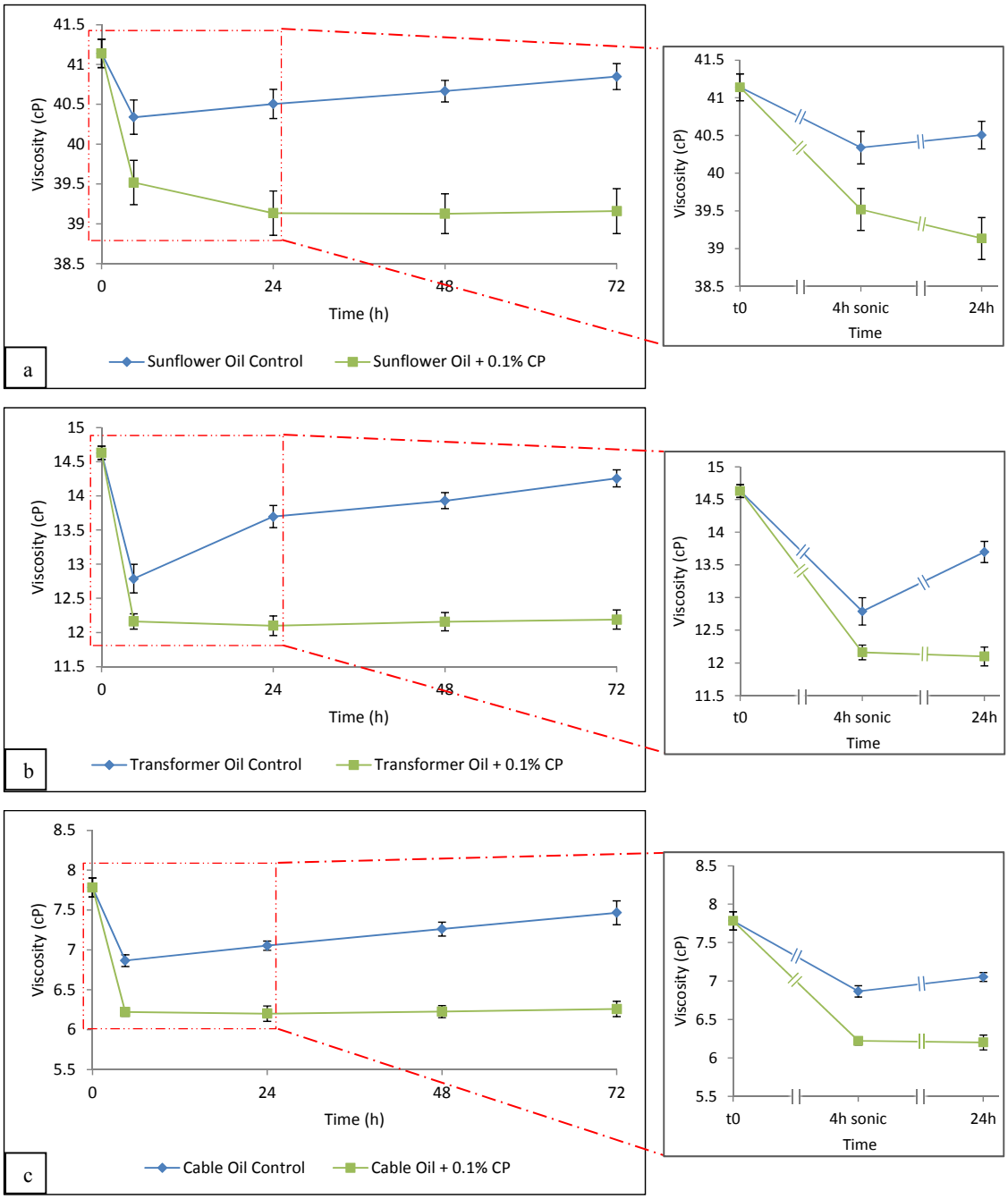

Figure 6.3 Effects of long time sonication with the addition of the nucleating agent and of the radical scavenger on sunflower oil (a), transformer oil (b), cable oil (c). 4-tert-butylphenol was added after 24 hours from the sonication to the samples which were sonicated in the presence of carbon black (green line). The measurements were performed in triplicate with the standard error being shown.

6.4 Ultrasound and the effect upon the viscosity of oils when a radical scavenger is introduced

In order to confirm the hypothesis of the radical formation previously described, 4-tert-butylphenol at 0.1 mM was added to two samples of sunflower, transformer and cable oil to allow the scavenger to dissolve into the oils. The following day 0.1% w/w of carbon black (CP) was added to one sample of each of these oils and then all the samples plus a fresh sample for each of the oils (control) were sonicated at 35 kHz frequency in a bath sonicator for 60 minutes. Immediately after the sonication, the samples to which carbon black was added were centrifuged at 4000 rpm for 15 minutes to remove the carbon. The viscosity measurements were made before sonication, after the sonication time (having allowed the samples to cool down to room temperature - resting time 30 minute), and every day of storage (3 days at room temperature within a dark cabinet).

As could be seen in figure 6.4, the addition of the radical scavenger before the sonication also inhibits the viscosity decrease in the samples to which carbon was added thus supporting the hypothesis of radical formation following sonication exposure.

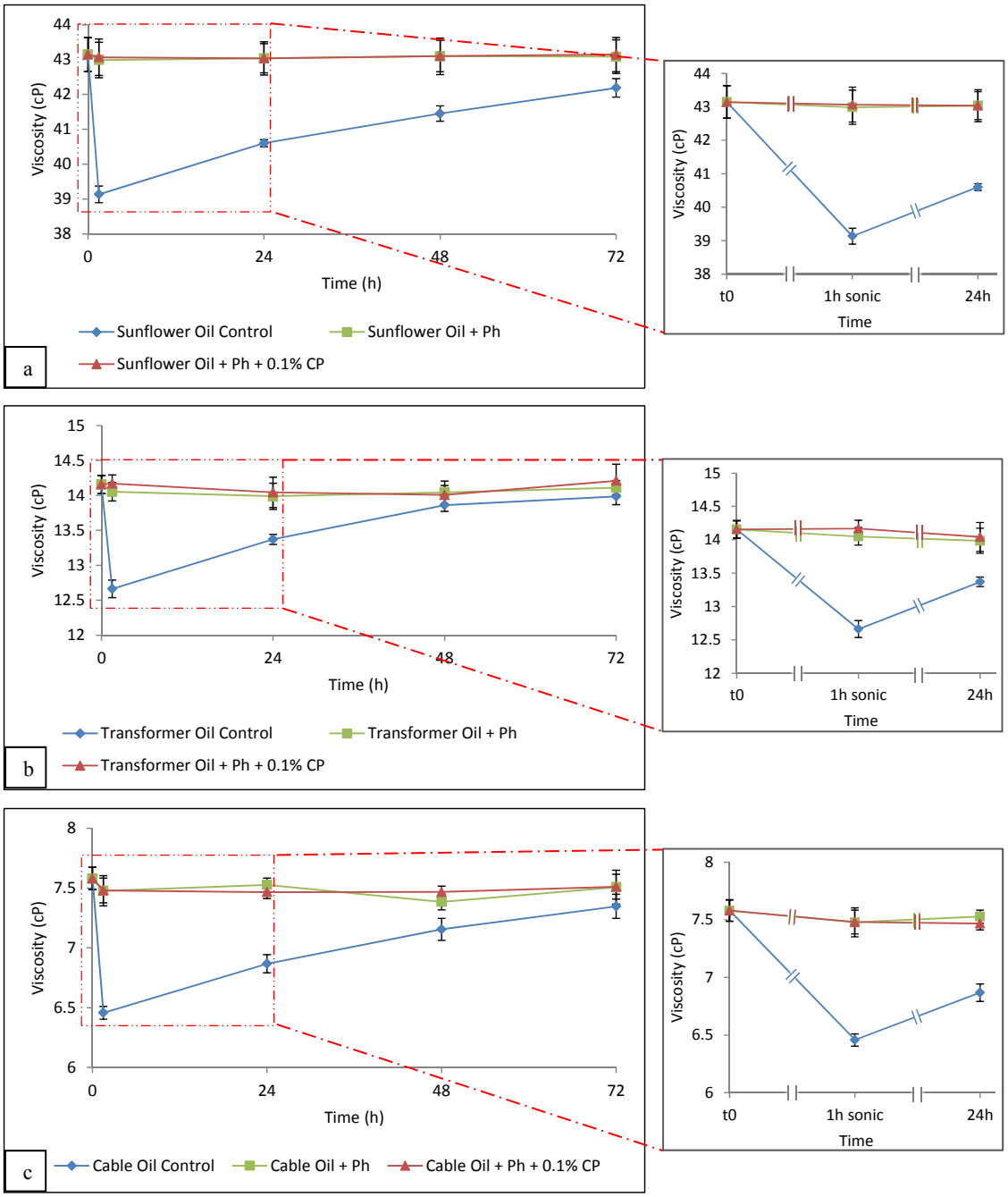

Figure 6.4 Effects of the addition of the radical scavenger before the sonication on sunflower oil (a), transformer oil (b), cable oil (c). The measurements were performed in triplicate with the standard error being shown. Ph= 4-tert-butylphenol.

6.5 Investigation on the "thermal effect"

As described in section 2.1.3, the cavitation phenomenon generates localised high temperatures within the vicinity of the collapse of the micro-bubble. This leads to a generalised increase of the temperature of the whole sample over time by some degrees which in turn can affect the viscosity of the sample.

In order to investigate this phenomenon, two samples of sunflower oil were sonicated in a bath sonicator at 35 kHz frequency for 60 minutes. After sonication 4-tert-butylphenol at 0.1 mM was added to both the samples to stabilise the lower viscosity level achieved; to one of the samples it was added 30 minutes after the sonication, while to the other it was added immediately after the sonication. Viscosity measurements were made before sonication, immediately after the sonication (0m), 30 minutes after the sonication (to allow the sample to cool back down to room temperature), and every 24 hours after the sonication for 3 days. The samples were stored at room temperature in glass bottles within a dark cabinet.

As can be seen in figure 6.5, the level of viscosity of the samples immediately after the sonication, whilst samples are still elevated in temperature (about 40°C), is approximately 15-17% lower than after 30 minutes from the sonication, which is the time needed for the samples to cool down to room temperature. This drop in viscosity is solely dependent on the temperature generated during the sonication process and can be identified with the expression "thermal effect" to distinguish this from the physical-mechanical breakage of the chains of the oil driven by cavitation.

Moreover the addition of 4-tert-butylphenol immediately after the sonication stabilises the viscosity decrease; this suggests the presence of short lived radical species which start reacting as soon as the sonication ends. The advantage of the possibility to stabilise the viscosity decrease at this lower level, which is dependent on the "thermal effect", could be of great importance for many applications in the energy and transports sectors.

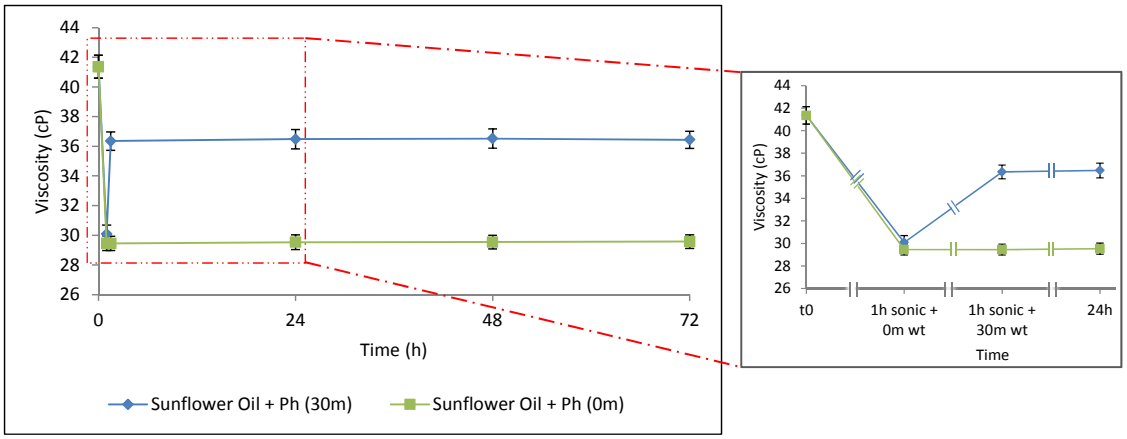

Figure 6.5 The "thermal effect" on the viscosity of sunflower oil. 4-tert-butylphenol (Ph) was added immediately after the sonication (green line) or after 30 minutes from the sonication (blue line). The measurements were performed in triplicate with the standard error being shown.

6.6 The effect of degassing (sparging) on viscosity

Degassing, or partial degassing, is essentially a method to replace one active gas (usually oxygen) with an inert gas, such as nitrogen; this procedure is also known as sparging. The replacement of oxygen with nitrogen should clarify the nature of the radicals formed during sonication and also their effects on the viscosity of the samples.

Two samples of sunflower oil were sonicated in a bath sonicator at 35 kHz frequency for 60 minutes. Prior to sonication, one of the samples was bubbled with nitrogen (N_2) for 30 minutes in order to remove the oxygen. Bubbling with nitrogen was also continued during the sonication process. Viscosity measurements were undertaken before sonication, 30 minutes after the sonication (to allow the sample to cool down to room temperature), and every 24 hours after the sonication for 3 days. The samples were stored at room temperature in glass bottles within a dark cabinet.

As could be seen in figure 6.6, treatment with bubbled N_2 diminishes the influence of the ultrasound on the viscosity of sunflower oil. The drop in the viscosity achieved in the sample bubbled with N_2 is 5% lower than that achieved in the control sample. As stated previously, the treatment with nitrogen removes the oxygen naturally present in

the oil; this could possibly limit the formation of oxygen-related radicals like peroxides. This result shows not only that a part of the radicals formed during sonication are oxygen-related, but also that radical species of different nature, such as alkyl radicals, are also formed during the sonication process. This can further support the hypothesis of the molecular cleaving action of the ultrasound, along with the formation of radicals on the broken chains.

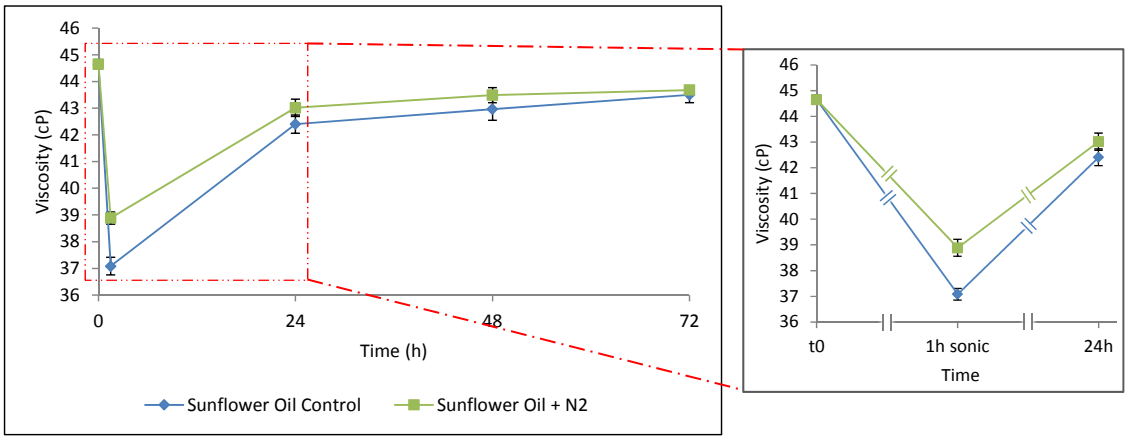

Figure 6.6 The effect of degassing (sparging) on the viscosity of sunflower oil. The measurements were performed in triplicate with the standard error being shown.

6.7 Chapter summary

This chapter has shown that the addition of a radical scavenger to sonicated samples stabilises the lower level of viscosity initially obtained through the sonication process, preventing the molecular rearrangements due to the action of the radicals. Moreover it has also been shown that the addition of the radical scavenger before the sonication prevents the molecular cleaving action of the ultrasound on the oils' chains. These findings support the hypothesis of the formation of radical species, whose nature is either oxygen- and non-oxygen- related, during the sonication process and of their action in causing chain rearrangements during the storage time.

Chapter 7

Viscosity analysis on other oils

7.1 Introduction

Having described the effects of the ultrasound on some model oils in the previous chapters, these effects will be further investigated within this chapter on other commercially available mineral and synthetic oils which differ in molecular structure and/or chemical composition. These data will give a broader vision on the possible applications of the ultrasound.

7.2 Viscosity analysis on 'Dow Corning' silicone oil

In order to obtain some insight into the effects of the chemical structure of the oils on sonication, samples of 'Dow Corning' silicone oil were sonicated at 35 kHz frequency in a bath sonicator for a total amount of 4 hours. To one sample 0.1% w/w carbon black (CP) was added prior to sonication and then removed, by centrifuging at 4000 rpm for 15 minutes, to allow the viscosity measurements. These measurements were undertaken before sonication, after the sonication (having allowed the samples to cool down to room temperature - resting time 30 minutes), and after 24 hours from the termination of sonication.

As can be observed in figure 7.1 silicone oil samples appear not to be affected by ultrasound in this instance. This particular behaviour can be explained by considering the different chemical structure of the core chain of silicone oil (Si-O chain) in contrast to the other oils considered within this work (C-C chains); these chains are characterised by different bond energies, C-C bonds having an energy of 346 $kJ\ mol^{-1}$ and Si-O bonds of 452 $kJ\ mol^{-1}$ [94]. Moreover, as described in section 2.1.3, the lower vapour pressure of silicone oil increases the tensile strength of the liquid, limiting the formation of the cavities and thus inhibiting the action of the ultrasound [3; 95].

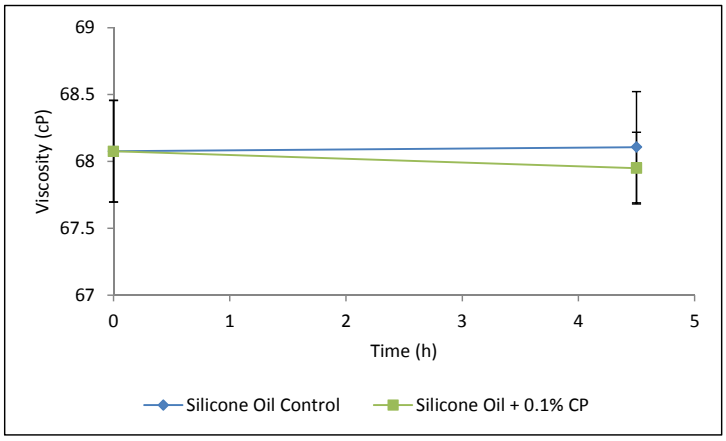

Figure 7.1 Ultrasound effects on the viscosity of 'Dow Corning' silicone oil. The measurements were performed in triplicate with the standard error being shown.

7.3 Viscosity analysis on commercially available motor oil samples

7.3.1 'Total' motor oil

As described in section 2.3.1, motor oils are a range of lubricating oils mainly used in internal combustion engines, whose molecular formula is based on medium/long hydrocarbon chains (18-34 atoms of carbon) [41]. The effects of ultrasound are here investigated on 'Total' motor oil (Quartz Ineo ECS 5W-30) which is a petroleum-derived highly refined motor oil designed to enhance the engine performance, to lower fuel consumption and improve the post-treatment systems.

Seven samples of 'Total' motor oil were sonicated at 35 kHz frequency in a bath sonicator for 60 minutes. 24 hours before the sonication 4-tert-butylphenol at 0.1 mM (Ph) was added to two of the samples to allow the scavenger to dissolve into the oil. The following day 0.1% w/w of carbon black (CP) was added to one of these two samples and to two further samples; all the samples were then sonicated as described above. As it is summarised in figure 7.2, the seven samples sonicated were: three samples of fresh motor oil; two samples of motor oil to which CP was added prior to sonication; two samples of motor oil to which Ph was added 24 hours before sonication, one of which

had also CP added before the sonication exposure. Immediately after the sonication of all seven samples, the samples to which CP was added were centrifuged at 4000 rpm for 15 minutes to remove the CP. 30 minutes after sonication exposure, 4-tert-butylphenol at 0.1 mM was added to one of the fresh oil samples and also to one of the samples sonicated in the presence of CP. At a time period of 24 hours after sonication 4-tert-butylphenol at 0.1 mM was added to another one of the fresh oil samples and to the other sample sonicated in the presence of CP. The viscosity measurements were taken before sonication, after the sonication exposure having allowed the samples to cool down to room temperature (resting time 30 minutes), and every day of storage (3 days at room temperature within a dark cabinet). The results summarised in figure 7.2 have been reported with more details in figure 7.3 for ease of analysis.

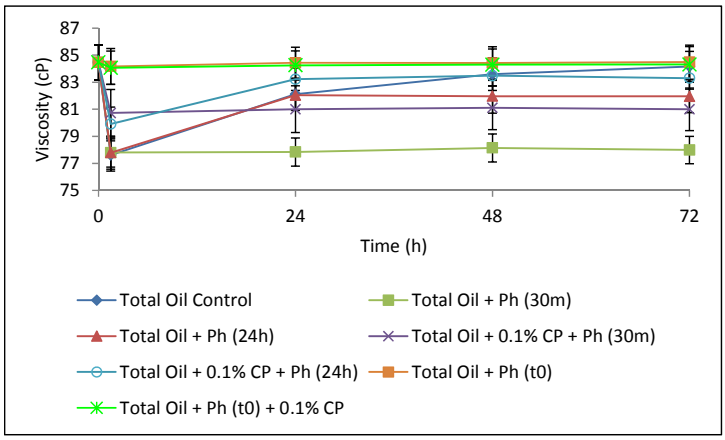

Figure 7.2 List of the sonicated samples. Carbon black (CP) was added to the samples before the sonication, while 4-tert-butylphenol (Ph) was added either 24 hours before the sonication (0h), or 30 minutes after the sonication (1.5h), or 24 hours after the sonication (24h).

As could be seen in figure 7.3a, ultrasound is effective in lowering the viscosity of the fresh motor oil samples, and the addition of 4-tert-butylphenol stabilises the level of viscosity achieved after sonication whether it is added 30 minutes after the sonication or 24 hours after the sonication. The addition of the nucleating agent (figure 7.3b) appears to interfere with the action of the ultrasound, not allowing the greater decrease in the viscosity which was expected, from the results described in chapters 5 and 6. This behaviour could possibly be due to the presence of additives, such as detergents, which are normally added to these oils to improve their performance characteristics, in

particular to remove ashes and particulates from the engine. The addition of 4-tert-butylphenol before the sonication (figure 7.3c) inhibits the action of the ultrasound, as previously described (section 6.4).

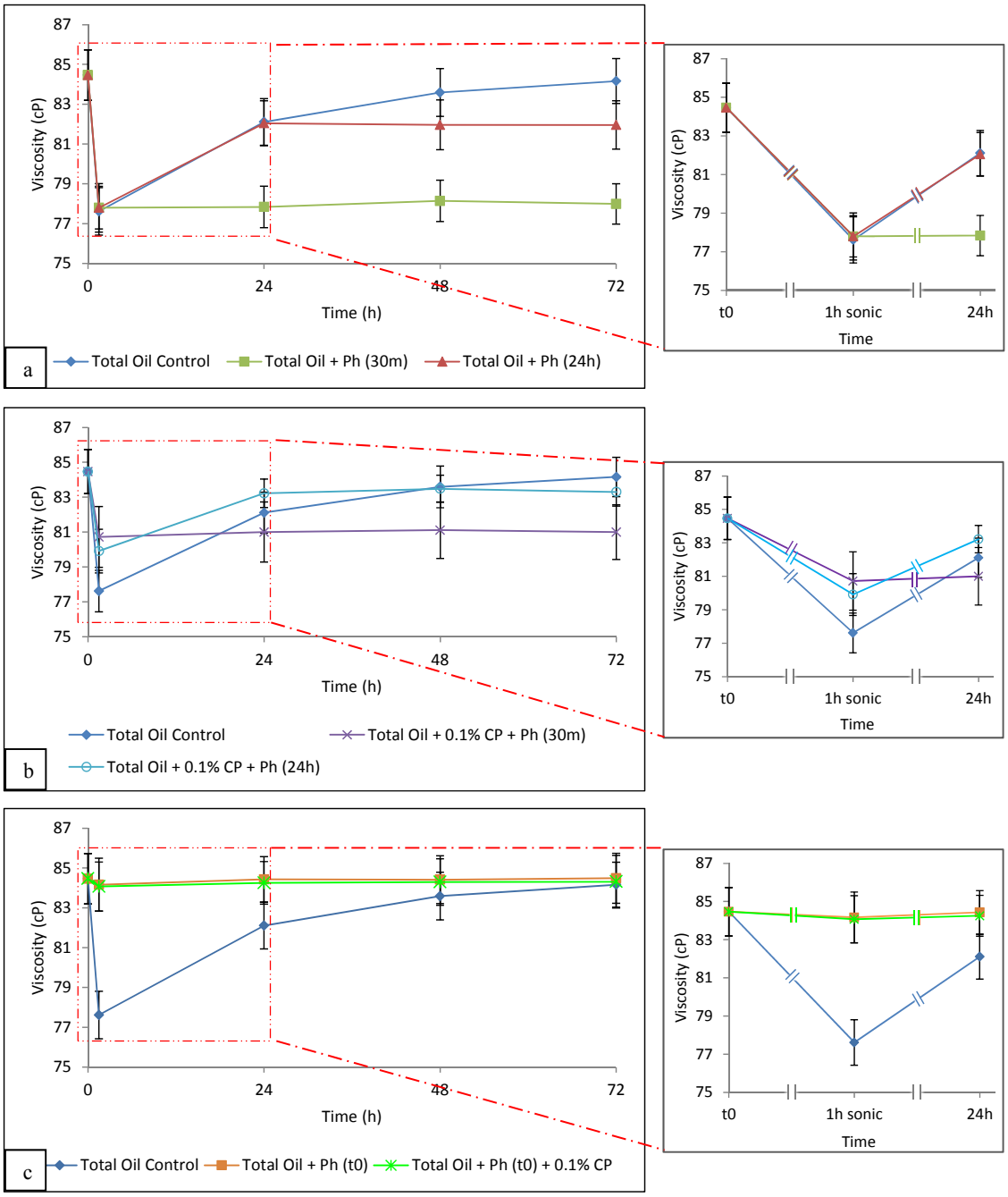

Figure 7.3 Viscosity analysis on 'Total' motor oil samples. The chart has been split into three different charts for ease of analysis; the control sample (dark blue line) is thus reported in every chart to allow comparison. a) fresh motor oil samples, 4-tert-butylphenol (Ph) was added 30 minutes after the sonication (green line) or 24 hours after the sonication (red line). b) motor oil samples with carbon black (CP), Ph was added 30 minutes after the sonication (purple line) or 24 hours after the sonication (light blue line). c) samples to which Ph was added 24 hours before the sonication, one of the samples was also added with CP (light green line). The measurements were performed in triplicate with the standard error being shown.

7.3.2 'Comma' motor oil

The effects of ultrasound are here investigated on 'Comma' motor oil (Multigrade Premium 20W-50) which is a synthetic motor oil specifically designed for older, higher mileage vehicles to help lower the oil consumption in these older vehicles.

Seven samples of 'Comma' motor oil were sonicated at 35 kHz frequency in a bath sonicator for 60 minutes. 24 hours before the sonication 4-tert-butylphenol at 0.1 mM (Ph) was added to two of the samples to allow the scavenger to dissolve into the oil. The following day 0.1% w/w of carbon black (CP) was added to one of these two samples and to two further samples; all the samples were then sonicated as described above. As it is summarised in figure 7.4, the seven samples sonicated were: three samples of fresh motor oil; two samples of motor oil to which CP was added prior to sonication; two samples of motor oil to which Ph was added 24 hours before sonication, one of which had also CP added before the sonication exposure. Immediately after the sonication of all seven samples, the samples to which CP was added were then centrifuged at 4000 rpm for 15 minutes to remove the CP. 30 minutes after sonication exposure, 4-tert-butylphenol at 0.1 mM was added to one of the fresh oil samples and also to one of the samples sonicated in the presence of CP. At a time period of 24 hours after sonication 4-tert-butylphenol at 0.1 mM was added to another one of the fresh oil samples and to the other sample sonicated in the presence of CP. The viscosity measurements were taken before sonication, after the sonication exposure having allowed the samples to cool down to room temperature (resting time 30 minutes), and every day of storage (3 days at room temperature within a dark cabinet). The results summarised in figure 7.4 have been reported with more details in figure 7.5 for ease of analysis.

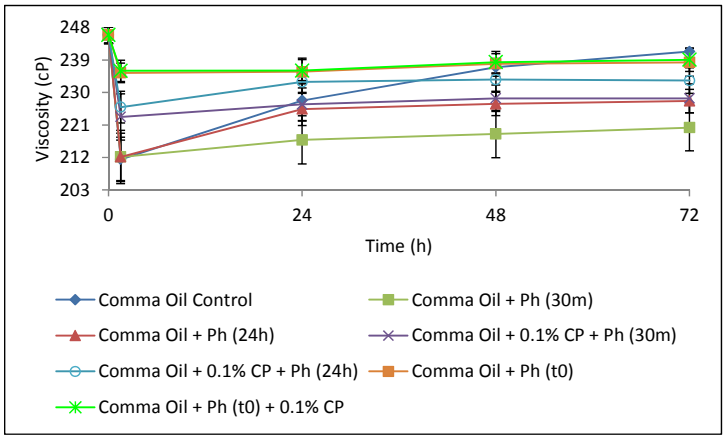

Figure 7.4 List of the sonicated samples. Carbon black (CP) was added to the samples before the sonication, while 4-tert-butylphenol (Ph) was added either 24 hours before the sonication (0h), or 30 minutes after the sonication (1.5h), or 24 hours after the sonication (24h).

As could be seen in figure 7.5a, ultrasound is effective in lowering the viscosity of the fresh motor oil samples. As described in section 7.3.1, the addition of the nucleating agent (figure 7.5b) seems to interfere with the action of the ultrasound; this further supports the hypothesis according to which the detergents added to the oil may interfere with the carbon particles lowering their action as nucleating agents. The addition of 4-tert-butylphenol though effective in stabilising the achieved lowered viscosity in the samples, is not as effective in doing so as previously described for the Total motor oil samples (figure 7.5a); this is also reflected in a lower efficiency in inhibiting the action of the ultrasound when 4-tert-butylphenol is added before the sonication (figure 7.5c).

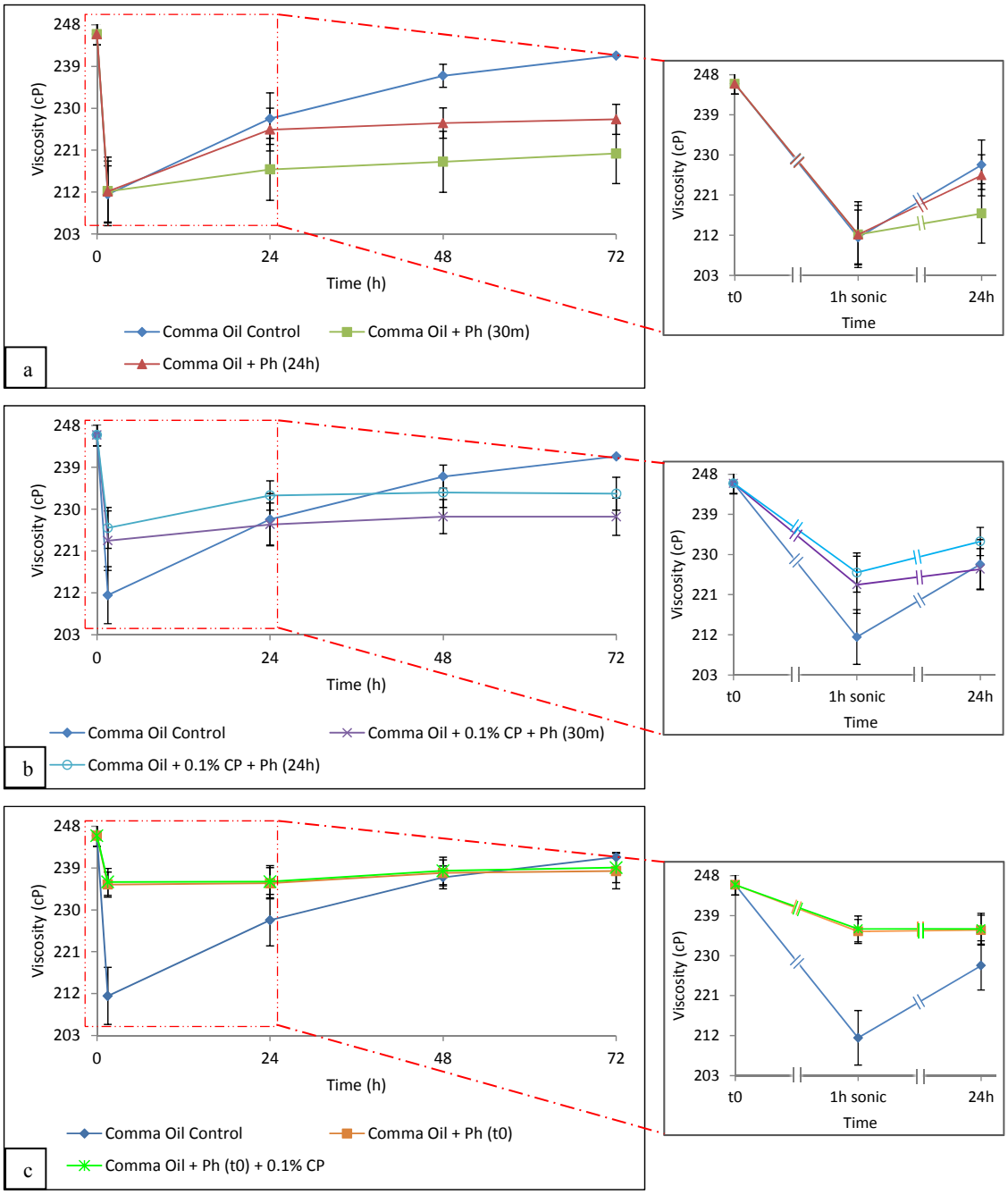

Figure 7.5 Viscosity analysis on 'Comma' motor oil samples. The chart has been split into three different charts for ease of analysis; the control sample (dark blue line) is thus reported in every chart to allow comparison. a) fresh motor oil samples, 4-tert-butylphenol (Ph) was added 30 minutes after the sonication (green line) or 24 hours after the sonication (red line). b) motor oil samples with carbon black (CP), Ph was added 30 minutes after the sonication (purple line) or 24 hours after the sonication (light blue line). c) samples to which Ph was added 24 hours before the sonication, one of the samples was also added with CP (light green line). The measurements were performed in triplicate with the standard error being shown.

7.3.3 'Halfords' motor oil

The effects of ultrasound are here investigated on 'Halfords' motor oil (Classic Oil 20W-50) which is a mineral multi-grade motor oil specifically designed for old engines and classic vehicles dating back to the 60's, 70's, and 80's to help minimising oil loss and leakage.

Seven samples of 'Halfords' motor oil were sonicated at 35 kHz frequency in a bath sonicator for 60 minutes. 24 hours before the sonication 4-tert-butylphenol at 0.1 mM (Ph) was added to two of the samples to allow the scavenger to dissolve into the oil. The following day 0.1% w/w of carbon black (CP) was added to one of these two samples and to two further samples; all the samples were then sonicated as described above. As it is summarised in figure 7.6, the seven samples sonicated were: three samples of fresh motor oil; two samples of motor oil to which CP was added prior to sonication; two samples of motor oil to which Ph was added 24 hours before sonication, one of which had also CP added before the sonication exposure. Immediately after the sonication of all seven samples, the samples to which CP was added were then centrifuged at 4000 rpm for 15 minutes to remove the CP. 30 minutes after sonication exposure, 4-tert-butylphenol at 0.1 mM was added to one of the fresh oil samples and also to one of the samples sonicated in the presence of CP. At a time period of 24 hours after sonication 4-tert-butylphenol at 0.1 mM was added to another one of the fresh oil samples and to the other sample sonicated in the presence of CP. The viscosity measurements were taken before sonication, after the sonication exposure having allowed the samples to cool down to room temperature (resting time 30 minutes), and every day of storage (3 days at room temperature within a dark cabinet). The results summarised in figure 7.6 have been reported with more details in figure 7.7 for ease of analysis.

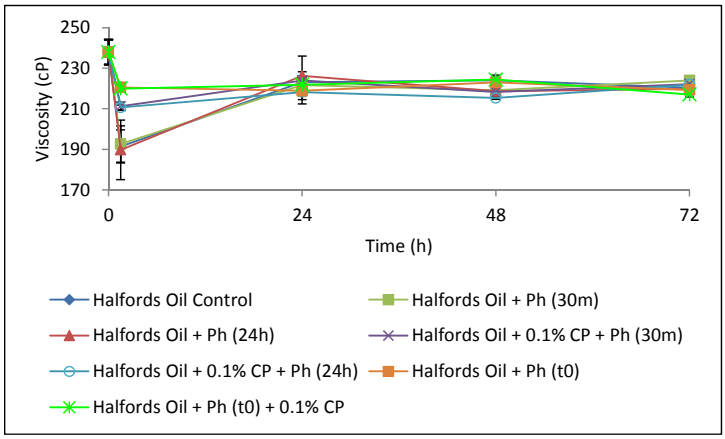

Figure 7.6 List of the sonicated samples. Carbon black (CP) was added to the samples before the sonication, while 4-tert-butylphenol (Ph) was added either 24 hours before the sonication (0h), or 30 minutes after the sonication (1.5h), or 24 hours after the sonication (24h).

As could be seen in figure 7.7a, ultrasound again is effective in lowering the viscosity of the fresh motor oil samples. As described for the other motor oils analysed in sections 7.3.1 and 7.3.2, the addition of the nucleating agent (figure 7.7b) lowers the effects of the ultrasound on the viscosity; this further support the hypothesis according to which the detergents added to the oil may interfere with the carbon particles lowering their action as nucleating agents. The addition of 4-tert-butylphenol does not seem to stabilise the viscosity of the samples when it is added after sonication (figure 7.7a and b); this could be due to a poor dissolution of 4-tert-butylphenol in this particular motor oil. This hypothesis is supported by the results presented in figure 7.7c, where a mild action of 4-tert-butylphenol is visible when it is added to the samples 24 hours before the sonication allowing more time for its dissolution into the samples.

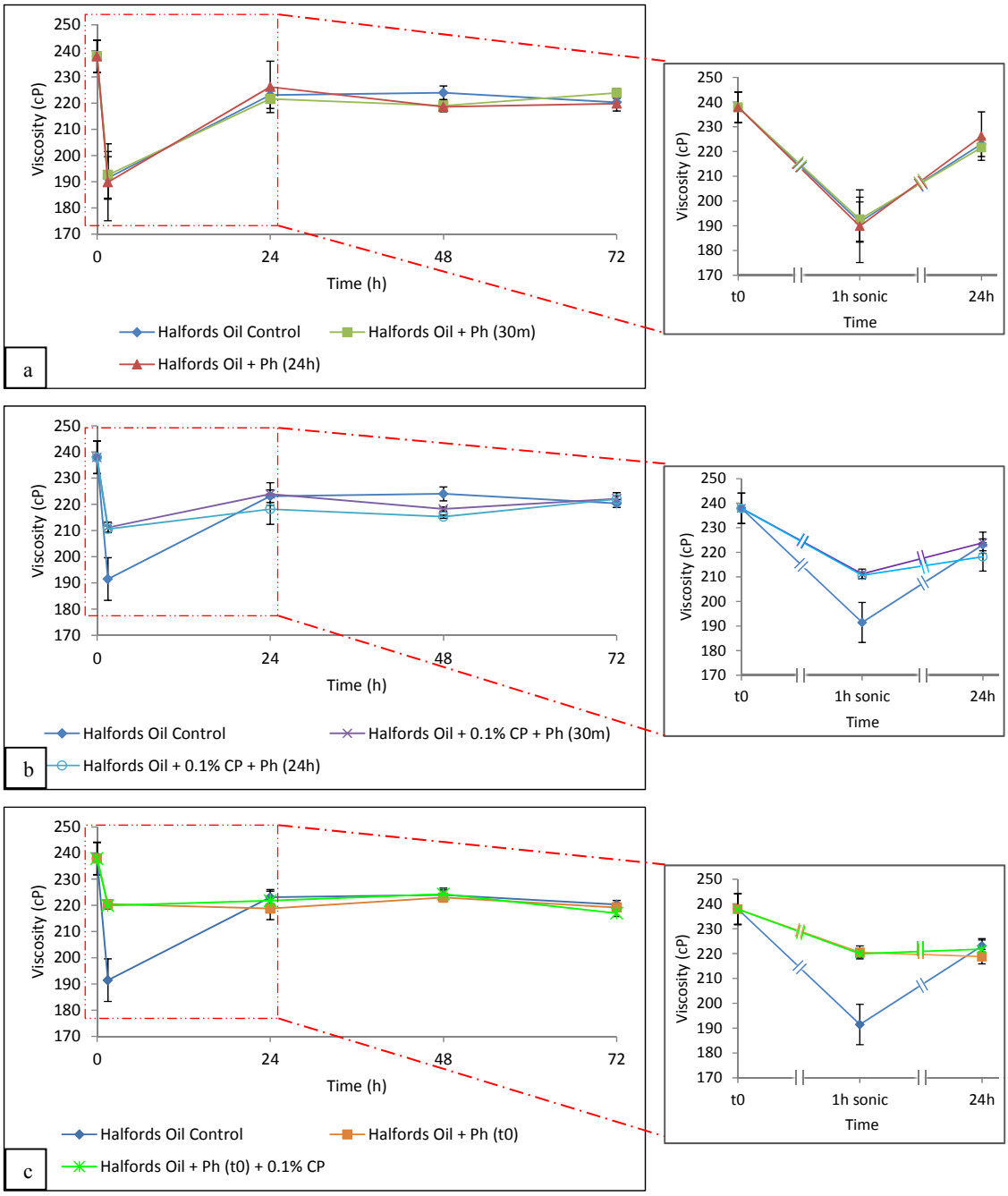

Figure 7.7 Viscosity analysis on 'Halfords' motor oil samples. The chart has been split into three different charts for ease of analysis; the control sample (dark blue line) is thus reported in every chart to allow comparison. a) fresh motor oil samples, 4-tert-butylphenol (Ph) was added 30 minutes after the sonication (green line) or 24 hours after the sonication (red line). b) motor oil samples with carbon black (CP), Ph was added 30 minutes after the sonication (purple line) or 24 hours after the sonication (light blue line). c) samples to which Ph was added 24 hours before the sonication, one of the samples was also added with CP (light green line). The measurements were performed in triplicate with the standard error being shown.

7.4 Viscosity analysis on diesel

In order to investigate the effects of ultrasound on samples of commercial diesel fuel, seven samples of diesel oil were sonicated at 35 kHz frequency in a bath sonicator for 60 minutes. 24 hours before the sonication 4-tert-butylphenol at 0.1 mM (Ph) was added to two of the samples to allow the scavenger to dissolve into them. The following day 0.1% w/w of carbon black (CP) was added to one of these two samples and to two further samples; all the samples were then sonicated as described above. As it is summarised in figure 7.8, the seven samples sonicated were: three samples of fresh diesel; two samples of diesel to which CP was added prior to sonication; two samples of diesel to which Ph was added 24 hours before sonication, one of which had also CP added before the sonication exposure. Immediately after the sonication of all seven samples, the samples to which CP was added were then centrifuged at 4000 rpm for 15 minutes to remove the CP. 30 minutes after sonication exposure, 4-tert-butylphenol at 0.1 mM was added to one of the fresh diesel samples and also to one of the samples sonicated in the presence of CP. At a time period of 24 hours after sonication 4-tert-butylphenol at 0.1 mM was added to another one of the fresh diesel samples and to the other sample sonicated in the presence of CP. The viscosity measurements were taken before sonication, after the sonication exposure having allowed the samples to cool down to room temperature (resting time 30 minutes), and every day of storage (3 days at room temperature within a dark cabinet). The results summarised in figure 7.8 have been reported with more details in figure 7.9 for ease of analysis.

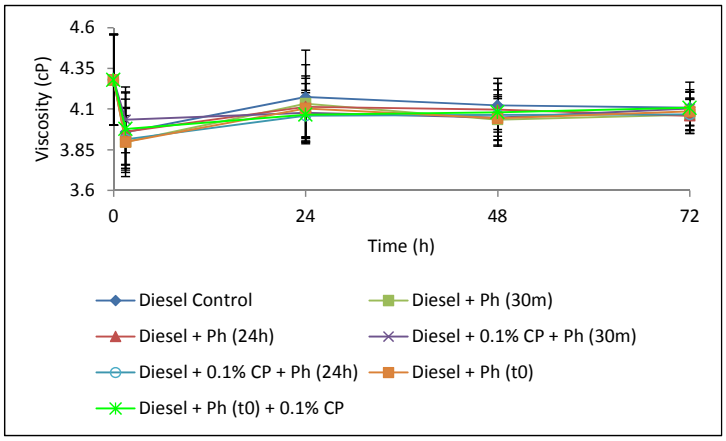

Figure 7.8 List of the sonicated samples. Carbon black (CP) was added to the samples before the sonication, while 4-tert-butylphenol (Ph) was added either 24 hours before the sonication (0h), or 30 minutes after the sonication (1.5h), or 24 hours after the sonication (24h).

As can be seen in figure 7.9a, a decrease in the viscosity level of about 7.5% is achieved in all the samples. While is possible to say that ultrasound is able to affect the viscosity of diesel, it is impossible to quantitatively define the extent and the efficiency of the process since the error which characterises the viscosity measurements is, in this instance, too broad. As is shown in figure 7.9b, carbon black does not enhance the effect of the ultrasound; this could be attributable to the detergents which are added to the diesel during the manufacturing process. From these results it remains impossible to define the effects of 4-tert-butylphenol, but it does not seem to inhibit the effects of ultrasound when it is added before the sonication (figure 7.9c).

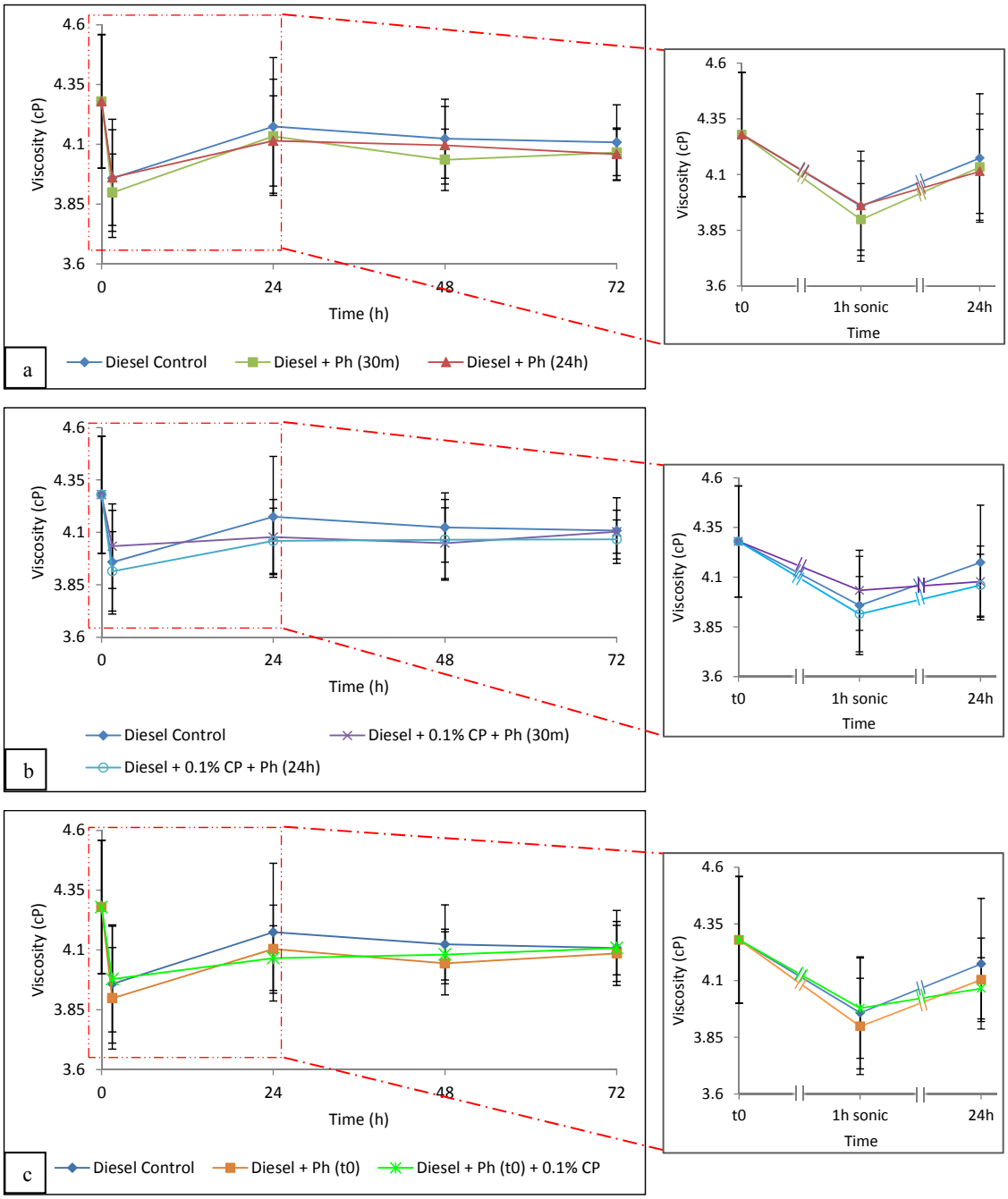

Figure 7.9 Viscosity analysis on diesel fuel samples. The chart has been split into three different charts for ease of analysis; the control sample (dark blue line) is thus reported in every chart to allow comparison. a) fresh diesel samples, 4-tert-butylphenol (Ph) was added 30 minutes after the sonication (green line) or 24 hours after the sonication (red line). b) diesel samples with carbon black (CP), Ph was added 30 minutes after the sonication (purple line) or 24 hours after the sonication (light blue line). c) samples to which Ph was added 24 hours before the sonication, one of the samples was also added with CP (light green line). The measurements were performed in triplicate with the standard error being shown.

7.5 Chapter summary

This chapter has highlighted some variances in the effects of ultrasound on mineral and synthetic oils with different molecular structure and chemical composition. In particular ultrasound at operational frequency of 35 kHz is not able to break the chains of silicone oil; this behaviour is thought to be attributable to the higher bond energy of the Si-O bonds. A lowering of the viscosity is obtained for the motor oil samples; their response to the ultrasound and to the radical scavenger is comparable to that described for the other carbon-based oils in chapters 5 and 6. In the motor oil samples the presence of detergents and of other additives lowers the effect of the nucleating agent; a smaller decrease in the viscosity of the samples is obtained, when compared to the decrease obtained on the samples which were not added with the nucleating agent. A similar behaviour seems to be present also in the diesel samples added with carbon black, but it remains impossible to define the extent and the efficiency of the sonication process, since the viscosity achieved after treatment with ultrasound is within the range of the error bars. This could be due to the already low level of viscosity of the samples before the sonication which adversely affects the efficiency of the measuring system.

Chapter 8

Chemical and structural characterisation of oils

8.1 Introduction

Having described, in the previous chapters, the physical changes caused by the application of an ultrasonic field to oil samples, a deeper understanding of the chemical changes would also be highly beneficial. In order to get this insight several different kind of analysis were performed on samples of the model oils investigated in chapters 5 and 6 namely: sunflower oil, transformer oil, and cable oil.

8.2 FTIR analysis

In an attempt to determine the chemical changes occurring within the sample oils during sonication, sunflower, transformer, and cable oils were sonicated in a bath sonicator at 35 kHz frequency for times up to 4 hours. To one sample (of each of the oils) 0.1% w/w of carbon black (CP) was added before sonication to increase the cavitation events. Immediately after sonication these samples were centrifuged at 4000 rpm for 15 minutes in order to remove the carbon. The samples were analysed with Fourier Transform Infrared Spectroscopy (FTIR) in the total reflection mode (ATR) after 1 and 4 hours of exposure to sonication respectively and a non-sonicated sample, of each of the oils, was used as negative control.

As could be seen in figure 8.1 the spectra fails to show differences among the samples before and after sonication, neither after a total of 4 hours sonication - nor when the CP is added. Therefore infrared analysis does not seem to be effective to show the chemical changes which affect the oils during sonication in this instance, and therefore other methods were used for further analysis.

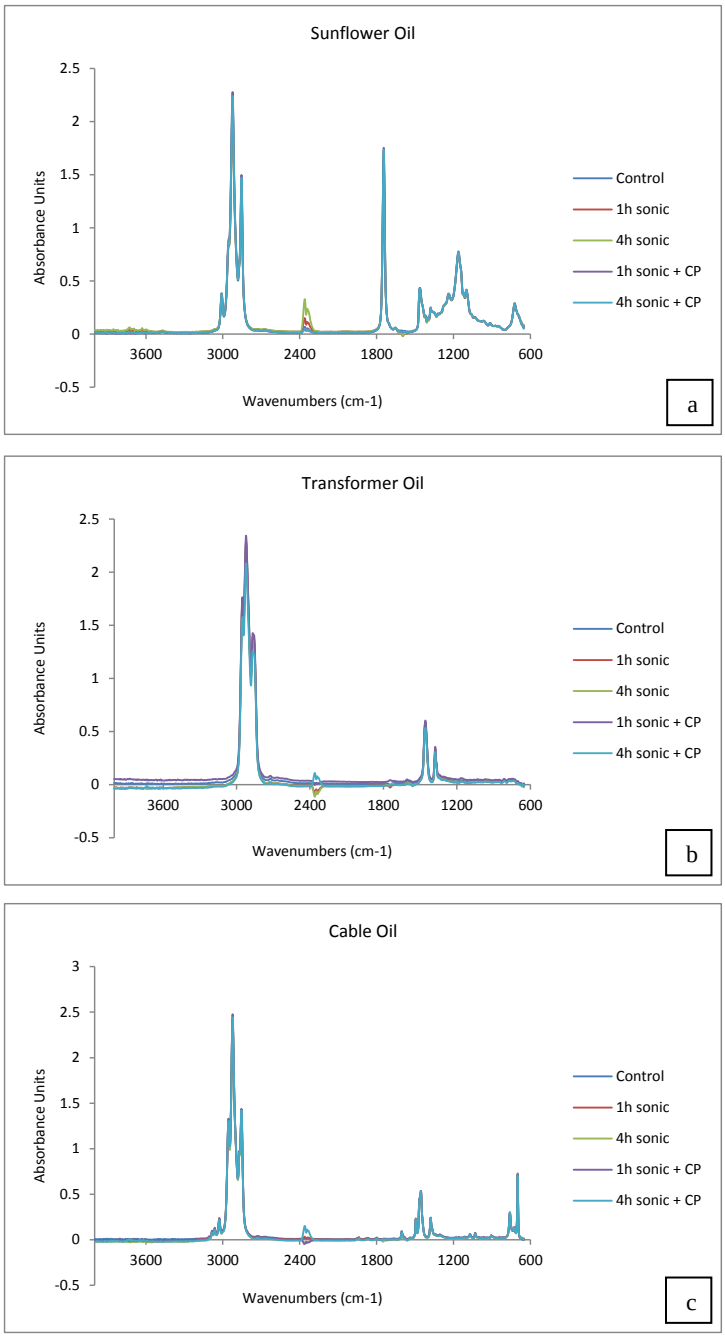

Figure 8.1 FTIR spectra of sunflower (a), transformer (b), and cable oil (c). For each of the oils are shown the spectra of the samples before sonication (control), after 1 and 4 hours of sonication both with and without the addition of carbon black (CP). Peaks at 2360 cm^{-1} are due to atmospheric CO_2.

A Nuclear Magnetic Resonance analysis (^{1}H-NMR) was also performed on the same samples, but the spectra did not show any difference between the samples before and after sonication (^{1}H-NMR spectra are reported in appendix A).

8.3 SIFT-MS analysis

Selected Ion Flow Tube Mass Spectrometry (SIFT-MS) analysis was performed on samples of sunflower, transformer, and cable oil sonicated for 60 minutes in a bath sonicator at 35 kHz frequency, and on non-sonicated (control) samples. Analyses were performed on 2.5 ml of samples which were allowed to equilibrate to 30°C for 15 minutes in the bags to allow the volatiles of the oils to disperse into the air-filled bags. A bag filled just with air (zero air sample) was used as internal control.

The principal volatiles identified before and after the ultrasound treatment of the oils are those listed in figure 8.2. The composition of the volatiles potentially indicates an oxidative process taking place within the samples during sonication, but it could also be possible that the volatiles are formed from the smaller fragments of the chains broken by the ultrasound.

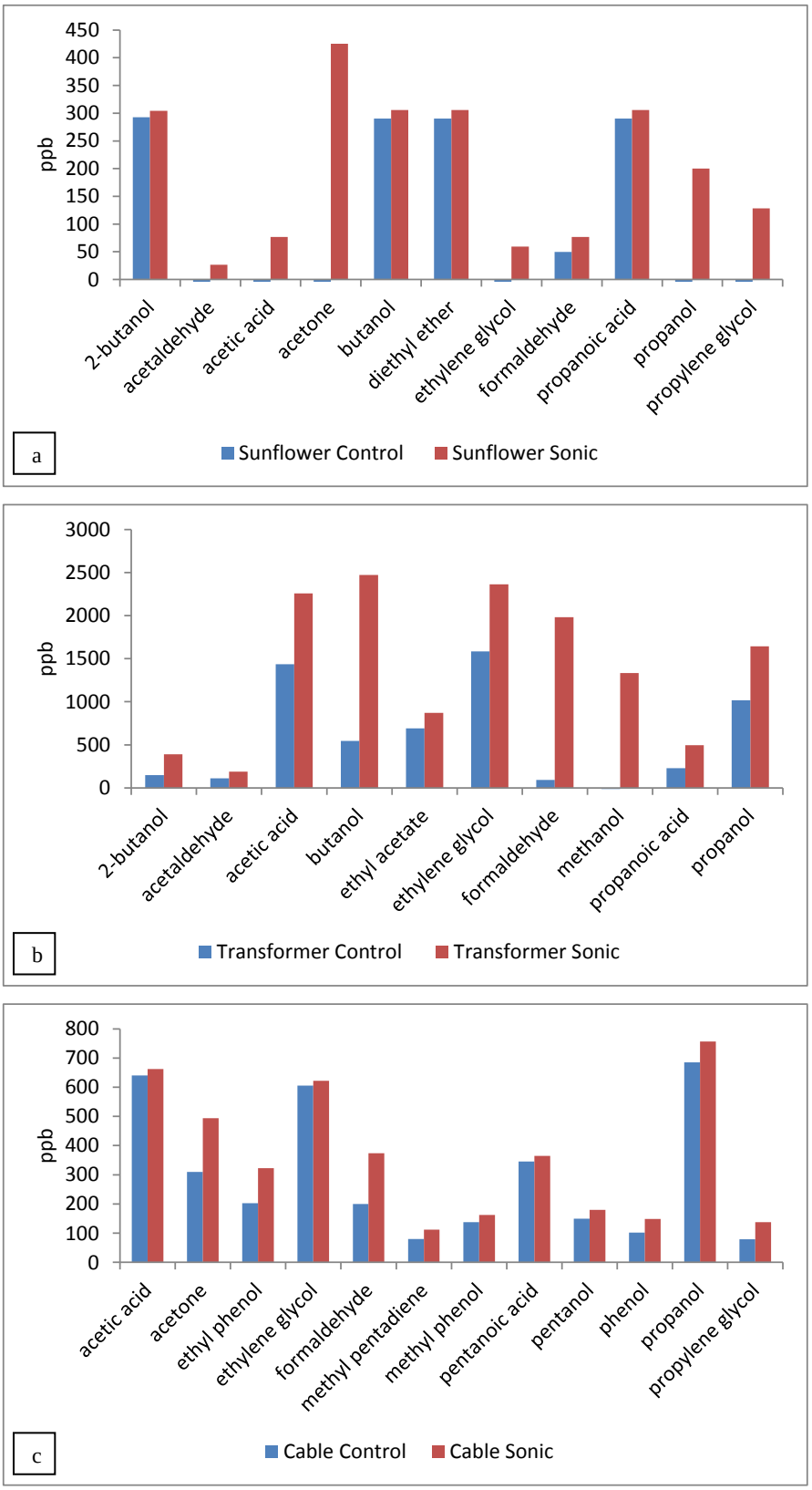

Figure 8.2 Principal products identified from the analysis of the volatiles for sunflower (a), transformer (b), and cable oil (c) before and after treatment with ultrasound. Amounts are expressed in parts per billions (ppb).

8.4 ATD-GCMS analysis

The Automated Thermal Desorption – Gas Chromatography Mass Spectrometry (ATD-GCMS) analysis was undertaken using the same samples used for the SIFT analysis, after having refilled the bags with air and re-equilibrated them at 30°C for 15 minutes. The volatile were then extracted and analysed as described in section 3.2.4.

The total ion chromatograms (TIC) of each sample were analysed and compared with the AMDIS library in order to obtain the best hit for each ion. The principal products, which were identified for each of the oils after the treatment with ultrasound, are listed in figure 8.3 which reports the products with their relative percentage abundance. Since it was not possible to clearly identify any specific compound in the cable oil control sample, only the compounds identified after sonication are reported (figure 8.3c). For the other samples ATD-GCMS analysis seems to confirm the hypothesis of an oxidative process taking place during sonication, as proposed when discussing the results of the SIFT analysis of the volatiles.

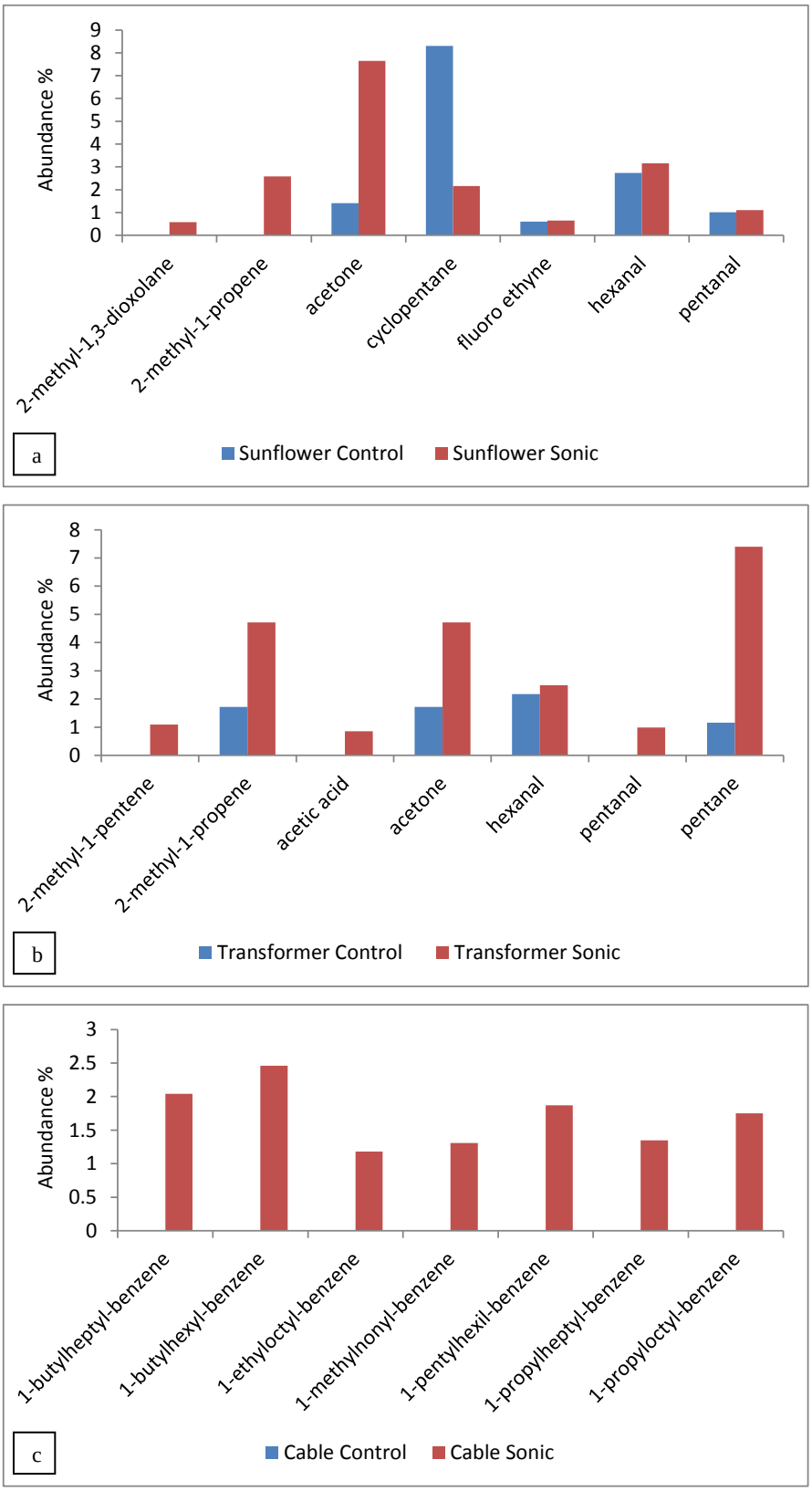

Figure 8.3 Principal products and relative percentage abundance, identified from the analysis of the TIC for sunflower (a), transformer (b), and cable oil (c) before and after treatment with ultrasound.

8.5 LC/MS analysis

Liquid Chromatography – Mass Spectrometry (LC/MS) analysis was performed on samples of sunflower oil. As reference standards both glyceryl trilinoleate and glyceryl trioleate were chosen since linoleic and oleic acid are the major components of the triglycerides of sunflower oil. One sample of sunflower oil and one sample of each of the standard were sonicated for 60 minutes in a bath sonicator at 35 kHz frequency. Following sonication, these samples and their relative non-sonicated samples were diluted in the solvent described in section 3.2.5 to a concentration of 1 mg/ml and then injected at a dilution of 100 μg/ml.

The total ion chromatograms (TIC) of the non-sonicated and sonicated glyceryl trilinoleate standard are shown in figure 8.4, while the TIC of the non-sonicated and sonicated glyceryl trioleate standard are shown in figure 8.5. Figure 8.6 shows the TIC for the non-sonicated and sonicated sunflower oil samples. Each single peak was analysed to determine the presence of the expected ion adducts (H^+, NH_4^+, Na^+, K^+), with the data reported in appendix B. No differences are visible between the TIC of the oil and the standards before and after the sonication as well as on the pattern of the ion adducts. This result may suggest that either the structural changes are too small to be detected with this technique, or that the radicals species generated during sonication are too short lived. It is possible in this context that the molecular rearranging of the cleaved chains takes place immediately after the sonication.

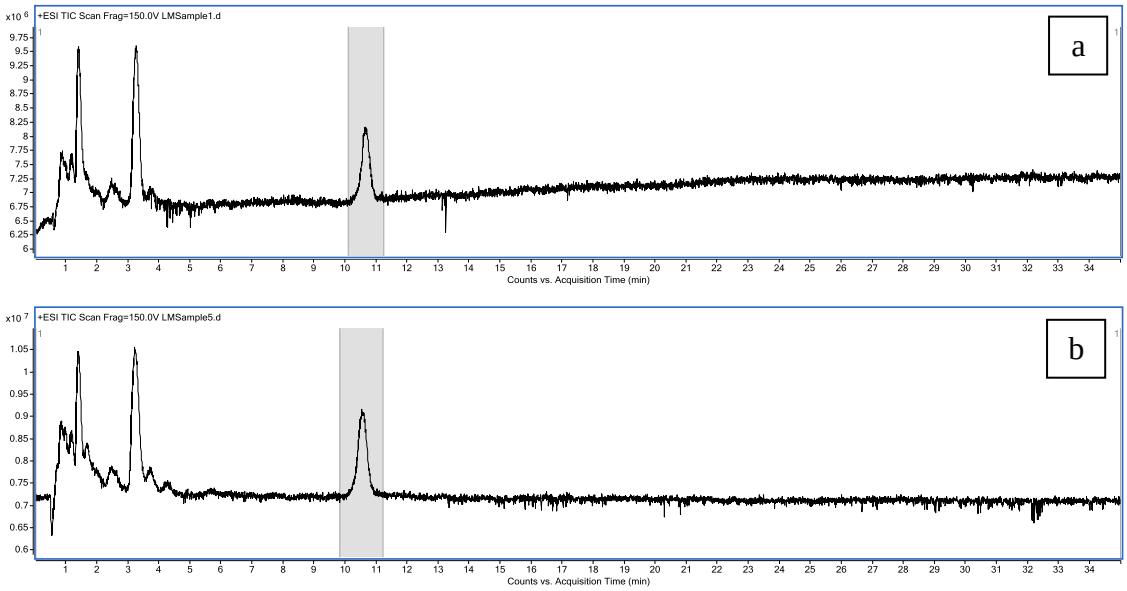

Figure 8.4 TIC of non-sonicated (a) and sonicated (b) glyceryl trilinoleate.

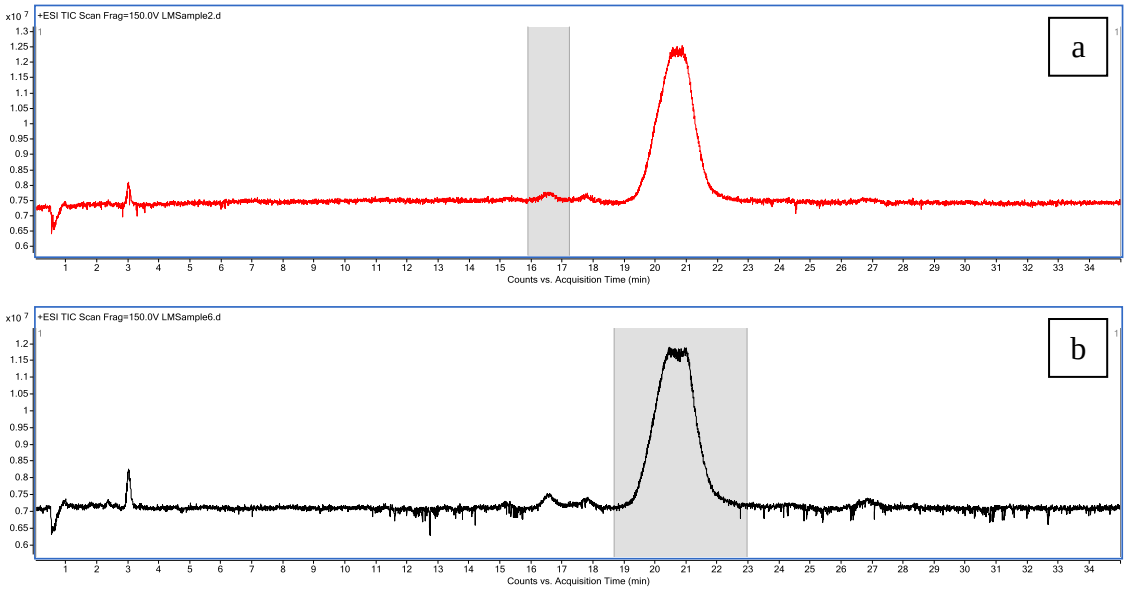

Figure 8.5 TIC of non-sonicated (a) and sonicated (b) glyceryl trioleate.

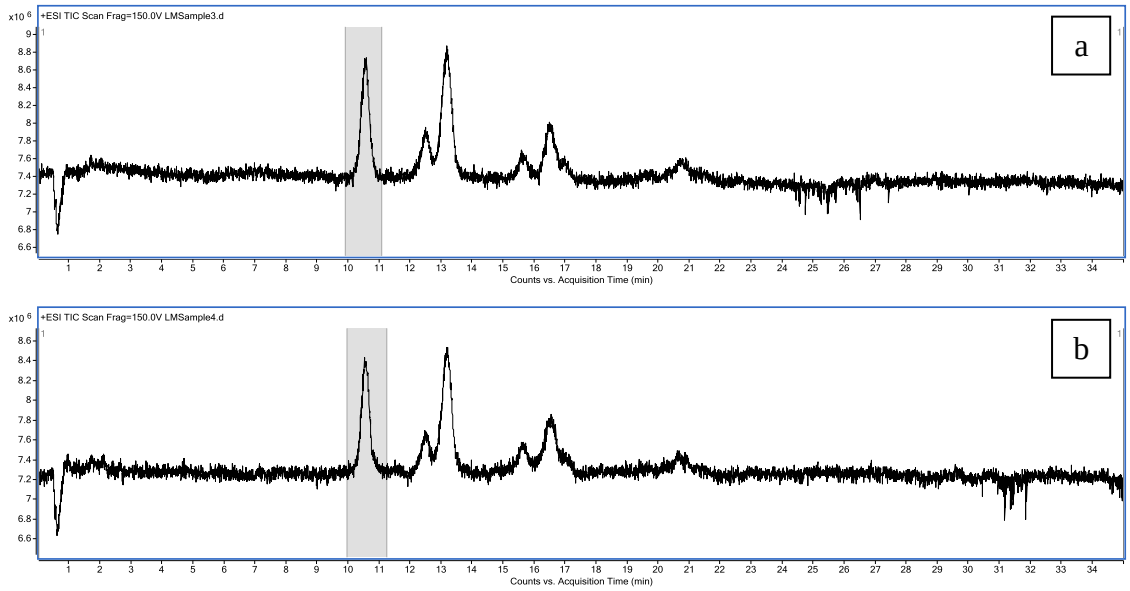

Figure 8.6 TIC of non-sonicated (a) and sonicated (b) sunflower oil.

In order to verify if the lack of response obtained with this technique is attributable to the generation of short lived radical species during sonication or to the small size of the structural changes obtained, the analysis was performed again on new freshly sonicated standards and sunflower oil. 4-tert-butylphenol at 0.1 mM was added after the sonication to these samples in order to act as radical scavenger preventing the chain rearrangements described in the previous chapters. Again however it was not possible to identify visible differences between the TIC of the oil and the standards before and after the sonication (data reported in appendix C). This result supports the hypothesis according to which the structural changes obtained with sonication are too small to be identified by the LC/MS technique using the parameter here employed.

8.6 ESR analysis

In order to obtain data on the nature of the radical species generated during sonication, Electron Spin Resonance (ESR) analyses were performed on three samples of sunflower oil. N-tert-butyl-α-phenyl nitrone (PBN) at 10 mM concentration was used as a radical trap and was added to two of the samples before the sonication. One of these samples was then sonicated for 60 minutes in a bath sonicator at 35 kHz frequency. Following

sonication each sample was placed in a glass capillary and some nitrogen gas was injected in the capillary before its closure. The closed capillaries were inserted in a quartz cell to record the spectra. As an internal control the ESR spectra of a closed empty capillary was also recorded. The scan time was set to 8 minutes to allow an accurate scanning of the whole field from 0 to 1000 mT.

As reported in section 6.6, at least a part of the radicals generated during sonication are oxygen-related and, for this reason, N-tert-butyl-α-phenyl nitrone was chosen as preferred radical trap. The trap interacts with the free radical forming nitroxide-based spin adducts which can be defined as persistent radicals with a distinctive ESR spectrum. As reported in the literature, PBN shows a characteristic primary nitrogen triplet and a β-hydrogen doublet [96].

As can be seen in figure 8.7, all the samples show the same radical modulation. As this modulation is also present in the spectra of the internal control, it seems likely that some radicals are being generated during the closure of the glass capillaries, which requires the flame heating of the extremities of the capillary. These glass-related radicals may interfere with the reading of the radicals formed during the sonication of the oil.

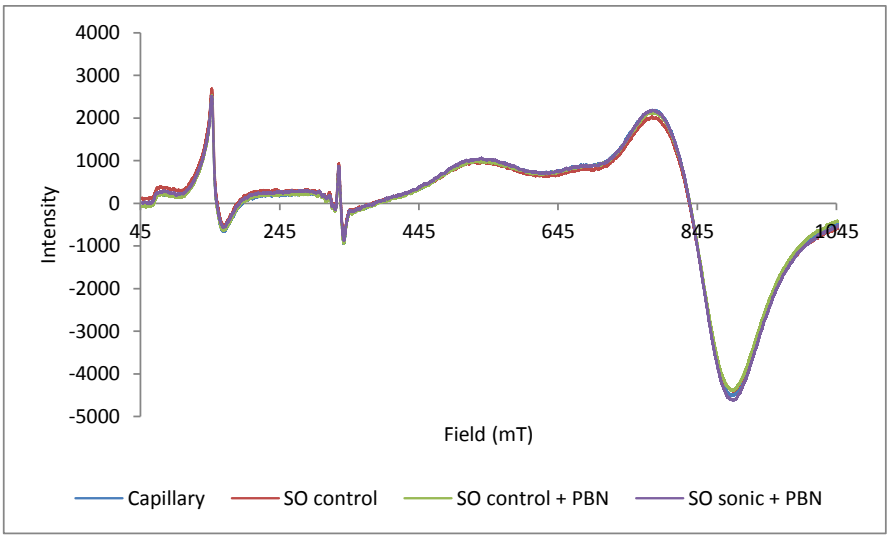

Figure 8.7 ESR spectra of sunflower oil samples using glass capillaries. PBN was added to one non-sonicated (green line) and to one sonicated (purple line) sample before the sonication. The spectra of the internal control (blue line) and of the oil control-non-sonicated sample (red line) are also shown.

In order to investigate if the glass capillary is interfering with the recording of the ESR spectra, the previous experiment has been repeated preforming the reading using cap-sealable quartz capillaries which fit the spectrometer chamber. The scan time was set to 8 minutes to allow an accurate scanning of the whole field from 0 to 1000 mT.

As it is shown in figure 8.8, again no radical modulation is visible for the samples while they are analysed inside quartz capillaries. This result support the hypothesis previously reported about the formation of glass-related radicals when the analysis is performed inside glass capillaries. The modulation visible in the far region of the field is similar for both the analysis, though it is of lower intensity in figure 8.8, and might be attributable to instrument imprecision during the scanning of such a broad field.

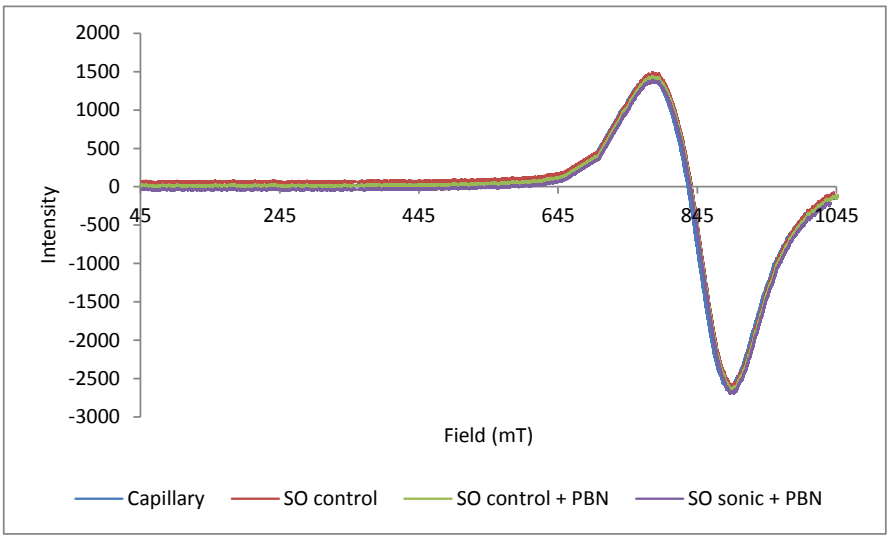

Figure 8.8 ESR spectra of sunflower oil samples using quartz capillaries. PBN was added to one non-sonicated (green line) and to one sonicated (purple line) sample before the sonication. The spectra of the internal control (blue line) and of the oil control-non-sonicated sample (red line) are also shown.

8.7 Calorimetric analysis

In order to determine if the sonication process described in the previous chapters can improve the thermodynamic characteristics of a model oil, a calorimetric analysis was performed evaluating the calorific value and the burning rate of a model vegetable oil. This oil is a 100% vegetable oil with a certain amount of unlisted solvent added specifically designed to increase its burning characteristics in order to be used in oil lamps.

The calorific value (CV) of the sample before the sonication has been determined using equation 3.2 and the procedure reported in section 3.3.3; the amount of deionised water used was 40 g, whilst the burning time was 10 minutes. The sample was then sonicated at 35 kHz frequency in a bath sonicator for 60 minutes, and the procedure for the measurement of the calorific value was repeated immediately after the sonication (termed 0m AS). 4-tert-butylphenol at 0.1 mM was then added to the sample and the procedure for the measurement of the calorific value was repeated 30 minutes and 24 hours after the sonication. The burning rate (BR), being expressed as the amount of oil burned during a certain amount of time, was calculated for each of the samples using equation 8.1:

Equation 8.1 $$BR = (W_1 - W_2)/t$$

where W_1 and W_2 represent the mass of the oil before and after the burning (g), and t is the time of the burning expressed in minutes.

As can be seen in figure 8.9, the calorific value of the vegetable lamp oil increases after sonication exposure meaning that more heat is generated by the burning of the same amount of oil. Encouragingly, it is also worth noting that the burning rate tends to decrease after the sonication meaning that less oil is consumed to generate that heat. Both these results might indicate that the performance of the oil as a combustible material is improved by the sonication process.

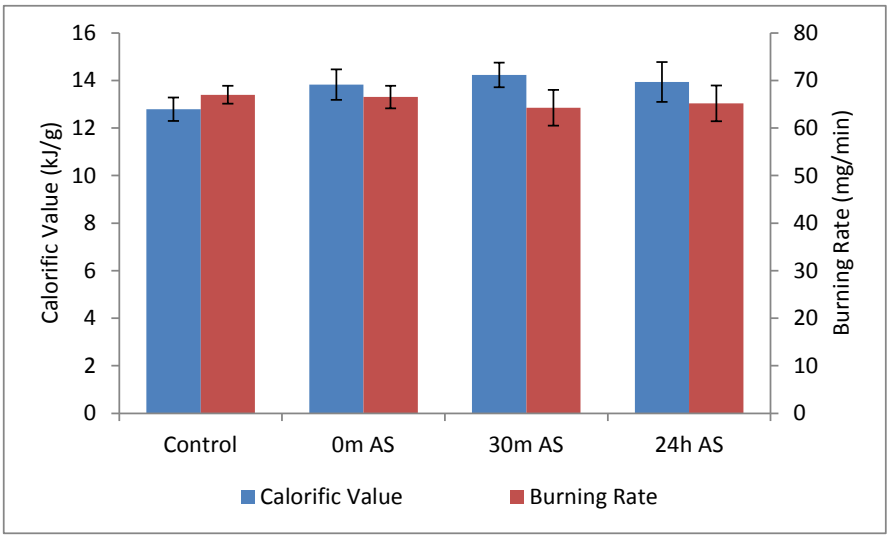

Figure 8.9 Calorific value and burning rate levels for vegetable lamp oil samples. Blue bars represent the calorific value and refer to the left vertical axis, while the red bars represent the burning rate and refer to the right vertical axis. The measurements were performed in triplicate with the standard error being shown.

In an attempt to evaluate the energy required for the sonication process here described and of the energy generated while burning the sonicated oil, the following consideration may be made. The water bath utilised for this analysis has a power of 85 W and its volume capacity is 2.75 litre; when applying the sonic power for 60 minutes the energy consumption equals 306 kJ, but not all the power is transferred to the sample due to the volume of the water bath (as discussed in section 4.4.2). After 60 minutes of sonication the calorific value of the vegetable lamp oil is increased by 1.44 kJ g^{-1}. Since the total mass of the oil used for this analysis was 26 g, the increase in the calorific value corresponds to a total 37.5 kJ of additional energy generated by burning the entire oil sample. If, for hypothesis, the bath sonicator was filled with oil and the same increase of calorific value was obtained after sonication in the same conditions, the additional energy generated from the burning of the oil would be 3207.6 kJ (vegetable lamp oil density 0.81 g cm^{-3}), while the energy consumption for the sonication would remain 306 kJ.

Further calorimetric analyses will be required to confirm this preliminary result since some errors, due to the nature of the present procedure, have to be taken into account. Some of these errors can be identified as: the heat lost in the surrounding area since the

"home-made" calorimeter is not enclosed in an insulating box; the heat lost by the beaker since its thermal capacity has not been taken into account in the equation; the incomplete or inefficient combustion since the experiment has been performed in air and not in an oxygen atmosphere. However, the preliminary results are encouraging since they show that the sonication procedure offers a method to increase the efficiency of the burning process of the oil.

8.8 Chapter summary

The techniques investigated here were not sufficient to characterise the chemical and structural changes which the oils undergo during treatment with ultrasound. In the case of the FTIR analysis, the chemical structures of the oils before and after sonication are still too similar to allow a proper distinction between the samples. In the case of SIFT and ATD-GCMS analyses, the main limit is that they solely identify the volatiles emitted giving an indication of the possible chemical changes within the chains of the oils examined, however this is insufficient to determine the real chemical structure of the chains of the oils before and after treatment with ultrasound. Moreover some of the products detected with these techniques may be attributable to an environmental contamination of the volatile samples. With the LC/MS analysis, which provides the liquid injection of the sample, it was not possible to highlight differences in the TIC and the ion adducts before and after sonication for both the samples and the standards. Similarly the ESR analysis, for the characterisation of the radical species, was not able to show positive results.

Even though it was not possible to gain definitive results from the structural analysis performed, the preliminary result obtained from the calorimetric analysis indicates that the sonication process improves the combustion characteristics of the oil. This, coupled with the results obtained in chapter 6 on the effects of the radical scavenger, support the hypothesis of the ultrasound being able to alter the chemical structure of carbon-based oils.

Chapter 9

Other application of ultrasound

- Saponification reaction -

9.1 Introduction

As shown this far, the ultrasound is able to induce chemical changes on the oils' chemical structure, which results in measurable physical changes (viscosity and calorimetry). In this chapter ultrasound will be tested as source of power to drive organic chemistry reactions such as the alkaline hydrolysis of the fatty acids constituting the triglycerides contained within the oil; this reaction is better known as the saponification reaction [28; 29]. As discussed in section 2.1.6 ultrasound has been used, in other works, to drive the reaction with the addition of phase transfer catalyst [33; 34]; in this work the reaction will be improved to achieve higher yield of saponification in a lower reaction time, whilst avoiding the use of PTC.

In all the following experiments the reaction will be considered as completed (end-point) when the majority of the oil is converted into a solid and the application of further ultrasonic energy is not possible due to a separation of the probe and the semi-solid sample, even if this does not correspond to the complete chemical conversion of the oil into the soap salt. The reaction yield will be determined through FTIR in the ATR mode (section 3.2.2) by measuring the height of the peak at around 1565 cm^{-1} which represents the C=O stretching vibrational mode of the salt of the obtained carboxylic acid, while the peak at 1750 cm^{-1} is attributable to the aliphatic C=O stretching of the ester in the triglyceride [97]. The yield of the reaction is expressed as the percentage of conversion of the triglycerides' ester into the salts over the total concentration of the esters of a control non-sonicated oil sample.

9.2 Test of the effectiveness of bath and probe sonicator in driving the saponification reaction

The saponification reaction was performed on three samples of sunflower oil (10 g). Potassium hydroxide (KOH), at a stoichiometric amount (1.9 g), was added to two of these samples as powder, while to the third sample potassium hydroxide was added as a highly concentrated solution (1.9 g in 2 ml deionised water). This last sample and one of

those with powder KOH were sonicated with a probe sonicator at 40 kHz frequency until the reaction reached the end-point described in section 9.1; samples were taken at five minutes intervals and analysed with FTIR to follow the development of the reaction. The remaining sample, to which KOH was added as powder, was sonicated with a bath sonicator at 35 kHz frequency for one hour and was then analysed with FTIR. Before the sonication all the samples were manually stirred for a couple of minutes to allow the mixing of the KOH with sunflower oil. In order to perform the FTIR analysis, only a minimal amount of the reaction mixture is removed so as not to detrimentally affect the balance of the reaction.

As can be seen in figure 9.1, the bath sonicator appears to be ineffective in driving the reaction, with no differences being shown between the sample and the non-sonicated sample of sunflower oil (with no KOH added) used as a negative control for the reaction.

The reaction however was observed to occur in the samples sonicated with the probe sonicator. The characteristic peak for the products is at 1565 cm^{-1}; the reaction is faster for the sample to which KOH was added as a solution. The oil is converted in just 15 minutes of total power application (figure 9.2). The additional peak at 1650 cm^{-1} is due to the presence of water in the reaction sample. When the sample is spread on the prism surface a phase separation occurs and the water creates a lower layer in contact with the prism, thus interfering with the recording of the spectra for the oil/reaction phase which constitutes the upper layer. While this alteration makes it impossible to calculate the exact rate of conversion, it is still evident that the reaction is occurring. Figure 9.3 shows, for comparison, a reference FTIR spectrum for deionised water; in the spectrum, the O-H symmetric and asymmetric stretching are seen at 3280-3920 cm^{-1}, and the H-O-H bending can be seen at 1650 cm^{-1} [97].

The saponification reaction for the last sample (sonicated with the probe sonicator in the presence of powder KOH) takes 40 minutes to reach the end-point; as can be seen in figure 9.4, the products' peak is defined, but the yield is still low since not all the KOH was reacted. This can be seen by the presence of crystals of potassium hydroxide still

visible at the bottom of the sample. The maximum level of ester conversion achieved is 5.8%.

Differences in the delivery of the sonic power to the sample between the water bath and probe sonicator explain the greater efficiency of the latter in driving the saponification reaction. These differences are due to the position of the sample within respect to the ultrasonic power source; in particular the probe sonicator is directly immersed in the reaction mixture so that all the power is transferred to the sample, while in the case of the water bath the sample is placed in its centre and, as discussed in section 4.4.2, dissipation of power occurs leading to a lower efficiency of the water bath.

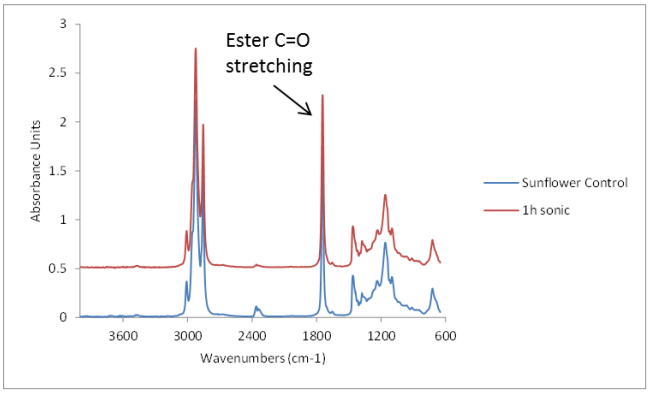

Figure 9.1 Saponification reaction driven with bath sonicator, potassium hydroxide was added as powder to the oil. For clarity the spectrum of the sonicated sample has been displaced upwards by 0.5 absorbance units (red line).

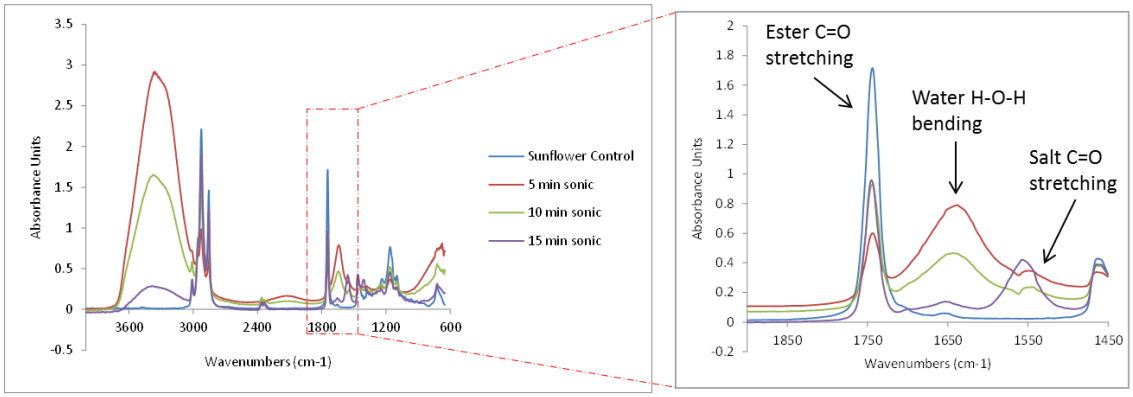

Figure 9.2 Saponification reaction driven with probe sonicator, potassium hydroxide was added as high concentrate solution. The characteristic peaks for the ester and the salt are highlighted as well as the interfering peak caused by the water.

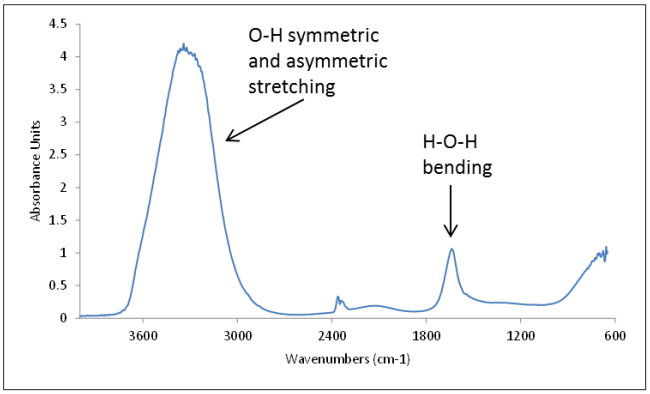

Figure 9.3 Reference FTIR spectrum for deionised water. The characteristic peaks for the O-H and H-O-H vibrational modes are highlighted.

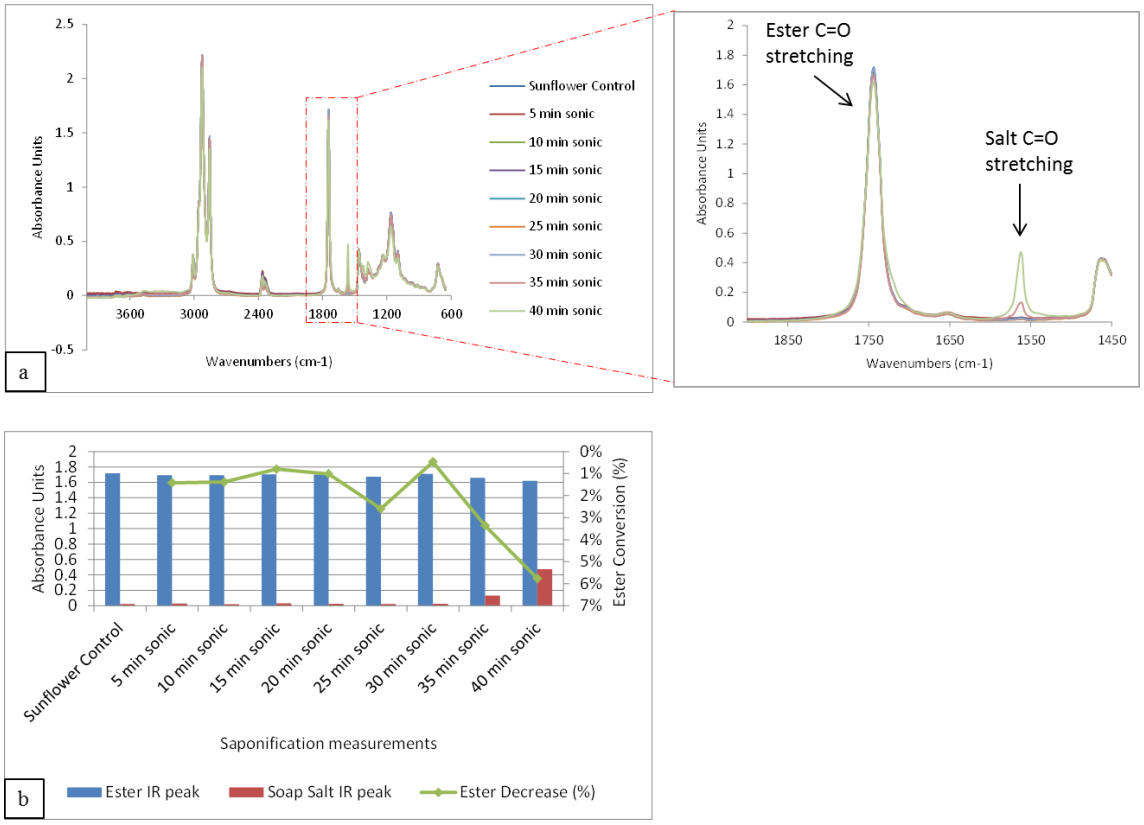

Figure 9.4 Saponification reaction driven with the probe sonicator, potassium hydroxide was added as powder to the oil. a) FTIR spectra with a zoom-in in the region of interest. b) blue and red bars are obtained respectively from the ester and salt IR peaks; green line represents the percentage of the ester converted over the total ester calculated from the IR peak at 1750 cm^{-1}.

9.3 Analysis of the yield of the saponification reaction obtained with different concentrations of potassium hydroxide

After having demonstrated the greater efficiency of the probe sonicator in comparison to the bath sonicator in driving the saponification reaction, the former was then used for the following investigations. As described in section 9.2 unreacted crystals of potassium hydroxide were visible on the bottom of the sample after the reaction, causing the reaction to produce a lower yield. In an attempt to increase the reaction yield, different concentrations of KOH were tested. Three samples of sunflower oil (10 g) were mixed prior to sonication with powder KOH in the following amounts: 0.5 g, 1.0 g, 1.9 g. These amounts were chosen since they are below or equal to the stoichiometric amount required for the reaction, being one of the objectives of the present procedure to avoid the use of excess alkali in order to reduce the eventual purification steps. All the samples were manually stirred for a couple of minutes to allow the mixing of the KOH with sunflower oil. The samples were then sonicated with a probe sonicator at 40 kHz frequency for a total amount of 15 minutes. The samples were analysed with FTIR after the reactions were completed (end-point); as controls for the reaction a sample of sunflower oil non-sonicated (control) and a sample of sunflower oil sonicated under the same conditions (sonic), were used.

As can be seen in figure 9.5, the best yield (14.9%) is achieved with the higher concentration of KOH (1.9 g), but as occurred previously not all the KOH is reacted. However the quality of the soap, in terms of visible and tactile consistency, achieved with this concentration is higher than the quality achieved in the other two lower concentration samples.

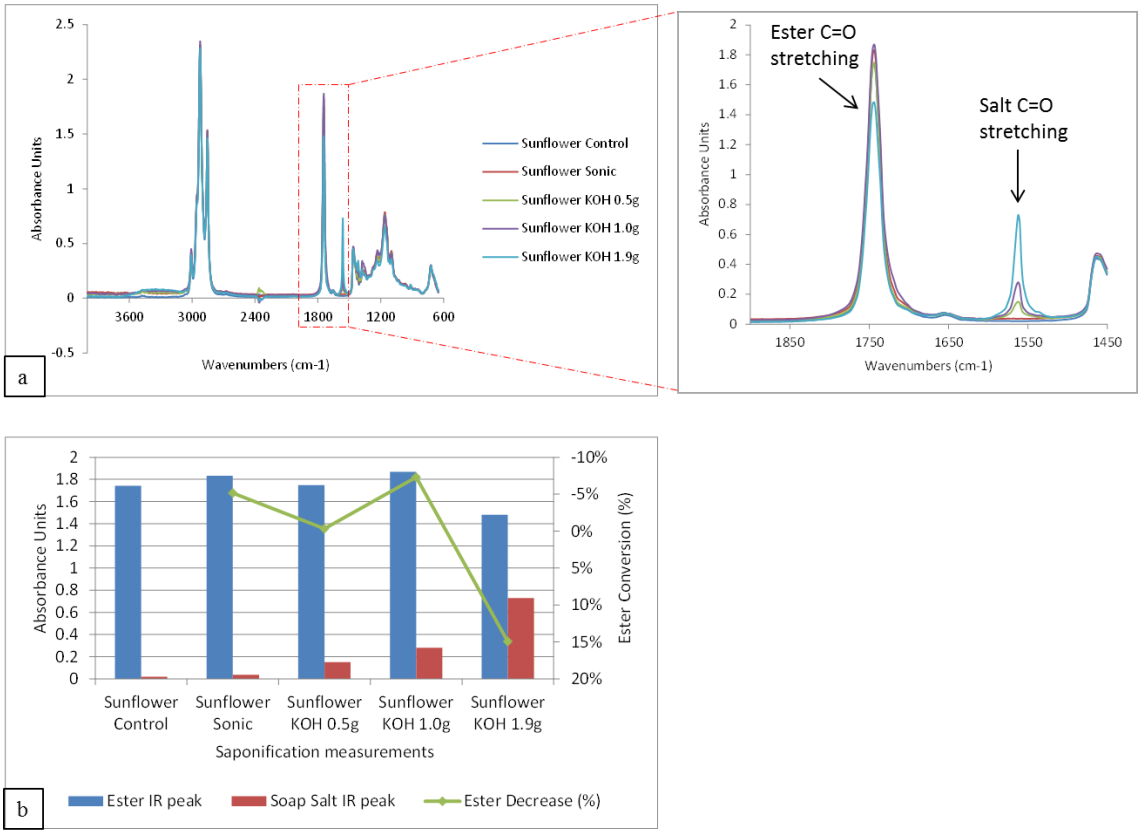

Figure 9.5 Saponification reaction performed on samples of sunflower oil added with different concentrations of powder potassium hydroxide. a) FTIR spectra with a zoom-in in the region of interest. b) blue and red bars are obtained respectively from the ester and salt IR peaks; green line represents the percentage of the ester converted over the total ester calculated from the IR peak at 1750 cm^{-1}.

9.4 Increasing the yield of the saponification reaction

As previously described when the potassium hydroxide is added as a powder to sunflower oil, not all of the reactants give rise to products leading to a low final yield. In order to rectify this, 0.5 ml of deionised water was added to 1.9 g of potassium hydroxide, the solution was stirred for 5 minutes and then 10 g of sunflower oil was added to the solution. The sample was sonicated with a probe sonicator at 40 kHz frequency, and from time to time the sample was manually stirred to improve the mixing between the oil and KOH solution. Every five minutes a sample of the reaction was taken and analysed with FTIR until the reaction reached its end-point. As a

negative control for the reaction, a sample of sunflower oil non-sonicated was also used. As described in sections 3.3.4 and 9.1, the reaction end-point - reached when the application of the ultrasound to the sample is no longer possible - does not correspond to the complete chemical conversion of the oil into the soap salts and the reaction is likely to proceed also after the ultrasonic irradiation is terminated. In order to investigate this phenomenon a sample of the reaction mixture was also analysed with FTIR after an overnight rest at room temperature, the sample was stored in a dark cabinet.

As it is shown in figure 9.6, the reaction reached the end-point after 10 minutes of ultrasound application. The yield of the reaction reaches 17.7% of ester conversion and the solid compound obtained had a uniform appearance since no KOH crystals are visible. Moreover the reaction continues during the overnight rest period (termed ON), thus further increasing the yield to 51.3% of ester conversion.

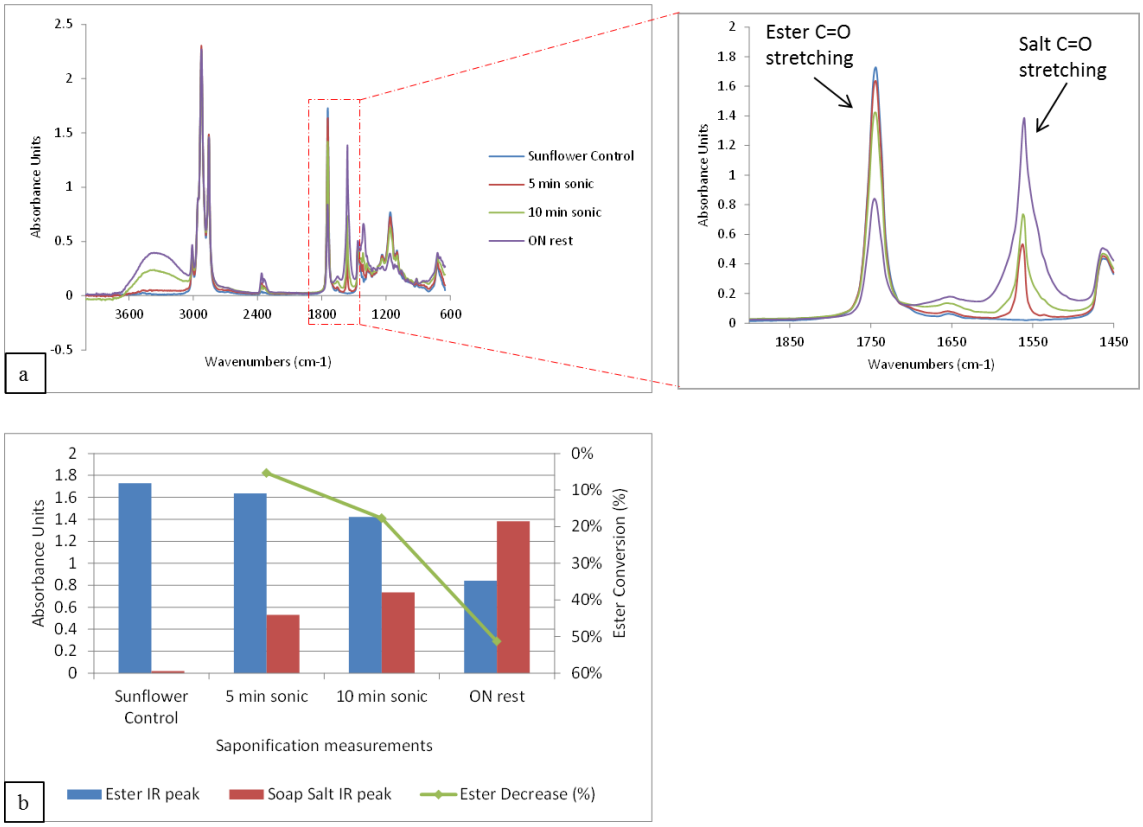

Figure 9.6 Saponification reaction performed on sunflower oil with potassium hydroxide powder pre-dissolved in 0.5 ml of deionised water. a) FTIR spectra with a zoom-in in the region of interest. b) blue and red bars are obtained respectively from the ester and salt IR peaks; green line represents the percentage of the ester converted over the total ester calculated from the IR peak at 1750 cm^{-1}. ON= overnight.

9.5 Achieving a higher yield out of the saponification reaction by lengthening the reaction time

In an attempt to further increase the final yield of the saponification reaction by lengthening the reaction time, the experiment described in section 9.4 was carried on in an ice bath. The solution of 1.9 g potassium hydroxide in 0.5 ml of deionised water was stirred for 5 minutes and then 10 g of sunflower oil was added to the solution. The sample was sonicated with a probe sonicator at 40 kHz frequency; from time to time the sample was manually stirred to improve the mixing between the oil and KOH solution. A sample of the reaction was taken every five minutes and was analysed with FTIR till

the reaction was completed. As a negative control for the reaction, a sample of sunflower oil non-sonicated was used. The sample was also analysed with FTIR after an overnight rest at room temperature, the sample was stored in a dark cabinet.

The presence of the ice bath helps to maintain the constant sample temperature preventing overheating and thus allowing more time for the development of the reaction; in these conditions the separation of the product from the probe occurs after 15 minutes of total power application. As can be seen in figure 9.7 these conditions seem to greatly increase the yield of the reaction after 15 minutes reaching a 43.6% of ester conversion, when compared to the yield achieved in 9.4 (17.7%) after 10 minutes of reaction (figure 9.6). The yield of the reaction is further increased overnight achieving a final yield of 61.3% of ester conversion.

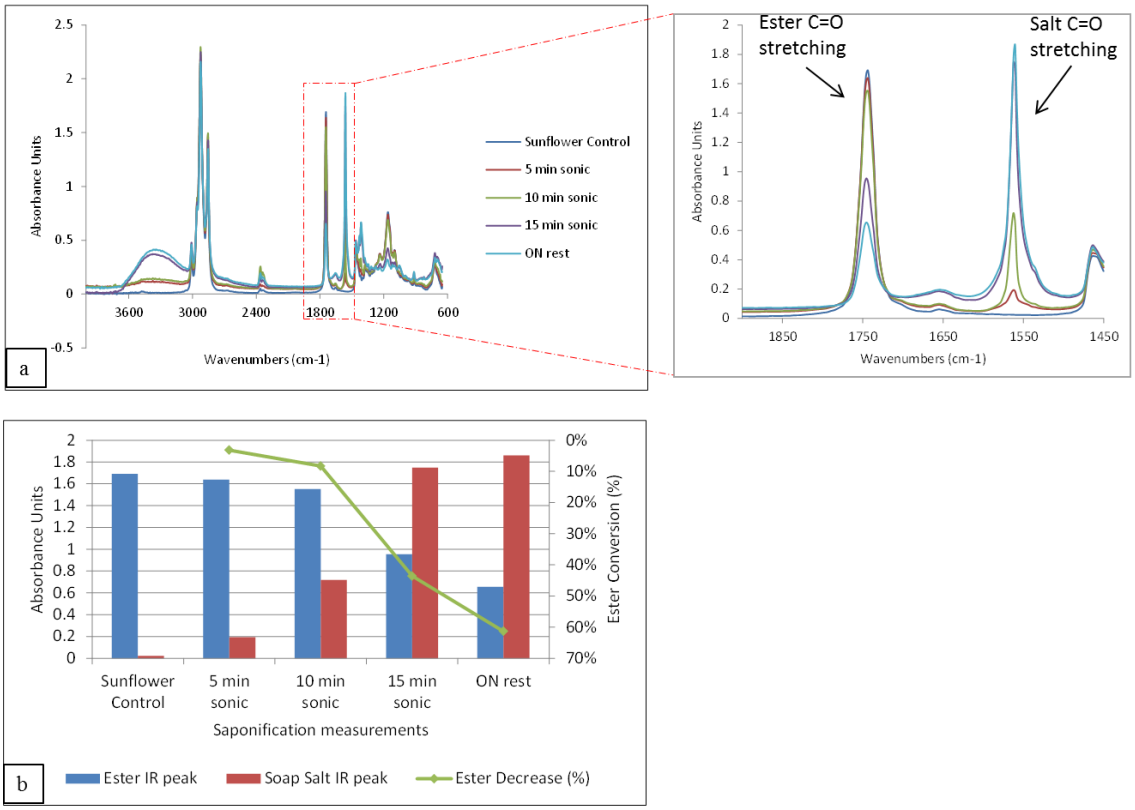

Figure 9.7 Saponification reaction performed on an ice bath. a) FTIR spectra with a zoom-in in the region of interest. b) blue and red bars are obtained respectively from the ester and salt IR peaks; green line represents the percentage of the ester converted over the total ester calculated from the IR peak at 1750 cm^{-1}. ON= overnight.

9.6 Chapter summary

This chapter has shown that the ultrasound can be used as power source to drive organic chemistry reactions such as the hydrolysis of the triglycerides present in sunflower oil. The reaction has been optimised to achieve a higher yield in a relative low reaction time (15 minutes) and at room temperature, with consequently lower energy consumption: 180 kJ/hour rather than the 270 kJ/hour of a typical small heating mantle (50 ml flask) utilised for the traditional reaction process, which would also require extra energy for stirring [29]. The probe sonicator has proved to be both more effective and efficient than the bath sonicator, being the probe sonicator immersed in the reaction mixture with all the sonic power directly transferred to the reaction. The highest reaction yield (61.3% of ester conversion) was achieved when the reaction was performed in an ice bath with a highly concentrated solution of potassium hydroxide.

Chapter 10

General Discussion

The aim of this study was to investigate and characterise the sonochemical breakdown of a various range of oils, in order to obtain products amenable to further processing. The rationale behind this work is the possibility to apply an ultrasonic field to the oil samples to generate lower viscosity products.

The application of ultrasound to a liquid medium, known as sonication, generates the cavitation phenomenon which implies the formation, growth and implosive collapse of micro-bubbles. Results of the cavitation phenomenon are the generation of high temperatures and pressures due to the collapsing micro-bubbles, as well as the formation of micro-currents and strong shear gradients due to the oscillation of the cavitating micro-bubbles. These effects are responsible for the physical-mechanical and chemical changes which will affect the liquid medium. In the particular case of ultrasound applied to polymeric-like structures, the shear forces generated during the growth step of cavitation stretches the polymeric chains which are eventually cleaved during the implosive collapse step. This results in the formation of highly reactive radical species and in the decrease of the viscosity of the liquid medium.

The preliminary investigations of this work were aimed at demonstrating the effect of ultrasound on the viscosity of some model oils in order to investigate the feasibility of the process. Chapter 4 has shown the effectiveness of the ultrasound in lowering the viscosity of the model oils, analysed as well as the efficiency of different sonicators in delivering their sonic power to the samples. In particular it has been shown that the two water baths tested (Camlab Trannsonic T460 and Ultrawave U100) have an essentially identical efficiency, while the water tank (custom-built with an Ultrawave SFE590 ultrasonic generator) shows about 25% of the efficiency obtained with the two smaller water baths due to the larger volume of the water tank and to differences in the amount of sonic power delivered to the sample. Since the main aim of the present study was the characterisation of the effects of the sonication process, the experiments described in all the following chapters were performed using the small scale provided by the two water baths, leaving the scale-up - using the custom-built water tank - for the future developments of the process.

Chapters 5 and 6 investigated the mechanism through which the decrease of the oil viscosity takes place; this mechanism has been hypothesised to be related to the breakage of the oils' chains with the formation of lower molecular weight radical species. Some preliminary results have shown that the nature of these radicals is both oxygen- and non-oxygen- related. If left free, the radical species react with themselves forming new chains, leading to an increase in the viscosity.

Chapter 7 highlighted the effectiveness of the ultrasound on lowering the viscosity of various commercially available oils with a carbon-based chain, whist illustrating the inefficiency of the process on complex non-organic oils, such as silicone oil. This difference in action is due to the difference in bond energies between the carbon-based oil and silicone oil being higher for the latter; moreover the lower vapour pressure which characterises silicone oil increases the tensile strength of the liquid limiting the formation of the cavities.

The investigations reported in chapters 5, 6, and 7 also showed that the viscosity decrease is further enhanced by the addition of a nucleating agent such as carbon black; this action has been shown to be possibly inhibited by the detergents added to some of the oils (motor oil and diesel) during the manufacturing process. The addition of a radical scavenger after the sonication was able to stabilise the lower viscosity levels achieved and thus avoiding the chains rearrangements during the storage time mentioned previously. The addition of the radical scavenger before the sonication inhibits the chain-breaking action of the ultrasound on the oils, thus supporting the hypothesis of the formation of highly reactive radical species during the sonication process. It has also been shown that an influence of the so called "thermal effect" on the viscosity decrease is visible mainly during the first 30 minutes after the sonication. This could be of some importance for those applications which require a lower level of viscosity when it does not matter if that was generated by the cavitation-driven physical-mechanical cleavage of the oil chains, or by the generalised effect that any increase in temperature has on the viscosity of any sample.

Throughout these chapters some differences in the rate of viscosity percentage decrease across different experiments were noticeable. These differences have to be related to the use of different batches of the oils; fluctuations of the laboratory temperature could also be a possible cause for this behaviour, but should be excluded due to a fine control of the temperature achieved with an air conditioning and ventilation system.

Chapter 8 has shown that most of the techniques used to characterise the chemical changes, to which the oils undergo during exposure to ultrasound, were not effective in producing quantitative results and no definitive conclusions can be obtained. The techniques used for the analysis of the volatiles do potentially indicate an oxidative process taking place within the samples during sonication, but this indication is at present insufficient to determine the real changes in the chemical structure of the chains of the oils before and after treatment with ultrasound. In addition to this, the chromatographic analysis of the liquid sample and the electron spin resonance, for the characterisation of the radical species, gave no further useful information.

Chapter 8 also reported the calorimetric analysis; these preliminary results indicate that the combustion characteristics of the model carbon-based oil are improved by the sonication process. This supports the hypothesis of the ultrasound being able to alter the structure of carbon-based oils.

Moreover chapter 9 has shown that the ultrasound has proved to be effective to drive the alkaline hydrolysis of the fatty acids constituting the triglycerides contained within the oil (saponification reaction), which implies a structural change of the oils' chains. The reaction has been optimised to achieve a higher yield in a relative low reaction time (15 minutes) and at room temperature, with consequently potentially lower energy consumption when compared with the traditional process. Further benefits of this process include the absence of detectable by-products, which simplifies any eventual procedure for the purification of the product, as well as negating the need to add extra chemicals (such as PTC) to the reaction mixture.

Having seen the favourable results in chapters 5, 6, and 7 relating to the effectiveness of ultrasound to cleave the chains of carbon-based oils, the promising preliminary results of the calorimetric analysis in chapter 8, and the positive results obtained from the saponification reaction (chapter 9), the sonication approach is confirmed as a viable process to alter the structure of carbon-based oils, and it will be worthwhile attempting to use other analytical techniques to obtain some more definitive results relating to the structural changes ultrasound generates on the oils' chains.

Possible future applications of the sonication process described herein include: its application as method to lower and stabilise the viscosity of a wide range of carbon-based oil to improve their pumpability and transport; a new process for the treatment of oil waste possibly coupled with some thermal energy recovery system, as in the case of the cogeneration plants, which can use an internal combustion engine to burn several different substrates and recover the generated thermal energy/power [98]; a new process to produce biofuel or improve its characteristics.

Future applications are also foreseen for the scale-up of the saponification process in conjunction with the traditional reaction mechanism. A possible approach could be to perform the main part of the reaction using ultrasound and completing the conversion of the remaining esters in the traditional manner with the aid of heat.

Chapter 11

Conclusions and Further work

Conclusions

This work has shown that the ultrasound is effective in cleaving the chains of carbon-based oils. However, despite the success in carbon-based oils, this approach has proven to be ineffective on complex non-organic oils, such as silicone oil. This difference in behaviour is suggested to be due to the different bond energies between the C-C and Si-O bonds constituting the core chains of the oils.

The proposed mechanism through which the ultrasound breaks the chains of the oils (thus leading to a drop in the viscosity) is based on the generation of radical species whose nature is either oxygen- or non-oxygen related. After sonication is terminated, the generation of lower molecular weight species ceases and the radicals formed can recombine thus leading to an increase in the viscosity.

The efficiency of the ultrasound, in breaking the oils' chains, was found to be increased by the addition of a nucleating agent such as carbon black, although its action is inhibited when detergents are present within the oil, as in the case of motor oil and diesel. To prevent chain rearrangements, due to the presence of radicals, the addition of a radical scavenger has also proven to be effective.

The techniques used within this work for the chemical analysis of the oils before and following sonication have proven to be insufficient in gaining a better understanding of the structural changes to which oils undergo during sonication. Some indications can be obtained from the analysis of the volatiles, which seem to indicate the potential of an oxidative process occurring within the samples. Moreover the preliminary calorimetric analysis performed indicates that the sonication process improves the combustion characteristics of the model carbon-based oil. These findings, whilst not conclusive, seem to confirm the hypothesis of the chains cleaving action of the ultrasound.

Furthermore the effectiveness of the ultrasound in causing chemical changes in oils has been shown whilst using it as power source to drive the saponification reaction. The optimisation of the reaction has allowed obtaining a high yields in low reaction times coupled to lower energy consumption in comparison to the traditional process.

Suggestions for further work

Frequency investigation: the present work has mainly investigated the effects of ultrasound at an operational frequency of 35 kHz, which was found to be effective in breaking the C-C bonds of carbon-based oils giving a good level of viscosity decrease; the investigation of the effects of other frequencies of ultrasound will be beneficial to determine if higher or lower ultrasonic frequencies are able to break the chains of samples characterised by higher energy bonds (such as silicone oil). Moreover, of particular interest, could be the application of ultrasound with lower frequency but higher power which could speed up the growth step of the cavitation phenomenon, thus having a stronger effect on the samples, i.e. leading to a potentially greater viscosity decrease, possibly for shorter exposure times.

Chemical characterisation: as discussed before the analytical methods used so far have proven to be insufficient in obtaining clear and definitive data on the chemical changes to which the oils undergo during sonication. The continuation of the Liquid Chromatography – Mass Spectrometry analysis would be advantageous in particular on samples sonicated for a longer time and/or with ultrasound at higher/lower operational frequencies in order to obtain stronger, and hopefully, more detectable chemical effects/changes on the structure of the oils' chains. The addition of the radical trap (PBN) or of the radical scavenger (4-tert-butylphenol) to these oil samples will be highly beneficial to respectively stabilise the radical species formed, or prevent the chain rearrangements. These treatments of the samples after sonication should allow the stabilisation of the products, so that they may be more easily detected by the analytical method.

Further investigations on the nature of the radicals generated during sonication will be also advantageous; the oil samples could be treated, during sonication, with air to simulate the addition of extra oxygen to the sample, or with H_2O_2 to simulate an oxidative process. Both these treatments should not only clarify the nature of the radicals formed during sonication, but also have some effects on the modification of the viscosity of the samples following the sonication.

Combustion investigation: in order collect data on the energy which can be obtained from the oils, on their efficiency as possible fuels, and on their carbon release, other calorimetric and combustion analyses are required. A suggested calorimetric approach would be to use oxygen bomb calorimetry; this will provide more accurate data on the calorific value of the oils than those obtained with the "home-made" calorimeter here described, which, as previously discussed, might be affected by some errors due to the nature of the experimental set-up. For the combustion investigation a diesel engine is suggested, since the chemical characteristics of the non-treated oils and of the sonicated products are analogous with those of biodiesel. These experiments will again have to be performed on the oil samples before and after sonication exposure; the addition of the radical scavenger following the sonication (so as to stabilise the lower viscosity level achieved with sonication) could also be beneficial in order to investigate the combustion properties of the stable lower viscosity product. These data will show if the process of producing sonicated oils offers environmental benefits and if their chemical characteristics are improved so as to be used as general fuels.

Thermodynamic evaluation: an evaluation of the energy required to drive the sonication of the oils will be highly beneficial; these data could then be related to the data obtained from the combustion of the oils after sonication to determine whether the process, of producing low viscous oils, is energetically favourable.

Process scale-up: some preliminary data on the scale-up of the sonication process are already presented in this work. This demonstrated the efficiency of the large custom-built water tank in affecting the viscosity of the samples; however it still remains to be established the effects of the sonication of an increased volume of sample within the water tank, and also the effects of increasing the time of sonication. Moreover all the investigations involving the use of the nucleating agent and of the radical scavenger will have to be reproduced on the larger scale, as well as the analysis of the combustion characteristics of the products obtained after sonication in the custom-built water tank.

References

[1] Wolfson, R.; Pasachoff, J. M. (1999). *Physics - With modern physics for scientists and engineers*, 3rd ed. Addison-Wesley.

[2] Leighton, T. G. (2007). What is ultrasound? - Review. *Progress in Biophysics and Molecular Biology*, 93, p. 3-83.

[3] Mason, T. J.; Peters, D. (2002). *Practical sonochemistry: power ultrasound uses and application*, 2nd ed. Woodhead Publishing (Cambridge).

[4] Ince, N. H.; Tezcanli, G.; Belen, R. K.; Apikyan, I. G. (2001). Ultrasound as a catalyzer of aqueous reaction systems: the state of the art and environmental applications. *Applied Catalysis B: Environmental*, 29, p. 167-176.

[5] Mason, T. J. (2003). Sonochemistry and sonoprocessing: the link, the trends and (probably) the future. *Ultrasonics Sonochemistry*, 10, p. 175-179.

[6] Chemat, F.; Grondin, I.; Costes, P.; Moutoussamy, L.; Shum Cheong Sing, A.; Smadja, J. (2004). High power ultrasound effects on lipid oxidation of refined sunflower oil. *Ultrasonics Sonochemistry*, 11, p. 281-285.

[7] Mason, T. J. (2007). Developments in ultrasound - Non-medical. *Progress in Biophysics and Molecular Biology*, 93, p. 166-175.

[8] Mason, T. J. (2000). Large scale sonochemical processing: aspiration and actuality. *Ultrasonics Sonochemistry*, 7, p. 145-149.

[9] Capote, F. P.; Luque de Castro, M. D. (2007). Ultrasound in analytical chemistry. *Analytical & Bioanalytical Chemistry*, 387, p. 249-257.

[10] Gogate, P. R.; Kabadi, A. M. (2009). A review of applications of cavitation in biochemical engineering/biotechnology. *Biochemical Engineering Journal*, 44, p. 60-72.

[11] Kim, Y. U.; Wang, M. C. (2003). Effect of ultrasound on oil removal from soils. *Ultrasonics*, 41, p. 539-542.

[12] Gopinath, R.; Dalai, A. K.; Adjaye, J. (2006). Effects of ultrasound treatment on the upgradation of heavy gas oil. *Energy and Fuels*, 20, p. 271-277.

[13] Soloff, R. S. (1964). Sonic drying. *The Journal of the Acoustical Society of America*, 36 (5), p. 961-965.

[14] Raman, G.; Srinivasan K. (2009). The powered resonance tube: from Hartmann's discovery to current active flow control applications. *Progress in Aerospace Sciences*, 45, p. 97-123.

[15] Gogate, P. R. (2008). Cavitational reactors for process intensification of chemical processing applications: A critical review. *Chemical Engineering and Processing*, 47, p. 515-527.

[16] Ji, J.; Wang, J.; Li, Y.; Yu, Y.; Xu, Z. (2006). Preparation of biodiesel with the help of ultrasonic and hydrodynamic cavitation. *Ultrasonics*, 44, p. 411-414.

[17] Suslick, K. S.; Price, G. J. (1999). Applications of ultrasound to materials chemistry. *Annual Reviews of Material Science*, 29, p. 295-326.

[18] Paulusse, J. M. J.; Sijbesma, R. P. (2006). Ultrasound in polymer chemistry: revival of an established technique. *Journal of Polymer Science Part A: Polymer Chemistry*, 44, p. 5445-5453.

[19] Earnshaw, R. G.; Appleyard, J.; Hurst R. M. (1995). Understanding physical inactivation processes: combined preservation opportunities using heat, ultrasound and pressure. *International Journal of Food Microbiology*, 28, p. 197-219.

[20] Brennen, C. E. (1995). *Cavitation and bubble dynamics*. Oxford University Press (New York).

[21] Majumdar, S.; Senthil Kumar, P.; Pandit, A. B. (1998). Effect of liquid-phase properties on ultrasound intensity and cavitational activity. *Ultrasonics Sonochemistry*, 5, p. 113-118.

[22] Price, G. J. (1996). Ultrasonically enhanced polymer synthesis. *Ultrasonics Sonochemistry*, 3, p. 229-238.

[23] Price, G. J.; West, P. J.; Smith, P. F. (1994). Control of polymer structure using power ultrasound. *Ultrasonics Sonochemistry*, 1 (1), p. 51-57.

[24] Rice, F. O. (1931). The thermal decomposition of organic compounds from the standpoint of free radicals. I. Saturated hydrocarbons. *Journal of American Chemical Society*, 53, p. 1959-1972.

[25] Suslick, K. S.; Gawlenowski, J. J.; Schubert, P. F.; Wang, H. H. (1983). Alkane sonochemistry. *Journal of Physical Chemistry*, 87, p. 2299-2301.

[26] Kuijpers, M. W. A.; Iedema, P. D.; Kemmere, M. F.; Keurentjes, J. T. F. (2004). The mechanism of cavitation-induced polymer scission; experimental and computational verification. *Polymer*, 45, p. 6461-6467.

[27] Pandit, A. B.; Joshi, J. B. (1993). Hydrolysis of fatty oils: effect of cavitation. *Chemical Engineering Science*, 48 (19), p. 3440-3442.

[28] Solomons, T. W. G.; Fryhle, C. B. (1998). *Organic chemistry*, 7th ed. John Wiley & Sons, Inc. (New York).

[29] Norris, M. H.; McBain, J. W. (1922). A study of the rate of saponification of oils and fats by aqueous alkali under various conditions. *Journal of the Chemical Society, Transactions*, 121, p. 1362-1375.

[30] Moon, S.; Duchin, L.; Cooney, J. V. (1979). Application of ultrasound to organic reactions: Ultrasonic catalysis on hydrolysis of carboxylic acid esters. *Tetrahedron Letters*, 41, p. 3917-3920.

[31] Davidson, R. S.; Safdar, A.; Spencer, J. D.; Robinson, B. (1987). Application of ultrasound to organic chemistry. *Ultrasonics*, 25 (1), p. 35-39.

[32] Robinson, B.; Safdar, A.; Davidson, R. S. (1986). Saponification of fats and oils. UK patent GB 2170507A.

[33] Bhatkhande, B. S.; Samant, S. D. (1998). Ultrasound assisted PTC catalyzed saponification of vegetable oils using aqueous alkali. *Ultrasonics Sonochemistry*, 5, p. 7-12.

[34] Entezari, M. H.; Keshavarzi, A. (2001). Phase-transfer catalysis and ultrasonic waves II: saponification of vegetable oil. *Ultrasonics Sonochemistry*, 8, p. 213-216.

[35] Liu, Y.; Jin, Q.; Shan, L.; Liu, Y.; Shen, W.; Wang, X. (2008). The effect of ultrasound on lipase-catalyzed hydrolysis of soy oil in solvent-free system. *Ultrasonics Sonochemistry*, 15, p. 402-407.

[36] Huang, J.; Liu, Y.; Song, Z.; Jin, Q.; Liu, Y.; Wang, X. (2010). Kinetic study on the effect of ultrasound on lipase-catalyzed hydrolysis of soy oil: Study of the interfacial area and the initial rate. *Ultrasonics Sonochemistry*, 17, p. 521-525.

[37] Siatis, N. G.; Kimbaris, A. C.; Pappas, C. S.; Tarantilis, P. A.; Polissiou, M. G. (2006). Improvement of biodiesel production based on the application of ultrasound: monitoring of the procedure by FTIR spectroscopy. *Journal of the American Oil Chemists' Society*, 83 (1), p. 53-57.

[38] Yustianingsih, L.; Zullaikah, S.; Ju, Y. -H. (2009). Ultrasound assisted in situ production of biodiesel from rice bran. *Journal of the Energy Institute*, 82, p. 133-137.

[39] Deng, X.; Fang, Z.; Liu, Y. (2010). Ultrasonic transesterification of Jatropa curcas L. Oil to biodiesel by a two-step process. *Energy Conversion and Management*, 51, p. 2802-2807.

[40] Lima, L. P.; Santos, F. F. F.; Costa, E.; Fernandes, F. A. N. (2012). Production of free fatty acids from waste oil by application of ultrasound. *Biomass Conversion and Biorefinery*, July, DOI 10.1007/s13399-012-0056-0.

[41] Goodger, E. M. (2000). *Transport Fuels Technology*, Landfall Press (Norwich).

[42] Yusuf, N. N. A. N.; Kamarudin, S. K.; Yaakub, Z. (2011). Overview on the current trends in biodiesel production. *Energy Conversion and Management*, 52, p. 2741-2751.

[43] Lee, C. S.; Park, S. W.; Kwon, S. I. (2005). An experimental study on the atomization and combustion characteristics of biodiesel-blended fuels. *Energy and Fuels*, 19, p. 2201-2208.

[44] Ramadhas, A. S.; Jayaraj, S.; Muraleedharan, C. (2004). Use of vegetable oils as I.C. engine fuels - A review. *Renewable Energy*, 29, p. 727-742.

[45] Altim, R.; Cetinkaya, S.; Yucesu, H. S. (2001). The potential of using vegetable oil fuels as fuel for diesel engines. *Energy Conversion and Management*, 42, p. 529-538.

[46] Kegl, B. (2011). Influence of biodiesel on engine combustion and emission characteristics. *Applied Energy*, 88, p. 1803-1812.

[47] Thamsiriroj, T.; Murphy, J. D. (2011) A critical review of the applicability of biodiesel and grass biomethane as biofuels to satisfy both biofuel targets and sustainability criteria. *Applied Energy*, 88, p. 1008-1019.

[48] Benjumea, P.; Agudelo, J. R.; Agudelo, A. F. (2011). Effects of the degree of unsaturation of biodiesel fuels on engine performance, combustion characteristics, and emissions. *Energy and Fuels*, 25, p. 77-85.

[49] Xue, J.; Grift, T. E.; Hansen, A. C. (2011). Effect of biodiesel on engine performances and emissions. *Renewable and Sustainable Energy Reviews*, 15 (2), p. 1098-1116.

[50] Fazal, M. A.; Haseeb, A. S. M. A.; Masjuki, H. H. (2011). Biodiesel feasibility study: an evaluation of material compatibility and engine durability. *Renewable and Sustainable Energy Reviews*, 15 (2), p. 1314-1324.

[51] Yu, C. W.; Bari, S.; Ameen, A. (2002). A comparison of combustion characteristics of waste cooking oil with diesel as fuel in a direct injection diesel engine. *Proceedings of the Institution of Mechanical Engineers, Part D: Journal of Automobile Engineering*, 216, p. 237-243.

[52] Ozsezen, A. N.; Canakci, M.; Sayin, C. (2008). Effects of biodiesel from used frying palm oil on the performance, injection, and combustion characteristics of an indirect injection diesel engine. *Energy and Fuels*, 22, p. 1297-1305.

[53] Ya-fen, L.; Yo-ping, G. W.; Chang-Tang, C. (2007). Combustion characteristics of waste-oil produced biodiesel/diesel fuel blends. *Fuel*, 86, p. 1772-1780.

[54] Holland, B.; McCance, R. A.; Widdowson, E. M. (1991). *McCance and Widdowson's The composition of food*, 5th ed. Royal Society of Chemistry and Ministry of Agriculture, Fisheries and Food.

[55] Gunstone, F. D.; Herslöf, B. G. (2000). *Lipid Glossary 2*, The Oily Press (Bridgwater).

[56] Oilseed Glossary. In: *Soya & Oilseed Bluebook* (2006), Soyatech.
Citing Internet resources (WWW document accessed 11th January 2010).
http://www.soyatech.com/oilseed_glossary.htm

[57] Marth, J. S. (2007). Chapter 13 - Non-renewable types of lubricants. In: *Renewable Lubricants Manual - Biobased Oils, Fluids, & Greases*, United Bio Lube.
Citing Internet resources (WWW document accessed 11th January 2010).
http://www.renewablelubricants.com/Renewable_Lubricants_Manual.html

[58] Johnson, S. J.; Barry, D. A.; Christofi, N.; Patel, D. (2001). Potential for anaerobic biodegradation of linear alkylbenzene cable oils: literature review and preliminary investigation. *Land Contamination & Reclamation*, 9 (3), p. 279-291.

[59] Bewley, R. J. F.; Alexander, J. G.; Webb, G. H. (2001). *Ex situ* and *in situ* bioremediation of former oil distribution terminals. *Land Contamination & Reclamation*, 9 (2), p. 175-189.

[60] Sobiecka, E.; Cedzynska, K.; Bielski, C.; Antizar-Ladislao, B. (2009). Biological treatment of transformer oil using commercial mixtures of microorganisms. *International Biodeterioration & Biodegradation*, 63 (3), p. 328-333.

[61] Kirk-Otmer (1995). *Encyclopedia of chemical technology*, 4th ed., vol. 22. John Wiley & Sons Inc. (New York) (executive editor Kroschwitz, J. I.; editor Howe-Grant, M.).

[62] De, S.; Perkins, M.; Dutta, S. K. (2006). Nitrate reductase gene involvement in hexachlorobiphenyl dechlorination by *Phanerochaete chrysosporium*. *Journal of Hazardous Materials*, 135 (1-3), p. 350-354.

[63] Montagnolli, R. N.; Lopes, P. R. M.; Bidoia E. D. (2009). Applied models to biodegradation kinetics of lubricant and vegetable oils in wastewater. *International Biodeterioration & Biodegradation*, 63 (3), p. 297-305.

[64] Lin, Y. J.; Chen, Y. L.; Huang, C. Y.; Wu, M. F. (2006). Photocatalysis of 2,2',3,4,4',5'-hexachlorobiphenyl and its intermediates using various catalytical preparing methods. *Journal of Hazardous Materials B*, 136 (3), p. 902-910.

[65] Manzano, M. A.; Perales, J. A.; Sales, D.; Quiroga, J. M. (2004). Catalyzed hydrogen peroxide treatment of polychlorinated biphenyl contaminated sandy soils. *Water, Air, and Soil Pollution*, 154 (1-4), p. 57-69.

[66] Whitfield Åslund, M. L.; Zeeb, B. A.; Rutter, A.; Reimer, K. J. (2007). *In situ* phytoextraction of polychlorinated biphenyl - (PCB) contaminated soil. *Science of the Total Environment*, 374, p. 1-12.

[67] Ma, F.; Hanna, M. A. (1999). Biodiesel production: a review. *Bioresource Technology*, 70, p. 1-15.

[68] Maher, K. D.; Bressler, D. C. (2007). Pyrolysis of triglyceride materials for the production of renewable fuels and chemicals. *Bioresource Technology*, 98, p. 2351-2368.

[69] Demirbas, A. (2008). Comparison of transesterification methods for production of biodiesel from vegetable oils and fats. *Energy Conversion and Management*, 49, p. 125-130.

[70] Gornay, J.; Coniglio, L.; Billaud, F.; Wild, G. (2009). Steam cracking and steam reforming of waste cooking oil in a tubular stainless steel reactor with wall effects. *Energy Fuels*, 23 (11), p. 5663-5676.

[71] Ong, Y. K.; Bhatia S. (2010). The current status and perspectives of biofuel production via catalytic cracking of edible and non-edible oils. *Energy*, 35 (1), p. 111-119.

[72] Stumborg, M.; Wong, A.; Hogan, E. (1996). Hydroprocessed vegetable oils for diesel fuel improvement. *Bioresource Technology*, 56, p. 13-18.

[73] Marquevich, M.; Farriol, X.; Medina, F.; Montané, D. (2001). Hydrogen production by steam reforming of vegetable oils using nickel-based catalysts. *Industrial & Engineering Chemistry Research*, 40, p. 4757-4766.

[74] Tooley, J. (2008). Process for Cracking of Waste Oil by Microwave. Patent Publication Number: US 2008/0202982 A1.

[75] Stavarache, C.; Vinatoru, M.; Nishimura, R.; Maeda Y. (2005). Fatty acids methyl esters from vegetable oil by means of ultrasonic energy. *Ultrasonics Sonochemistry*, 12, p. 367-372.

[76] Stavarache, C.; Vinatoru, M.; Maeda Y. (2006). Ultrasonic versus silent methylation of vegetable oils. *Ultrasonics Sonochemistry*, 13, p. 401-407.

[77] Stavarache, C.; Vinatoru, M.; Maeda Y. (2007). Aspects of ultrasonically assisted transesterification of various vegetable oils with methanol. *Ultrasonics Sonochemistry*, 14, p. 380-386.

[78] Georgogianni, K. G.; Kontominas, M. G.; Pomonis, P. J.; Avlonitis, D.; Gergis V. (2008). Conventional and *in situ* transesterification of sunflower seed oil for the production of biodiesel. *Fuel Processing Technology*, 89, p. 503-509.

[79] Abramov, O. V.; Abramov, V. O.; Myasnikov, S. K.; Mullakaev, M. S. (2009). Extraction of bitumen, crude oil and its products from tar sand and contaminated sandy soil under effect of ultrasound. *Ultrasonics Sonochemistry*, 16, p. 408-416.

[80] Muller, G.; Abraham, K.; Schaldach, M. (1981). Quantitative ATR spectroscopy: some basic considerations. *Applied Optics*, 20 (7), p. 1182-1190.

[81] Greener, J.; Abbasi, B.; Kumacheva, E. (2010) Attenuated total reflection Fourier transform infrared spectroscopy for on-chip monitoring of solute concentrations. *The Royal Society of Chemistry - Lab Chip*, 10, p. 1561-1566.

[82] Vongsvivut, J.; Heraud, P.; Zhang, W.; Kralovec, J. A.; McNaughton, D.; Barrow, C. J. (2012). Quantitative determination of fatty acid compositions in micro-encapsulated fish-oil supplements using Fourier transform infrared (FTIR) spectroscopy. *Food Chemistry*, 135, p. 603-609.

[83] Sherazi, S. T. H.; Talpur, M. Y.; Mahesar, S. A.; Kandhro, A. A.; Arain, S. (2009). Main fatty acid classes in vegetable oils by SB-ATR-Fourier transform infrared (FTIR) spectroscopy. *Talanta*, 80, p. 600-606.

[84] Khanmohammadi, M.; Kojidi, M. H.; Garmarudi, A. B.; Ashuri, A.; Soleymani, M. (2009). Quantitative monitoring of the amidation reaction between coconut oil and diethanolamine by attenuated total reflectance Fourier transform infrared spectrometry. *Journal of Surfactants and Detergents*, 12, p. 37-40.

[85] Rohman, A.; Che Man, Y. B.; Ismail, A.; Hashim, P. (2010). Application of FTIR spectroscopy for the determination of virgin coconut oil in binary mixtures with olive oil and palm oil. *Journal of the American Oil Chemists' Society*, 87, p. 601-606.

[86] Mazurek, S.; Szostak, R. (2012). Quantitative analysis of thiamine hydrochloride in tablets - Comparison of infrared attenuated total reflection, diffuse reflectance infrared and Raman spectroscopy. *Vibrational Spectroscopy*, 62, p. 10-16.

[87] Meléndez, L. V.; Lache, A.; Orrego-Ruiz, J. A.; Pachon, Z.; Mejia-Ospino, E. (2012). Prediction of the SARA analysis of Colombian crude oils using ATR-FTIR spectroscopy and chemometric methods. *Journal of Petroleum Science and Engineering*, 90-91, p. 56-60.

[88] Smith, D.; Spanel, P. (2005). Selected ion flow tube mass spectrometry (SIFT-MS) for on-line trace gas analysis. *Mass Spectrometry Reviews*, 24, p. 661-700.

[89] Zeb, A.; Murkovic, M. (2010). Analysis of triacylglycerols in refined edible oils by isocratic HPLC-ESI-MS. *European Journal of Lipid Science and Technology*, 112, p. 844-851.

[90] Laborde, J.-L.; Bouyer, C.; Caltagirone, J.-P.; Gérard, A. (1998). Acoustic cavitation field prediction at low and high frequency ultrasounds. *Ultrasonic*s, 36, p. 581-587.

[91] de Nevers, N. (2005). *Fluid mechanics for chemical engineers*, 3rd ed. McGraw – Hill (International Edition).

[92] Zima, P.; Marsik, F.; Sedlar, M. (2003). Cavitation rates in water with dissolved gas and other impurities. *Journal of Thermal Science*, 12 (2), p. 151-156.

[93] Health and Safety Executive (2011). Risk management of carbon nanotubes – Information sheet part of the Nanotechnology publications.
Citing Internet resources (WWW document accessed 15th February 2011).
http://www.hse.gov.uk/pubns/web38.pdf

[94] Carraher, C. E. Jr (2003). *Seymour/Carraher's Polymer chemistry*, 6th ed. Marcel Dekker, Inc. (New York).

[95] Chivate, M. M.; Pandit, A. B. (1995). Quantification of cavitation intensity in fluid bulk. *Ultrasonics Sonochemistry*, 2 (1), p. S19-S25.

[96] Castellano, M. M.; Reyman, D.; Sieiro, C.; Calle, P. (2001). ESR-spin trapping study on the sonochemistry of liquids in the presence of oxygen. Evidence for the superoxide radical anion formation. *Ultrasonics Sonochemistry*, 8, p. 17-22.

[97] Stuart, B. H. (2004). *Infrared spectroscopy: fundamentals and applications*. John Wiley & Sons Inc. (New York).

[98] COGEN Europe – The European Association for the Promotion of Cogeneration Citing Internet resources (WWW document accessed 13th October 2011). http://www.cogeneurope.eu/

Appendices

Appendix A

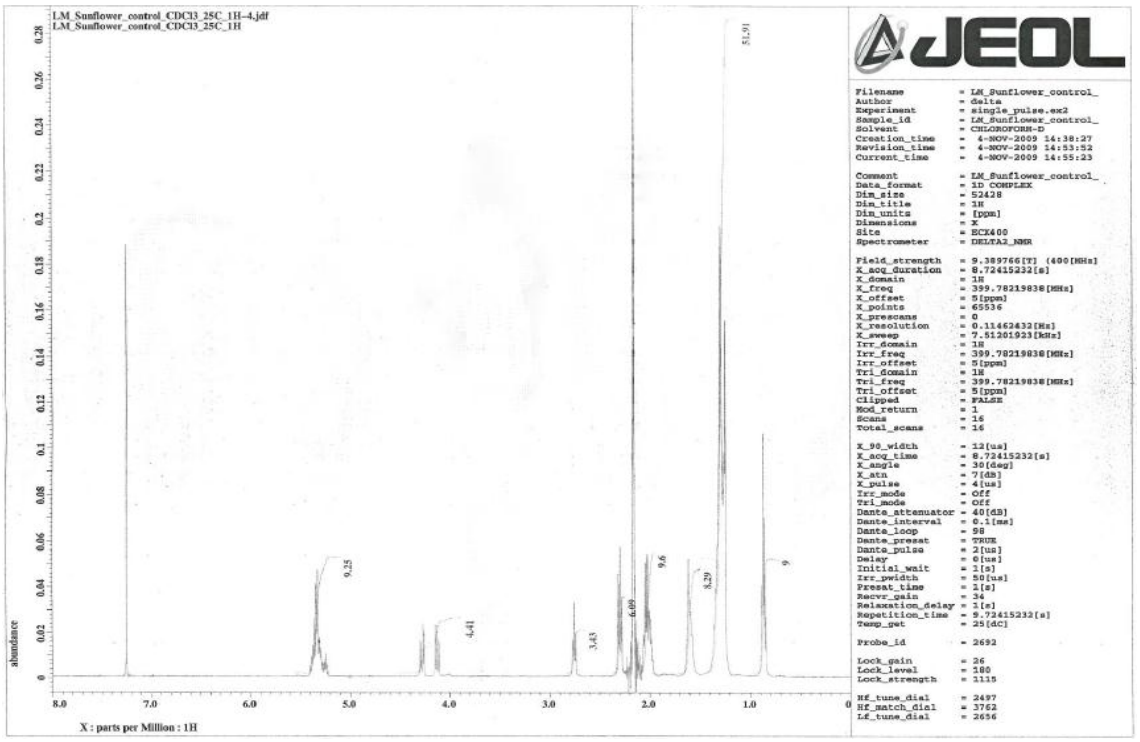

Figure A.1 ^{1}H-NMR spectra of non-sonicated sunflower oil (control).

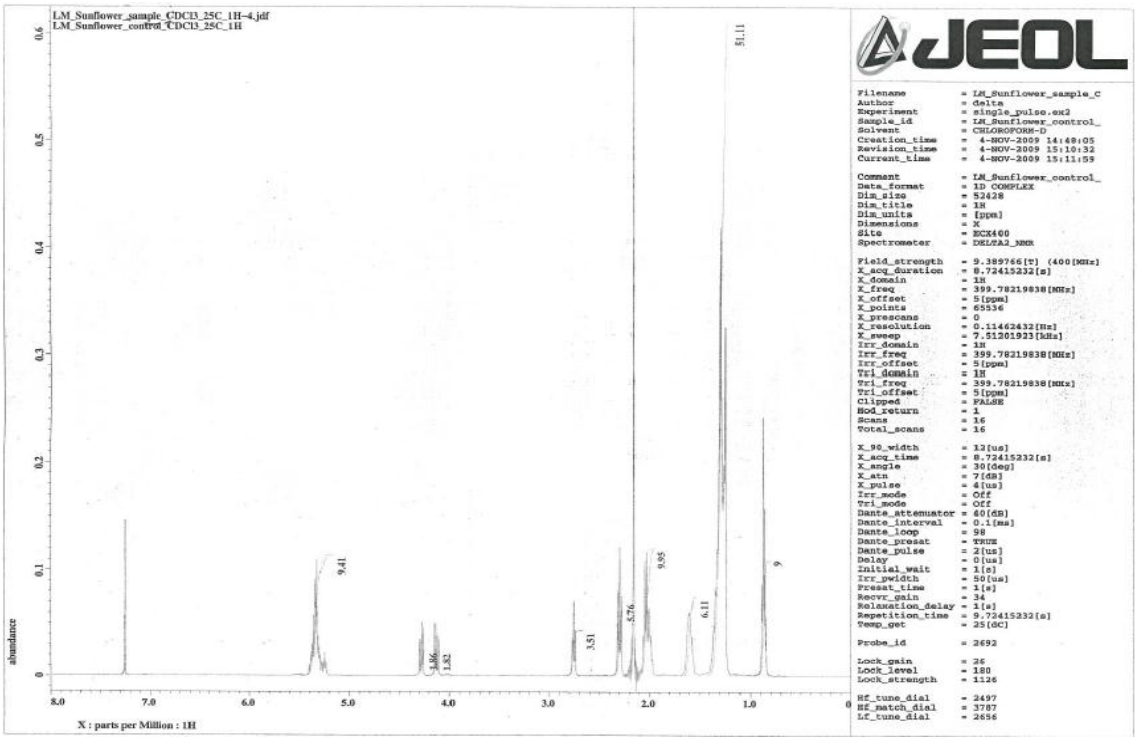

Figure A.2 ^{1}H-NMR spectra of sonicated sunflower oil (1 hour - 35 kHz frequency).

Appendix B

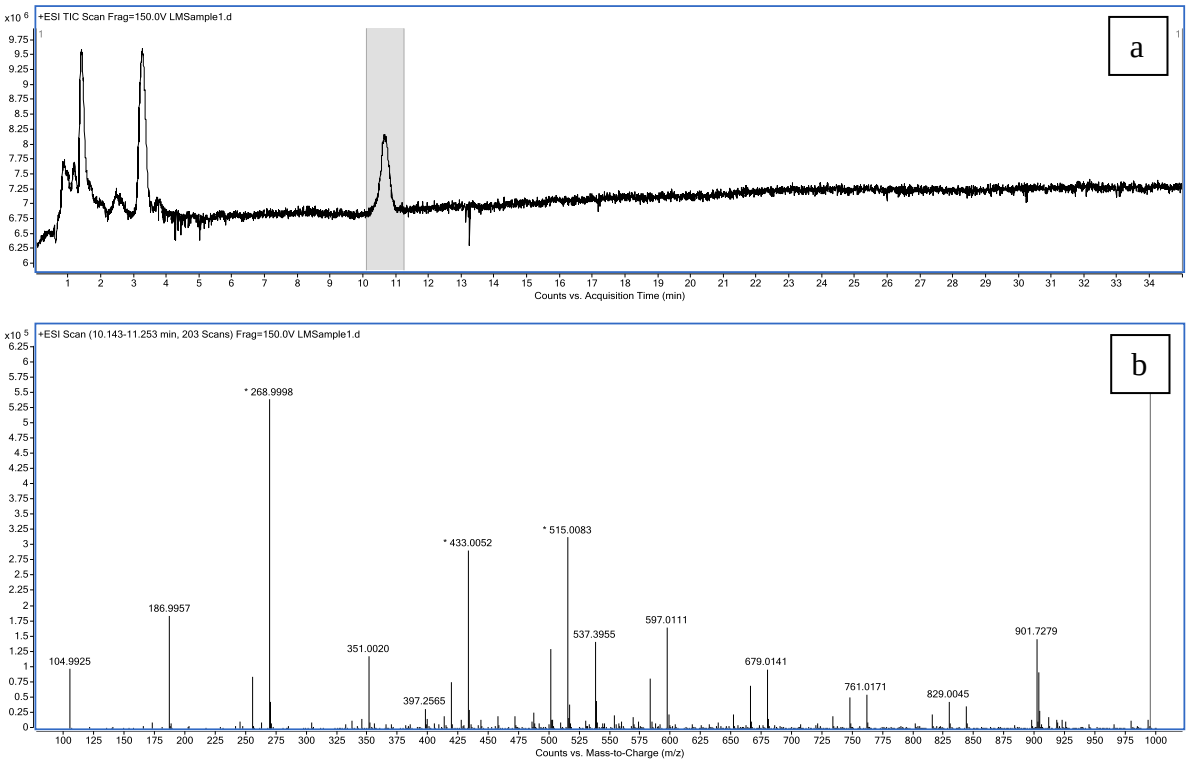

Figure B.1 TIC of non-sonicated glyceryl trilinoleate (a) and ion spectra of peak n°1 (b).

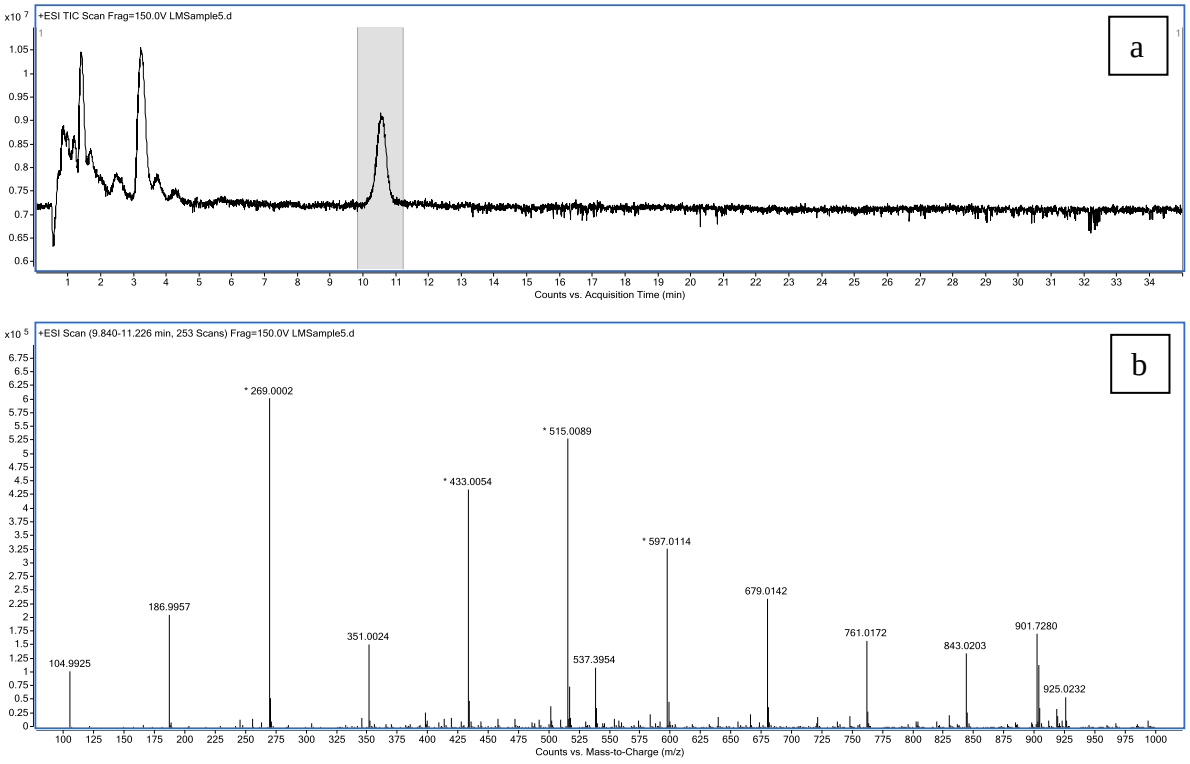

Figure B.2 TIC of sonicated glyceryl trilinoleate (a) and ion spectra of peak n°1 (b).

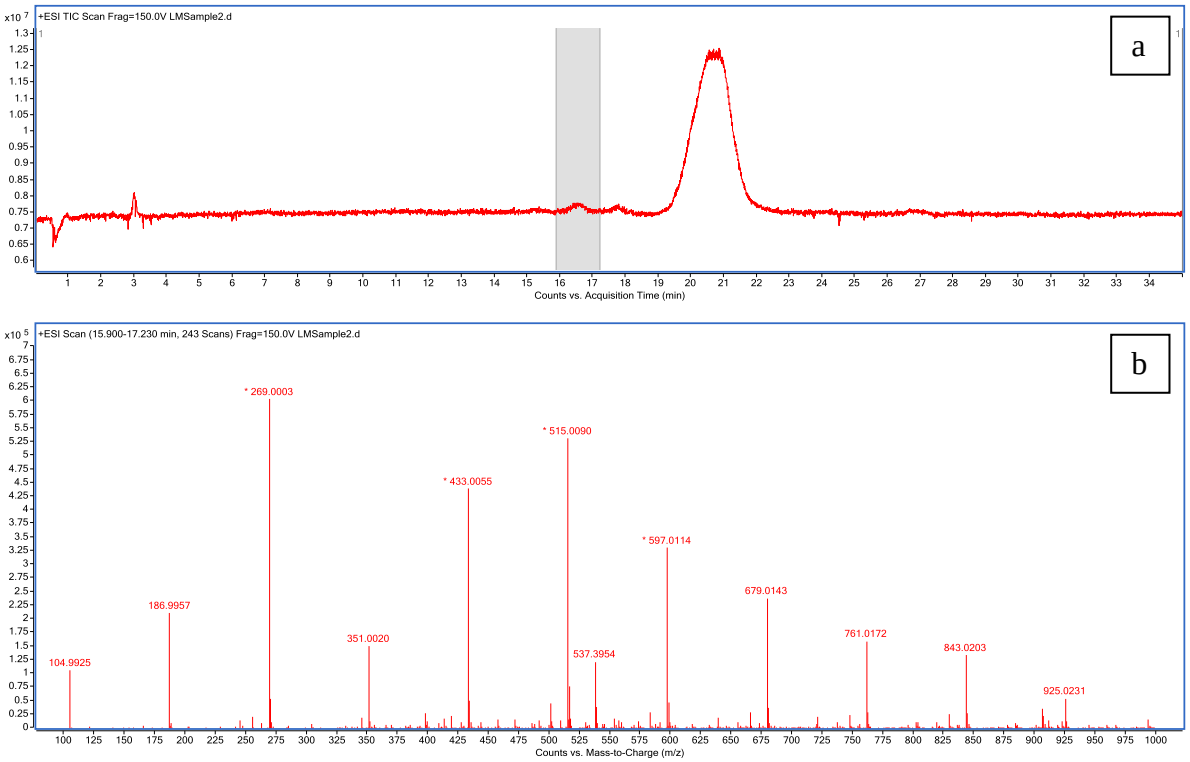

Figure B.3 TIC of non-sonicated glyceryl trioleate (a) and ion spectra of peak n°1 (b).

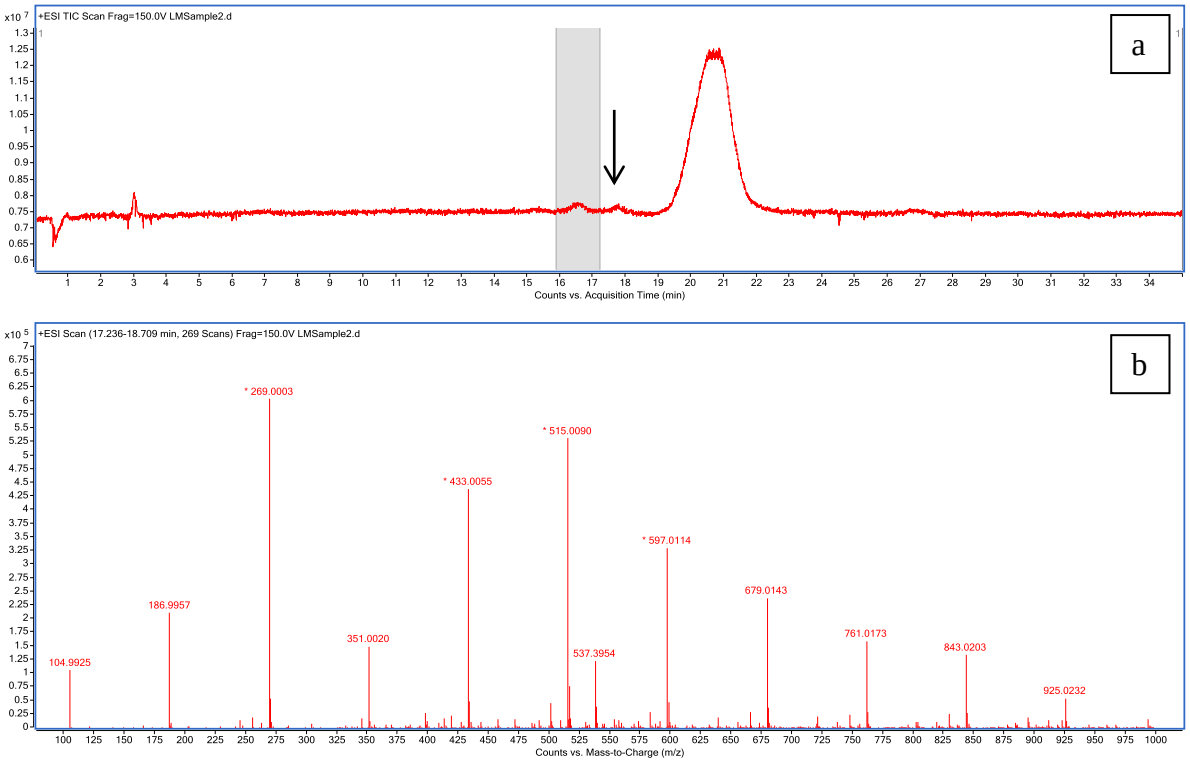

Figure B.4 TIC of non-sonicated glyceryl trioleate (a) and ion spectra of peak n°2 (b).

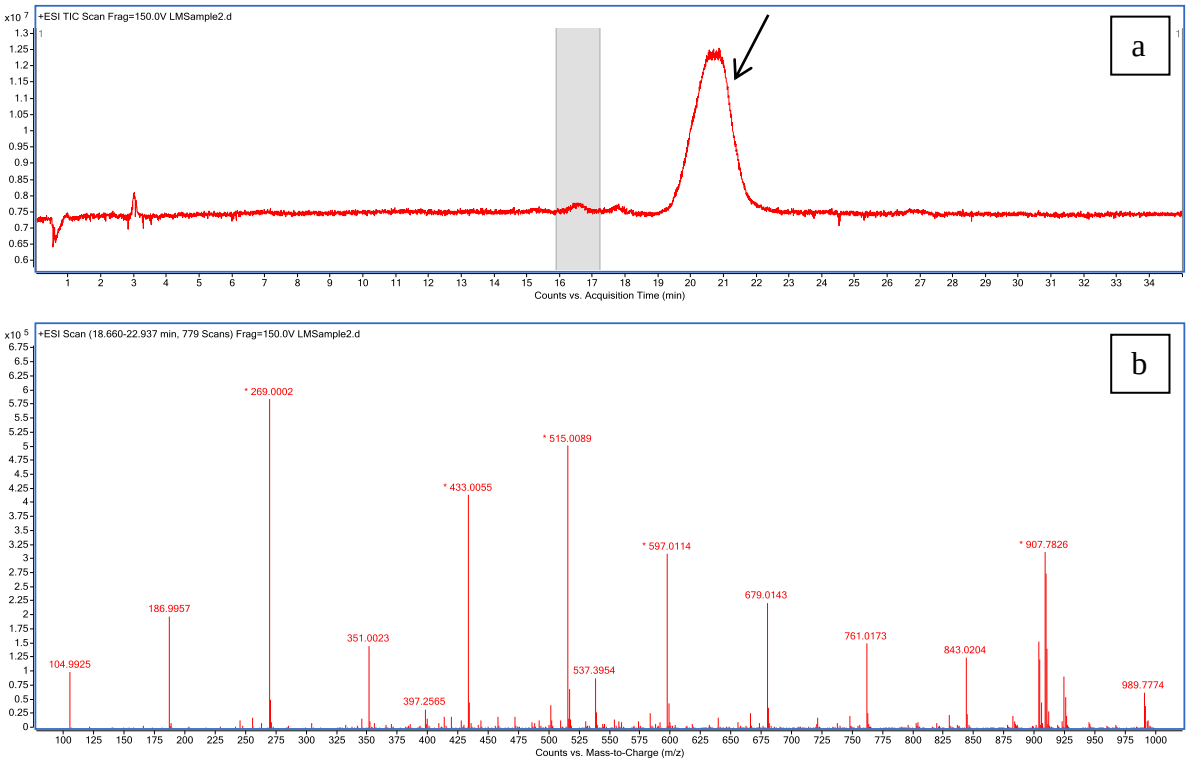

Figure B.5 TIC of non-sonicated glyceryl trioleate (a) and ion spectra of peak n°3 (b).

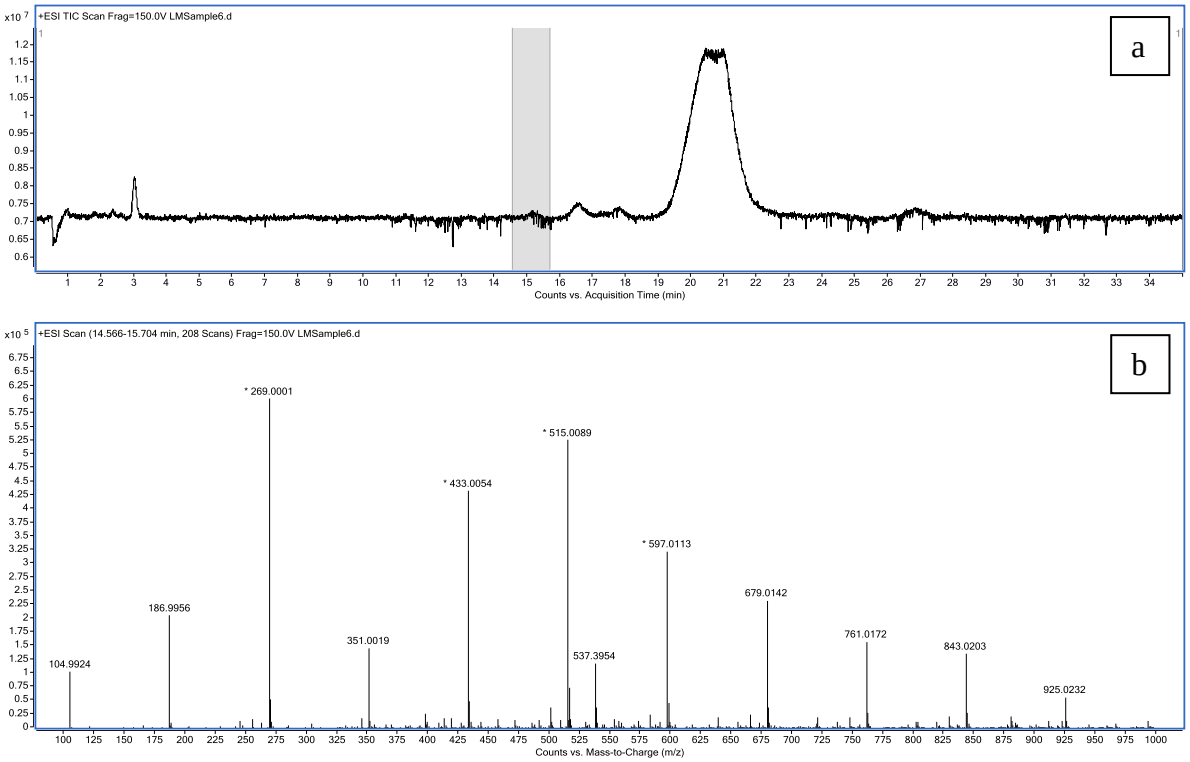

Figure B.6 TIC of sonicated glyceryl trioleate (a) and ion spectra of peak n°1 (b).

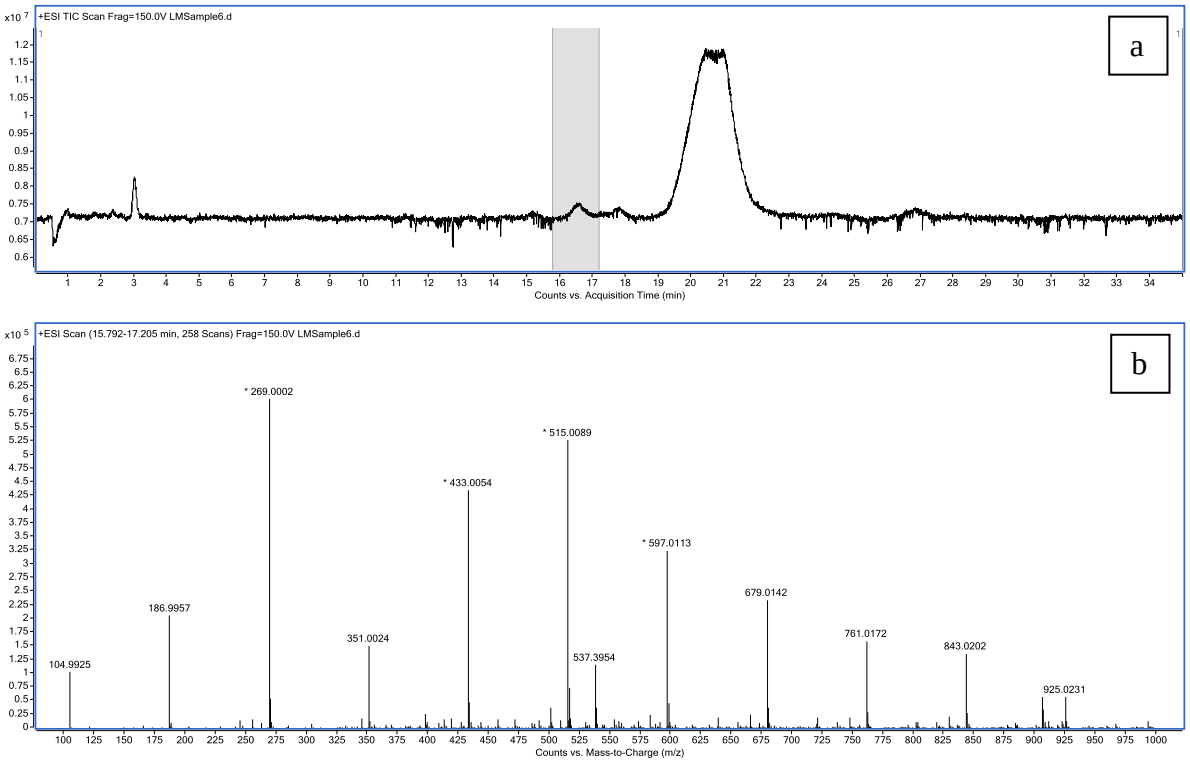

Figure B.7 TIC of sonicated glyceryl trioleate (a) and ion spectra of peak n°2 (b).

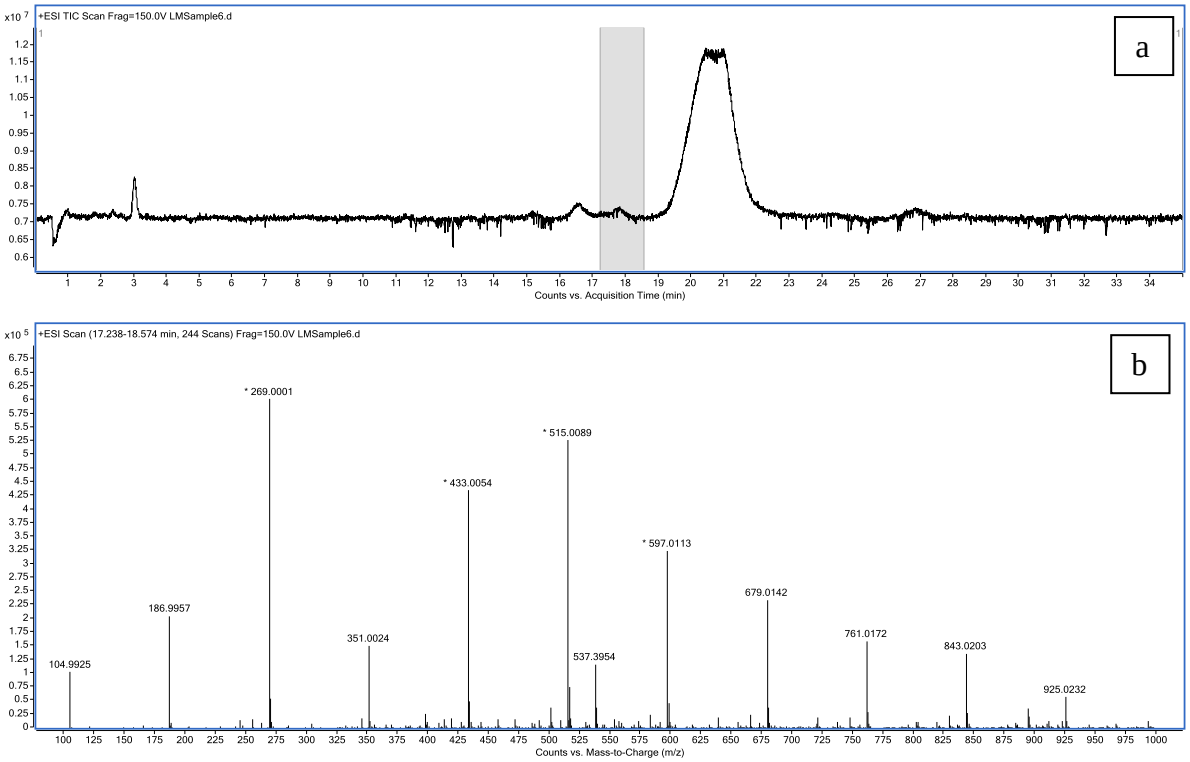

Figure B.8 TIC of sonicated glyceryl trioleate (a) and ion spectra of peak n°3 (b).

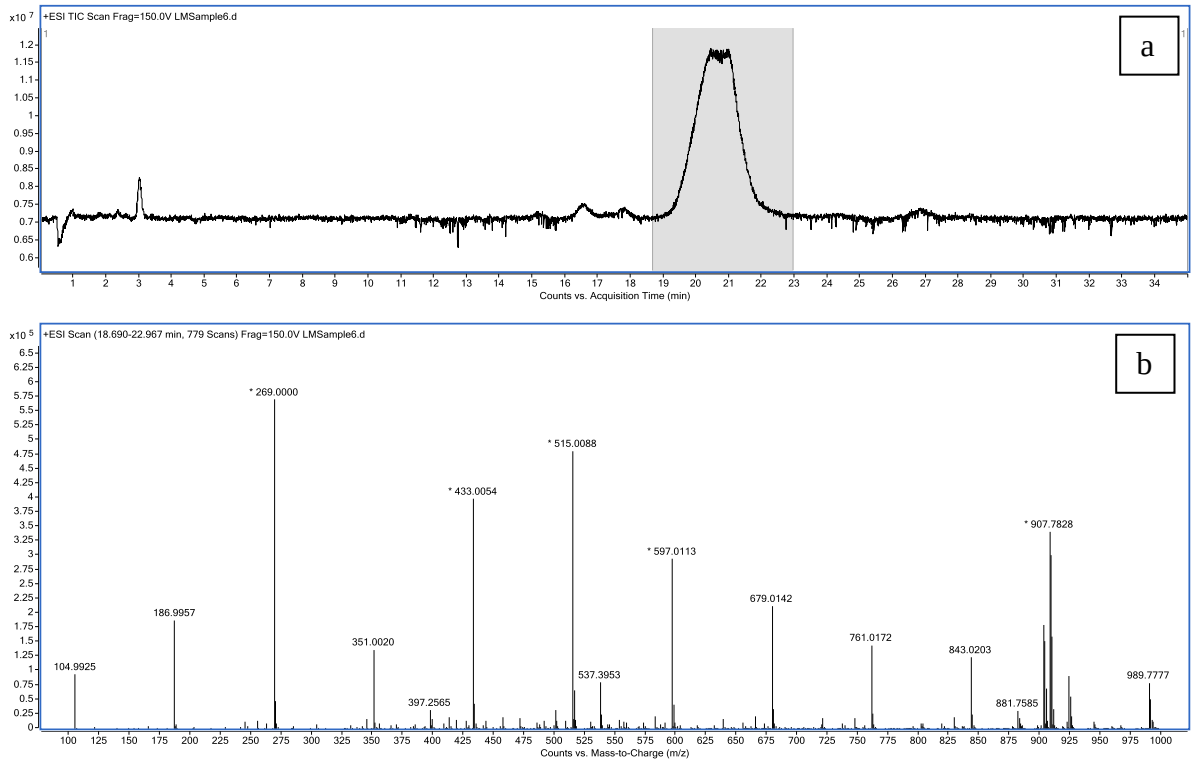

Figure B.9 TIC of sonicated glyceryl trioleate (a) and ion spectra of peak n°4 (b).

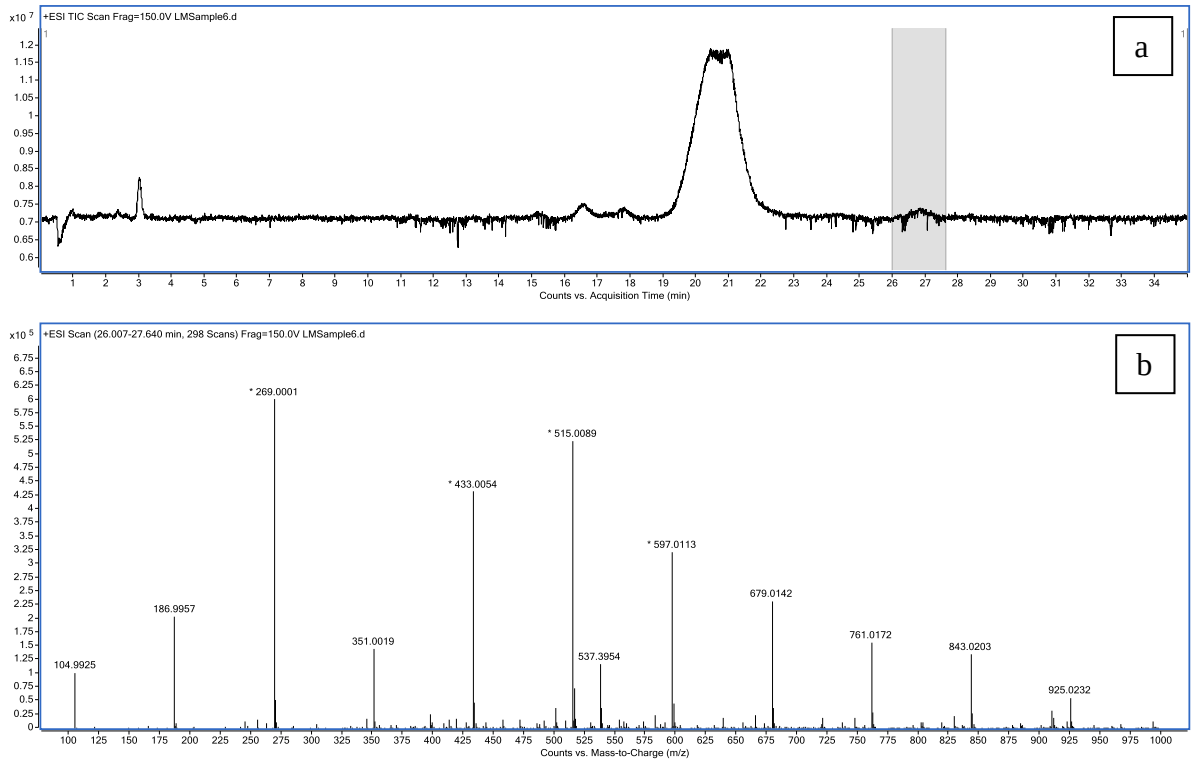

Figure B.10 TIC of sonicated glyceryl trioleate (a) and ion spectra of peak n°5 (b).

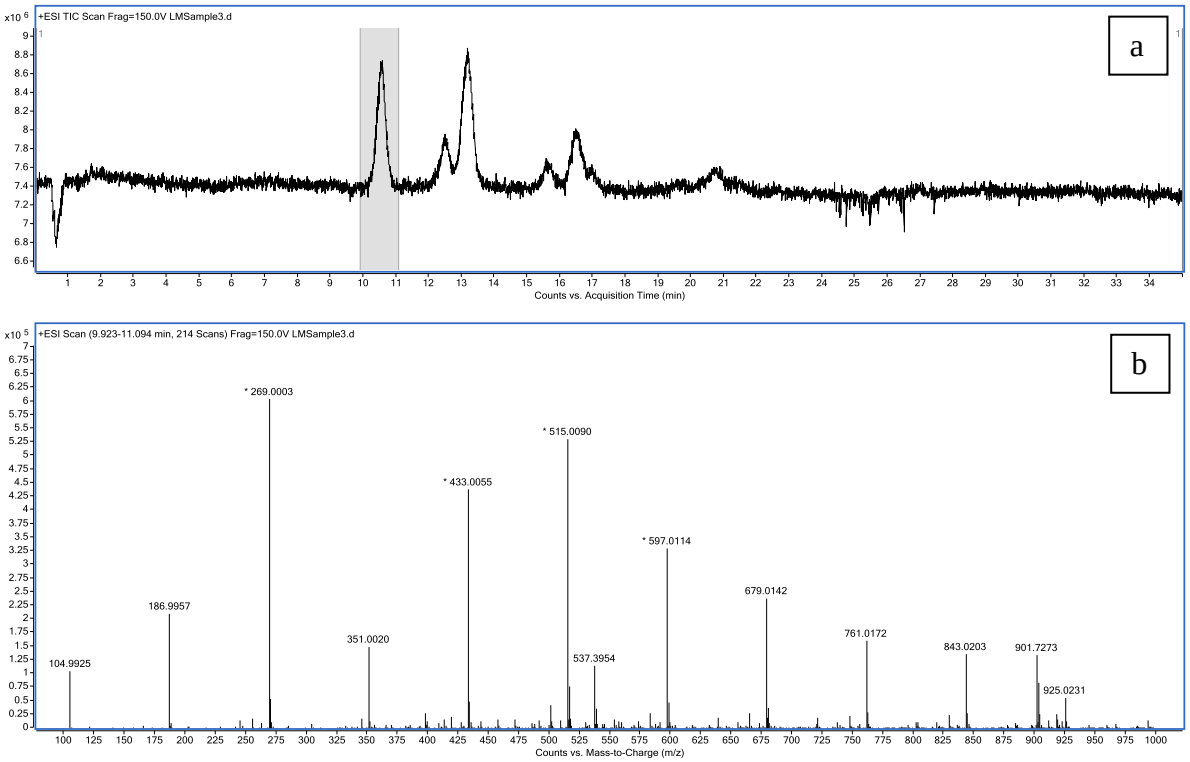

Figure B.11 TIC of non-sonicated sunflower oil (a) and ion spectra of peak n°1 (b).

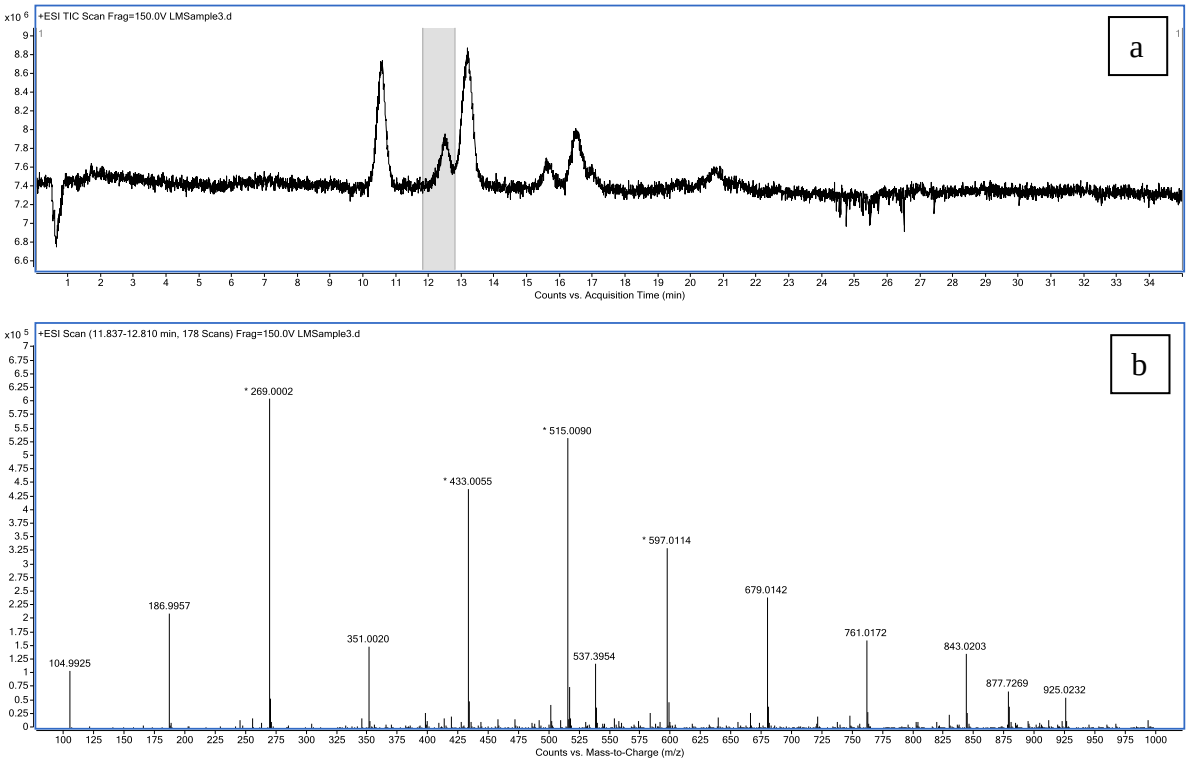

Figure B.12 TIC of non-sonicated sunflower oil (a) and ion spectra of peak n°2 (b).

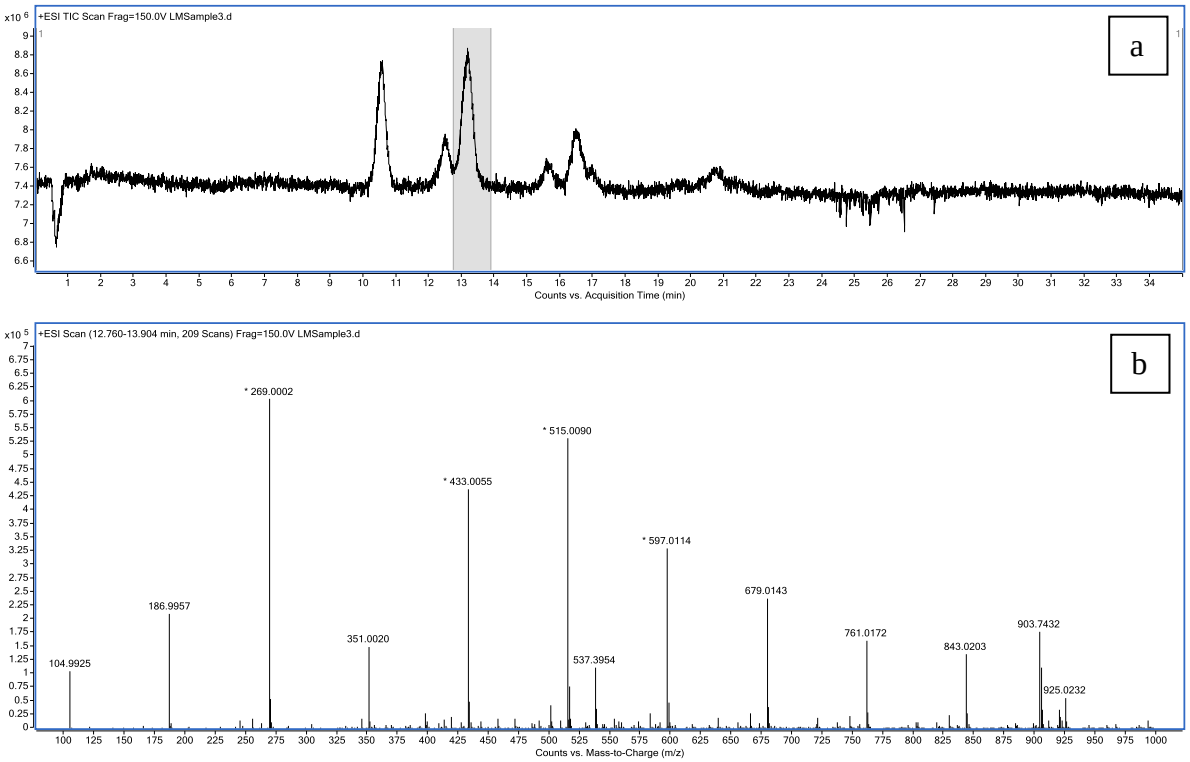

Figure B.13 TIC of non-sonicated sunflower oil (a) and ion spectra of peak n°3 (b).

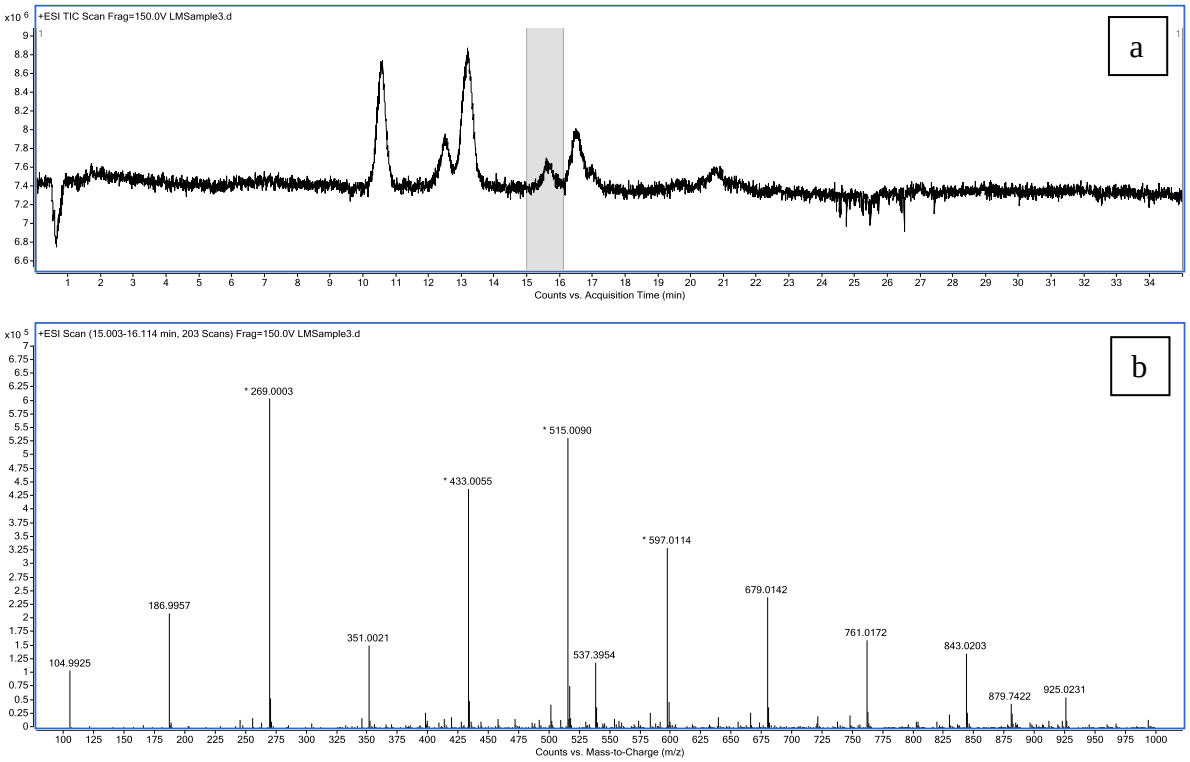

Figure B.14 TIC of non-sonicated sunflower oil (a) and ion spectra of peak n°4 (b).

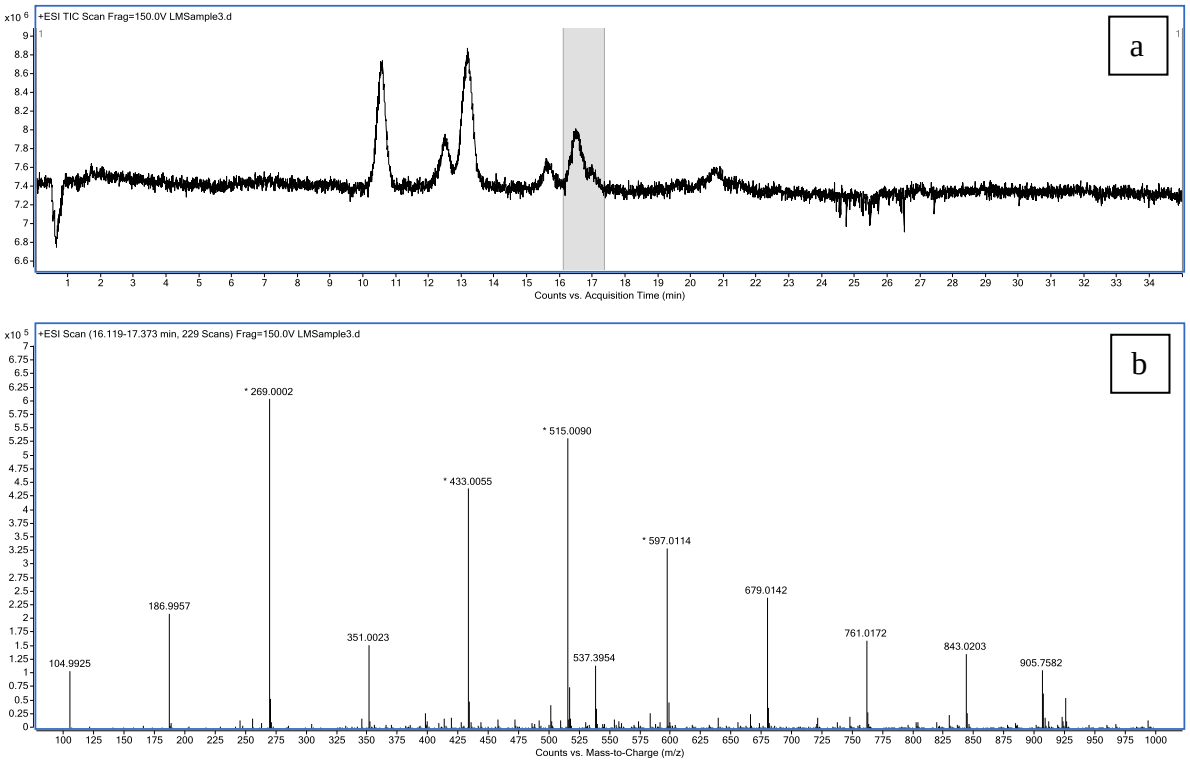

Figure B.15 TIC of non-sonicated sunflower oil (a) and ion spectra of peak n°5 (b).

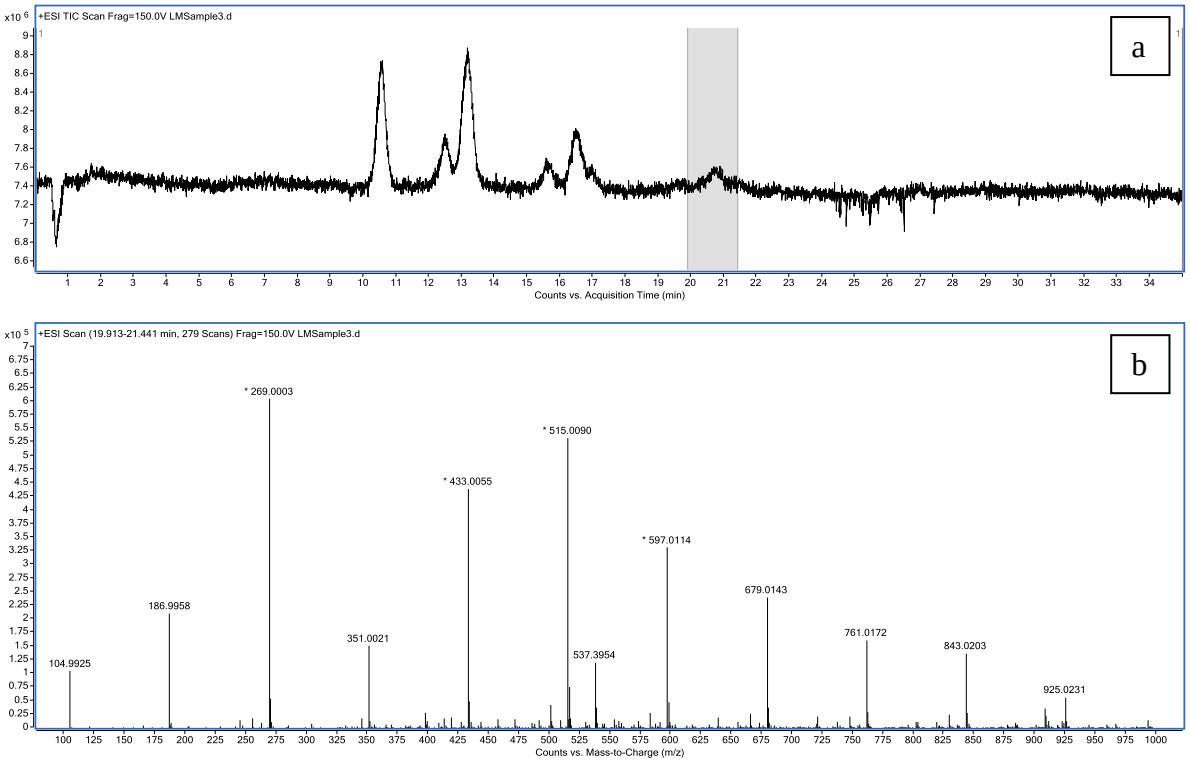

Figure B.16 TIC of non-sonicated sunflower oil (a) and ion spectra of peak n°6 (b).

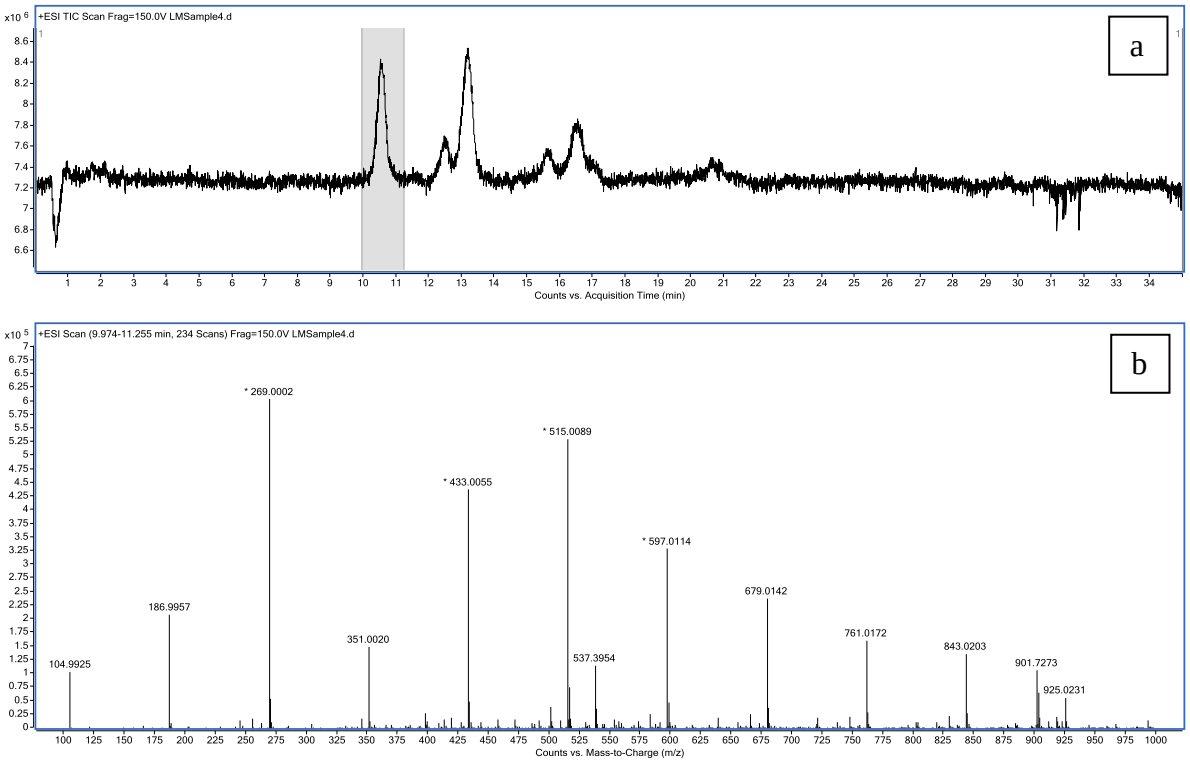

Figure B.17 TIC of sonicated sunflower oil (a) and ion spectra of peak n°1 (b).

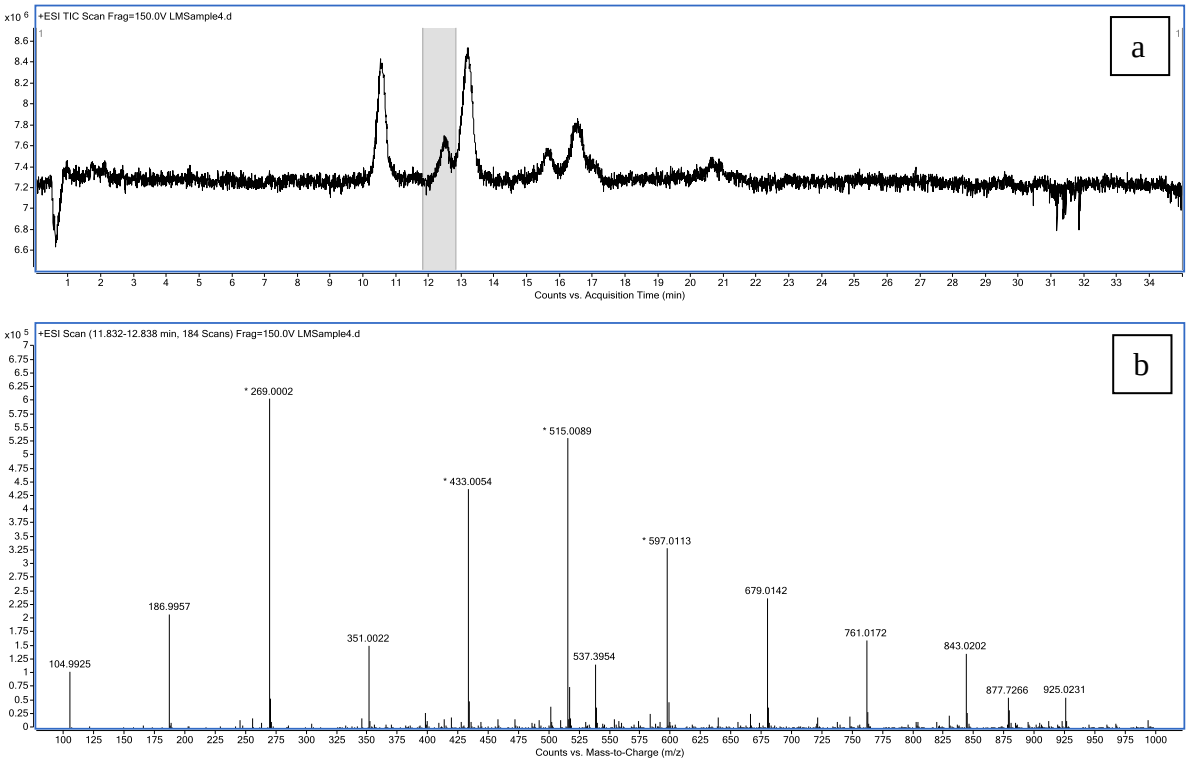

Figure B.18 TIC of sonicated sunflower oil (a) and ion spectra of peak n°2 (b).

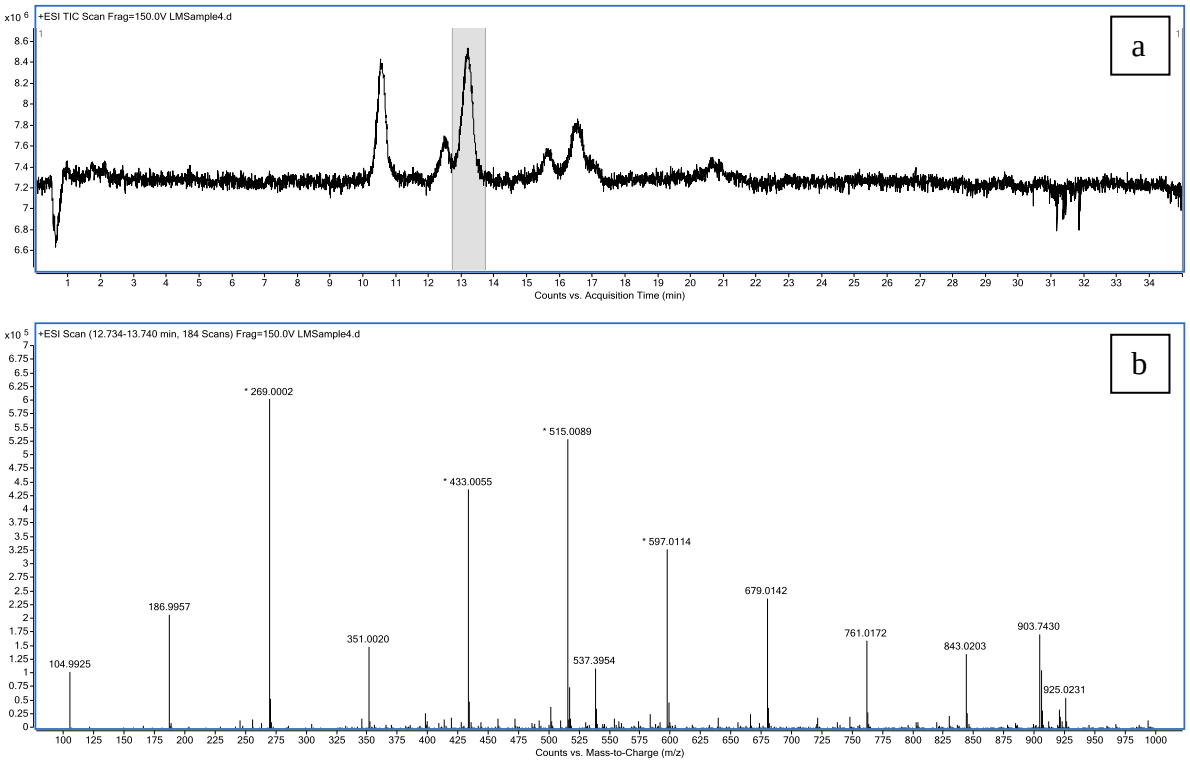

Figure B.19 TIC of sonicated sunflower oil (a) and ion spectra of peak n°3 (b).

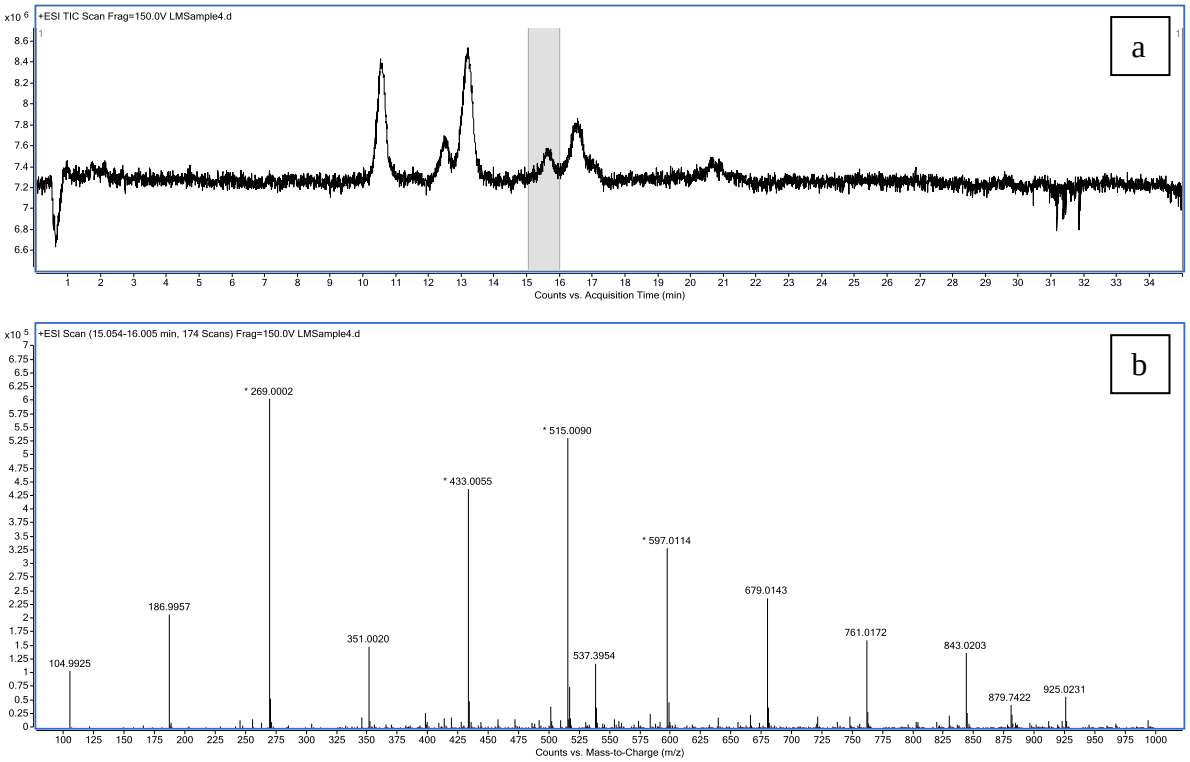

Figure B.20 TIC of sonicated sunflower oil (a) and ion spectra of peak n°4 (b).

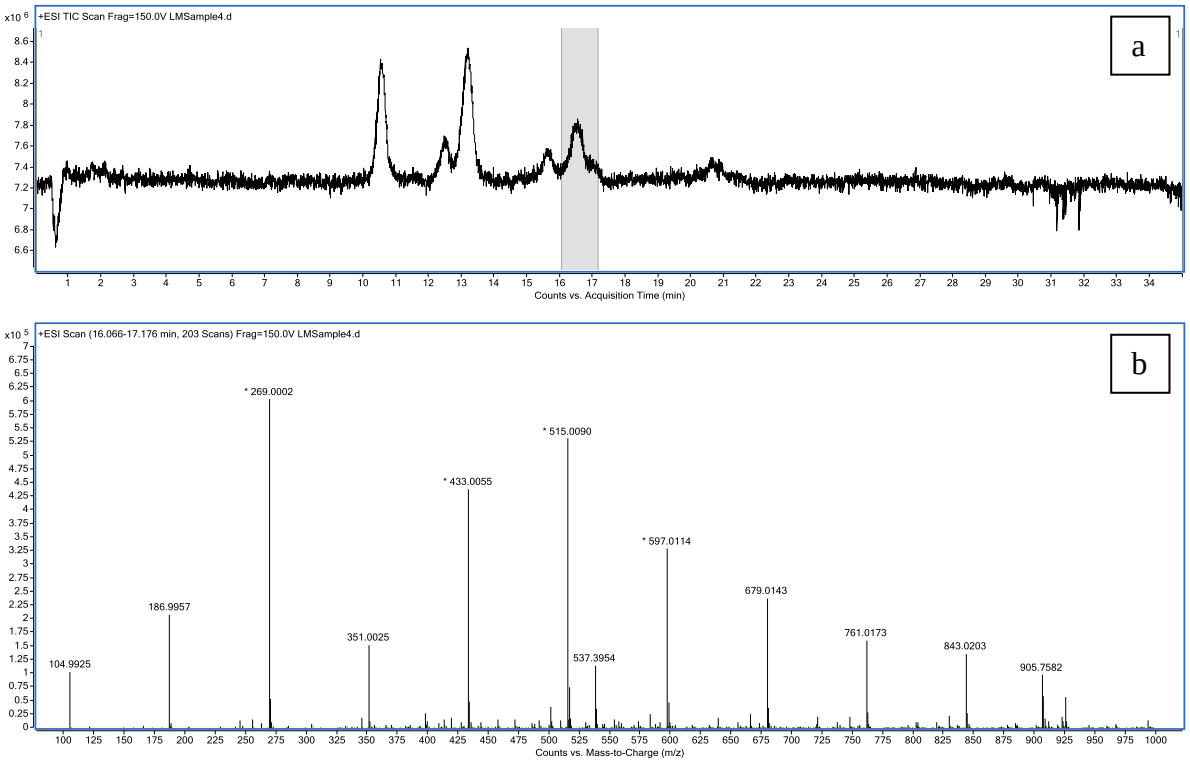

Figure B.21 TIC of sonicated sunflower oil (a) and ion spectra of peak n°5 (b).

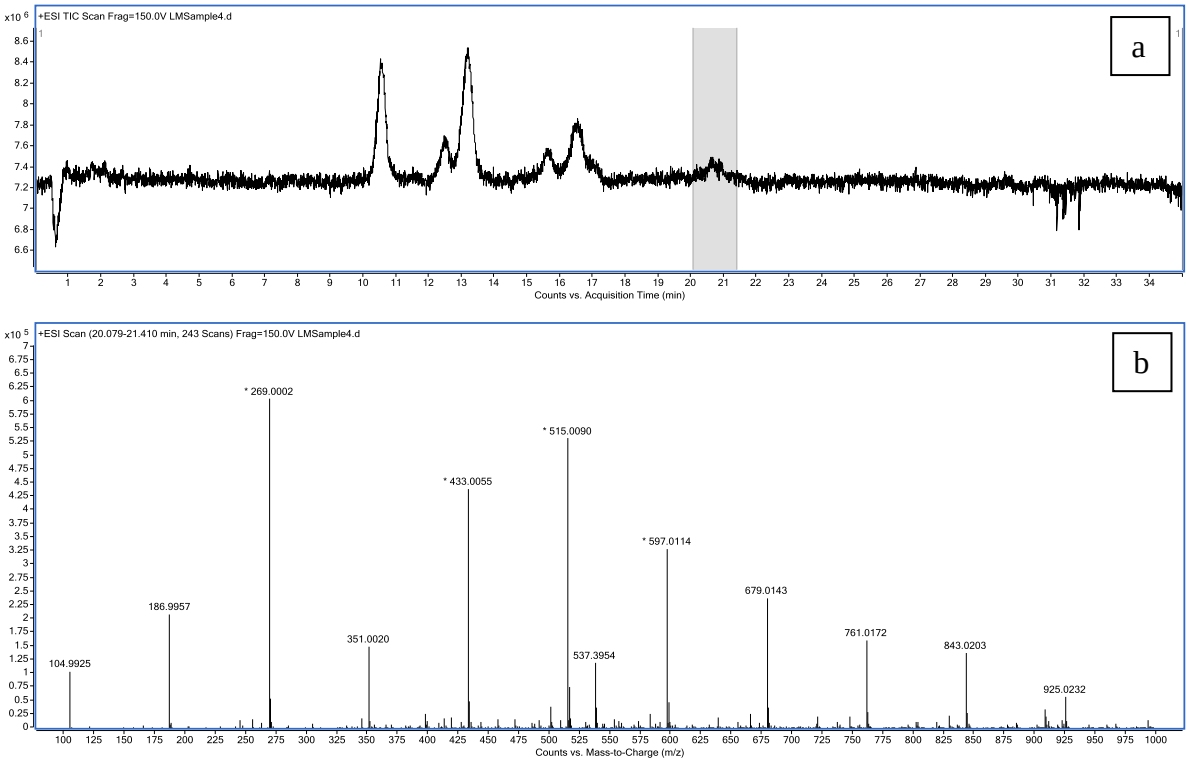

Figure B.22 TIC of sonicated sunflower oil (a) and ion spectra of peak n°6 (b).

Appendix C

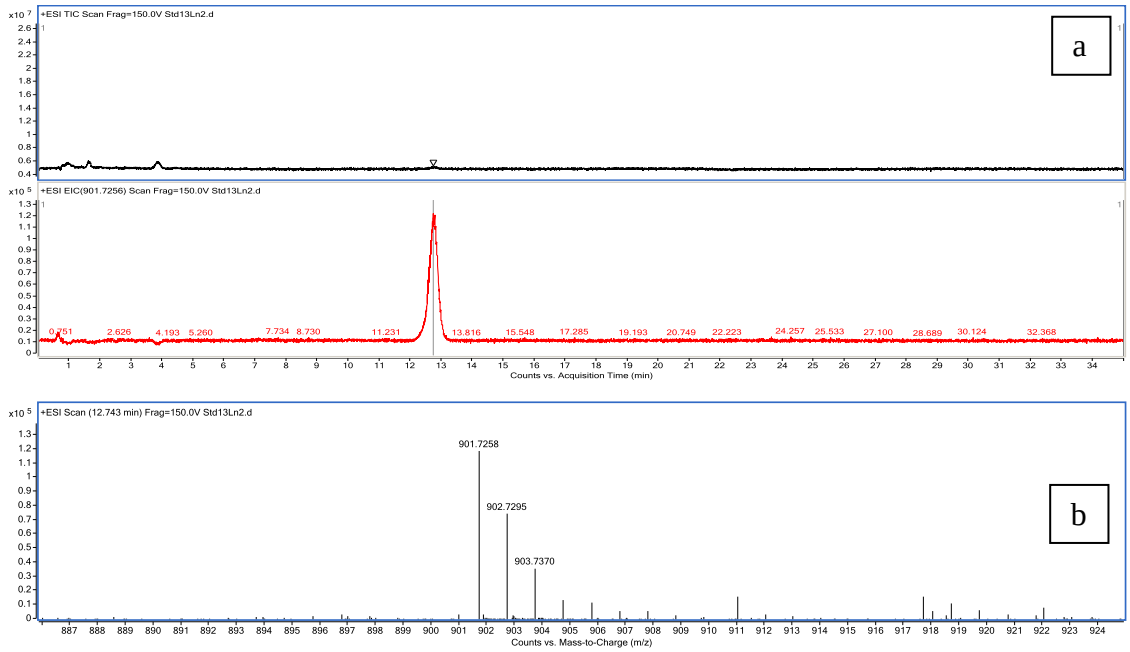

Figure C.1 TIC of sonicated glyceryl trilinoleate with zoom-in on the peak (a) and ion spectra of the peak (b).

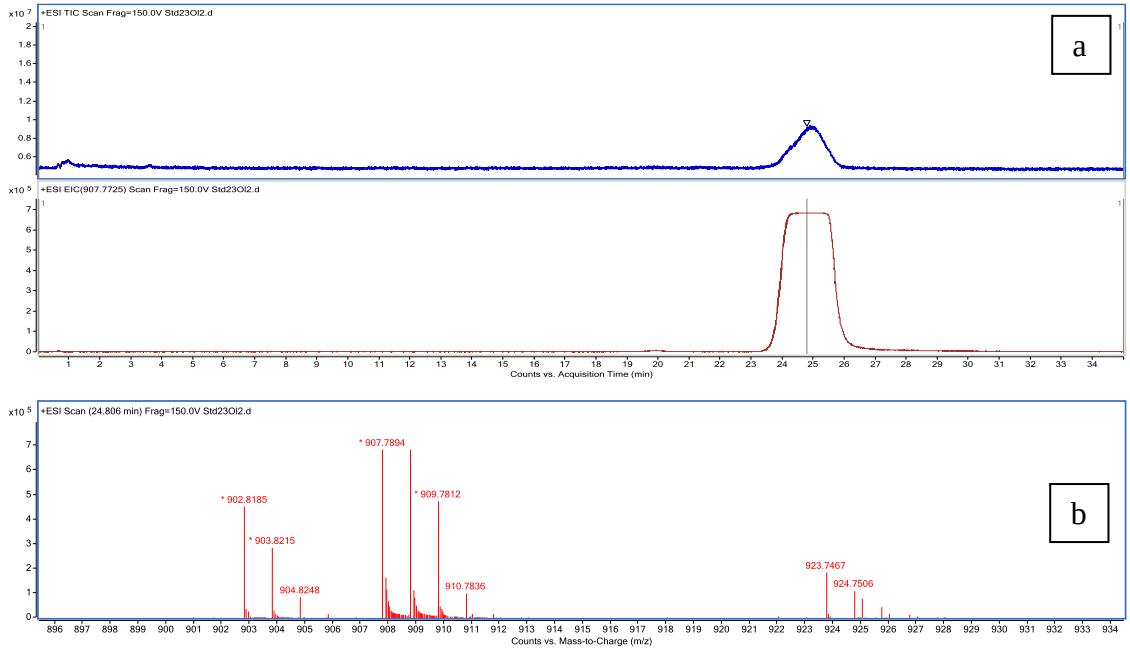

Figure C.2 TIC of sonicated glyceryl trioleate with zoom-in on the peak (a) and ion spectra of the peak (b).

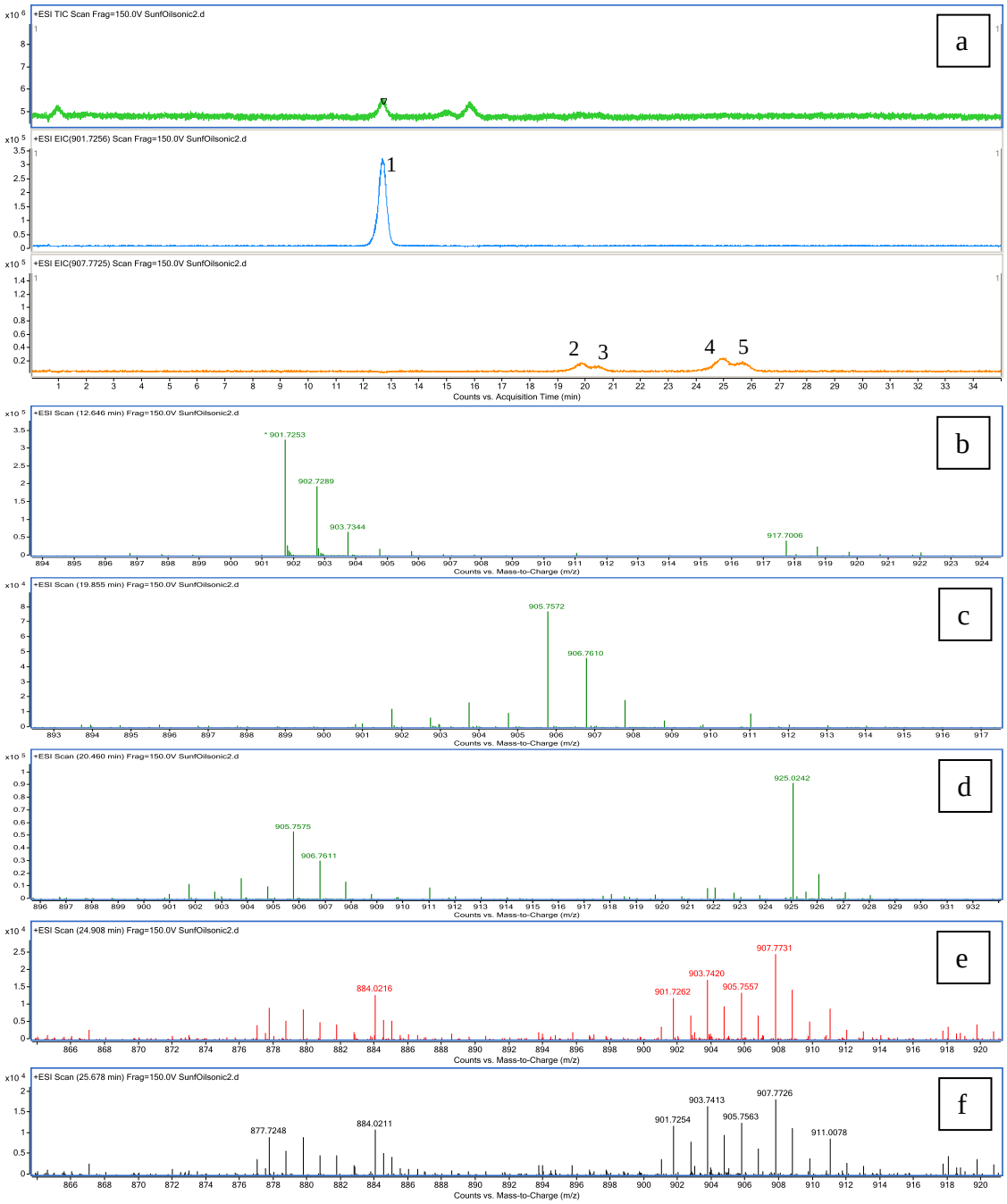

Figure C.3 TIC of sonicated sunflower oil with zoom-in to differentiate the five main peaks (a) and ion spectra of peaks n°1 (b), n°2 (c), n°3 (d), n°4 (e), n°5 (f).